

Department of the Interior
U.S. Geological Survey

LANDSAT 7 IMAGE ASSESSMENT SYSTEM (IAS) RADIOMETRIC ALGORITHM THEORETICAL BASIS DOCUMENT (ATBD)

Version 1Draft

June 2003



Document History

Document Number	Document Version	Publication Date	Change Number	Keywords
	Version 1	June 2003		Original

Contents

Document History	iii
Contents	iv
List of Figures	vi
List of Tables	vii
Section 1 Introduction	1
1.1 Purpose	1
Section 2 Overview and Background Information	3
2.1 Experimental Objective	3
2.2 Historical Perspective	3
2.3 Instrument Characteristics	4
2.3.1 Internal Calibrator	4
2.3.2 Partial Aperture Solar Calibrator (PASC)	7
2.3.3 Full Aperture Solar Calibrator	10
Section 3 Algorithm Descriptions	12
3.1 Radiometric Preprocessing Algorithm.....	13
3.1.1 Process PCD	13
3.2 Radiometric Characterization Algorithms.....	13
3.2.1 CHARACTERIZE IMPULSE NOISE	14
3.2.2 CHARACTERIZE MEMORY EFFECT	18
3.2.3 CHARACTERIZE SCAN-CORRELATED SHIFT (SCS).	27
3.2.4 CHARACTERIZE COHERENT NOISE	33
3.2.5 CHARACTERIZE DROPPED LINES.....	38
3.2.6 CHARACTERIZE DETECTOR SATURATION	40
3.2.7 CHARACTERIZE DETECTOR OPERABILITY	42
3.2.8 CHARACTERIZE MODULATION TRANSFER FUNCTION (MTF).....	47
3.2.9 CHARACTERIZE RANDOM NOISE	52
3.2.10 HISTOGRAM ANALYSIS.....	56
3.3 Radiometric Calibration Algorithms.....	61
3.3.1 PARTIAL APERTURE SOLAR CALIBRATOR (PASC)	61
3.3.2 FULL APERTURE SOLAR CALIBRATOR (FASC).....	75
3.3.3 PROCESS IC DATA	87
3.3.4 PROCESS IC DATA - REFLECTIVE BAND	94
3.4 Radiometric Correction Algorithms	106
3.4.1 PRE-1R CORRECTION OF RADIOMETRIC ARTIFACTS.....	106
3.4.2 CORRECT MEMORY EFFECT	109
3.4.3 CORRECT SCAN-CORRELATED SHIFT (SCS).	113
3.4.4 CORRECT COHERENT NOISE	115
3.4.5 SEPARATE IMAGE AND IC DATA	120
3.4.6 APPLICATION OF RADIOMETRIC CALIBRATIONS.....	122
3.4.7 RESCALE RADIANCE TO SCALED 8-BIT INTEGERS	125
3.4.8 POST-1R CORRECTION OF RADIOMETRIC CHARACTERISTICS....	127
3.4.9 STRIPING.....	130
3.4.10 BANDING	132

3.5	Miscellaneous Radiometric Processing Algorithms	135
3.5.1	CORRECT DETECTOR TEMPERATURE SENSITIVITY.....	135
3.5.2	GAIN FITTING FUNCTION.....	137
3.5.3	COMBINED RADIOMETRIC MODEL (CRaM)	144
Section 4	Processing Flows and Descriptions	147
4.1	Level 1R Processing (Day Scenes)	148
4.2	Night Scene Processing/Characterization.....	154
4.3	FASC Scene Processing/Characterization	161
4.4	PASC Scene Processing/Characterization	168
Appendix A	Acronyms.....	173
Appendix B	SBRS Algorithm Documents.....	180
Appendix C	Sample IAS Output Reports	181
References	236

List of Figures

Figure 2-1. ETM+ Internal Calibration System	6
Figure 2-2. ETM+ Band 4, Detector 1, Low Gain, Internal Calibrator Data, 12/7/96, Primary Lamp.....	7
Figure 2-3. ETM+ PASC Drawing Showing Light Path from the Sun (Modified SBRS Drawing).....	8
Figure 2-4. Enlargement of Partial Aperture Calibrator Hardware (SBRC Drawing)	9
Figure 2-5. ETM+ PASC Scene	9
Figure 2-6. ETM+ FASC in Deployed Position in front of ETM+ Aperture (SBRS drawing)	11
Figure 3-1. Partial Aperture Calibrator Geometry	62
Figure 3-2. Simulated ETM+ Band 3, Diffraction Image of Solar Disk.....	65
Figure 3-3. ETM+ FASC in the Deployed Position (Based on SBRS Drawing).....	76
Figure 4-1. Symbols and Terms	147
Figure 4-2. Step 1. 0R Radiometric Characterization	148
Figure 4-3. Step 2. Pre-1R Correction.....	149
Figure 4-4. Step 3. 0Rc Radiometric Characterization/Calibration	150
Figure 4-5. Step 3a. Process IC	151
Figure 4-6. Step 4. 1R Correction	152
Figure 4-7. Step 5. 1R Radiometric Characterization/Correction	153
Figure 4-8. Step 1. 0R Radiometric Characterization	154
Figure 4-9. Step 2. Scan Correlated Shift Characterization.....	155
Figure 4-10. Step 3. Coherent Noise Characterization.....	156
Figure 4-11. Step 4. Memory Effect Characterization	157
Figure 4-12. Step 5. 0Rc Radiometric Characterization/Calibration	158
Figure 4-13. Step 6. 1R Correction	159
Figure 4-14. Step 7. 1R Radiometric Characterization/Correction	160
Figure 4-15. Step 1. 0R Radiometric Characterization	161
Figure 4-16. Step 2. Scan Correlated Shift Characterization.....	162
Figure 4-17. Step 3. Coherent Noise Characterization.....	163
Figure 4-18. Step 4. Memory Effect Characterization	164
Figure 4-19. Step 5. Process FASC Data.....	165
Figure 4-20. Step 6. 1R Correction	166
Figure 4-21. Step 7. Radiometric Characterization/Correction	167
Figure 4-22. Step 1. 0R Radiometric Characterization	168
Figure 4-23. Step 2. Memory Effect Characterization	169
Figure 4-24. Step 3. Process PASC Data	170
Figure 4-25. Step 4. 1R Correction	171
Figure 4-26. Step 5. 1R Radiometric Characterization/Correction	172

List of Tables

Table 2-1. L7 ETM+ Salient Characteristics	4
Table 3-1. ETM+ SNR Requirements (Low Signal)	44
Table 3-2. ETM+ SNR Requirements (High Signal)	44
Table 3-3. L7 System Spec	46
Table 3-4. ETM+ PASC Radiometric Calibration Uncertainty for Initial In-orbit Deployment	63
Table 3-5. ETM+ FASC Radiometric Calibration Uncertainty for Initial In-orbit Deployment	76
Table 3-6. Component Index	91
Table 3-7. Symbols	92

Section 1 Introduction

1.1 Purpose

This document describes the radiometric algorithms used by the Landsat 7 (L7) Image Assessment System (IAS). These algorithms are implemented as part of the IAS Level 1 (L1) processing, radiometric characterization and radiometric calibration software components. These algorithms are used to create accurate L1 output products, characterize the Enhanced Thematic Mapper Plus (ETM+) radiometric performance (noise, dynamic range, anomalies), and derive improved estimates of the absolute and relative radiometric calibration parameters. These algorithms produce output that is stored in the IAS Database and routinely trended as part of the radiometric performance monitoring. This document presents background material describing the ETM+ sensor and its radiometric calibration devices as well as descriptions of the IAS processing algorithms and processing flows.

The Core L1 radiometric processing algorithms include:

- Process Payload Correction Data (PCD)
- Characterize Dropped Lines
- Correct Coherent Noise (CN) (partial - pan band only)
- Characterize Impulse Noise (IN) (shutter only)
- Characterize Detector Saturation
- Process Internal Calibrator (IC) Data
 - Reflective Bands
 - Emissive Band
- Apply Radiometric Correction
- Correct Dropped Lines (if required)
- Rescale data to LMIN, LMAX (part of 1G processing)

The following correction algorithms (with their associated necessary characterizations) are also available within the L1 radiometric processing:

- Correct Temperature Sensitivity
- Correct Inoperable Detectors
- Histogram Analysis
- Correct Striping
- Characterize CN (partial – all bands)
- Correct CN (all bands)

In addition, several radiometric characterization algorithms are typically turned on during L1 processing. These do not affect the L1R product, but generate the following reports and trending data for off-line analysis:

- Characterize Detector Operability
- Characterize Random Noise

- Histogram analysis (complete)

Several algorithms were included in the L1 processing to account for radiometric artifacts present in Landsat 4 (L4) and Landsat 5 (L5) Thematic Mapper (TM) data. These artifacts have not been observed in L7 ETM+ data at sufficient levels to operationally turn on these algorithms as part of processing. These include:

- Characterize Scan-Correlated Shift (shift locations only)
- Correct Scan-Correlated Shift
- Correct Memory Effect (ME)
- Characterize Banding
- Correct Banding

There are sets of algorithms designed to be used on specialized scenes only (e.g., night scenes) to perform more detailed characterizations. These algorithms include:

- Characterize Scan-Correlated Shift (complete)
- Characterize CN (image portion)
- Characterize Random Noise (image portion)
- Characterize ME
- Characterize IN (image portion)

Finally, there are radiometric calibration algorithms applicable to each of the on-board calibration devices:

- Process Full Aperture Solar Calibrator (FASC)
- Process Partial Aperture Solar Calibrator (PASC)
- Process IC

Each of these algorithms is based, at least in part, on those provided by the instrument vendor, Santa Barbara Remote Sensing (SBRS). Appendix B includes the algorithm descriptions provided by SBRS.

Section 3 describes each algorithm; Section 4 describes the processing flows.

Section 2 Overview and Background Information

The L7 ETM+ continues the Landsat Project's multispectral space-borne Earth remote sensing satellites that began with the launch of Landsat 1 in 1972. L7 will provide data consistent with the Landsat historical record from 1999 to the introduction of successor instruments based on newer technology. The basic sensor design used in the ETM+ is to the same as the TM instruments flown on L4 and L5, and the Enhanced Thematic Mapper (ETM) built for Landsat 6 (L6), which suffered a launch failure. The radiometric processing, characterization, and calibration algorithms described in this document take into account the new 15-meter panchromatic band (also present in L6), the higher resolution thermal band, the use of two gain states, the use of a single internal calibration system lamp with a backup lamp, and the addition of two new radiometric calibration devices: the PASC and the FASC, in adapting the processing techniques applied to L4/L5 TM data to the L7 ETM+.

The inclusion of an IAS as an integral part of the L7 ground system illustrates the more systematic approach to instrument calibration and in-orbit monitoring and characterization necessitated by the more stringent calibration requirements of the L7 ETM+ as compared to earlier Landsat missions. This is especially true of the radiometric calibration requirements, which include using partial and full-aperture solar calibrations to monitor the stability and performance of the ETM+ detectors and on-board calibration lamps. The IAS also provides the platform for systematic geometric performance monitoring, characterization and calibration.

2.1 Experimental Objective

The objective of the L7 ETM+ mission is to provide global, seasonally refreshed, high-resolution (15-meter panchromatic, 30-meter multispectral, 60-meter thermal) imagery of Earth's land areas from a near polar, sun-synchronous orbit. These data will:

- Extend the continuous data record collected by Landsats 1-5
- Provide greater calibration accuracy to support new and improved analysis applications
- Provide the high-resolution component for the Earth Observing System (EOS), complementing and validating datasets from the moderate resolution systems, i.e, Moderate Resolution Imaging Spectroradiometer (MODIS), and Multiangle Imaging Spectroradiometer (MISR).

The L7 IAS and the L1 Product Generation System (LPGS) will use the radiometric algorithms described in this document to ensure that the radiometric behavior of the ETM+ is sufficiently characterized to meet the more stringent radiometric calibration requirements.

2.2 Historical Perspective

The L7 ETM+ mission continues the evolutionary improvement of the Landsat family of satellites, which began with Landsats 1, 2, and 3 carrying the Multi-Spectral Scanner

(MSS), and builds on the L4 and L5 TM heritage. The ETM+ adds a 15-meter GSD panchromatic band similar to that used in the ETM instrument built for L6. It improves the thermal band spatial resolution from 120 meters (TM/ETM) to 60 meters (ETM+), and improves the radiometric calibration accuracy from 10% (TM/ETM) to 5% (ETM+). The L7 system is also taking a more systematic approach to monitoring and measuring system performance in flight than that applied to L4 and L5, which were turned over to commercial operations in October 1985.

2.3 Instrument Characteristics

Table 2-1 shows the principal characteristics of the ETM+. The basic optical design of the ETM+ is unchanged from the earlier systems. An oscillating scan mirror provides the cross-track scanning. A Ritchey-Chretien telescope focuses the energy on the primary focal plane (PFP), where the silicon detectors for bands 1-4 and 8 (panchromatic) are located. The spectral filters for the bands are located directly in front of the detectors. The spectral filters for the ETM+ are of Ion-Assisted Deposition (IAD) design to reduce changes due to outgassing in a vacuum. A portion of the energy bypasses the PFP and goes into the relay optics to the Cold Focal Plane (CFP). The Indium Antimonide detectors for bands 5 and 7 and the Mercury Cadmium Telluride detectors for band 6 are located on the CFP. The temperature of the CFP is maintained at a predetermined temperature (using a radiative cooler) of 91K, with two higher set point temperatures available: 95K and 105K. The 15-meter panchromatic band has 32 detectors, the 30-meter reflective bands have 16 detectors/band and the 60-meter thermal band has eight detectors.

Band (#)	Bandpass (mm)	Spatial Resolution (Meters)	NED _p (%) [*]	Noise Equivalent Detector Temperature (NEDT) (K@300K)
1	0.452 – 0.514	30	0.19	
2	0.519 – 0.601	30	0.15	
3	0.631 - 0.692	30	0.19	
4	0.772 - 0.898	30	0.14	
5	1.547 - 1.748	30	0.18	
6	10.31 – 12.36	60		0.22
7	2.065– 2.346	30	0.28	
8 (pan)	0.515 – 0.896	15	0.39	
[*] High Gain Mode at ~6% exoatmospheric reflectance @ 30° solar zenith angle				

Table 2-1. L7 ETM+ Salient Characteristics

2.3.1 Internal Calibrator

The IC of the ETM+ consists of a shutter flag, a blackbody and two tungsten lamps (See Figure 2-1). The shutter flag, located immediately in front of the prime focal plane, oscillates in synchronization with the scan mirror. At the end of each scan, the shutter passes in front of the focal plane. The shutter flag also relays light from the internal calibration lamps and blackbody to the detectors. The two internal calibration lamps are situated near the base of the internal calibrator flag. Light from either or both lamps is

directed through optics at the pivot point of the flag into a sapphire rod in the flag itself. This rod transfers the light up the shutter flag, and within the flag, the light splits into separate paths for each of the spectral bands. The light is directed out of the shutter flag and onto the focal planes by additional optics in the head of the flag. The light for each band is aligned so it impinges upon the appropriate detectors.

The internal blackbody is situated off the optical axis of the instrument. When the shutter flag passes in front of the PFP, the blackbody-emitted energy reflects off a toroidal mirror on the shutter flag into the aft optics of the ETM+ so it impinges upon the band 6 detectors. The portion of the shutter flag imaged by band 6, exclusive of the area where the toroidal mirror is located, is coated with a high-emissivity paint and acts as the second blackbody source for band 6 calibration. This portion of the shutter flag is also instrumented with a thermistor.

The IC lamps are supplied with a regulated voltage across a combination of the lamp and a resistor, resulting in quasi-constant power supplied to the lamp. Each lamp can be commanded "on" or "off," so four lamp states are possible (both "off" [0,0], one "on" [0,1] or [1,0] or both "on" [1,1]). For reliability issues, the use of the [1,1] state was restricted to prelaunch testing. The IC was designed to have one lamp produce a usable signal in all bands; both lamps on will saturate some bands, particularly in high gain mode. The internal blackbody has three set point temperatures (30°C, 37°C and 46°C).

The ETM+ IC is essentially identical to the L6 ETM IC, although it has some differences compared to the IC on L4 and L5 TMs. The principal differences include: (1) Two lamps are used instead of three, (2) more compact lamp filaments result in a higher flux incident on the IC optics, although the lamps are nearly identical in terms of current and voltage ratings, (3) the control circuit utilizes the regulated voltage mode for both primary and backup control, whereas TM used a radiance-stabilized mode as the primary and the regulated voltage as the backup, (4) sapphire rods are used to transmit the energy from the base of the flag to the head of the shutter flag; the TM ICs used fiber optics, (this change was an attempt to improve the uniformity of the calibration flux at the focal plane) and (5) the lamp sequencer used on TM to automatically cycle through the lamp states was removed.

When the ETM+ is operating, the shutter flag oscillates in synchronization with the scan mirror and blocks the light entering the aperture from reaching the focal planes. The size of the shutter flag and its speed of movement combine to provide obscuration of the light to each detector for about 7.2 msec or 750 pixels for the 30-meter channels; the light pulse has a width of approximately 40 pixels (Figure 2-2). For band 6, the calibration signal is similar, with the blackbody pulse at about 40 pixels wide.

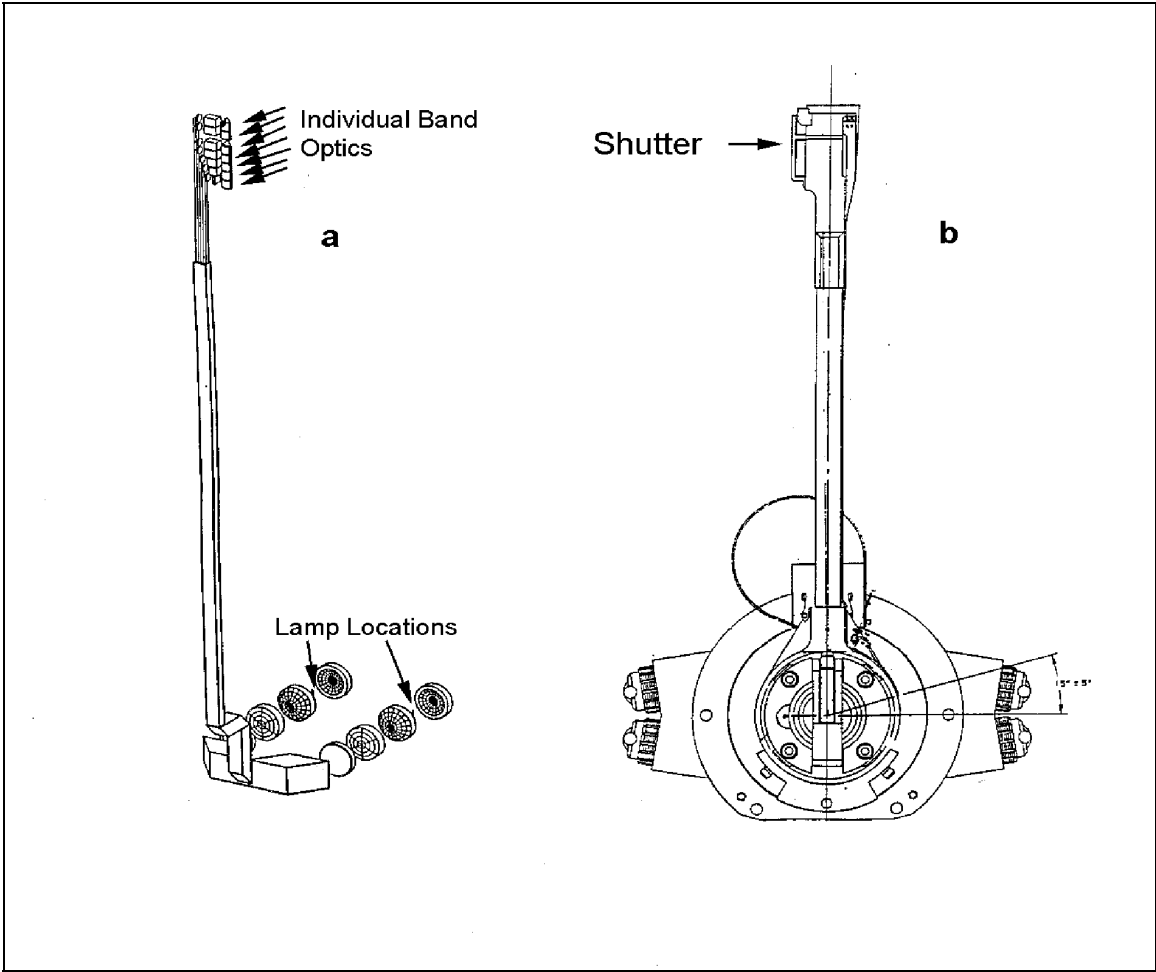


Figure 2-1. ETM+ Internal Calibration System

(a) optical drawing (b) mechanical drawing (SBRS drawings)

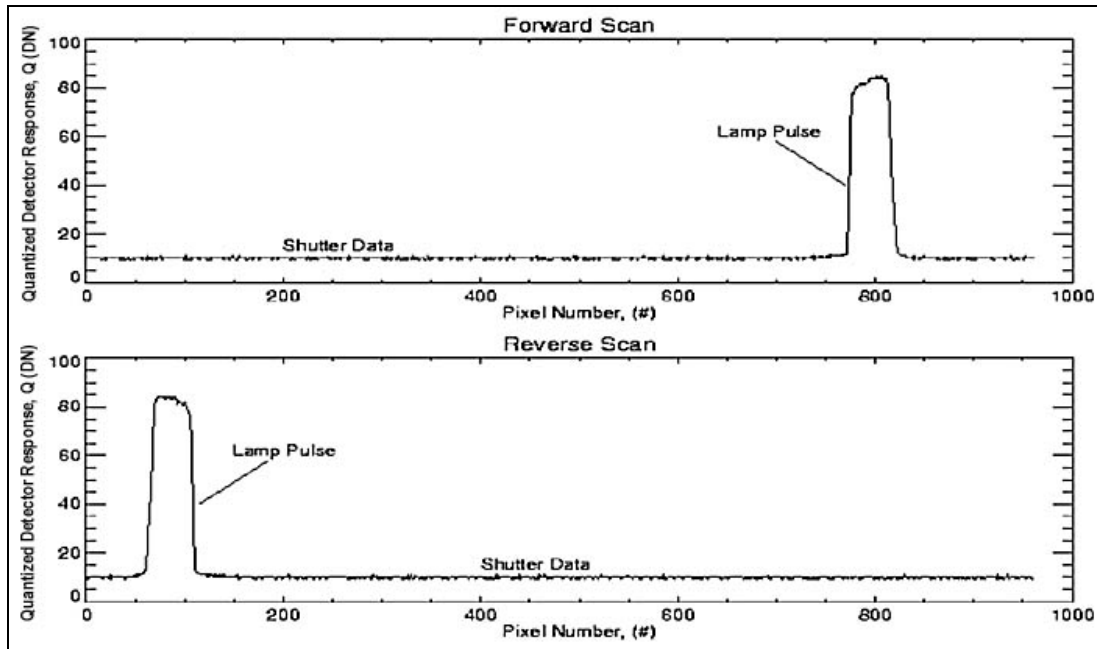


Figure 2-2. ETM+ Band 4, Detector 1, Low Gain, Internal Calibrator Data, 12/7/96, Primary Lamp

2.3.2 Partial Aperture Solar Calibrator (PASC)

The PASC is a small passive device that allows the ETM+ to image the sun while viewing a “dark Earth.” It is attached to the ETM+ sunshade and it permanently obscures a small portion (~0.5%) of the aperture.

The PASC consists of four essentially identical sets of optical elements, each in a slightly different orientation. Each set (or facet) consists of an uncoated silica reflector, a 45-degree mirror and an aperture plate with a precision-drilled small aperture (~4 mm) (Figure 2-3). The facets are oriented at a 9-degree dip angle relative to the velocity direction of the spacecraft, and 6 degrees apart in azimuth, at angles of 24, 30, 36 and 42 degrees to the left of the satellite velocity vector (for a 10:00 a.m. equatorial crossing) (Figure 2-4). The orientation is such that on any given orbit, as the satellite passes out of solar eclipse in the vicinity of the North Pole, at least one facet will reflect sunlight directly into the ETM+ aperture and the ETM+ will image the sun. The combination of the small aperture and the uncoated silica reflector reduces the signal amplitude sufficiently to bring it into the ETM+ dynamic range. The +/- 7.7 degrees nominal scan of the ETM+ causes each facet to trace out a swath in space. However, edge vignetting restricts the usable portion of the scan to about +/- 5.9 degrees.

Typical PASC images appear with a distorted sun image (glint) superimposed over a dark (Earth) background (Figure 2-5). The glint distortions are attributable to three major effects. First, the reduced resolution images are limited by the diffraction from small apertures, an effect that is wavelength dependent. For the 4 mm apertures, the diffraction blur circle (at the first dark ring) is 7, 8, 10, 12, 24, 164, 32, and 20 pixels in diameter, for all bands 1-8 respectively. Second, the glints are over sampled and

elongated in the along-track direction. This results from the along-track rate at which the ETM+ images the sun, which in turn comes from the spacecraft pitch rate, which is ~9 times slower than the apparent rate at which the Earth is scanned in “normal” ground images. This factor derives explicitly from the pitch rate, whereby the along-track movement across the solar disk is approximately 360 degrees in ~100 minutes or ~3.6 degrees/minute, while the ground is normally scanned at 16 IFOVs ($16 * .0024^\circ = .039^\circ$) per scan (72 msec) or ~32.5 degrees/minute. (NOTE: The along-track dimensions may vary if the pitch rate varies anomalously, as has occurred on previous satellites exiting eclipse). Third, the scanning direction is not perpendicular to the motion of the sun - the angle between the two can be as small as 45° . Hence, the combined effects of diffraction, over sampling, and non-orthogonal scanning render solar imagery that is blurred, elongated, and skewed (Figure 2-5). The number of image pixels across the solar disk from limb to limb at disk center is ~200 for bands 1-5 and 7, and ~410 for band 8.

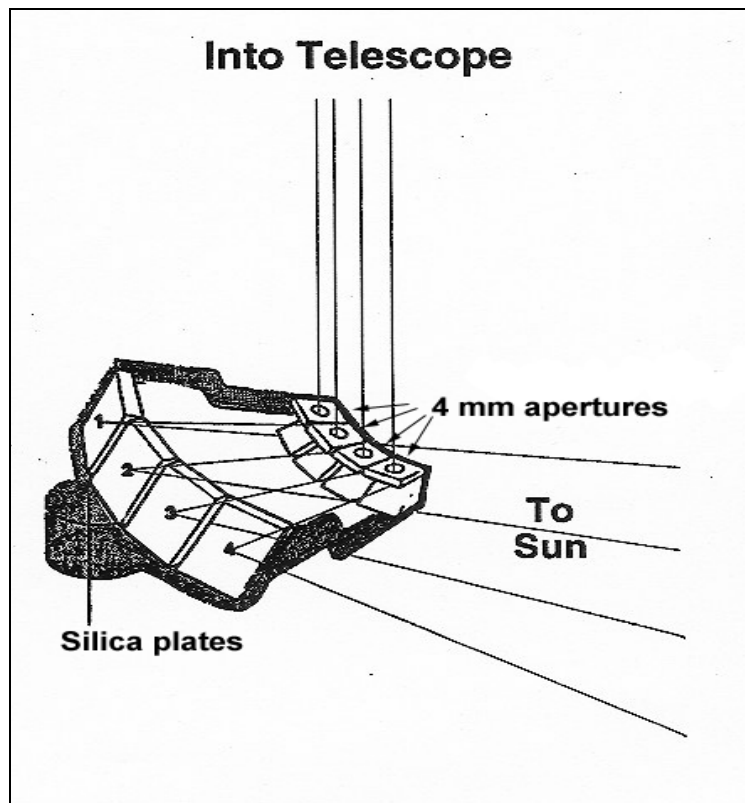


Figure 2-3. ETM+ PASC Drawing Showing Light Path from the Sun (Modified SBRS Drawing)

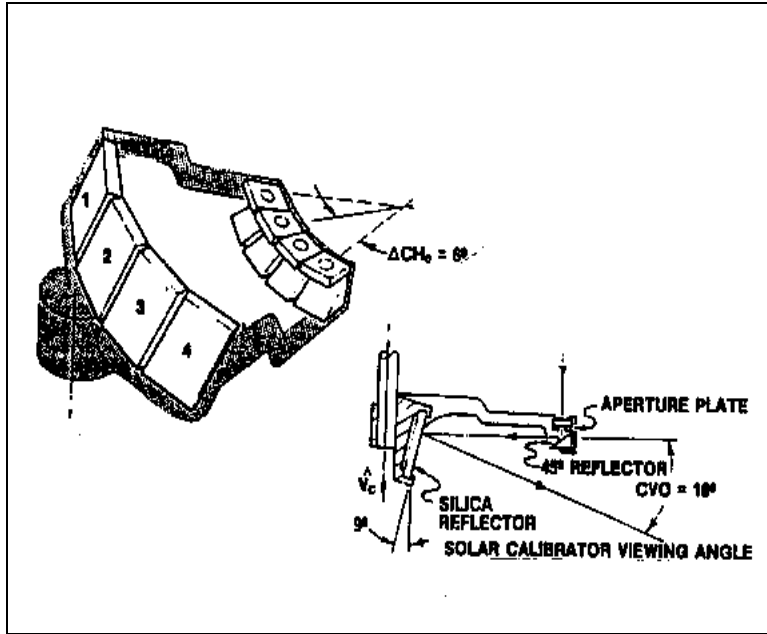


Figure 2-4. Enlargement of Partial Aperture Calibrator Hardware (SBRC Drawing)

CV is the dip (vertical) angle wrt the Spacecraft (S/C) velocity; CH is the hour (azimuthal) angle wrt to the velocity vector.

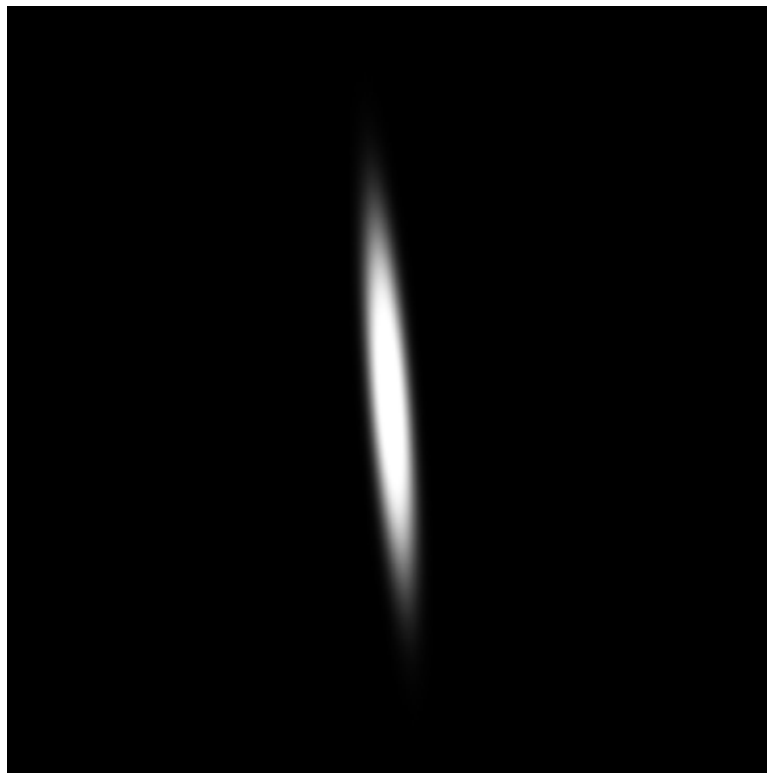


Figure 2-5. ETM+ PASC Scene

2.3.3 Full Aperture Solar Calibrator

The FASC is a white painted panel that diffusely reflects solar radiation into the ETM+ aperture.

The panel is an aluminum, octagon-shaped honeycomb, mounted on a motorized arm. The center 51 cm of the panel is painted with the classic formulation of YB71, an inorganic flat white paint selected for its spacecraft thermal control properties, near Lambertian characteristics, high reflectance, (~90% in the visible) and apparent stability in a space environment.

When not in use, the panel rests adjacent to its stow cover, thereby reducing exposure to contaminants and UV radiation. During calibration, the motorized arm rotates the panel from its stowed position to an inclined position (a nominal angle of 23.5 degrees relative to the nadir view direction of the ETM+) in front of the aperture (Figure 2-6). The panel deploys as the satellite passes over the terminator near the North Pole. Shortly after the satellite passes out of eclipse, the sun rises on the panel (at a 90-degree solar zenith angle). The solar illumination on the panel increases and remains unobstructed until an approximate solar zenith angle of 67 degrees, when the instrument structure begins to shadow the panel. The nominal calibration condition occurs at a 70-degree solar zenith angle, and a relative solar azimuth that varies approximately 14 degrees over the year (from about 23 to 37 degrees from the fore scatter direction at 0 degrees).

FASC imagery appears as an essentially flat field with vignetted cross-track edges. The image increases in brightness along track as the Solar Zenith Angle (SZA) on the panel decreases (roughly at $1/\cos(\text{SZA})$). Specifications require the FASC to fill the ETM+ aperture for the central 1000 pixels (approximately 1/6 of each scan line); the design nominally fills the aperture for the central ~50% of the scan line. As the scan mirror moves, the view angles to the panel change. If the nadir viewing pixel has the nominal 23.5 degree view angle and a 0 degree view azimuth angle, the view zenith angle increases by about 1 degree at the extreme ends of the scan, and the view azimuth angle varies by +/- 30 degrees. Prelaunch measurements of the Bi-directional Reflectance Distribution Function (BRDF) show an approximate 1% variation of radiance across the scan with view geometry. Across the central 1000 pixels, this translates into a 0.1% effect.

Thus, with a known surface reflectance, solar irradiance and geometry conditions, the FASC device behaves as a full system, full aperture calibration device.

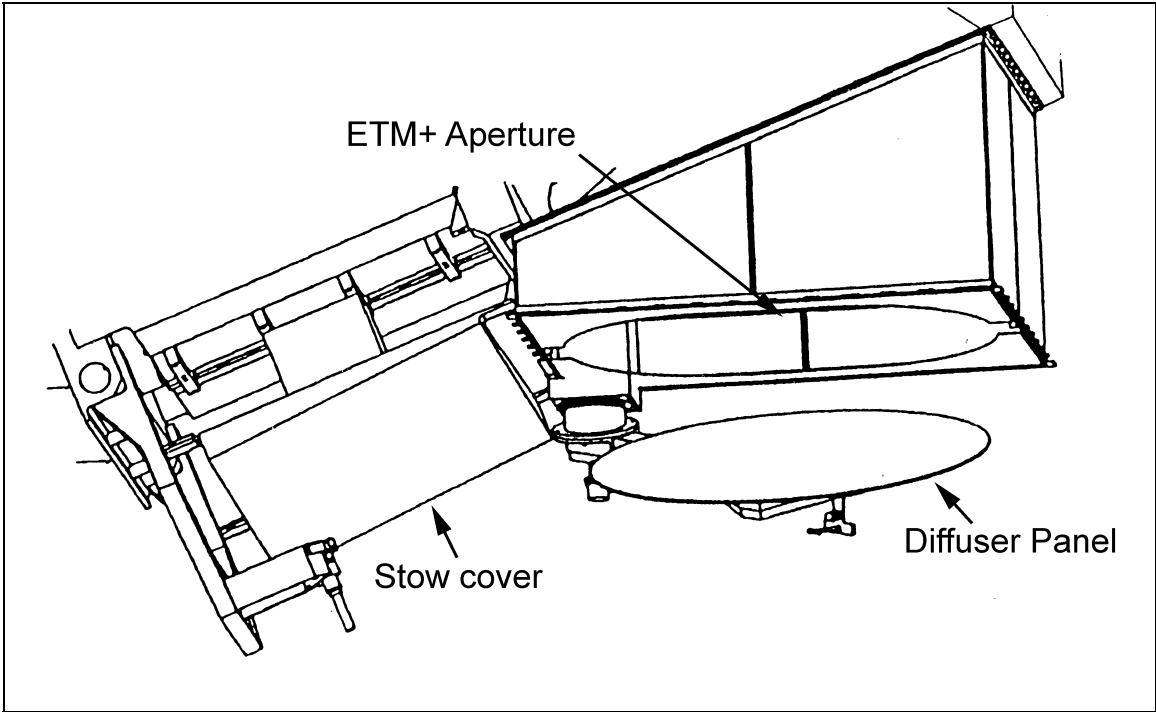


Figure 2-6. ETM+ FASC in Deployed Position in front of ETM+ Aperture (SBRS drawing)

Section 3 Algorithm Descriptions

This section provides the underlying theory, mathematical development, and coding schemes for the IAS radiometric algorithms.

The radiometric processing within the IAS and LPGS begins with the Level Zero-R (0Rp) data product as provided by the EOS core system (ECS). The Level 0Rp product is derived from the Level 0Ra (archive) data product that is provided to the ECS by the Landsat Processing System (LPS). The Level 0Rp product contains the uncalibrated image and internal calibration “wide-band” data, in addition the PCD, which contains temperatures, ephemeris and related information, and the Mirror Scan Correction Data (MSCD), which contains attitude and related information.

Additional processing inputs come from:

- The Calibration Parameter File (CPF)
- Operator inputs that may override the CPF settings
- The Modeling and Analysis Database**
- The IAS Labeled Mask (LM) (see below)
- The IAS Trending Database
- Temporary IAS internal storage from previously executed algorithms

Outputs from radiometric processing are available in several forms, including:

- A Level 1R “product” (not all processing produces a product)
- The IAS Trending Database values (permanently retained)
- The IAS internal reports (detailed reports, temporarily retained)
- The IAS LM, an internal IAS file that contains the line and pixel coordinates for any identified radiometric artifacts
- Temporary IAS internal storage

The IAS Trending Database contains results that may be trended or analyzed off-line.

The algorithms are loosely categorized into:

- Preprocessing (See Section 3.1)
- Characterization (See Section 3.2)
- Calibration (determination of absolute calibration parameters) (See Section 3.3)
- Correction (application of calibration parameters) (See Section 3.4)
- Miscellaneous Algorithms (developed for off-line data analysis as opposed to in-line data processing) (See Section 3.5)

3.1 Radiometric Preprocessing Algorithm

3.1.1 Process PCD

Before radiometric processing, a scene is first ingested into the IAS. During the ingest process, instrument state parameters for that scene are extracted from the instrument PCD file, a file that is generated for the entire subinterval of acquired data. Specific scene parameters extracted and tracked include IC lamp states (e.g., no lamps, lamp 1, lamp 2, both lamps), lamp current, lamp voltage, gain state (by band), instrument temperatures (all), FASC status, etc. These time-dependent parameters are output to a file and are accessible by all follow-on processing functions.

INPUTS:

- PCD file for interval
- "Time" file for specific scene to be processed

OUTPUTS:

- Processed PCD file for interval including values/equations to provide each instrument PCD parameter at any point in the interval. When a specific scene is to be input, the outputs are the values of each parameter for each swath of the scene.

ALGORITHM:

1. Ingest PCD file.
For binary parameters, check validity of PCD, and identify starting state and locations of transitions (gain state, lamp states) in terms of instrument time/scan line.
For "analog" telemetry, check validity of PCD data points, generate interpolation or least squares (probably third order) equation to provide value for any time-in interval along with estimated uncertainty in predicted value.
Ingest time file for scene to be processed – provide values of each parameter for each swath.

REPORTS:

1. Initial states and time-tagged transitions for each binary parameter
2. Plots of analog telemetry superimposed with predictive equation
3. Option to print/view all values of any parameter

3.2 Radiometric Characterization Algorithms

1. Read in from the CPF the median filter window width and the threshold factors by which the IN output value differ from the signal in units of standard deviation of the RN in the detector.
2. Read in a band from the data set and its associated radiometric anomaly label mask.

3. Obtain the standard deviation of the RN in each detector within the band from the CPF.

3.2.1 Extract all data of a given detector, excluding mf's marked as saturated nodes in CHARACTERIZE IMPULSE NOISE

3.2.1.1 Algorithm Description

3.2.1.1.1 Background

Impulse noise (IN) within a digital signal manifests itself in the occasional sample as a departure from the signal trend far in excess of that expected from Random Noise (RN). The characteristics of this noise are important clues of the state of the instrument. Analysis of some L4/L5 TM data indicates that most if not all occurrences of IN are simply due to flips of one or two of the more significant bits. Analysis also revealed that the occurrence rate could vary strongly.

The signals in the calibration (IC, PASC, and FASC) data and in the night scene data of ETM+ are fairly smooth. Consequently, samples corrupted by IN in these data will be easy to identify. In contrast, the structure of the scanned surface can drive strong variations in output value from sample to sample in day scenes. This algorithm description describes the algorithm for calibration and night data only.

3.2.1.1.2 Inputs

Primary input:

- IC, PASC, FASC, or night scene data (8-bit integer per pixel).

Input from the process flow:

- Radiometric anomaly label mask (8-bit string per pixel).

Input from the CPF:

- The width in minor frames (mf) of the median filter explained below (8-bit integer).
- The IN threshold factors by which the absolute difference between the IN output value and the median value in units of the standard deviation of the RN. There are two threshold factors for each case, as explained below.
- Standard deviation of RN in each detector (32-bit floating point number per detector).

3.2.1.1.3 Outputs

Output for process flow, including correction for IN:

- Updated radiometric anomaly label mask

- A vector of structures, in which the number of elements corresponds to the number of IN occurrences identified by the algorithm and where a structure contains the location and output value of the IN and other pertinent information necessary for evaluation and correction. Each structure contains:
 - The type of data, e.g., shutter, night scene (16-character string)
 - The spectral band name (4-character string)
 - The detector number (8-bit integer)
 - The scan number (16-bit integer)
 - The mf number (16-bit integer)

Output for the IAS Database:

- The begin and end times of the processed data set since launch in units of seconds (two 32-bit integers)
- The above vector of structures
- A three-element array containing the output values of the corrupted mf and its neighbors (3*8 bit integer)

3.2.1.1.4 Algorithm

The algorithm treats IN as two separate cases, both of which use the absolute difference between an output value of a pixel of interest and a median filtered value as a comparison value. Though a linear filter is faster, a median filter is more robust at predicting the true signal value. The data are processed serially, line-by-line, band after band.

The “unequal” case occurs when the difference between the two pixels adjacent to the pixel of interest is greater than twice the standard deviation of RN. IN is identified if the comparison value is greater than the difference between the adjacent pixels times the first IN threshold factor (~5). This avoids false positive identifications of IN in regions where the signal is changing significantly (such as in the slopes of the calibration pulse).

The “equal” case occurs when the difference between the two adjacent pixels is zero. IN is then identified if the comparison value is greater than the standard deviation of RN times the second IN threshold factor (~15). This avoids false positive identifications of IN in dark regions with very low detector noise.

The process flow:

4. The label mask.
5. For each block of mf's between saturated nodes, perform the following IN characterization steps only if the width is greater than the median filter window width.
6. Within each block of mf's, calculate the absolute difference between the output value and its median-filtered value, and calculate the absolute difference between the output values of bordering mf's.

7. If the bordering mf difference is:

- Greater than twice the standard deviation of RN, it is marked as case 1 and the comparison value is set to the bordering mf difference times the case 1 threshold value divided by two.
- Less than twice the standard deviation of RN, it is marked as case 2 and the comparison value is set to the standard deviation of RN times the case 2 threshold value.

8. Identify an occurrence of IN if the absolute difference between the output value and its median-filtered value exceeds the comparison value.

9. Store into an array a structure containing the data type, band name, detector number, scan number, mf number, and output values of the corrupted mf and its bordering frames.

10. Update the radiometric anomaly label mask to include the mf identified as corrupted by IN and output for ingest by downstream processes.

11. Repeat steps 4-10 until all detectors of a band have been processed.

12. Repeat steps 2-11 until all bands of the data set have been processed.

13. Output to the IAS Database the begin and end times of the data set since launch in units of seconds, and the structure array containing the data type, band names, detector numbers, scan numbers, mf numbers, output values of the corrupted mf's, and the output values of the bordering mf's.

14. Keep the above output vector as input for the algorithm for IN correction.

3.2.1.1.5 Evaluation

At ingest of this algorithm's output into the IAS Database, the database manager should insert the begin and end times into a structure that also contains a pointer to the appropriate IN characteristics vector stored in the database. The structure containing the pointer should be stored as an element of a vector of such structures, where each element contains the begin and end times of a processed data set (scene/swath) and contains a pointer to the IN characteristics vector for that data set. With the data stored this way in the database, a user can easily see the kind of coverage the data set has and can specify a time span for which the appropriate IN characteristic vectors can be extracted for analysis.

Because most IN occurrences flagged by this algorithm are expected to arise from flips of the four most significant bits, the first step in evaluating the algorithm output is to identify which bits flipped in each occurrence.

This identification analysis requires the output value of the corrupted mf and the output values of the bordering mf's. With these output values, the analyst obtains the bit flips that convert the output value of a border frame to the output value of the IN-corrupted frame. Then, given these two sets of bit flips and ignoring those flips that likely arise from RN and variation in signal, the analyst decides which bit flips caused the occurrence of IN.

After each IN occurrence is classified by bit flip, the analyst can determine as a function of time the occurrence rate of each bit flip class on each mf in a line. The analyst can determine if the spatial distribution of IN occurrences in a given detector is random or tends to occur in certain locations. What should be reported for each detector is the occurrence rates of IN in each bit flip class at each mf in a line, the total occurrence rate in each bit flip class, and any trends of these quantities.

3.2.1.1.6 References

None

3.2.2 CHARACTERIZE MEMORY EFFECT

3.2.2.1 Algorithm Description

3.2.2.1.1 Background

Memory Effect (ME) is an artifact that has plagued TM data from the beginning. It is manifested in a noise pattern commonly known as banding. It can be observed as alternating lighter and darker horizontal stripes that are 16 pixels wide in data that has not been geometrically corrected. These stripes are most intense near a significant change in brightness in the horizontal (along scan) direction, such as a cloud/water boundary. Because of this, it was formerly termed Bright “Target Saturation” or “Bright Target Recovery.” Another artifact known as “Scan Line Droop” was originally thought to be a separate phenomenon, but has since been shown to be simply another manifestation of ME. Because of its nature, ME has historically been the cause of significant error in calibration efforts because its effect on IC calibration data is scene-dependent. It is present in bands 1 through 4 of the PFP, and nearly absent in the CFP.

ME is caused by circuitry contained in the pre-amplifiers immediately following the detectors in the instrument electronics. It is primarily due to a portion of a feedback circuit that contains a resistor/capacitor combination with a time constant of approximately 10 ms. This directly corresponds to time constants of approximately 1100 mf’s that have been derived from night scenes. Therefore, ME has been modeled as a simple first order linear system and only three model parameters need to be identified to characterize it (actually one of the three is simply detector bias).

$$(1) \quad g(mf = b - k(1 - \exp(t \div \tau)))$$

Where

(mf) is the ME pulse response,
b is detector bias,
k is ME magnitude,
tau is the ME time constant.

Although the exact approach taken to characterize ME is dependent upon data type, response of the detector to some type of pulse is measured and averaged over many scan lines. Because the response will be exponential in form, the data are manipulated by subtracting out the appropriate bias level, linearized via the natural logarithm, and linearly regressed to determine the model parameters.

Characterization of ME can only be completed on the scenes in which the detectors are stimulated by a known input and allowed to respond without further stimulus. Thus, only FASC, PASC, and night scenes are used. Use of night scenes for characterization of ME on L4 and L5 has been done extensively. Because PASC and FASC data will not be available until after launch, validation of these algorithms will have to wait until then.

However, prelaunch integrating sphere data may provide some insights into the use of the FASC data. For night scenes, detector stimulus is the IC calibration pulse and detector response is recorded for the following mf's until the next pulse occurs. For PASC scenes, the detectors are stimulated over a portion of the scene by observation of the sun. Response is recorded until the next observation. The calibration lamp should be off during this period. For a FASC scene, the procedure is reversed. Detectors are observing the sun during a full scan, which allows them to reach a (quasi-) steady state condition. Following this, the detectors are stimulated by the calibration shutter for approximately 800 mf's. Response of the detectors is then observed until the following shutter interval. The IC lamps should be off during this period.

3.2.2.1.2 Inputs

- 0R Image and IC Data from Night Scenes
- 0R Image and IC PASC Data
- 0R Image and IC FASC Data
- IC Lamp State
- LM
- Detector Bias

3.2.2.1.3 Outputs

- ME magnitude for each detector
- ME time constant for each detector

3.2.2.1.4 Algorithm

Information contained in the LM is used to avoid including any pixels in ME parameter calculations that are corrupted by other noise or artifacts. For a given detector, if a scan includes pixels flagged by the LM, it will not be used. Although not stated explicitly, this policy will be followed in the algorithms described below.

NIGHT SCENES:

For night scenes, IC calibration pulses are used to characterize ME. Because this stimulus is short in duration, detector response over a significant number of scans must be averaged to obtain an adequate signal. Depending on how often the lamp is on, several contiguous scenes will be necessary.

1. For all scans subsequent to a calibration pulse, obtain data beginning at the trailing edge mf that is 10% of the net pulse height, and continue until reaching 100 mf before the 10% point of the rising edge of the next pulse.
2. Find the average of all data collected for each detector in a scan-by-scan fashion to obtain the detector response function, $g(\text{mf})$.
3. Find the minimum of $g(\text{mf})$ and remove from the data set all values obtained before the minimum occurred resulting in a truncated $g_1(\text{mf})$.

4. Average the last 1000 mf of $g_1(mf)$ to obtain detector bias b_0 .
5. Remove the bias from the response function: $g_2(mf) = b_0 - g_1(mf)$. (Rev 1/12/99)
5. Apply a 51-point boxcar noise filter to the bias subtracted data. (End Rev 1/12/99)
6. Truncate $g_2(mf)$ by removing all data values occurring after the first zero crossing to obtain $g_3(mf)$.
7. Linearize the data: $g_4(mf) = \ln [g_3(mf)]$
8. Fit a regression line to the data using a weighted least squares approach. The weighting function is $w(mf) = \exp(mf/\tau)$ in which τ is the ME time constant (obtained from ME Database). Regression coefficients are ME model parameters according to:

$$\begin{aligned} \text{slope} &= -1/\tau \\ \text{intercept} &= \ln(k) \end{aligned}$$

where k = ME magnitude parameter

The above steps are performed for each detector. The model parameters derived above are the system's calibration pulse response. It is necessary at this point to deconvolve the pulse and the pulse response to obtain the ME response to a unit pulse. This will be performed in an approximate manner because the calibration pulses are not rectangular.

- For all scans used in the above ME parameter estimation procedure, determine an average calibration pulse width and height: 1) Find the 10% point locations on the Net Pulse skirts. 2) Use these values to determine an average pulse width, T , by averaging all pulses for a given detector. 3) Integrate each pulse over the width, T , using a trapezoidal integration procedure to obtain P_{int} . 4) Average these values for all calibration pulses. 5) Find the average net pulse height (P) by dividing the integrated pulse height by the pulse width and subtracting out the bias. $P = (P_{int}/T) - b_0$. This procedure uses floating-point values similar to the pulse integration method described in the Process IC Reflective Bands algorithm (See Section 3.3.4).
- The ME unit pulse response magnitude, k_{ME} , is then obtained according to:

$$(2) \quad k_{ME} = -k / \{ P * [\exp(-T/\tau) - 1] \}.$$

ME parameters determined from night scene analysis are:

$k_{ME(N)}$ = k_{ME} ME unit pulse response magnitude, night scenes
 $b_0(N)$ = b_0 ME bias level, night scenes (should equal bias from Process IC algorithm)
 $\tau(N)$ = τ ME time constant, night scenes

Each of these parameters is stored in an ME parameters database along with the standard deviation of the estimate.

PASC SCENES:

Because these scenes will not be available until after launch, the algorithm described here is based on assumptions derived from limited engineering knowledge of how this system will work. Thus, it will be subject to significant review and possible modification immediately following launch and acquisition of PASC scene data.

The going-in assumptions here are that the PASC pulses are well behaved, repeatable, have steep skirts, and are relatively flat-topped. They will be modeled as square pulses, and a pulse response will be derived for ME. The pulses will be of unequal width, which will be taken into account in the form of an appropriate scaling factor so many scans can be averaged. This will allow better estimation of ME parameters and processing similar to that used with night scenes. Calibration lamps should be off when estimating ME parameters.

The following processing is performed on a per-detector basis. Pulse Processing:

1. For each scan, locate the PASC pulse by using a simple threshold detector, all Digital Number (DN) > 20 will be designated as PASC pulse (consistent with LM information).
2. Using a procedure similar to Process IC Reflective Bands, integrate over 50 mf in the center of each pulse to find a Pseudo-Average Pulse Height (PAPH). Use this information to locate the mf locations corresponding to 10% of the net pulse height (both the rising edge and trailing edge of the pulse).
3. Using information from the preceding step, determine the pulse width, T, as the distance, in mf, between the 10% points. Find the integrated pulse height, Pint, by integrating over the width of the pulse. Lastly, find the average pulse value, P = (Pint/T) - b0 (in which b0 is detector bias).
4. Determine the location of the pulse relative to the center of the image region. If the pulse is on the "left" (west) side of the image, use forward scans of that pulse to determine ME parameters. If the pulse is on the "right" (east) side of the image, use reverse scans. Determine, through a thresholding operation (DN < 10), that the following 3000 mf are suitable for ME parameter calculation (i.e., no corrupted pixels as indicated by the LM or presence of another PASC pulse).

Varying PASC pulse width will not affect the ME time constant. However, the magnitude of the pulse response is dependent upon the pulse width. Unfortunately, it is dependent in a non-linear fashion. It is necessary, therefore, to derive ME parameters in a more complicated process that first estimates ME time constant, uses this information to normalize for non-uniform pulse width, and then performs a second estimation of the ME magnitude and time constant.

ME Parameter Estimation

1. Using the regions of the PASC pulse that are greater than 50 mf in width, obtain data beginning at the trailing edge mf that is 10% of the net pulse height, and

continue until reaching 100 mf before the 10% point of the rising edge of the next pulse.

2. Average all data collected for each detector in a scan-by-scan fashion to obtain the detector response function, $g(mf)$.
3. Find the minimum of $g(mf)$ and remove from the data set all values obtained before the minimum occurred, resulting in a truncated $g1(mf)$.
4. Average the last 1000 mf of $g1(mf)$ to obtain detector bias $b0$.
5. Remove the bias from the response function: $g2(mf) = b0 - g1(mf)$.
6. Truncate $g2(mf)$ by removing all data values that occur after the first zero crossing to obtain $g3(mf)$.
7. Linearize the data: $g4(mf) = \ln[g3(mf)]$.
8. Fit a regression line to the data using a weighted least squares approach. The weighting function is $w(mf) = \exp(mf/\tau)$ in which τ is the ME time constant (obtained from ME Database). A first estimate of the ME time constant is obtained from the regression coefficients as slope = $-1/\tau$ int.

Knowledge of τ int is used to normalize the data obtained from PASC pulses that are not of maximum width.

1. Determine the maximum width of the PASC pulse, T_{max} , for each detector. For each scan obtained using a non-maximum width pulse, use the following relation to normalize the data obtained after the pulse.

$$(3) \quad fN(mf) = [b0 - f(mf)] * [1 - \exp(T_{max}/\tau \text{ int})] / [1 - \exp(T/\tau \text{ int})]$$

where

$fN(mf)$ are the normalized scan values

$f(mf)$ are the original scan values obtained after the PASC pulse

2. Use the normalized scan values, $fN(mf)$, to repeat the above steps describing the weighted regression procedure:
 - Average the scan
 - Truncate $fN(mf)$ to remove negative values
 - Linearize the data
 - Fit a weighted regression line to the data to obtain the ME parameter estimates
 - Slope = $-1/\tau$, intercept = $\ln(k)$ where k = ME magnitude parameter

3. The ME unit pulse response magnitude, kME , is then obtained according to:

$$(4) \quad kME = \{ -k \} / \{ P [\exp(-T_{max}/\tau) - 1] \}.$$

ME parameters determined from PASC scene analysis are:

$kME(P) = kME$ ME unit pulse response magnitude, PASC scenes

$b_0(P)$ = b_0 ME bias level, PASC scenes (should equal bias from Process IC algorithm)
 $ME(P)$ = ME Memory Effect time constant, PASC scenes

Each of these parameters is stored in an ME parameters database, along with the standard deviation of the estimate.

FASC SCENES:

These scenes provide a unique opportunity to characterize ME from the opposite direction. It is assumed that sun illumination will provide a constant radiance level that is only interrupted by the shutter. If the calibration lamps are off, a “negative” pulse is recorded by the detectors for approximately 800 mf. After this, the sun is once again in view. As long as the channels are not saturated, the detector response as the sun is again viewed should overshoot and settle back down to a constant value with a time constant of (F). This algorithm characterizes ME based on overshoot after a shutter (cal lamps off).

1. Determine the edges of the shutter region by finding fractional mf location of 90% points of net illumination skirts (DN_{sun} – Detector (Det) bias). Distance between these points is shutter width, T_s . “Average pulse” value is $P = DN_{sun} - \text{Det. bias}$. DN_{sun} is determined by averaging 1000 mf occurring 1100 mf to 100 mf before a shutter interval.
2. For all scans subsequent to a shutter interval, obtain data beginning at the mf that is 90% of the net pulse height, and continue until reaching 100 mf before the 90% point of the falling edge of the next pulse.
3. Average all data collected for each detector in a scan-by-scan fashion to obtain the detector response function, $g(mf)$.
4. Find the maximum of $g(mf)$ and remove from the data set all values obtained before the maximum occurred, resulting in a truncated $g_1(mf)$.
5. Average the last 1000 mf of $g_1(mf)$ to obtain average sun radiance, DN_{sun} .
6. Remove the bias from the response function: $g_2(mf) = g_1(mf) - DN_{sun}$.
7. Truncate $g_2(mf)$ by removing all data values that occur after the first zero crossing to obtain $g_3(mf)$.
8. Linearize the data: $g_4(mf) = \ln[g_3(mf)]$.
9. Fit a regression line to the data using a weighted least squares approach. The weighting function is $w(mf) = \exp(mf/\tau)$ in which τ is the ME time constant (obtained from ME Database). Regression coefficients are ME model parameters according to:

$$\begin{aligned} \text{slope} &= -1/\tau, \\ \text{intercept} &= \ln(k) \text{ where } k = \text{ME magnitude parameter.} \end{aligned}$$

The parameters listed above are the ME response to a “shutter region” pulse. This pulse input was again deconvolved to obtain an unit pulse ME response. The approach is similar to those used in the other algorithms.

The ME unit pulse response magnitude, k_{ME} , is then obtained according to:

$$(5) \quad k_{ME} = \{ -k \} / \{ P [\exp(-T/\tau) - 1] \}.$$

ME parameters determined from FASC scene analysis are:

$k_{ME}(F)$ = k_{ME} ME unit pulse response magnitude, FASC scenes

$b_0(F)$ = b_0 ME bias level, FASC scenes (should equal bias from Process IC algorithm)

$\tau(F)$ = τ ME time constant, FASC scenes.

Unfortunately, because the detectors are not in a zero-state condition for this analysis, the unit pulse response magnitude for the FASC case is actually a combination of the true unit pulse response magnitude multiplied by the true DN response of the detectors. Each of these parameters is stored in an ME parameters database, along with the standard deviation of the estimate.

ME PARAMETER DATABASE

ME parameters are estimated using three types of scenes: FASC, PASC, and night scenes. Each of these types of estimations is trended as a function of time. Due to the nature of the artifact, it is expected that the parameters will not change significantly over the life of the instrument. As a check on this, a regression analysis will be performed on a monthly interval for night-estimated parameters, quarterly on PASC-estimated parameters, and annually on FASC-estimated parameters. A standard hypothesis test will be performed to determine if the slope of the regression line is nonzero. If a nonzero slope is determined, a flag will be set.

Because three different methods of determining ME parameters are available, comparison of the estimates provides an important method of validating the algorithms. Hypothesis checks that test whether the estimates are the same should be conducted on a monthly basis. If estimates are determined to be different, a flag will be set.

Because multiple estimates of ME parameters are available, a method is needed to combine the estimates in an attempt to produce an overall result that is more accurate than any individual estimate. The approach taken here will follow the example set by the CRaM algorithm. Individual estimates will be weighted in a manner inversely proportional to the standard deviation of the estimate, and combined. All information available in the database will be used to form this estimate.

3.2.2.1.5 Evaluation

Evaluation of this algorithm can be performed at two levels. One is an internal consistency check, and the other is an external check based on the correct banding algorithm. L4 and L5 TM instruments have provided a heritage that allows a significant understanding of ME.

Within the algorithm, ME is determined using three different approaches. The approach using night scenes will have the poorest Signal-to-Noise Ratio (SNR) because calibration pulses provide input stimulus for only a short period. PASC scenes should provide significantly improved SNR and, for L7, should be acquired on a regular basis equal to that of night scenes. Consistency between these two estimation approaches will be the most regularly available evaluation of the algorithm. FASC scenes provide an estimation approach independent of the other two. Consistency of this method with the other two is a second means of the algorithm's internal evaluation.

Figures of merit for internal evaluation of the algorithm will consist of standard deviations of the individual estimates. Over time, the standard error of the combined estimates will provide another figure of merit.

Early in the life of the instrument, regular evaluation of ME parameters is necessary to ensure that the artifact is stable and parameters are not changing with time. Following this, regular inspection of ME parameters on a quarterly basis should occur to ensure that the artifact is behaving as expected and trending models are adequate.

External evaluation of the algorithm consists of using the Characterize Banding algorithm to assess the adequacy of the ME characterization and correction methods. PASC and FASC scenes are especially well suited for this task. These scenes should be processed by Characterize Banding both before and after ME correction. The difference image produced by Characterize Banding provides a visual inspection tool to assess algorithm performance, and the Characterize Banding figure of merit provides a quantitative means of assessment. If banding is not significantly reduced, this indicates either an inadequate model parameterization/estimation or inadequate correction.

3.2.2.1.6 References

J.L Barker. Characterization of Radiometric Calibration of Landsat 4 TM Reflective Bands. NASA Landsat 4 Scientific Characterization Early Results. Vol. 2. Pt. 1. 373-474. January 1985.

JL Barker. Relative Radiometric Calibration of Landsat TM Reflective Bands. Proceedings of the Landsat 4 Science Characterization Early Results Symposium, Greenbelt, MD. NASA Conference Publication 2355. Vol. 55. No. 3. Feb. 22-24, 1983.

D. Fischel. Validation of the Thematic Mapper Radiometric and Geometric Correction Algorithms. IEEE Transactions on Geoscience and Remote Sensing. Vol. GE-22, No. 3. p. 237-242. May 1984.

D. Helder. A Radiometric Calibration Archive for Landsat TM. SPIE AeroSense. 1996. SPIE Proc. Vol. 2758.

M.D. Metzler and W.A. Malila. Characterization and Comparison of Landsat 4 and Landsat 5 Thematic Mapper Data. Photogrammetric Engineering and Remote Sensing. Vol. 51, No. 9. p. 1315-1330.

D. Helder et al. A Technique for the Reduction of Banding in Landsat Thematic Mapper Images. Photogrammetric Engineering and Remote Sensing. Vol. 58. No. 10. p. 1425-1431.

D. Helder et al. "Short Tem Calibration of Landsat TM: Recent Findings and Suggested Techniques. IGARSS '96. May 27-31, 1996. Lincoln, Neb. 8. D.

Helder et al. An Adaptive Debanding Filter For Thematic Mapper Images in review for IEEE Transactions on Geoscience and Remote Sensing.

3.2.3 CHARACTERIZE SCAN-CORRELATED SHIFT (SCS).

3.2.3.1 Algorithm Description

3.2.3.1.1 Background

Scan-Related Shift (SCS) is a sudden change in bias that occurs simultaneously in all detectors. The bias level switches between two states. (It is assumed that L7 will behave like L5). Not all detectors are in phase; some are 180 degrees out of phase (i.e., when one detector changes from low to high, another may change from high to low). All detectors shift between two states that are constantly time varying, or slowly time varying on the order of days to months. Measurement of SCS levels is affected by another instrument artifact known as ME.

Characterization of SCS is performed at three levels. First, SCS states are obtained for each detector in each line of the scene. This must be completed on all scenes that require removal of SCS. Second, the value for the SCS levels is calculated for each detector. Third, the exact location of the transition from one SCS state to another within a scan line is determined (assuming that a continuous flow of data from the detectors is available).

The second and third levels of SCS characterization can only be performed on night scenes. Night data is largely unaltered by ME except for detector response to calibration pulses. Measurement of SCS level values will only be performed on portions of night scenes unaffected by calibration lamp pulses (i.e., when the lamps are off).

Standard data input to this process will be artifact-corrected night data used to calculate SCS Levels and SCS Transition Location. However, any scene may be input to determine SCS state as a function of scan line. Additionally, 1R data can be input to determine the effectiveness of the algorithm for determining SCS state and levels.

3.2.3.1.2 Inputs

For SCS state determination

- 0R IC Data
- SCS levels for reference detectors (from CPF)

For SCS value determinations (See Steps 2 and 3 below)

- Artifact Corrected 0R Imagery and IC (logically or physically combined)
- Labeled radiometric anomaly mask including SCS states

For Evaluation

- 1R Image Data and 1R IC Data (logically or physically combined)

3.2.3.1.3 Outputs

To Labeled Radiometric Anomaly Mask

- SCS state mask (per detector, per scan)

To Trending Database and reports

- SCS state mask (per detector, per scan)
- SCS levels (2) per detector (determined only from night scenes)
- SCS level differences and statistics (determined only from night scenes)
- SCS mask indicating transition location from start of scan, by scan, per detector (determined only from night scenes)
- SCS Fourier coefficients of scan state mask

3.2.3.1.4 Algorithm

1. Identify Bias Level Transitions and State

The purpose of this block is to identify whether each detector is in a high or low SCS state for each scan line. This process needs to be available for an arbitrary scene, so it will be performed using IC data. Three detectors that are most sensitive to SCS will be used as "flags" for the remainder of the detectors. A voting arrangement will be used to determine SCS state. For these three detectors, the dark current portion of the IC (approx. 550 mf's) will be averaged for each scan. Only the values that have not been flagged as "bad" by the LM will be used in the calculation. If it is determined that the SCS state is high, a "+1" will be recorded for that scan. If it is determined that the SCS state is low, a "-1" will be recorded.

The output from this block will be an array indicating SCS state for each scan of the instrument. A "+1" will be recorded for a scan in the high state, and a "-1" will be recorded for a scan in the low state. This data will also be stored in the SCS Trending Database.

Initialization: The initialization procedure for this block during IOC will determine which three detectors to use as flags and what their SCS levels are. (Alternatively, prelaunch information can be used to determine which detectors to use as reference detectors). During IOC, all scenes will be passed through this block to determine the average value for each detector on every scan. For each detector, this data will tend to be characterized as the sum of two Gaussian distributions. Histograms of the data will be fitted in that fashion to determine two means (m_1 and m_2) and standard deviations (actually $1 = 2$). The three detectors exhibiting the largest $(m_2 - m_1)/$ will be selected. The means, m_1 and m_2 , will be used for the SCS levels for the three detectors. When ten night scenes become available, this process will be repeated to validate the selection.

2. Measure SCS Level

The purpose of this activity is to identify the two SCS levels for each detector. Input for this process is the image data and the mask generated in the previous step, as well as the LM. Night data is used for this process because SCS level is affected by ME. To eliminate the effects of calibration lamps, only the image lines that correspond to zero calibration lamp states will be used. Furthermore, of those image lines, the first two after lamp state transition will not be used. Contiguous subintervals of night data are recommended. SCS levels are calculated by averaging entire scan lines of image data (assuming that SCS transition does not occur during normal image acquisition), along with the other scan lines in the same state. Only the data values that have not been flagged as "bad" by the LM will be used in this calculation. Standard errors of the estimates will also be calculated. A hypothesis test will be conducted to determine if the values calculated agree with the predicted values from the SCS Trending Database. If a statistical difference exists, a flag will be set.

SCS estimates from all scans will be stored in the SCS Trending Database, along with standard deviations of those estimates.

The output from this procedure will be SCS levels (2) for each detector, their magnitude (difference in SCS levels), and standard error.

Initialization: During prelaunch and IOC, the initialization procedure described in Step 1 can be used to obtain estimates of SCS levels for all detectors. When 10 night scenes become available, these estimates will be replaced with values obtained from the night scenes using this process.

3. Locate SCS Transition

The purpose of this process is to locate where the SCS transition occurs within a scan line. Use of this process assumes that either a continuous stream of data is available from the L7 detectors, or SCS transitions occur within image/IC data regions, and that the transition occurs abruptly. This process can only be performed on night data.

Using OR data, the SCS state changes will be determined by observation of SCS state scan mask obtained from Step 1. When a state change is identified, a search of the scan line will determine the exact mf where it occurred. This will be performed using a moving window filter of width 50 mf, with left half coefficients of "1" and right half coefficients of "-1," followed by a magnitude detector. Only the data values that have not been flagged as "bad" by the LM will be used in this calculation. MF location of SCS transitions will be performed for each detector.

SCS Transition Locations will be tracked in the SCS Trending Database. For single scenes, an average value and standard deviation will be calculated from

all scans, and stored. For data collected from contiguous scenes, SCS Transition Location will be recorded for each scan.

The output of this step will be an SCS mask indicating transition location from start of scan, for each scan line, for each detector.

Initialization: Not applicable because only night data can be used and verification of the phenomenon existence must occur.

4. Perform 1-D Fourier Analysis

The purpose of this process is to determine if any periodicities exist with SCS transitions. Using the SCS state scan mask generated from a contiguous subinterval, a time series obtained from this data will be subdivided into intervals roughly corresponding to one scene (28=256 scans is convenient). The Fourier transform of each interval will be obtained. These results will be averaged in the Fourier domain to isolate spectral peaks in the magnitude plots. Recommended number of intervals for averaging is 15. Visual evaluation may be necessary. NOTE: 0th term indicates relative amount of time spent in high or low state. The output of this analysis is the Fourier coefficients of SCS state mask.

Initialization: Not applicable. Values can be obtained whenever SCS state mask is available.

5. SCS Trending Database

The purpose of this block is to determine and validate the SCS levels for each detector using data from the current scene, as well as past SCS estimates. Values of SCS estimates obtained over time will be used to predict the current SCS value for each detector. Based on this comparison, the current estimate will be either accepted or rejected. If the current estimate is accepted, the SCS value for that detector will be updated and stored in the database (D1344 SCS Levels).

Time series analysis will be performed at two sampling intervals: a contiguous single orbit, and over the life of the instrument. This implies that whenever night data is available, SCS values will be calculated for each scan, as well as standard deviations of those estimates. A linear model will be fitted to data collected from a contiguous swath. Gain and intercept will be recorded in the data, along with standard errors of the estimates. These data will be used to ascertain whether any changes occur during this time. These values will be stored in the database for each detector. An exponential model will be used at least initially to fit the data over the life of the instrument. As knowledge of SCS over time improves, this model may be updated and/or simplified (i.e., replaced with a linear model). The outputs for this block are predicted SCS levels per detector.

6. Determine and Validate SCS Transition Locations

In a manner similar to Step 5, SCS transition locations will be validated via the SCS Trending Database time series analysis. NOTE: This will only be possible if the data stream from the detectors is recorded during the time that an SCS transition occurs. It is anticipated that a single orbit and lifetime time series will be generated in a manner similar to the above discussion. Because no precursor data is available to do this with L5 TM, this algorithm cannot be developed further until prelaunch L7 information is obtained. The outputs for this step are predicted SCS locations.

3.2.3.1.5 Evaluation

1. Evaluation of this algorithm will involve monitoring the various SCS parameters that are tracked in the databases. Because SCS has been observed historically as a very stable artifact, evaluation of SCS levels for sudden changes will provide an indicator of instrument performance and adequacy of the algorithm. It will also be important to watch long-term trends.
2. If data flow permits an estimate of when SCS changes state within a scan, it will be necessary to characterize that change of state in terms of stability and duration. In addition, the performance of the algorithm for determining that change will need to be monitored for adequacy and possible improvement, because it will not have been previously implemented or simulated due to lack of data.
3. Monitoring of the algorithm and its output should be frequent near the beginning of life. However, as confidence in the instrument increases with time on orbit, monitoring frequency can be reduced significantly.

3.2.3.1.6 References

J.L Barker. Characterization of Radiometric Calibration of Landsat 4 TM Reflective Bands. NASA Landsat 4 Scientific Characterization Early Results. Vol. 2. Pt. 1. p. 373-474. January 1985.

JL Barker. Relative Radiometric Calibration of Landsat TM Reflective Bands. Proceedings of the Landsat 4 Science Characterization Early Results Symposium, Greenbelt, MD. NASA Conference Publication 2355. Vol. 55. No. 3. Feb. 22-24, 1983.

D. Fischel. Validation of the Thematic Mapper Radiometric and Geometric Correction Algorithms. IEEE Transactions on Geoscience and Remote Sensing, Vol. GE-22. No. 3. p. 237-242. May 1984.

D. Helder. A Radiometric Calibration Archive for Landsat TM. SPIE AeroSense. 1996. SPIE Proc. Vol. 2758.

M.D. Metzler and W.A. Malila. Characterization and Comparison of Landsat 4 and Landsat 5 Thematic Mapper Data. Photogrammetric Engineering and Remote Sensing. Vol. 51. No. 9. p. 1315-1330.

D. Helder et al., A Technique for the Reduction of Banding in Landsat Thematic Mapper Images, Photogrammetric Engineering and Remote Sensing, Vol. 58, No. 10, pp. 1425-1431.

D. Helder et al. Short Term Calibration of Landsat TM: Recent Findings and Suggested Techniques. IGARSS '96. May 27-31. 1996. Lincoln, Neb.

3.2.4 CHARACTERIZE COHERENT NOISE

3.2.4.1 Algorithm Description

3.2.4.1.1 Background

CN manifests a rich variety of behavior in L4/L5 TM reflective band data. Consequently, it is difficult to characterize and correct. Some CN components are locked to the start of scan, but the more dominant components are not. The most persistent and dominant component is scan-free and has a varying frequency. Analysis of a swath of L5 TM night data showed the frequency of this component generally increased with time, with episodic and strong jumps occurring at lamp state transitions. In addition, there is a bursting broadband component that is also not locked to start of scan. The power of this component varies strongly even within a scan. Its amplitude can be as strong as 1 DN. In addition, its peak frequency varies widely over a range of 0.1 inverse mf's (imf). Consequently, this component is difficult to filter out. A common scan-locked component manifests as a spike every 16 mf's. Its amplitude may reach up to .1-.2 DN. Another scan-locked component appears in only a few detectors. It is quite strong in one detector, having amplitude of 0.6 DN. Interestingly, the power of this component varies significantly. Analysis of the swath of night data referred above reveals its power to decrease exponentially from an amplitude of 0.6 DN to an amplitude of 0.3 DN over a timescale of about one thousand scan cycles. Finally, the power of most, if not all, CN components and the Background Noise (BN) correlates positively with SCS state.

The set of parameters characterizing a CN component in a detector will be the phase (relative to a reference mf), the frequency, and the total power in the line in excess of that of the BN. These parameters will be obtained per scan. In order to obtain the total power in excess of the BN, the BN must be characterized itself. Thus, this algorithm will characterize the continuum of the power density spectrum before it identifies CN components. Analysis of the swath of night data showed a strong dependence of the continuum on detector and SCS state. It also showed a dependence on lamp state, but the effect is weak. Thus, this algorithm assumes that the continuum depends only on detector, scan direction, and SCS state.

Because most CN components appear in all detectors on a given focal plane, this algorithm groups the bands of detectors into band groups. Within each band group, it identifies the CN components; then obtains the total net power in each component at each scan for each detector in the group. Because the frequency of the component is equal for all detectors, and CN correction requires an extremely accurate value of the frequency, this algorithm derives the frequency of the component as a function of scan from the detector with the strongest signal at this frequency. Finally, given a precise frequency, the algorithm obtains the phase per scan per detector in the band group.

The parameters used to detect and characterize CN are contained in a CN control file in the IAS system.

3.2.4.1.2 Inputs

From the process flow:

- IC data of day scene or stitched IC and night scene data; radiometric anomaly label mask
- SCS state per scan

From the CN control file:

- The maximum frequency bin width for a one-sided power spectral density spectrum
- The maximum order of a linear combination of Legendre polynomials fitted to the continuum of a one-sided Power Spectral Density (PSD) spectrum
- The filter window width used in filtering the power spectrum to characterize the noise sub floor of the scene
- The minimum total net power in a CN component above which the component is considered significant
- The minimum uncertainty in the value of the frequency of a CN component

From the CPF:

- The mean, minimum, maximum, and standard deviation of the magnitude, frequency, and phase of the CN sources to be corrected

3.2.4.1.3 Outputs

The output of this algorithm will not only characterize the CN components in the data, but will also characterize the BN.

- The output characterizing the BN consists of the values of the coefficients to the Legendre polynomials in the fit of a linear combination of Legendre polynomials to the continuum of the average PSD spectrum of data in scans of a given scan direction and SCS state, and their one standard deviation uncertainties. A set of coefficients is produced for each scan group, detector, and spectral band.
- The output characterizing the CN components consists of the phase, the reference mf, the lower bound frequency, the peak frequency, the upper bound frequency, and the total net power per CN component, per scan, per detector, per spectral band.

This algorithm will divide the bands into groups. One group will consist of the pan band only, another of the reflective bands, and another of the thermal band. Within each band group, the algorithm will find the significant CN components. Output will be produced independently for each band group.

3.2.4.1.4 Algorithm

The algorithm processes the data a group of bands at a time. For L7, there will be three groups of bands: the pan band group, the reflective band group, and the thermal band group. Within each band group, the algorithm will identify the significant CN components, calculate the total net power per component per scan per detector per band, estimate precisely the frequency of each component at each scan, and then determine the phase of each component at each scan for each detector and band. When all of this analysis is complete, the algorithm then tests, for each CN component, whether the phase, frequency, or total net power is constant as a function of scan number. If it is, all values of the constant variable are replaced by the constant value. The algorithm writes as output the phase, the reference sample number, the lower frequency, the peak frequency, the upper frequency, and the total net power of each CN component at each scan for each detector and band. The following steps detail this algorithm.

1. The algorithm identifies the CN components. Before a CN component can be identified, a baseline of power density must be established from which one measures the excess power in a CN component. This baseline is the continuum of the PSD spectrum. It is assumed that the continuum depends on scan direction, SCS state, detector, and band only. Thus, for each band and detector, the algorithm groups the scans by scan direction and SCS state, and within each scan group, it creates the average one-sided PSD spectrum by application of the Fast Fourier Transform (FFT) to the flat signal segment of each scan in the scan group. The size of the FFT window is determined by the maximum frequency bin width provided by the CN control file and the length of the flat signal section of each scan. The power estimate at zero frequency is replaced by the relative error of the other power estimates. Points that are within one standard deviation of its neighbors are classified as power estimates of the continuum. The algorithm fits a linear combination of Legendre polynomials to the continuum points, obtaining the values and their one standard deviation uncertainties of the coefficients to the Legendre polynomials. These coefficient values and uncertainties are output as characteristics of the continuum for that given scan group, detector and band. The maximum order of the Legendre polynomials is a CN control file parameter.
2. Given the continuum as determined by the fit of linear combination of Legendre polynomials, the algorithm then identifies frequency bins in the average one-sided PSD spectrum in which the difference between the natural log of the power and the natural log of the power in the continuum exceeds five times the expected standard deviation of the power estimate. These bins are classified into groups of contiguous bins. A group of contiguous bins is kept as a CN component candidate if the total power in that group in excess of the continuum exceeds some minimum value provided by the CN control file. Each remaining group of contiguous bins are then examined for local maxima and minima in power density to determine if this group contains more than one CN component. If the difference between the natural log of the minimum and the minimum of the natural log of the neighboring maxima exceeds the uncertainty in these values by at least a factor of ten, each of the neighboring maxima represents the peaks of

separate CN components. After the groups of contiguous bins have been reduced to CN components, the CN component is kept as significant if the total power in excess of the continuum exceeds the minimum threshold value. The algorithm collects the lower frequency indices, peak frequency indices, upper frequency indices, total net power, detector and band of all CN components identified in the band group. It then reduces the number of components by identifying groups with the same peak frequency index and choosing from the group the component with the greatest strength.

3. After the algorithm has the CN components of a band group identified by their lower frequency bin index, peak frequency bin index, upper frequency bin index, and detector and band of strongest signal, it takes the lower and upper frequency bin indices and calculates the total net power in each component at each scan for each detector and band in the band group by applying the same FFT as above to obtain the average one-sided PSD spectrum.
4. The IAS provides two options for CN correction, subtraction method or filter method.

For filter method correction, first a normalized notch filter is constructed by generating a Gaussian signal with a peak at the CN component frequency and a width equal to the standard deviation of the CN component frequency. These values are from the CPF. A discrete Fourier transform is then applied to each scan line in the image, and the notch filter is multiplied with the real and imaginary components of the DFT. A reverse Fourier transform is then applied.

For subtraction method correction, the frequency, phase, and magnitude of the CN component must be known with sufficient precision. The CPF is read to obtain the nominal values and the maximum and minimum values of these parameters. The CN component is a candidate for subtraction method correction if the difference between the frequency maximum and minimum is less than 0.0000150 mf's per cycle, the difference between the phase maximum and minimum is less than 0.157, and the difference between the magnitude maximum and minimum is less than ten percent of the maximum magnitude. If the CN component is eligible for subtraction method correction, an inverse signal is created using the nominal frequency, phase, and magnitude, and this inverse signal is subtracted from each scan line.

Figure of Merit

3.2.4.1.5 Evaluation

The analyst will trend the power and frequency of each CN component with respect to previous data sets; then will trend these quantities within the present data set for those components in which these quantities were found to not be constant.

In addition, the analyst will trend the coefficients resulting from fits to the continua and will integrate the continua to obtain estimates of the variance in the RN; then compare these values to those obtained from the histogram analysis algorithm (See Section 3.2.10).

3.2.4.1.6 References

S.A. Teukolsky, W.T. Vetterling and B.P. Flannery . Numerical Recipes in FORTRAN.
W.H. Press.

3.2.5 CHARACTERIZE DROPPED LINES

3.2.5.1 Algorithm Description

3.2.5.1.1 Background

This algorithm describes automated Dropped Lines characterization. Any automated process may be supplemented by visual evaluation of scene data when dropped lines are known or suspected to exist.

Statistics on dropped lines (occurrence count, frequency) are to be kept by the LPS for all data transferred to the LPDAAC. The LPS also replaces corrupt mf's in both scene and cal data with a fixed byte pattern of 0s for odd detectors and 255 for even detectors. This procedure merely scans for the "dropped line" pattern, and logs location and extent of the dropped lines in the LM.

This process is to be completed first, BEFORE any additional characterization functions.

3.2.5.1.2 Inputs

- The "minf_filled" fields and "filled_scan_flag" for each line in the scene (or interval) being processed from MSCD
- 0R (Raw) Scene Data (byte, DN)
- 0R (Uncorrected) IC Data (the entire shutter interval) (byte, DN)

3.2.5.1.3 Outputs

- Locations of Dropped Lines for the Scene & IC Files under consideration, by line, starting mf and length. This contributes to the "Labeled Mask" used in the algorithm Characterize Detector Saturation (See Section 3.2.6) and other characterization algorithms.

3.2.5.1.4 Algorithm

Scan MSCD for "filled_scan_flag" to determine whether a scan has any fill data, on a scan-by-scan basis. For those scans with fill data, test mf's for the 0,255 fill pattern. Verify minf_filled count in the MSCD.

Log the line, detector channel starting mf, and extent of each dropped line in the LM. If discrepancies between the number of dropped mf filled per line are detected between LPS statistics and the IAS algorithm LM entries, generate a discrepancy report.

3.2.5.1.5 Evaluation

None

3.2.5.1.6

“Landsat 7 Processing System (LPS) Output Files Data Format Control Book.”
510-3FCD/0195. June 14, 1996 (TBR).

“Landsat 7 OR Distribution Product DFCB.” GSFC 430-11-06-007-0. Draft
7/2/96.

Email correspondence with Dennis Crehan. LPS systems engineering. Friday
Dec 8, 1995.

3.2.6 CHARACTERIZE DETECTOR SATURATION

3.2.6.1 Algorithm Description

3.2.6.1.1 Background

This algorithm flags pixels in image data that have saturated digital counts.

There are several types of saturation that may occur, including:

1. Normally observed saturation, in which the input signal exceeds the input radiance (a count of 254 at the Analog/Digital (A/D) output). The resulting high saturation output count of 255 has an unknown corresponding radiance, and using these data can lead to erroneous results. A similar situation occurs at 0 counts for low saturation levels, and therefore it is essential to flag pixels at both levels.
2. An A/D converter may saturate below 255 counts at the high end, or above 0 at the low end. This can be determined via histogram analysis, and once known, the pixel saturation level for a given detector (below 255 or above 0) can be flagged. This is done at the 0R level. This has not been observed to occur on previous TM instruments or in prelaunch ETM+ testing.
3. The analog electronic chain may saturate at a radiance corresponding to a level below 255 counts. Here, with the analog portion saturated, the upper end of the digital range may not be as sharp as it is for A/D converter saturation as "noise," and artifacts can toggle several bits. The characterization of this pixel saturation should occur at the 0Rc level of processing. This has not been observed to occur on previous TM instruments or in prelaunch ETM+ testing.

NOTE: This algorithm does not determine or update the saturation levels or DNs for the detectors; it simply flags pixels that meet previously defined criteria. These criteria come from either the defaults of 0 for low saturation, 255 for high saturation, prelaunch measurements, or on-orbit characterization using histogram analysis or other techniques.

3.2.6.1.2 Inputs

- 0R (byte, DN) or 0Rc (float, DN) IC data (the entire shutter interval)
- 0R (byte, DN) or 0Rc (float, DN) Scene data
- LM containing dropped line and IN locations
- Current High and Low saturation DN levels corresponding to analog saturation (by detector, by gain state, from CPF); (Byte, DN)
- Current High and Low saturation A/D DN levels (by detector, by gain state from CPF); (Byte, DN)

3.2.6.1.3 Outputs

- Locations of High and Low A/D saturated mf's (by detector, by band) from 0R data. Used to update "Labeled Mask"
- Locations of High and Low analog saturated mf's (by detector, by band) from 0Rc data. Used to update "Labeled Mask"
- Report relative number of saturated pixels per detector, per band (Real, unitless)

3.2.6.1.4 Algorithm

At the 0R level of processing:

1. Using input values of saturation DN's (normally 0s and 255s), flag each saturated pixel. Use a different flag for High and Low level saturation.
2. Count the number of pixels saturated by detector.
3. Calculate the average number of saturated pixels for a given band across detectors.
4. Calculate the relative number of saturated pixels by detector (relative to the band average). Ignore pixels flagged with IN or as dropped lines.

At the 0Rc level of processing:

1. Using an input value of saturation DN's, flag pixels at or above the saturation DN level.
2. Count the number of pixels saturated by detector.
3. Calculate the average number of saturated pixels for a given band across detectors.
4. Calculate the relative number of saturated pixels by detector (relative to the band avg.) Ignore pixels flagged with IN, as dropped lines, or as A/D saturated pixels.

3.2.6.1.5 Evaluation

None

3.2.6.1.6 References

None

3.2.7 CHARACTERIZE DETECTOR OPERABILITY

3.2.7.1 Algorithm Description

3.2.7.1.1 Background

This algorithm describes automated Detector Operability characterization. In addition to the obvious case of a "dead detector" (one that provides no change in output DN for changes in input radiance), the IAS must also have the ability to determine when a detector channel has fallen out of acceptable performance limits. A starting point for such a determination is a test to see if each detector meets the performance criteria established in the L7 System Specification (See). This specification provides a detector to be classified as degraded if its SNR or dynamic range is below the specification levels. Degraded detectors are generally useable by most algorithms until the degradation exceeds some level. This level is currently defined in the IAS Specification Document as a dynamic range that is less than 0.7 times specification, or greater than two times specification, or with a noise level that exceeds two times specification. Detectors below this level of performance are categorized as inoperable.

The algorithm consists of two parts that operate within the normal Level 1R data processing flow. The first piece takes the outputs of RN characterization to determine compliance with the instrument noise specifications. The second piece of the algorithm takes the output of the current gain selection and the currently indicated saturation bins, and assesses the dynamic range of the channels. If either portion of the algorithm indicates that a detector is out-of-spec or inoperable, a message is sent to the IAS operator or analyst to examine the results.

3.2.7.1.2 Inputs

- Noise Levels from Random Noise algorithm:
 - Dark noise levels (standard deviations) from normal Earth scene shutter data (Real, DN)
- Current gains from gain selection (Real, [DN/W/m²-sr-mm])
- Current biases from Perform IC (Real, DN)
- Current "Low_AD_Level" and "High_AD_Level" A/D saturation levels, in DN (by detector, by gain state), from CPF (Byte, DN)
- Current "Low Analog Level" and "High_Analog_Level" analog saturation levels (by detector, by gain state) from CPF

3.2.7.1.3 Outputs

For reporting/trending:

- Detector noise levels out-of-spec detectors
- Detector saturation radiances (high and low gain); out-of-spec detectors
- Flags to analyst when detectors are out-of-spec or inoperable

3.2.7.1.4 Algorithm

1. SNR out of limits:

The ETM+ system specification provides SNRs for two radiance (L) levels for high-gain mode. During normal Earth acquisitions, only the data taken when the shutter obscures the signal is uniform enough to use to assess the instrument noise. This uniformly dark data can be used to assess the noise at a zero radiance signal. This dark noise data can be used to assess approximate compliance to the specifications (i.e., if the dark noise level exceeds the noise levels for the illuminated scenes, the system is definitely out of specification). The dark noise level (Root-Mean-Square (RMS) in DN) as computed in the Random Noise algorithm from the shutter data is compared to the specified reference noise levels (noise-equivalent radiances) at the high and low signals. The noise equivalent radiances are only given for the reflective bands in the L7 specification for the low signals. The noise equivalent radiances for the high signal for the reflective bands are calculated by dividing the reference signal levels by the specified SNR at that signal level (see Table 3-2, in which an additional column has been added to provide the high signal reference noise levels). Also, note that the L7 specification is in units of mW/ cm² sr mm and the IAS uses W/m² sr mm). For the thermal band, band 6, noise is specified in terms of NEDT as <0.5 K at 300 K and <0.42 K at 320 K. These temperature noise values convert to noise-equivalent radiances of < 0.0066 mW/ cm² sr mm at 300K and < 0.0064 mW/ cm² sr mm at 320 K.

Spectral Band	Input Spectral Radiance (mW/cm ² -sr-μm)	SNR	Reference Noise Level (mW/cm ² -sr-μm)
PAN	2.29	15	0.153
1	4.00	31	0.129
2	3.00	33	0.091
3	2.17	25	0.087
4	1.36	28	0.049
5	0.40	24	0.017
7	0.17	18	0.009

Table 3-1. ETM+ SNR Requirements (Low Signal)

Spectral Band	Input Spectral Radiance (mW/cm ² -sr-μm)	SNR	Reference Noise Level (mW/cm ² -sr-μm)*
PAN	15.63	88	0.178
1	19.00	103	0.184
2	19.37	137	0.141
3	14.96	115	0.130
4	14.96	194	0.077
5	3.15	134	0.024
7	1.11	96	0.012
* This column was not in the original table from the L7 system specification			

Table 3-2. ETM+ SNR Requirements (High Signal)

The RMS dark noise levels in DN are converted to equivalent radiances by dividing the current gain value used for processing the scene being evaluated. If the noise levels exceed the specified noise levels, the detector is flagged as noisy:

- 0 - in specification
- 1 - noisy low signal
- 2 - noisy high signal
- 3 - noisy both signals
- 4 - inoperable due to noise (noise more than twice the specification value)

2. Detector Saturation Radiances:

- a. Use the smaller of the “High_AD_Level” and the “High_Analog_Level” for the High Saturation Signal (QSATH) and the higher of the “Low_AD_Level” and the “Low_Analog_Level” for the Low Saturation Signal (QSATL).
- b. Convert QSATH and QSATL (in DN) to saturation radiances, High Saturation Radiance (LSATH) and Low Saturation Radiance (LSATL) (in

W/(m² sr mm)) for each detector using current gain (G) and current bias (B) values (i.e., $LSATH=(QSATH-B)/G$ and $LSATL = (QSATL-B)/G$).

- c. Compare these calculated values against appropriate Low Gain or High Gain values in 7 System Spec, Table 3-3, to determine if detector response exceeds specification for "Minimum Saturation Spectral Radiance". NOTE: The "High end" spec. is not met if the detector has less than the specified minimum saturation level; the "Low-end" spec is not met if the detector has greater than the specified saturation level. The low-end saturation radiances are effectively "0" for all bands except band 6. This is to say that the system needs to record signals down to its noise level, which may result in "negative" values. For band 6, the low-end saturation radiances are 200K (0.110 mW/cm² -sr -mm) for low gain and 260K (0.483 mW/cm²- sr -mm) for high gain.
- d. Calculate $LSATH-LSATL$ and compare to specification values [$LSATL$ should be set to "0" for this calculation if $LSATL$ is less than "0"]. If this difference is less than 0.7 times or greater than 2 times the difference between the low-end and high-end saturation radiance specifications, the detector is inoperable due to dynamic range.
- e. Categorizations will be:

0 - in specification

- 1 - fail high-end saturation radiance
- 2 - fail low-end saturation radiance
- 3 - fail both ends saturation radiances
- 4 - inoperable due to dynamic range

Spectral Band	Minimum Saturation Spectral Radiance [High end] (mW/cm ² -sr-μm)	
	Low Gain	High Gain
PAN	23.50	15.63
1	28.57	19.00
2	29.13	19.37
3	22.50	14.96
4	22.50	14.96
5	4.73	3.15
6(1)	[1.568] 340K	[1.232] 320K
7	1.67	1.11
(1) Specification was in terms of brightness temperature converted to radiance here.		

Table 3-3. L7 System Spec

3.2.7.1.5 Evaluation

None

3.2.7.1.6 References

GSFC/NASA. Landsat 7 System Spec. Tables 3-20, 3-21. Rev K. March 1998.

3.2.8 CHARACTERIZE MODULATION TRANSFER FUNCTION (MTF)

3.2.8.1 Algorithm Description

3.2.8.1.1 Background

The algorithm described here characterizes the blurring function of a system from an image of a target containing a sharp "knife-edge" (or discontinuous) transition from a dark field to a bright field. All imaging systems, including the L7 instruments, cause a blurring of the scene radiance field during image acquisition. This blurring is attributable to optical diffraction, focal-plane integration by the detectors, analog signal processing, and other physical processes. In most well-designed imaging systems, this process is accurately modeled as a linear, shift-invariant process that can be characterized by the system's impulse response or transfer function. In imaging systems, the impulse response is called the PSF and the transfer function is called the optical transfer function (OTF). The magnitude of the OTF is called the modulation transfer function (MTF). The Line spread Function (LSF) describes the system's response in one dimension (i.e., the response perpendicular to direction of a line in the scene). The transform of the LSF is a one-dimensional slice of the OTF.

Proper interpretation of pixel values in images requires an accurate characterization of the blurring introduced during image acquisition. This is particularly true in spatial regions with relatively non-uniform "brightness" because spatial blurring will push the measured values in such regions closer to one another and away from the true values. Restoration processing compensates and corrects for systemic degradations to yield greater radiometric accuracy. Restoration algorithms are premised on a model of the imaging system (and its degradations). Such models require characterizations of the system performance, such as MTF.

The L7 prelaunch testing includes measuring the optical system MTF for bands 1 - 5, 7, and Pan [SBRC TP32015-522] to demonstrate compliance with the system specification. The system specification contains a minimum response at 0.50, 0.67, and 1.00 the Nyquist frequency. The prelaunch test is conducted under thermal vacuum conditions.

The algorithm described here is intended to be compared to the prelaunch test results and to monitor long-term performance. It is based on an approach described by Reichenbach et al.[REICH91]. The method is based on the traditional knife-edge technique, but explicitly deals with fundamental sampled system considerations: aliasing, sample/scene phase shifts, and asymmetrical system functions. Subpixel registration of the knife-edge scan lines achieves subpixel resolution sufficient to sufficiently sample the system and eliminate the effects of aliasing. Line averaging removes variability associated with sample/scene phase-shift and increases the effective SNR. The technique can be applied to assess system symmetry or separability or to generate a two-dimensional estimate.

3.2.8.1.2 Inputs

- A rectangular subimage with appropriate target, extracted from a Level 1R image with post-1R corrections.

The algorithm requires a two-dimensional subimage of a target containing a sharp "knife-edge" (or discontinuous) transition from a dark field to a bright field. Ideally, the dark and bright fields should have uniform brightness and the transition between the fields should be sharp (i.e., blurred only by the system).

The input subimage is extracted (from a Level 1R image with post-1R corrections) using general image processing utilities not described in this document. Specifically, the system must provide a utility to examine pixel values on an individual basis, along user-designated lines, or in user-designated regions and to extract one or more subimages (in or convertible to a format that the MTF characterization software can use). Both text and graphical presentations of the pixel values should be available so the user can easily identify an appropriate subimage. A graphical point-and-click interface should be available both for examining pixel values and for specifying the subimage extent. In order to provide band-specific, detector-specific, and scan-direction-specific MTF estimates, there should be utilities for extracting a subimage specific to a band, detector, and/or scan direction. Finally, the prototype software included with this Algorithm Theoretical Basis Document (ATBD) operates only on images with a nearly vertical edge. Images with edges at other orientations must be preprocessed with other software to rotate the image.

3.2.8.1.3 Outputs

- A sequence of values at uniformly spaced points estimating the LSF across the edge. The DFT of the LSF gives a one-dimensional slice of the OTF (or MTF).

3.2.8.1.4 Algorithm

In the approach described here, the knife-edge scan lines are aligned to subpixel accuracy to achieve subpixel resolution (resolution greater than the sampling rate). This technique alleviates the problems caused by undersampling. In order to achieve resolution, the knife-edge must be aligned slightly sloped relative to perpendicular. Tescher and Andrews characterized this unavoidable shift as unfortunate, but here it is the key to increasing the effective sampling rate and averaging sample/scene phase. In an image with the knife-edge slightly askew, the edge shifts slightly relative to the samples from scan line to scan line. If the scan lines are first registered (so the edge-points in each scan line are aligned) and then combined, the result contains many more sample points along the edge response than any single scan line. Although the averaging process used to compute the subsampled edge scan reduces noise, noise will remain a problem when a small number of scan lines are used. The algorithm employs some additional techniques to reduce the effect of noise.

The algorithm proceeds as follows.

1. Build a single high-resolution edge scan from the many scan lines in the image.

- a. Obtain an initial estimate for the edge location and direction (up or down in brightness) in each successive scan line by finding the points of maximum and minimum difference between neighboring pixels. For example, assume the last scan line in an image contains the following values:

37 42 40 40 37 49 61 69 75 106 178 225 229 235 235 222

The maximum change is at the 10th pixel (numbering from 0) where the brightness jumps up from 106 to 178 on the left and from 178 to 225 on the right.

- b. Estimate the mean brightness value on each side of the edge in each scan line. Do not include pixels in a buffer zone around the edge. The size of the buffer is an operational parameter. In the scan line above, accepting a buffer of 2 pixels at the edge in each computation, the average on the left is 50 and the average on the right is 230.25.
- c. Normalize each scan line so the average on the left (excluding the buffer) is 0 and the average on the right is 1. For the example above, the scan line is normalized by subtracting 50 from each brightness value and dividing by $230.5 - 50 = 180.5$.
- d. Fit a curve through the brightness values of each individual scan line and determine where the brightness curve crosses the midpoint between the brightness mean on the left (which, after normalization, is 0) and the brightness mean on the right (now 1). This second and final estimate of the edge location is more accurate than the initial estimate. Using piecewise cubic interpolation, in the example above, the brightness curve crosses the midpoint of the normalized scan line (0.5) at coordinate 9.50238.
- e. Register the many scan lines and, for each desired subinterval, average the values. For the example above, if we desire subintervals of 1/2 the original sampling interval, the scan line given above (registered by shifting -9.50238 pixels) would contribute values to the averages in the subintervals -10.0 to -9.5, -9.0 to -8.5, -8.0 to -7.5, . . . , and 5.0 to 5.5. Fill in the average in any empty subintervals on the left with 0.0 and on the right with 1.0 (or opposite for a step down). As the subinterval averages compute, calculate the mean-square difference between the averages and 0.0 on the left and 1.0 on the right (or opposite for a step down). This is an estimate of the residual noise variance. In the first of the example images, the high-resolution edge scan created in this way process is:

0.000 -0.068 -0.079 -0.047 -0.030 -0.034 0.008 -0.025 0.011 0.001
0.016 0.017 0.014 0.002 -0.018 -0.003 0.054 0.120 0.063 0.184
0.471 0.816 0.921 0.944 1.008 1.002 1.019 1.019 1.015 1.017
0.998 1.007 0.977 0.989 0.934 1.009 1.000 1.017 1.000 1.000

Note that the interval between these values is 1/2 the original sampling interval. The edge location is at the center of the scan (with value 0.471). The estimated residual noise variance is 0.000898. The root-mean-square (RMS) SNR is only about 30 even after averaging.

2. Apply optional smoothing to the high-resolution edge scan. Values close to the edge (within the defined buffer region) are not changed. Values far from the edge are set to the "background" value (either 0 or 1) under the assumption that the LSF has a limited effective extent and therefore noise is dominant in points distant from the edge. The size of the transition region between the buffer and the smoothed region is an operation parameter. Moving from the edge of the buffer region through the transition region, smoothing is increased linearly. After smoothing with a 2-pixel transition region, the example high-resolution edge scan is:

0.000 0.000 0.000 0.000 -0.009 -0.002 0.054 0.120 0.063 0.184
 0.471 0.816 0.921 0.944 1.008 1.001 1.009 1.004 1.000 1.000

3. Invert the equation defining the high-resolution scan line. The inverse filter described in [REICH91] is herein replaced by the least-squares optimal estimator (i.e., the Wiener filter). The system model for the high-resolution edge scan (in the frequency domain) is:

$$R(u) = S(u) H(u) \text{sinc}(u/r) + E(u)$$

where u is the spatial frequency, R is the transform of the high-resolution edge scan, S is transform the step-edge scene, H is the system transfer function, the sinc function accounts for averaging over each of r subintervals per pixel, and E is the transform of the residual noise. This algorithm uses the standard Wiener approach to estimate $H(u)$ and assumes white noise. In this example, we have (at the center of the response):

0.262 -0.174 0.385 -0.385 0.163 0.419 3.297 -0.686 -0.184 6.810
 10.603 7.992 -0.209 2.345 0.636 -0.069 0.261 -0.224 0.048 0.063

The MTF slice corresponding to this LSF is:

1.000 0.892 0.764 0.611 0.495 0.468 0.495 0.513 0.465 0.361 0.209 0.066

3.2.8.1.5 Evaluation

The system utilities should provide the capacity to display the LSF, OTF, and MTF estimates on a graph, to compare (both arithmetically and visually) estimates with other estimates and with the system specification and prelaunch measures, and to examine time sequences of the estimates. The system should maintain an archive of past estimates, including a specification of the source image and creation process of the

subimage used in the estimate. The system should also provide for the recall of the system specification and prelaunch measures.

3.2.8.1.6 References

[REICH91] S E Reichenbach, S K Park, and R Narayanan. Characterizing Digital Image Acquisition Devices. Optical Engineering. 30(2):170-177. 1991.

[SBRC TP32015-522] Santa Barbara Research Center, ETM+ System Modulation Transfer Functions of Bands: Pan, 1-5 & 7. Test Procedure for ETM+ Test BL16, 1992.

3.2.9 CHARACTERIZE RANDOM NOISE

3.2.9.1 Algorithm Description

3.2.9.1.1 Background

This function characterizes the noise level of the ETM+ instrument and ETM+ data products. It specifically attempts to measure the random component of the noise by operating on data that have been corrected for radiometric artifacts (e.g., CN, scan correlated shifts and ME). This function is also applied to data without the corrections, and as such, it can be considered to give a measure of "total" noise. Applying this function before and after the corrections also measures the effectiveness of the corrections. In order to provide a measure of system or instrument noise, this function must operate on "images" where the scene content is essentially zero. Examples of such imagery are the IC shutter region, night scenes in the reflective bands, FASC scenes (e.g., some ocean, snow or desert scenes). This function evaluates noise per detector. Calculations are performed on a per scan basis.

3.2.9.1.2 Inputs

- IC Data
 - Raw (0R)
 - Artifact corrected (0Rc)
- Scene Data
- FASC scenes (0R, 0RC, 1R)
 - Night scenes (0R, 0Rc)
 - Other scenes (e.g., Ocean, Desert, Snow)

3.2.9.1.3 Outputs from other functions

- IN Mask - identifies noise-contaminated pixels
- Dropped Line Mask - identifies dropped lines
- Saturated Pixel Mask - identifies high and low saturated pixels (normally 0 and 255)
- Reflective band bias - from perform IC calibration for FASC data
- Parameters for scene data
 - Number of scans to process
 - Number of scans to overlap
 - Starting pixel number

3.2.9.1.4 Output

For Trending:

IC Data, Night and other data (only per scene values trended)

- Scene mean and standard deviation per detector, per section, per scan direction
- Scene bias corrected mean per detector, per section, per scan direction
- Average per scan mean and standard deviation, per detector, per section, per scan direction
- Scene SNR per detector, per section, per scan direction

FASC Data (per scan values trended):

- Mean and standard deviation per scan, per detector, per section, per scan direction
- Bias corrected mean per scan, per detector, per section, per scan direction
- SNR per scan, per detector, per section, per scan direction

For Reports:

- Scene mean and standard deviation per detector, per section, per scan direction (except for FASC data)
- Tests of equivalence of means and standard deviations between sections per scan direction
- Average per scan mean and standard deviation per section
- Tests of randomness of per scan means and standard deviations per scan direction (except FASC data)
- Correlation (r), Coefficient of Determination (r^2) and test of significance of regression of per scan means between detectors within a band per scan direction (except FASC data)
- Selected plots of per scan means, per scan standard deviations, histograms, and FFTs, for forward, reverse and all scans

Parameters to Track:

- Gain state
- Time
- Lamp state
- Time since on
- Temperatures (IC, Focal Planes)

3.2.9.1.5 Algorithm

The basic algorithm is a calculation of sample means and standard deviations. The primary considerations are the samples from which they are determined.

Predecessor Functions

Always performed:

- Characterize Dropped Lines
- Characterize IN
- Characterize Detector Saturation

To be performed for ORc:

- Characterize SCS
- Characterize CN
- Correct Scan-Related Shifts
- Correct CN
- Correct ME

To be performed for FASC data:

- Perform IC Calibration

For all IC data, FASC scenes, and night scenes:

1. Check the PCD for within-scene changes in lamp state or gain state. If the lamp state or gain state changes, generate results for different states separately. Extract scene acquisition time and all temperatures from the PCD.
2. Extract usable RN region. For IC data, the region is defined by the bias location parameters in the CPF. For FASC data, the center pixel region is defined within the code. For night scenes (and other image data), the region is defined by the Scan Line Offsets in the CPF. Divide each window into three sections; left, right and center.
3. Calculate sample mean and standard deviation per scan line, per section for forward scans, reverse scans and all scans. Disregard dropped lines, IN and saturated pixels from calculations.
4. Test regions for equivalence of means (via T-test) and variances (via F-test) to check for residual ME.
5. Evaluate randomness of per scan standard deviations and means. Correlate/regress per scan means between detectors within a band (to assess residual SCS). Test significance of regressions.
6. Calculate the average of the per scan standard deviations per section (this is an attempt to exclude line-to-line variations, e.g., scan correlated shifts from one of the noise measures).
7. Calculate FFTs of full scan line per scan and compute average magnitude of the FFT per detector for the scene (to check for CN).
8. Calculate bias-corrected scene mean by subtracting the per scan bias (from IC processing) from per scan per section mean (except band 6).
9. Calculate SNR (excluding band 6) per scan, per section, per scan direction.

3.2.9.1.6 Evaluation of Random Noise

This function performs the trending and comparison of the noise to instrument specifications. Evaluations are to be performed periodically (e.g., after each FASC scene processed and each night scene processed).

3.2.9.1.7 Inputs

- Table of ETM+ SNR/Noise Equivalent Detector Radiance (NEDL) specifications
- Output of Characterize RN
- Gain History from CRaM

3.2.9.1.8 Outputs

- Plots of "dark" noise from IC and night data, as a function of time and temperature
- Converted FASC radiances based on CRaM parameters
- Plot of NEDL vs. L
- Flags for degraded or inoperable detectors

3.2.9.1.9 Algorithm

1. Plot dark noise, scene averages, and average line-by-line values from IC as a function of time, temperature (After Direct Current (DC) Restore (ADC), Before DC Restore (BDC), DC, forward, reverse, all scans), by detector. User-selectable parameters include time interval (e.g., since launch, one subinterval). Perform fitting/moving window averages.
2. Plot dark noise, scene averages and average line-by-line values from night scenes as a function of time and temperature (forward, reverse, all) by detector. User-selectable parameters include time interval (e.g., since launch, one subinterval) and gain state. Perform fitting/moving window averages.
3. Convert FASC means and standard deviations to radiance, L based on current CRaM parameters. $L = (\text{mean} - \text{bias}) / \text{gain}$; $\text{NEDL} = \text{stdev} / \text{gain}$.
4. Plot/parameterize NEDL versus L, and SNR (except band 6) versus L. Plot one or both versus time, for fixed L (e.g., spec values).
5. Flag detectors that are below SNR or NEDL (band 6) specifications.
6. Flag detectors that are < 0.5 out-of-specification and update detector operability matrix.
7. Generate a table of current noise estimates for "weighting" various operations (e.g., parameterized noise level, in counts, as function of signal level, in counts).
8. Generate a report that includes the results.

3.2.9.1.10 References

None

3.2.10 HISTOGRAM ANALYSIS

3.2.10.1 Algorithm Description

3.2.10.1.1 Background

This function estimates the relative gains and biases of detectors by characterizing the behavior of individual detectors in a band relative to the other detectors in a band, based on scene content. Individual detector histograms are generated for forward scans, reverse scans, and all scans. Lines dropped by one detector and IN mf's in one detector are excluded from all the detectors in that band. The number of saturated pixels (0s or 255s) for each detector is tabulated based on masks generated in the Characterize Detector Saturation function (See Section 3.2.6). The detector with the maximum number of saturated pixels in the band is identified; for all other detectors in the band, the same number of the brightest or darkest pixels is excluded to provide an equal number of pixels per detector. The means and standard deviations are calculated for each detector from the adjusted histograms, The band average mean and band average standard deviations are calculated excluding any "dead", "degraded", and "inoperable" detectors. Relative detector-to-detector gains are calculated by two methods; the first determines ratios of the detector means, after subtracting the IC based biases, to the band average mean and a reference detector mean; and the second determines ratios of the standard deviations of the detectors to a band average (weighted or unweighted by detector noise levels) standard deviation and a reference detector standard deviation. Bias differences are estimated from a combination of the ratios of the standard deviations and the mean differences. Filters based on the scene standard deviations relative to the detector noise levels, and the overall number of excluded pixels, may be used to remove poor scene data from these calculations. This function is performed on all day scenes and night band 6 scenes processed by IAS . This function is applied at the 0Rc level of processing to characterize the inherent striping of the detectors. At the 1R level of processing, this function characterizes the residual striping, and the output could be used to remove residual striping if required. A reduced version of the histogram analysis is applied to scenes at the 0R level to determine the count at which the detectors saturate.

3.2.10.1.2 Inputs

- IC-based bias from Perform IC, for particular scene/interval on line-by-line basis
- Scene Data - Normal Earth scenes (0R (to characterize saturation levels), 0Rc, 1R)
- Masks from "Characterize Detector Saturation," "Dropped Lines" and "IN" functions
- Dead/degraded detector information (from CPF)
- Detector noise levels (from CPF)

Parameters to be set (from CPF):

- Number of scans in window used for calculation
- Number of scans to overlap between windows
- Starting pixel for calculation
- Number of pixels for each calculation
- Reference detector
- Saturation bin threshold
- Adjacent bin threshold
- Number of adjacent bin to test

3.2.10.1.3 Outputs

For Trending (also as input to correct striping if used):

- Gain ratios to reference detector and average of detectors, per detector, per scan direction
 - Based on ratios of standard deviations
 - Based on ratios of bias-corrected means
- Bias offsets from reference detector and average detector
- Number of pixels, including total used per detector, and number excluded on high end and low end
- Reference detector and average detector mean and standard deviations by band
- Gain ratios (based on standard deviations and means) for forward to reverse scans
- Saturation bins (at 0Rc and 0R)
- Magnitudes above background of FFT at striping-related frequencies

For Reporting:

- Raw histograms by detector and band
- Scene means and standard deviations, both weighted and unweighted by detector noise
- Means and standard deviations by detector (before bias correction), for all scans, forward scans and reverse scans
- Means and standard deviations by detector (after bias correction), for all scans, forward scans and reverse scans
- Number of high and low brightness pixels excluded per detector
- Number of pixels used in calculations per detector
- Computed gain ratios per detector; four sets per window (reference and average, based on mean and standard deviation)
- Computed relative biases per detector; two sets per window (reference and average)
- Differences of gains calculated between mean method and standard deviation method
- Differences in relative bias between forward and reverse scans
- Ratios of relative gains between forward and reverse scans (based on standard deviations and means)

- Saturation bins (at 0Rc and 0R)
- Temperatures

Parameters to track:

- Temperatures (IC, focal planes)
- Gain state (scene broken into two segments if gain change occurs)
- Time
- Lamp state
- Time since on
- Scan direction

3.2.10.1.4 Algorithm

The basic algorithm is simply a calculation of means and standard deviations (sample), much like the Characterize Random Noise function (See Section 3.2.9). While the Characterize Random Noise function runs on scenes with little or no signal (night scenes), this function requires scenes with variability in signal (day scenes), trusting that the mean of the scene over all the detectors is the same. This function attempts to estimate gain and bias differences as opposed to noise differences. As such, scenes are required that have some signal.

Predecessor Functions

- Always performed
- Characterize Dropped Lines
- Characterize IN

To be performed at 0Rc:

- Characterize Detector Saturation
- Characterize Scan-Correlated Shifts (SCS)
- Characterize CN
- Correct SCS
- Correct CN
- Correct ME
- Perform IC calibration

For normal Earth scenes (including all day scenes, night band 6 data and FASC data) at the 0Rc and 1R levels:

1. Generate histograms for each scan direction, for each detector, for each band, for the pixels within a window length (i.e., number of scan lines) and width (i.e., number of pixels). Window size can be less than a scene up to three scenes. Exclude IN pixels and dropped lines from all detectors in the band (i.e., if data from one detector are dropped, data for all the detectors in the same scan and

pixel number shall be excluded). Perform for all scans, and forward and reverse scans, separately. Also, generate a full scene histogram by band. For data in float format, one bin is 1/10 a DN.

2. For 0R and 0Rc data only, examine the histogram to assess/determine if saturation is occurring below 255 DN or above 0 DN. Start at 255 and count down until the first bin with greater than or equal to 1000 pixels is reached. Count pixels in next higher ~two bins. If both bins have less than or equal to 10 pixels (0 for 0R data), the bin with > 1000 pixels is the saturation bin. Repeat, starting from the low end of the histogram.
3. Tabulate the number of saturated pixels for each detector based on masks generated in the Characterize Detector Saturation function (See Section 3.2.6). Identify the detector with the maximum number of saturated pixels in the band.
4. For all other detectors in the band, exclude from the histograms the same number of brightest and darkest pixels to provide an equal number of pixels per detector.
5. Calculate the mean (m_i) and standard deviation (s_i) of each detector within the window, based on the adjusted histograms. For 0R data, this is considered the gross mean and gross standard deviation because the IC bias has not been removed. For 1R data, the bias was subtracted during image processing so this is the bias-corrected mean and standard deviation.
6. For 0Rc data only, subtract the IC bias from the Perform IC Calibration function and recalculate means and standard deviations by detector. This is considered the bias-corrected mean and standard deviation.
7. Calculate the ratios of the bias-corrected mean values per detector to the band average detector, and then to the reference detector. These are relative gain measures.

$$(1) \quad g_{rel} = \frac{m_i}{\bar{m}}$$

$$(2) \quad g_{rel} = \frac{m_i}{m_{ref}}$$

where ref indicates the mean of the reference detector and \bar{m} indicates the band average histogram mean.

8. Calculate the ratios of the standard deviation per detector to a band average standard deviation and a reference detector standard deviation. For level 0Rc, use the gross standard deviation. These ratios provide a second measure of relative detector-to-detector gains.

$$(3) \quad g_{rel} = \frac{s_i}{\bar{s}}$$

$$(4) \quad g_{rel} = \frac{s_i}{s_{ref}}$$

Where ref indicates the mean of the reference detector and \bar{s} indicates the band average histogram standard deviation.

9. Calculate the relative bias for detector (i) based on the means and standard deviations. For ORc data, use the gross mean and gross standard deviation.

$$(5) \quad b_{rel} = \bar{m} - \bar{s} \frac{m_i}{s_i}$$

$$(6) \quad b_{rel} = m_{ref} - s_{ref} \frac{m_i}{s_i}$$

10. Calculate the band average mean and standard deviation, both weighted and unweighted, by the detector noise level (i.e., the Standard Deviation (STDEV) of the shutter region). In this calculation, dead or inoperable detectors are not considered.
11. Calculate the ratios of the forward scan standard deviations and bias-corrected means to reverse scan standard deviations and bias-corrected means. Calculate relative bias to adjust forward-to-reverse scans.
12. Calculate ratios and differences of relative gains and biases, between methods.
13. Move to the next window and repeat the calculation until the scene/interval is complete.
14. Compute the FFT along track (for every column of image data within the window) and calculate the average magnitude of FFT, over all detectors. Plot the average FFT. Report magnitudes (above background) of striping related peaks (e.g., 1 cycle per 16 lines, 8 lines).

3.2.10.1.5 Evaluation

1. The gain ratios and relative bias are plotted vs. time, time since-"ON," focal plane temperatures, and IC flag temperatures, to determine trends.
2. Observed trends are fitted to develop an equation for predicting their behavior. This equation is used to adjust the output of CraM, and in application, to apply the radiometric calibration function. Lacking enough data to trend, weighted average values (weighted by the number of pixels in the calculation or the scene content as measured by the scene standard deviation) are determined.
3. Filters based on the detector noise level to scene content level are available during the trending. Thus, in the evaluation function, the detector noise levels need to be available as ancillary data (from the Characterize Random Noise function).
4. Processed scenes (1R), particularly FASC, are evaluated for residual striping with and without the application of relative correction applied to CRaM output.

3.2.10.1.6 References

None

3.3 Radiometric Calibration Algorithms

3.3.1 PARTIAL APERTURE SOLAR CALIBRATOR (PASC)

3.3.1.1 Calibration

3.3.1.1.1 Background

The PASC generates a usable signal when the sun is imaged. Because the solar disk is some five orders of magnitude brighter than the surface of the Earth normally imaged by the ETM+, attenuation of the signal is required in order to view the sun directly. The fused silica plates provide an order of magnitude signal reduction, while the reduced aperture accounts for the remaining four orders. The PASC can observe the sun on every orbit shortly after the satellite emerges from Earth eclipse near the North Pole (Figure 3-1). The solar image is superimposed on a dark Earth background before the terminator is reached. On any given orbit, at least one facet will be illuminated, depending on the time of year. On most orbits, adjacent facets will provide spatially distinct (though not always both non-vignetted) solar images.

Prelaunch component measurements provide an approximate calibration of the PASC throughput. Postlaunch, this calibration will be refined based upon the IC, assuming that the IC calibration is successfully carried into orbit.

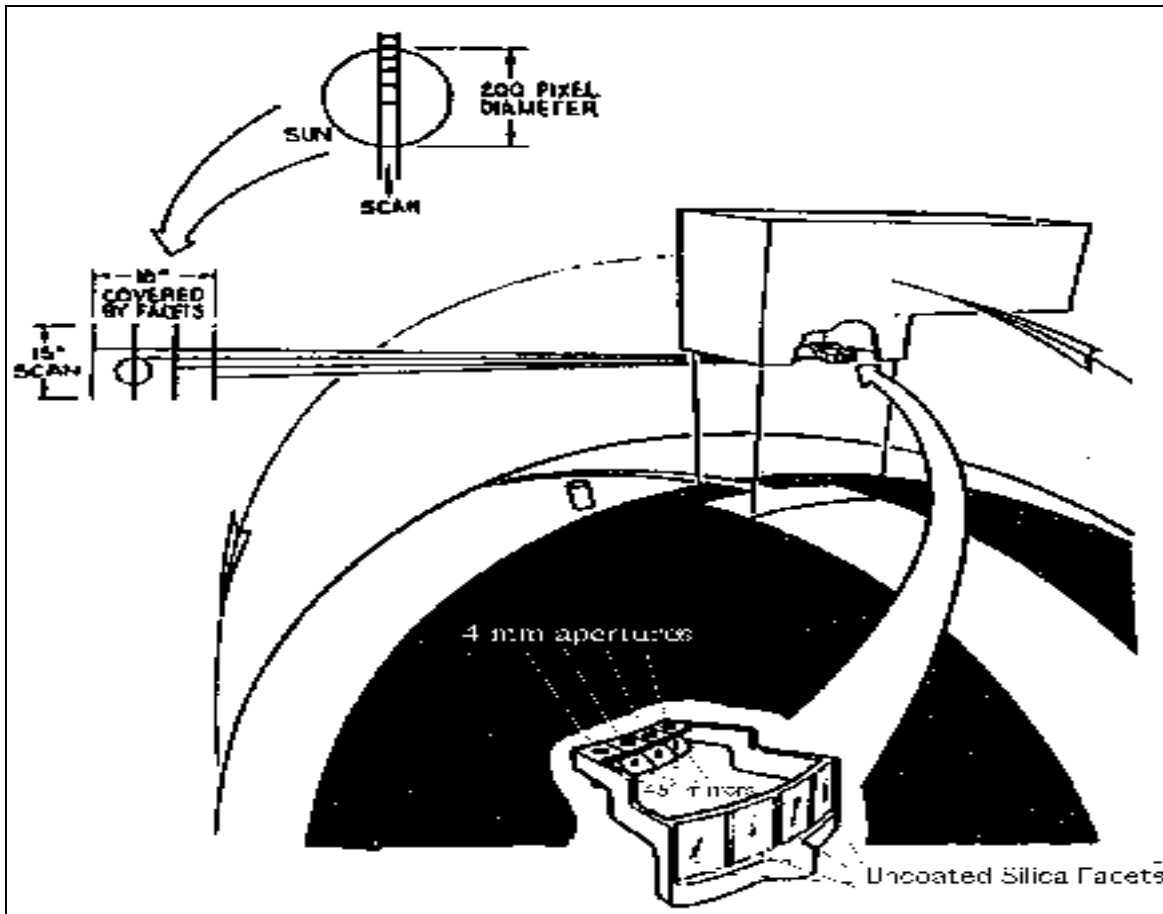


Figure 3-1. Partial Aperture Calibrator Geometry

3.3.1.1.2 Data Acquisition

Although the PASC can be used on every orbit, the current operations concept only calls for its use once per day. To acquire PASC data, the instrument must be turned on, warmed up and ready to acquire data when the sun is about 26 degrees below the S/C velocity vector at sunrise (about 7.1 minutes before the terminator is reached). For usable calibration signals, gains must be set for LOW in bands 1-4, 8, and HIGH or LOW for bands 5 and 7. Data will normally be acquired from about 45 seconds to several minutes after sunrise when the sun is 23 to 15 degrees below the velocity vector. If acquired, a second PASC image from an adjacent facet may appear approximately one minute later.

Uncertainties in PASC Data

The PASC produces a diffraction-limited image of the sun. This diffraction pattern results in the solar radiance being averaged over a larger solid angle than for normal Earth imaging. ETM+ pixels extracted from the center of the solar disk are used for calibration. The solar disk intensity decreases with distance from the center of the disk in a reproducible, spectrally dependent manner. For the extreme spectral wavelengths, band 1 and band 7, the blurring due to diffraction combined with the solar limb

darkening results in a less than 0.5% underestimation of the solar center radiance and is generally insignificant. In addition, the diffraction blur will result in the solar surface non-uniformity being averaged; this could result in contamination by sunspots or bright areas (faculae) in the particular area used for calibration. Sunspots are the greater concern, as they can be only as much as 0.15 the brightness of the rest of the photosphere (Chapman and Meyer, 1981). By example, large sunspots are visible in PASC imagery particularly in band 1, and thus can be filtered out of all bands. (Figure 3-2).

Table 3-4 summarizes the estimated uncertainties in the absolute calibration of the ETM+ using the PASC. Two potentially large sources of error due to contamination of the PASC silica facets, and differences between component based and the system level throughputs, are not included. It is anticipated that the component level measurements will not be adequate to use PASC as an independent absolute calibration source. As such, the PASC gain calibrations will be completed initially with Radio Frequency (RF) equal to unity in Eqs 1.0, with an expectation that recalibration factor will be updated postlaunch using the IC.

Parameter	Allocation	Source
PASC aperture area	1.3%	SBRC
PASC element reflectance	2.0%	SBRC
Non-uniformity of ETM + Optics	1.5%	SBRC
ETM+ aperture area	0.2%	SBRC
TRSS Total Payload	2.8%	SBRC
Center Disk Solar Radiance	1 % (VNIR)	GSFC
Knowledge	3 % Short Wavelength Infrared (SWIR)	GSFC
Sunspots/faculae	<1 %	GSFC

Table 3-4. ETM+ PASC Radiometric Calibration Uncertainty for Initial In-orbit Deployment

3.3.1.2 Algorithm Description

3.3.1.2.1 Background

The PASC uses the sun as a radiance calibration source in order to provide a calibration of the ETM+ reflective channels. In order to use the PASC as an absolute calibration source, the radiance of sun and the throughput of the PASC are required. The center of the solar disk provides the most uniform portion of the solar disk and should provide the best calibration. Determination of the effective radiance of the center of the solar disk through the PASC is as follows:

(1)

$$L_{\lambda}(b) = (R.F. \cdot A_{PASC} \int (L_{sun} \cdot \rho \cdot RSR) d\lambda) \div (A_{ETM} \cdot \int (RSR) d\lambda)$$

Where :

- $L_{\lambda}(b)$ = Equivalent ETM + At - Aperture - Radiance for Spectral Band (b)
- RSR = Relative Spectral Response
- A_{PASC} = PASC Aperture Area (~ .000012 m²)
- ρ = Product of PASC Optics Spectral Reflectances (Silica Reflector and Mirror)
- A_{ETM+} = ETM + Aperture Area (~ .1024 m²)
- $R.F.$ = Recalibration Factor (unitless)

- L_{SUN} = Solar Central Disk Spectral Radiance
= $E_{SUN\lambda} \div (f_{\lambda} \cdot \omega)$

Where :

- $E_{SUN\lambda}$ is the Solar Spectral Irradiance (W/m² - μ)
- f_{λ} is the ratio of the Mean Central Solar Intensity
- ω is the Sun Solid Angle (6.833E - 5 Ster)

Given the additional, and potentially more precise measurement of the instrument response to the sun, achieved by integrating the signal over the majority of the solar disk, this result will be calculated and evaluated for possible use in lieu of the central radiance values.

The absolute gain of the system is determined as:

(2)

$$G_{PASC} = (\langle Q_{SUN} \rangle - \langle B_{DARK} \rangle) \div L_{\lambda}(b)$$

Where :

- Q_{SUN} = Avg ETM+ Response to Solar Disk Center
- B_{DARK} = Avg Bias Using Dark Earth Background of PASC Image

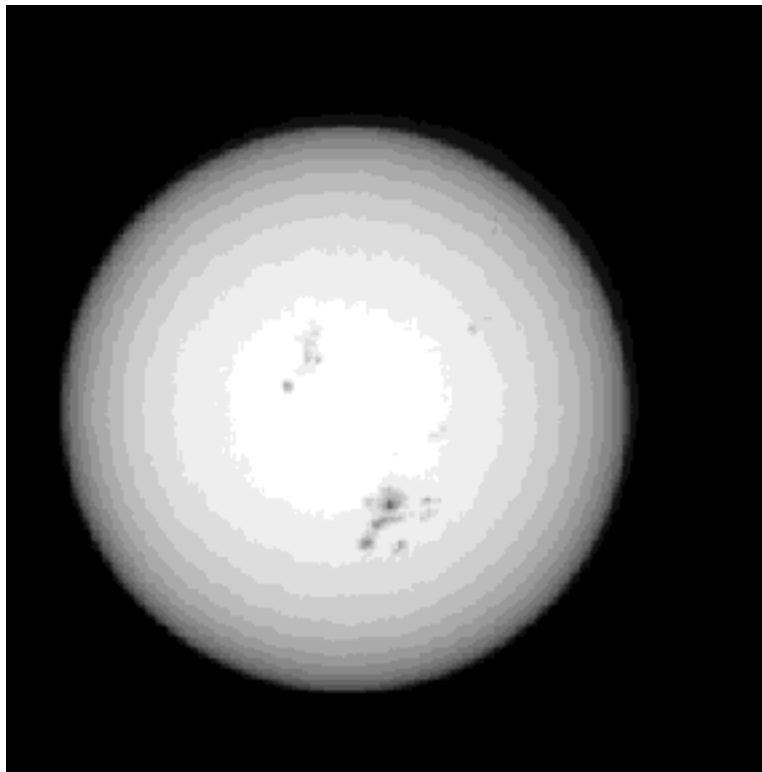


Figure 3-2. Simulated ETM+ Band 3, Diffraction Image of Solar Disk

Contours are at 5% intensity levels with respect to center brightness. (Solar data courtesy G. Chapman, San Fernando Observatory).

3.3.1.2.2 Inputs

- Artifact corrected 0Rc PASC imagery
- LM

The following inputs are measured prelaunch:

- Azimuth and zenith orientation angles (degrees) of PASC facets (8 values)
- Areas of PASC apertures (m^2) (4 values)
- Reflectances of fused silica plates (450-2400 nm) at 9-degree incidence angle
- Reflectance of mirror (450-2400 nm) at 45 degrees
- Area of ETM+ aperture (m^2)

Other inputs:

- Solar irradiance values file (from Moderate Resolution Transmittance Atmospheric Modeling Software (MODTRAN) 4.0) [Ref 1.0]
- Ratio of “mean-to-central” solar disk intensities file [Ref 2.0]
- Recalibration Factor (1 value/facet)

- Threshold values for PASC pulse locations (2 values/band)
- Percentages of disk (i.e., limits of pulse integration, along track and cross track)
- Offsets from pulse edge for extraction of dark background values and # of pixels (2 value/band)
- Thresholds for "2nd derivative" sunspot rejection (1 value/band, DN/Mf².)
- Pulse adjustment factor to correct for center disk value (1 value/band)
- Form of functional fit for "along track" profile

3.3.1.2.3 Outputs

- Average and STDevs of dark values per detector, for each of 4 regions above, below, left and right of the sun image
- Net pulse values per detector identified by facet (central 15% and larger integrated values, DN)
- Gain values per detector based on central and integrated values, per facet (DN / (W/m² - sr - mu))
- Number of rejected scans per detector
- Number of valid scans per detector
- Relative gain values identified by facet
- Mean pixel location (e.g., scan angle) of center of pulse (1 value/detector)
- Pulse adjustment factors for center disk value (1 value/detector)
- Band-to-band ratioed pulse values, identified by facet

3.3.1.2.4 Algorithm

The PASC calibration algorithm consists of four main steps:

1. Determination of PASC Sun Angles for Identification of PASC Facet
2. Calculation of PASC Radiances
3. Identification of PASC Image and Extraction of Disk Center Pixels
4. Determination of PASC Gains

Step 1 - Determination of PASC Sun Angles and Illuminated PASC facet

The orientation of each PASC facet, combined with the motion of the scan mirror, causes the ETM+ to image different swaths of space with each facet. This portion of the algorithm determines which facet is imaging the sun in the ingested scene. Before ingest, a PASC scene will have been identified from "browse" viewing to contain a full solar image. NOTE: Solar images that lie external to the central 75% of the scene width may not be useful for calibration due to vignetting.

Determination of facet illumination occurs in eight substeps:

1. Determine Sun Positions in Earth-Centered Coordinates
The sun state vectors (i.e., xyz positions) for a given time (i.e., YYYYMMDDHHSS) are determined from a Jet Propulsion Laboratory (JPL)

program [Ref 4.0]. This program uses a planetary ephemeris to generate vector components in km, in Earth-centered coordinates.

NOTES:

- It is adequate to calculate the sun position only once for a PASC pass.
- This JPL code has been checked against the code used by the Flight Dynamics Facility (FDF) for consistency and has been implemented.

2. Process Ephemeris

FOR each MF Record

Retrieve the MF time and check the MF flag.

IF the MF flag is "bad" THEN set the MF time = 0, set the outlier flag, and skip to the next MF.

ELSE retrieve the satellite ephemeris state vectors (i.e., xyz-position and velocity components), times and conversion coefficients.

END

Convert all vector components and times, and output arrays.

3. Process PCD for Scan Line Times

FOR each scan line

Check flags for bad data, sync losses, and quality code

IF flags are "bad" THEN set the scan line time = 0, set the outlier flag, and skip to next scan line

ELSE retrieve the raw scan values and conversion coefficients

ENDFOR

If scan line time values are missing over the desired interval, apply a linear interpolation. Convert all times, and output to arrays.

4. Correlate Scan Line and Ephemeris Data and Perform Quality Assurance (QA) Check.

Correlate scan line and ephemeris times, and use the corresponding state vectors, to calculate the S/C angular momentum (L). (Eq 3.0).

$$(3) \quad |r| \cdot |v| = m \quad \backslash \quad L$$

Where :

- m = s/c mass(constant)
- $|v|$ = absolute magnitude of s/c velocity
- $|r|$ = absolute magnitude of s/c position

The S/C angular momentum should remain fairly constant over the course of its lifetime with a variation of < .2% [Ref 4.0]. Any ephemeris record failing to meet these criteria is flagged and rejected. All flagged outliers are output to the IAS Database (DB).

5. Calculate PASC Angles (View and Illumination)

FOR each S/C state vector

- a. Use the sun position and S/C state vectors to calculate the S(un)-E(arth)-V(ehicle)-N(ormal) angles, namely, Sun-Earth-Vehicle Angle (SEV), Earth-Vehicle-Sun Angle (EVS), Sun-Vehicle-Normal Angle (SVN) “Earth-centered” coordinates.
- b. Transform the sun and S/C vectors from “Earth-centered” to “S/C sensor” coordinates, (Eq 4.0). [Ref 5.0]

(4.0)

$$\begin{bmatrix} X_s \\ Y_s \\ Z_s \end{bmatrix} = [Tr] \cdot \begin{bmatrix} X_{sun} \\ Y_{sun} \\ Z_{sun} \end{bmatrix} + \begin{bmatrix} 0 \\ 0 \\ R \end{bmatrix}$$

Where:

[Tr] = 3x3 matrix, the rows of which are normalized x,y,z, unit vectors, R/|R|, ZxV / |ZxV|, YxZ, respectively.

R = instantaneous radius vector, Earth centered (negative Earth pointing)

V = instantaneous velocity, Earth-centered

Xs,Ys,Zs = position components, sensor frame

Zsun,Ysun,Xsun = (Sun - S/C) position components Earth-centered

NOTES:

- In S/C sensor coordinates, Z is nadir pointing, X is in the S/C velocity direction, and Y is in the "cross product" direction of X and Z.
 - This transformation assumes the ETM+ “nadir vector” is truly nadir, and the scan direction is truly perpendicular to the velocity direction.
 - Operationally, it is intended that any misalignment between axes of the sensor and S/C frames be measured postlaunch and any correction be applied by trimming the S/C attitude. If a measurable misalignment is determined, and not corrected by flight operations, a correction matrix can be directly to [Tr].
6. Using these transformed vectors in sensor coordinates, calculate the sun incident angles CV (vertical) and CH (horizontal), wrt to the plane perpendicular to the S/C nadir; (when the S/C is over the terminator, the sun angle wrt this plane perpendicular to nadir = 0 degrees).

(5.0)

$$cv = a \tan \left(Z_{SUN} \bigg/ \sqrt{(X_{SUN}^2 + Y_{SUN}^2)} \right)$$

Where:

$$ch = a \tan \left(-Y_{SUN} \bigg/ X_{SUN} \right)$$

Xsun,Ysun,Zsun = transformed sun positions wrt S/C.

ENDFOR

7. Calculate PASC Scan Angles

In order to determine which facet is illuminated, it is necessary to calculate the angles CVV (vertical) and CHV (horizontal), which describe the ETM+ Line-of-Site (LOS) for a PASC optical path, for a given scan mirror angle.

To begin, ETM+ view normal vector components are calculated at each of three scan mirror angles, namely [-5.9, 0, +5.9] degrees, where 0 degrees corresponds to the mirror at center scan.

(6.0)

$$\begin{aligned}scx &= 0 \\scy &= -\sin(-5.9, 0, 5.9) \\scz &= \cos(-5.9, 0, 5.9)\end{aligned}$$

NOTE: +/- 5.9 degrees is used in lieu of the +/- 7.5 degree instrument spec. to avoid the vignetted regions of the PASC image.

Next, using the facet orientation angles wrt to the S/C velocity vector and S/C zenith, the normal vector components are calculated for each facet.

(7.0)

$$\begin{aligned}zpasc &= -\cos(pasc_el) \\xpasc &= \sin(pasc_el) \cdot \cos(pasc_az) \\ypasc &= -\sin(pasc_el) \cdot \sin(pasc_az)\end{aligned}$$

Where:

pasc_az = [21.,27.,33.,39.]degrees - azimuthal angles wrt S/C velocity vector

pasc_el = 54. degree - elev angle from S/C velocity vector

NOTE: These orientation angles are measured prelaunch.

Finally, Eqs 6.0 and 7.0 are used to calculate the CVV, and CHV, LOS angles for each of four facets, and each of three scan mirror angles.

(8.0)

$$cvv = a \tan \left(\frac{zvrr}{\sqrt{(xvrr^2 + yvrr^2)}} \right)$$

$$chv = a \tan \left(\frac{-yvrr}{xvrr} \right)$$

Where:

$$xvrr = x_2 / \sqrt{(x_2^2 + y_2^2 + z_2^2)}$$

$$yvrr = y_2 / \sqrt{(x_2^2 + y_2^2 + z_2^2)}$$

$$zvrr = z_2 / \sqrt{(x_2^2 + y_2^2 + z_2^2)}$$

The vector components of the LOS direction through the PASC

Where:

$$x_2 = (xvr - \begin{bmatrix} \end{bmatrix}) \cdot x_{PASC\ 2}$$

$$y_2 = (yvr - \begin{bmatrix} \end{bmatrix}) \cdot y_{PASC\ 2}$$

$$z_2 = (zvr - \begin{bmatrix} \end{bmatrix}) \cdot z_{PASC\ 2}$$

$$\begin{bmatrix} \end{bmatrix} = 2 \cdot (xvr \cdot x_{PASC\ 2} + yvr \cdot y_{PASC\ 2} + zvr \cdot z_{PASC\ 2})$$

$$xvr = x \div (x^2 + y^2 + z^2)$$

$$yvr = y \div (x^2 + y^2 + z^2)$$

$$zvr = z \div (x^2 + y^2 + z^2)$$

$$x = scx - \begin{bmatrix} \end{bmatrix} \cdot x_{PASC}$$

$$y = scy - \begin{bmatrix} \end{bmatrix} \cdot y_{PASC}$$

$$z = scz - \begin{bmatrix} \end{bmatrix} \cdot z_{PASC}$$

$$\begin{bmatrix} \end{bmatrix} = 2(scx \cdot x_{PASC} + scy \cdot y_{PASC} + scz \cdot z_{PASC})$$

8. Determine Facet Illumination

For each pair of CV,CH values, determine the perpendicular distance to the line defined by the CVV and CHV endpoint values, for each facet. If the perpendicular distance converges to zero, the facet is illuminated and flagged in array, (1 = illuminated, 0 = not illuminated). This array is output to the IAS DB, and a plot of the (CV,CH) and (CVV,CHV) angles is generated.

NOTES:

- PASC acquisitions will typically occur at CV = ~20 degrees.
- Due to the orientation of these facets, it is common for more than one facet to be illuminated during a PASC acquisition. Each PASC scene within a PASC acquisition will be processed separately.

Step 2 - Calculate PASC Radiances

FOR each illuminated facet

FOR each band

1. Retrieve the solar radiance (E/ω), the central-to-mean solar disk intensities (f), and relative spectral responses (RSR) corresponding to each band wavelength (λ).
2. Calculate the product of prism and silica reflectance (ρ) for the corresponding band.

NOTE:

- For testing and code validation, only one set of reflectances is used for all facets/bands. [Ref 6.0]
 - The reflectances will exhibit some variation with scan angle, which may not be characterized prelaunch.
3. Per Equation 1.0, combine ρ , f , RSR, solar radiance, and PASC and ETM+ aperture areas to determine a spectral radiance ($W/m^2\text{-sr}\cdot\mu$) for the given band.
NOTE: The prelaunch RSR for each band are used as weighting factors

ENDFOR

ENDFOR

For each illuminated facet, the band center wavelength vs. band avg radiance are plotted, and written to a file.

Step 3 - Identify, Extract, and Average Central Solar Disk and Background Pixels.

Read in the artifact-corrected PASC imagery and LM

Integrate Across Track:

FOR each detector per band

FOR each scan line

1. Read each pixel (mf) value. If flagged in LM, ignore. Compute the average of the first 20 "good" pixels in scan. Call this the base average. If the value of any subsequent pixel exceeds the base average by some Threshold Value ($THR = 20$ DN), check this value over the subsequent 20 pixels to ensure that a noise spike is not detected. Flag any noisy pixel as an outlier, and ignore.
2. Define Pulse "Start: and "End" pixels
The pulse "start" pixel is the first pixel of the 20 determined in Step 3.3.1, whose DN exceeds the mean base avg plus THR . The pulse "end" pixel is the fifth consecutive pixel whose DN is less than the mean base avg plus THR .
3. Determine Background
On scans where a pulse is detected, extract and average the background (dark) pixels, on either side of the pulse and average. Extract a window of 200 pixels at

offsets of +/- 200 pixels (bands 1-5,7), +/- 400 pixels (band) from the pulse start & end. Check values for outliers, and calculate avg and std devs (excluding outliers).

4. Subtract Background

Avg dark values before and after the pulse, and subtract from the scan line w/detected pulse, to obtain a new background-subtracted data set. These values are stored temporarily.

5. Define Pulse

Using the background-subtracted data, determine a MAX mf value, as well its location. Next, determine the 40% (of-peak) left and right edge values. Because 40% * MAX yields a floating-point number, linear interpolation is required to calculate the corresponding floating-point mf locations of the 40% edges. Next, compute the average of these 40% edges to obtain the floating-point mf location of the pulse center.

6. Integrate Net Pulse

Integrate between +/- 25 mf's of the pulse center location and divide by 51 to determine a PAPH. Next, determine the 10%-PAPH edge values in fractional mf's. Integrate between these values using trapezoidal integration. This gives the integrated pulse value for the scan.

7. Determine Central Pulse Value

Check scans for (sunspot) outliers in the center 30% portion and flag accordingly. These outliers are characterized as sharp dips in the pulse profile, and are flagged using derivatives. The second derivative of the center 30% pulse data, (P''(30%)) will have sharp peaks at precisely the mf's where the pulse shows sharp dips. If any peak in P''(30%) has a magnitude greater than a threshold (=5), flag the scan.

Compute central solar intensity of the central 15%. Integrate the center 15% or +/- 7.5% of the "Full Width" (FW) of the pulse where FW is the part of the pulse between the 10% points. As in the previous case, use trapezoidal integration. Calculate the mean and standard deviation of the center 30% (i.e., 2*15%) portion. Adjust the integrated center value to correct for a finite pulse width using an asymptotic correction factor (Alpha).

(9)

$$\textit{Alpha} = P0/Pw$$

Where

P0 = the limit of the integrated pulse value as "w" goes to 0,

Pw = the integrated pulse value, at pulse width "w"

This multiplicative factor should be GE 1.0. This input value is obtained by trending results from a number of scenes on a per scan basis.

NOTE: If outliers are detected, the entire scan line will be flagged and rejected.

ENDFOR
ENDFOR

Along-Track Direction:

For each Detector per band

8. Integrate Net Pulse (Apply Steps 4-6). Integrate between +/- 25 mf's of the pulse center location and divide by 51 to determine a PAPH. Finally, determine the 10%-PAPH edge values, and all values between the "left" 10% value and peak, and "right" 10% value and peak. For each set of values, apply a linear interpolation to determine the mf location of each 10%-PAPH value, and integrate between these values to yield an integrated pulse in two dimensions.
9. Determine Central Solar Intensity
Calculate the mean and standard deviation of all pixels within +/- 7.5% of the FW of the PAPH pulse in the along-track direction (approx. 11 scans for all bands 1-5, 7). Reject scans that have been flagged (possible sunspots) and replace by linearly interpolated values. Recompute the mean and standard deviation. After flagged scans have been removed from the along-track data, fit a polynomial of order 2 to the "good" remaining data. Integrate the center 15% of the along-track data using the polynomial fit, to determine the central solar intensity, and determine a peak value of the functional fit.
ENDFOR

All net pulse, center pulse (mean, std dev, fit integrated value, fit peak value and uncertainties), avg pulse center locations, figures of merit (std devs), and background values (4 regions) are output on a detector-by-detector basis. Flagged outlier values are stored in the IAS DB.

Step 4 - Calculate PASC Gains

FOR each detector, per band

1. Calculate Absolute Gains
Two sets of absolute gains are calculated. The first set uses the net pulse values divided by the spectral radiance, per Eq 2.0. NOTE: This calculation includes the RF, which is expected to change on-orbit. The second set of gains are again calculated using Eq 2.0, but with the radiance coming strictly from cross calibration with another calibration source (e.g., IC).
2. Calculate Relative Gains (Detector to Detector)
The net pulse values are ratioed to the band average or reference detector, pulse value.

ENDFOR

3. Calculate Relative Gains (Band to Band)
Once band average net pulse values are determined, these values are ratioed among themselves to characterize relative radiometry.

All absolute and relative gains are output on a detector-by-detector or band-to-band basis.

3.3.1.2.5 Evaluation

1. All gains and pulse values are trended/fitted vs. time, per facet.
2. Results from two methods of pulse integration are compared for stability.
3. Gains are plotted against pulse center locations to evaluate sensitivity to scan position.
4. Adjustment factors to correct central intensity will be trended and average values will be calculated for operational use.

3.3.1.2.6 References

MODTRAN. Version 4.0.

Neckel and Labs. The Solar Radiation Between 3000 and 12500A. Solar Physics V90. p205-258. 1984.

MAKE_EPHEM. Solar Ephemeris Code. JPL.

SBRS. ETM+ Algorithms Document. NAS5-32631. June 1995.

Lockheed Martin. Landsat 7 System - Program Coordinates Standard. REV B. NAS5-32633. December 2, 1994.

SBRS Memo, Modifications to ETM Solar Calibrator. Oct 1986.

3.3.2 FULL APERTURE SOLAR CALIBRATOR (FASC)

3.3.2.1 Calibration

3.3.2.1.1 Background

During calibration, the FASC panel is deployed in front of the ETM+ aperture as the satellite approaches the night-day terminator crossing. The nominal calibration occurs at a 70-degree solar zenith angle (incidence angle with panel vector normal). Following calibration, the panel is returned to its nominal stowed position. The FASC design supports 60 deployments over the life of the satellite or an average of one per month over the five-year design lifetime.

Uncertainties in the FASC Data

Table 3-5 illustrates the error allocation/estimates for calibration with the FASC. Most of the error is currently allocated to the measurement of the BRDF of the panel. Flight parts or witness samples have been measured by independent laboratories to validate the reflectance characterization. The uncertainty in the solar irradiance knowledge is allocated 1.0%; this is reasonable in the visible and near-IR (using MODTRAN 4 curves) and probably optimistic in the short-wave infrared. The actual variability in the solar irradiance is on the order of tenths of a percent on all time scales of interest to the Project (Foukal, 1981).

Parameter	Allocation	Source
BRDF measurement	2.5%	SBRS
Stray light	1.0%	SBRS
Panel position	1.5%	SBRS
Panel flatness	0.6%	SBRS
Panel Parallelness	0.6%	SBRS
Total payload	3.3%	SBRS
Solar irradiance (VNIR)	1 %	GSFC
Solar irradiance (SWIR)	3 %	GSFC
FASC Contamination Stray light Bias	+1.1%	SBRS

Table 3-5. ETM+ FASC Radiometric Calibration Uncertainty for Initial In-orbit Deployment

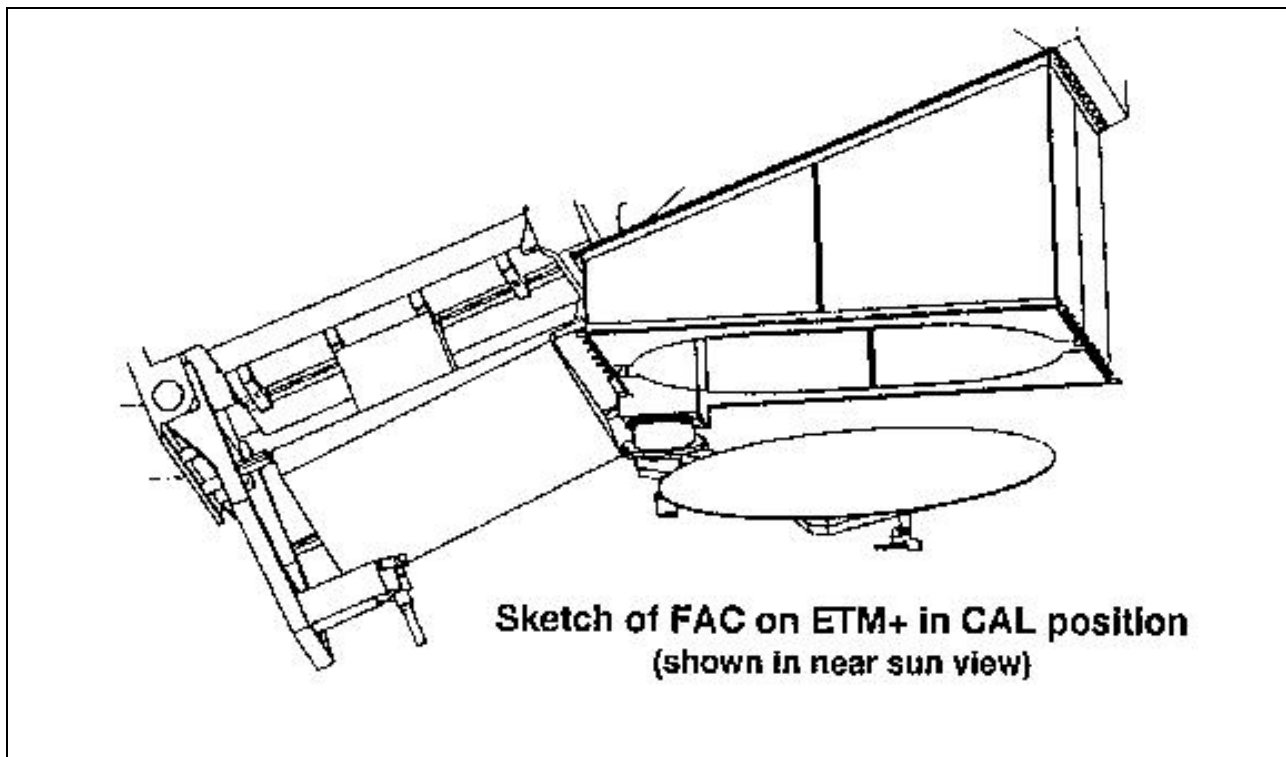


Figure 3-3. ETM+ FASC in the Deployed Position (Based on SBRS Drawing)

3.3.2.1.2 Data Acquisition

Current operations call for FASC acquisitions approximately once per month. Deployment takes approximately two minutes. To acquire FASC data, the instrument must be turned on, warmed up and ready to acquire data at the time of sunrise (the sun is about 26 degrees below the velocity vector at sunrise, or about 7.1 minutes before the terminator is reached).

In the primary mode of FASC data acquisition anticipated, both PASC and FASC data will be acquired during a single orbit following eclipse exit. The data from one to three minutes after eclipse will be used for PASC calibration. Three minutes after sunrise, the FASC will begin to deploy into the calibrate position, and two minutes later (at solar zenith angle of approx. 75 degrees), useable data will be acquired. Data collection will continue for another three minutes (to a solar zenith angle of approx 65 degrees). For this mode of acquisition, the gain will be selectable with low gain as the norm for bands 1-3, 8, and either low or high gain for bands 4, 5, and 7.

A secondary mode of acquisition (performed roughly twice per year) will have the FASC deployed by the time of eclipse exit. Data will be acquired from eclipse exit (as the sun rises on the panel) to a solar zenith angle of approximately 65 degrees (approximately 20 scenes). In addition to being useful for calibration, these acquisitions will allow a characterization of system performance (e.g., SNR) over most of the instrument dynamic range. The gain will be selectable, with the intention of alternating acquisitions between high and low gain.

3.3.2.1.3 Algorithm Description

3.3.2.1.4 Background

Radiometric calibration with the FASC, is provided per:

(1.0)

$$L_{\lambda} = [\cos(\theta_s) \cdot SF \cdot DF \cdot \int (R_{\theta_s \theta_v \phi \lambda} \cdot E_{sun \lambda} \cdot RSR_{\lambda}) d\lambda] \div [\pi \cdot d_{\oplus}^2 \cdot \int RSR_{\lambda} d\lambda]$$

Where:

L_{λ} = Spectral radiance for band(b), weighted by $RSR(\lambda)$

RSR_{λ} = Relative Spectral Response per band

θ_v = ETM+ view zenith angle to the panel (~ 23.5 degs)

θ_s = Solar zenith angle on the panel (~ 70 degs)

ϕ_s = Relative azimuth angle

$E_{sun \lambda}$ = Solar spectral irradiance per spectral band lambda, using Kurucz solar irradiance spectrum [Ref 1.0]

SF = Stray Light Enhancement Factor(~ 1.014). [Ref 2.0]

$R_{\theta_s \theta_v \phi}$ = Bi - directional reflectance factor

DF = Degradation factor per band (b) (approx 1.0)

d_{\oplus} = Earth - sun distance (1 AU)

NOTE: Variations in d can be accounted for as a multiplicative correction factor DCORR (Eq 2.0). This factor is derived by ratioing the mean sun-Earth distance to the current sun-Earth distance, and squaring the result. [Ref 3.0]

(2.0)

$$D_{corr} = (d \oplus \sqrt{(S_x^2 + S_y^2 + S_z^2)})^2$$

Where:

Sx,Sy,Sz = Instantaneous sun position components wrt Earth (km)

3.3.2.1.5 Inputs

Of the inputs required, principal prelaunch measurements will be made for following:

- The BRDF values of the FASC panel at view and illumination geometry provided by the sun panel, sensor.

- Spectral reflectance factors for fixed illumination geometry

Lambda(nm)	BRDF(fractional) @	(Thetas = 70 degrees,
420-940 by ~20nm increments		Thetav = 23.5 degrees,
1500-1800 by ~50nm increments		Phi = 30 degrees)
2050-2400 by ~50nm increments		

- BRDF values of the FASC for nominal range of illumination and view angles

(i.e., one set per wavelength region)

Lambda(nm)	Thetas(deg)	Thetav(deg)	Phi(deg)	BRDF(fractional)
------------	-------------	-------------	----------	------------------

490	65	23.5	0	.
490	65	23.5	15	.
490	65	23.5	30	.
490	65	23.5	45	.
490	65	23.5	60	.

490	70	23.5	0	.
490	70	23.5	15	.
490	70	23.5	30	.
490	70	23.5	45	.
490	70	23.5	60	.

490	75	23.5	0	.
490	75	23.5	15	.
490	75	23.5	30	.
490	75	23.5	45	.
490	75	23.5	60	.

560
660
830
1650
2200

NOTES:

- The θ_v is fixed by the orientation of the panel when deployed (nominally at 23.5 degrees). The variation in θ_v across the central 1000 pixels of the scan is insignificant (i.e., less than 0.1 degrees).
- BRDF values are tabulated in 3 band groups (bands 1-4, 8; band 5; and band 7).
- An absolute BRDF value is normalized to the optimum "70,23.5,30" deg. condition.
- The angle of the surface of the FASC in the deployed position relative to the ETM+ coordinate system specified in terms of 2 angles, a dip angle, (nominally 23.5 degrees), and a roll angle (nominally 0 degrees).
- Stray light contributions to the FASC signal indicate that the light reflected off external surfaces of the ETM+ and the FASC mounting structure are minimal (<.1%), whereas light internally reflected off the primary mirror back onto the FASC enhances the FASC radiance by 1.14%. [Ref 2.]
- Calibrator Degradation Factor for each band

Additional inputs are provided from the following data files:

- RSR Curve per band

Lambda(nm)	RSR (unitless)
420	0.0
421	0.1
.	.
.	.

- Solar irradiances from (MODTRAN) 4

Lambda(nm)	ESUN (W/m ² -sr-mu)
.	.
.	.

Input Parameters:

- MIN FASC angle for gain calc: (68)
- MAX FASC angle for gain calc: (75)
- Start pixel for processing: (2500)
- Number of pixels to process: (1000)
- Bands to process: (1-5,7,8)
- Reference Detectors (one per band): (9,9,9,9,9,9,9)
- Attitude correction matrix for ETM+: (3x3 matrix)

3.3.2.1.6 Outputs

A header page and summary report summarize the results from each FASC acquisition. Several data and plot files include detailed results.

The data files generated include:

- S/C State Vectors and Sun Angles
- FASC Panel Incident and Scatter Angles
- Spectral Radiances per Band
- FASC Image Statistics (with and without Bias)
- FASC Gains (Absolute), and Gain Ratios (wrt Mean Band Gain and D9)

The plot files generated include:

- L7 Orbit vs. ETM+ Sun Angles
- FASC Witness Sample Reflectance Measurements (BRDF vs. Wavelength)
- FASC BRDF Contours (BRDF vs. Incident and Scatter Angles)
- FASC Band Avg Radiance vs. Wavelength
- FASC Quantized Radiance (DN) vs. Spectral Radiance (L) per Band per Detector
- Q vs. L Fit Residuals

3.3.2.1.7 Algorithm

The FASC calibration algorithm consists of three main segments: 1) Determination of FASC Sun Angles, 2) Determination of FASC Radiances, and 3) Determination of FASC Gains.

Segment 1 - Determination of FASC Sun Angles

1. Determine Sun Positions

The sun state vectors (i.e., xyz positions) for a given time (i.e., YYYYMMDDHHSS) are determined by a JPL program. (Ref 4.0) This program uses a planetary ephemeris to generate vector components in km, in Earth-centered coordinates.

NOTES:

- It is adequate to calculate the sun position only once for a FASC pass, as the change in position during the pass has a less than .01% affect on the radiance.
- This JPL code has been verified against the code used by the Flight Dynamics Facility for consistency.

2. Process Ephemeris

FOR each MF Record

Retrieve the MF time and check the MF flag.

IF the MF flag is "bad" THEN set the MF time = 0, set the outlier flag, and skip to the

next MF.

ELSE retrieve the satellite ephemeris state vectors (i.e., xyz-position and velocity components), times and conversion coefficients.

ENDFOR

Convert all vectors and times, and output arrays.

3. Process PCD

FOR each scan line

Check flags for bad data, sync losses, and quality code.

IF flags are "bad" THEN set the scan line time = 0, set the outlier flag, and skip to the next scan line.

ELSE retrieve the raw scan values and conversion coefficients.

ENDFOR

If scan line data values are missing over the desired interval, apply a linear interpolation. Convert all times, and output to arrays.

4. Correlate Scan Line and Ephemeris Data and Perform Final QA Check

Correlate scan line and ephemeris times, and use the corresponding state vectors to calculate the S/C angular momentum (L).

(3.0)

$$|r| \cdot |v| = m \times J$$

Where:

m = S/C mass (constant)

|v| = magnitude of S/C velocity

|r| = magnitude of S/C position

The S/C angular momentum should remain fairly constant over the course of its lifetime with a variation of < .2% [Ref 6.0] Any ephemeris record failing to meet this criteria is flagged and rejected. All flagged outliers are output to the IAS DB.

5. Calculate FASC Angles (View and Illumination)

FOR each S/C state vector

6. Calculate an RA and DEC from each S/C state vector. For a DEC greater than 65 degrees, (in the ascending portion of the orbit), use the sun position, and S/C state vectors to calculate the S(un)-E(arth)-V(ehicle)-N(ormal) angles, namely, SEV, EVS, SVN in “Earth-centered” coordinates.
7. Transform the sun and S/C vectors from “Earth-centered” to “S/C sensor” coordinates, (Eq 4.0). [Ref 6.0]
(4.0)

$$\begin{bmatrix} X_s \\ Y_s \\ Z_s \end{bmatrix} = [\text{Tr}] \bullet \begin{bmatrix} X_{sun} \\ Y_{sun} \\ Z_{sun} \end{bmatrix} + \begin{bmatrix} 0 \\ 0 \\ R \end{bmatrix}$$

Where:

[Tr] = 3x3 matrix, the rows of which are the normalized x,y,z, unit vectors, R/|R|, Z x V/|Z x V|, Y x Z, respectively.

R = instantaneous radius vector, Earth centered (negative Earth pointing)

V = instantaneous velocity, Earth-centered

Xs,Ys,Zs = position components, sensor frame

Zsun,Ysun,Xsun = (Sun - S/C) position components, Earth-centered

NOTES:

- In S/D sensor coordinates, Z is nadir pointing, X is in the S/C velocity direction, and Y is the "cross product" direction of X and Z.
 - This transformation assumes the ETM+ “nadir vector” is truly nadir, and the scan direction is truly perpendicular to the velocity direction.
 - Operationally, it is intended that any misalignment between axes of the sensor and S/C is measured postlaunch and any correction is applied by trimming the S/C attitude. If measurable misalignment is determined, and not corrected by flight operations, a Correction matrix can be directly to [Tr].
8. Using these transformed vectors, and the panel orientation angles in sensor coordinates, calculate the sun incident angle CV, and view angles VH relative to the panel at the nadir position of the ETM+. In practice, only the relative azimuth is determined.

NOTE: These angles are calculated for every scan angle, though across the central 1000 pixels intended for use in calibration, the variation in view azimuth (Phiv) and zenith (Thetav) should produce less than 0.1% variation in panel radiance. (Eqs 5.0-7.0)

$$(5.0) \quad \theta = \arccos(X_n Y_n Z_n (X_s Y_s Z_s \cdot | X_s Y_s Z_s|))$$

$$(6.0) \quad \theta = \arccos(- (X_v Y_v Z_v \cdot X_n Y_n Z_n))$$

$$(7.0) \quad \phi = \arccos(X_{ns} Y_{ns} Z_{ns} \cdot X_{nv} Y_{nv} Z_{nv})$$

Where:

$X_n Y_n Z_n$ = FASC normal components

$X_v Y_v Z_v$ = ETM+ View direction components

$X_s Y_s Z_s$ = Sun position wrt the S/C

ENDFOR

Linearly interpolate all angles over scan line time intervals, and output all state vectors.

Segment 2 - Determination of FASC radiances

FOR each band

Retrieve the RSR and solar irradiance (E) data corresponding to each wavelength (λ).

1. Calculate BRDF

To determine the radiance of the FASC panel, a BRDF value is determined for each point of the RSR curve for each band. This is treated as a separable problem, in which the spectral dependence is distinguished from the angular dependence. The spectral reflectance as a function of wavelength is defined by polynomial fits of the BRDF values collected at the reference condition of (70,23.5,30 degrees). A polynomial of 3rd order is used for the fit.

Once derived, the spectral dependence of the BRDF is “fixed” for a given band, and may be scaled up or down to account for angular BRDF variation. This scaling is independent of wavelength. The angular variation of BRDF is expressed as a function of (Thetas=>x, Phiv=>y) for each of the bands (i.e., by fitting a 2nd order, 2 dimensional polynomial to the data).

(7.0)

$$BRDF(x, y) = \sum_{i=0,2} \sum_{j=0,2} [C_{ij} \cdot x^i \cdot y^j]$$

$$= C_{00} + C_{10} \cdot y + C_{20} \cdot y^2 + C_{01} \cdot x + C_{11} \cdot x \cdot y + C_{20} \cdot x \cdot y^2 + C_{02} \cdot x^2 + C_{12} \cdot x^2 \cdot y + C_{22} \cdot x^2 \cdot y^2$$

Where

y = phi (i.e., 0-60 degrees)

x = thetas (i.e., 65-75 degrees)

NOTE:

- Because the angular dependencies were similar for these bands (1 and 4), their values were averaged and used for all bands 1-4, 8.
- The YB71 paint used on the FASC panel is reasonably Lambertian at these incident angles such that the total variation across the angles used is approximately 2%.

Once the BRDF data are fitted, the fitted curve is normalized to provide a value of unity at the reference condition of (70, 23.5, 30 degrees) for each band. This normalized (BRDF-n) for band “b” is multiplied by the “absolute” spectral (BRDF-s) for band “b”, to obtain the equation for evaluating BRDF.

(8.0)

$$BRDF(\theta_s, \theta_v, \phi, \lambda) = BRDF_n(\theta_s, \theta_v, \phi, \lambda) \cdot BRDF_s(70, 23.5, 30, \lambda)$$

NOTE: Because the same BRDF-n and/or BRDF-s equations may cover more than one band, the total number of equations may be smaller than the number of bands. These equations are evaluated for each scan line, and the BRDFs output to an array.

2. Calculate Radiance

FOR each (thetai,phiv) per scan line

As per Equation 1.0, combine the RSR, solar irradiances, corresponding FASC angles, the rescaled BRDF distribution, and stray light enhancement factor, to determine a reflected panel radiance ($W/m^2\text{-sr}\cdot\mu$) for each band. NOTE: The measured prelaunch RSR for each band are used as weighting factors.

ENDFOR

ENDFOR

Output all angles and radiances to a file, and generate a plot of the band avg radiances per band center wavelength.

Segment 3 - Determination of FASC Gains

FOR each band

1. Extract FASC imagery.

Retrieve the artifact corrected (ORc) FASC imagery (DNs) and LM. Extract pixels (500 for bands 1-4, 5, 7 1000 for band 8) from the most uniform regions of each scan and generate means and standard deviations on this region, ignoring pixels

flagged with LM artifacts (i.e., saturation, IN, etc). Process this region for RN estimates.

NOTE: Due to possible panel degradation and/or contamination effects, changes in the uniformity may warrant changes in the pixel regions selected.

2. Remove Bias

Retrieve the corresponding bias values from the concurrently processed IC data, generate bias statistics, and subtract these values from the image to produce net FASC values.

3. Retrieve Radiance

Retrieve the band radiance from Step 2, and generate statistics.

4. Calculate Gain

FOR each detector

Ratio the pixel values of the FASC image to the FASC radiance, and derive an absolute gain per scan line. Average the gains across the range of angles specified in the "Input Parameters" (See Inputs). Regress the average FASC image values to the FASC radiance, limiting the regression to the same range of input angles. Plot regressions per detector, per band. Calculate two sets of "relative gains," wrt to the mean of all detector gains in a given band, and wrt to a reference detector in each band. Generate statistics for each gain.

ENDFOR

ENDFOR

5. Output all statistics to a file and the IAS DB. Band avg gains (excluding inoperable detectors) and inter-band ratios are determined here, as part of the relative radiometric characterization.

6. Generate Summary Report

For each FASC acquisition, the results from each intermediate file are presented in a summary report with an accompanying header page.

3.3.2.1.8 Evaluation

Output gain values will be trended and fitted. The residuals plots should be for non-random behaviors, and perhaps (based upon this analysis) reduce the range of angles used for the gain calculation.

3.3.2.1.9 References

MODTRAN4 Code. Version 4.0.

Some Stray Light Aspects of the ETM+ Full Aperture Calibrator. SBRC MEMO PL2807E-T00772 from Terry Ferguson to Mike Byers. 5 January 1995.

The Astronomical Almanac for Year 1997. p. c24. ISBN 0737-6421. 1996.

MAKE_EPHEM Code. JPL.

SBRS. ETM+ Algorithms Document. NAS5-32631. June 1995.

Lockheed Martin. "Landsat 7 System - Program Coordinates Standard." REV
B. NAS5-32633. December 2, 1994.

3.3.3 PROCESS IC DATA

3.3.3.1 THERMAL BAND

3.3.3.2 Algorithm Description

3.3.3.2.1 Background

Unlike the reflective bands incorporated in the L7 ETM+, which have multiple onboard calibration sources, the thermal band has only one source of onboard reference irradiance - a thermal blackbody visible to the detectors via a small mirror mounted on one edge of the calibration shutter. Using this mechanism, the thermal band detectors "see" the blackbody at the same time and roughly in the same manner that the reflective band detectors see irradiance from the calibration lamps, and the shutter flag is imaged just as in the reflective bands. Two issues complicate the analysis of thermal band shutter data. First, the detectors see more than the radiance contribution of the blackbody during the calibration pulse measurement. The entire structure of the ETM+ at normal operating temperature emits significant thermal energy in the pass band of the thermal band detectors. Because the detectors are not restricted to seeing only the blackbody, the measured radiance during the sampling of a calibration pulse is the sum of the blackbody plus all other sources of thermal energy emitted into the Field of View (FOV). This extraneous radiance must be adequately accounted for when processing the thermal band calibration pulse data. Second, the shutter is not at effective zero radiance for the thermal band. It must be adequately characterized (thermal spectral emittance) and adequately monitored (physical temperature) to allow determination of its net thermal spectral radiance in an unambiguous fashion.

The thermal band process (IC processing for Emissive bands (ICe)) operates on IC data from band 6, calculating pulse values and integrated shutter values on a per-scan basis, which are used in determining scene-based gains and scan-based offsets.

Analysis of archival L4 and L5 TM data showed that, while the calibration data was fairly noisy at times, the gain itself was relatively stable over periods on the order of a scene. Gains and offsets are initially determined from measurements made per scan to minimize the effects of changes in the net external radiance introduced by the ETM+ structure aft of the shutter (L_a). However, system noise precludes using scan-based gains to calibrate thermal data or to solve for net offset. Instead, a statistical outlier rejection and mean value approach is employed to calculate a scene-based gain for each detector. Thus, the scene-based gain is used with scan-based shutter values to calculate scan-based net offsets. Because many more raw shutter mf's than pulse mf's are collected during a scan, noise in scan-based shutter calculations is not as significant.

Both the radiance contribution of the ETM+ forward of the shutter (L_f) and the radiance contribution after the shutter (L_a) must be accounted for in the net radiance of scene mf's. L_a is not directly measurable, because no telemetry values monitoring temperature of those components are available in the PCD. However, the shutter

temperature is monitored, so it is possible to calculate the expected radiance emitted by the shutter from knowledge of its spectral emissivity and temperature. L_a is then the difference between the observed mean response during the shutter interval in a scan and the calculated expected response of the detectors to the shutter radiance (or to the blackbody) alone. Enough thermal monitor points exist on the forward structural elements to allow us to calculate L_f directly. These derived L_f and L_a values are additive components of the net observed radiance, and so may be "calibrated out" of scene m_f 's by simply treating them as offset terms. In practice they will be used to adjust the net offset parameter calculated above to yield an offset value that removes instrument-sourced radiance automatically with Level-1 thermal calibration.

Unlike the reflective bands, the thermal band is always acquired in both high and low gain states simultaneously. The high and low gain images are two separate image products. Each product goes through this process independently.

3.3.3.2.2 Inputs

- PCD-derived housekeeping temperatures and times bounding the scene being processed
- ORc calibration data
- Masks from Detector Saturation, Dropped Lines and IN functions
- Spectral emissivities of ETM+ structural elements as measured by SBRS
- Planckian radiance to temperature look up table
- Parameters to be set from CPF:
 - Shutter window
 - Pulse window

3.3.3.2.3 Outputs

For Subsequent Processing (Level-1, etc.):

- Gains by scene and offsets by scan for each detector
- Uncertainties in gains, based on standard deviation of blackbody values
- Scene offsets
- Uncertainties in scene offsets

For Trending:

- Scene gain, gain standard deviation and gain status per detector
- Scene offset, offset standard deviation and offset status per detector
- Total number of outliers in the shutter region over the entire scene per detector
- Average scene net pulse per detector
- Mean shutter values, shutter standard deviation, and number of outliers per scan
- Pulse height, width, minimum, location, mean and standard deviation per scan
- Scan gain and offset per scan
- Pulse, offset and gain status per scan

For Reporting:

- Scene mean gain and offset per detector
- Uncertainties in gain and offset, based on standard deviation of blackbody values
- Number of scans used in the scene mean estimates
- Total number of outliers in the shutter region
- PCD temperatures for relevant components

3.3.3.2.4 Algorithm

For all band 6 scenes (high and low gain independently):

1. Calculate scene average PCD temperatures. PCD temperatures are sampled multiple times per scene, but not with every scan line. The scene average temperature of the blackbody temperature (isolated), blackbody (control), baffle heater, CFP (control), baffle tube, CFP (monitor), baffle support, scan-line corrector, primary mirror, secondary mirror, telescope housing, calibration shutter flag and scan mirror are used in processing.
2. Convert scene average temperatures to spectral radiances using a Planckian lookup table specific to the L7 band 6 band pass. All but the scan mirror temperatures are stored in the Trending Database. The scan mirror temperature is not monitored on the instrument. The scan mirror temperature, T_{sc} , is estimated from the secondary mirror temperature, T_{sec} .

$$(1) \quad T_{sc} = a_2(T_{sec} - a_1) + T_{sec}$$

where a_2 and a_1 are from the CPF

Spectral radiance values are derived from physical temperatures using interpolation within a lookup table of temperature to spectral radiance formed from solutions to Planck's radiation equation over the temperature range of interest (75K to 350K) incorporating the spectral pass band characteristics of the ETM+ thermal band components. The Planck equation solution is integrated over the spectral pass band of the ETM+ thermal band and the result for a series of discrete temperatures forms the basis of the lookup table.

3. Check the calibration shutter window for outliers using a 3-sigma rejection criteria. Integrate shutter data over calibration shutter window, neglecting LM and outlier pixels for each scan. Calculate mean and standard deviation of shutter window.
4. Characterize pulse window, calculating or finding pulse height, width, relative minima, and location, neglecting any LM pixels. If the pulse cannot be found, do not calculate the mean pulse value. Integrate pulse data using a trapezoidal integration.
5. Calculate per scan gains from integrated pulse and shutter data. If no valid integrated pulse value is available for the current scan line, do not calculate a gain for that scan. ETM+ thermal band per detector per scan gains are given by:

$$(2) \quad G_{sd} = f_{rv} \frac{(Q_{bb} - Q_{sh})}{(V_{bb}L_{bb} - L_{sh})}$$

Where

Q_{bb} is the integrated per scan blackbody pulse value

Q_{sh} is the per scan shutter values per scan

L_{bb} is the spectral radiance of the blackbody calculated from the PCD blackbody monitor temperature

L_{sh} is the spectral radiance of the shutter calculated from the PCD shutter flag temperature

f_{rv} is the integrated instrument view factor, the ratio of the internal gain to the external gain, determined prelaunch and specified in the CPF

V_{bb} is the blackbody view factor, incorporating the non-unity emissivity and non-nadir view angle, determined prelaunch and specified in the CPF

6. Calculate per scene gain, G_d , based on average of per scan gains from equation (1). Use a 3-sigma rejection criteria to eliminate outliers from the per scan gains and calculate the scene mean gain and standard deviation without the outliers.
7. Calculate the effective shutter radiance, L_{esh} . The effective shutter radiance characterizes the radiance emitted by the shutter (L_{sh}) and the radiance entering the optical path from other instrument components (L_j).

$$(3) \quad L_{esh} = \frac{V_{sh}}{f_{rv}} L_{sh} + \sum_{j=1}^{11} a_j L_j$$

Where

a_j is the view factor for instrument component j . Table 3-6 lists the component index.

j	Component
1	Scan-line corrector
2	Baffle heater
3	Secondary mirror
4	Primary mirror
5	Scan mirror
6	Blackbody (isolated)
7	Blackbody (control)
8	CFP (control)
9	CFP (monitor)
10	Baffle tube
11	Baffle support

Table 3-6. Component Index

8. Compute per scan net offsets based on per scene or CPF gains and per scan integrated shutter values. The equation describing scene-based radiance in terms of instrument response:

$$(4) \quad L_{sc} = L_{esh} + \frac{(Q_{sc} - Q_{sh})}{G_d}$$

Offset is the response of the system to zero input target radiance, i.e., scene element spectral radiance (L_{sc}) = 0. Solving Equation (4) for the offset term, Q_{sc} , now known as Q_0 yields:

$$(5) \quad Q_0 = Q_{sh} - G_d L_{esh}$$

Note that G_d can either be the per scene gain calculated from the pulse and shutter, or it can be the gain specified in the CPF.

Q_{bb}	Digital Counts, response of a detector to radiance from the blackbody
Q_{sh}	Digital Counts, response of a detector to radiance from the IC Shutter Flag
Q_{sc}	Digital Counts, response of a detector to the scene input radiance
Q_0	Digital Counts, response of a detector to an input radiance of zero (the offset DN)
f_{rv}	Integrated instrument view factor
G_{sd}	Detector gain (counts/spectral radiance) per scan
G_d	Average detector gain (counts/spectral radiance) per scene
L_{sc}	Spectral radiance of the scene element
L_{sh}	Spectral radiance of the shutter
L_{bb}	Spectral radiance of the Thermal Blackbody
L_j	Spectral radiance of ETM+ component j
L_{esh}	Equivalent shutter spectral radiance of a scene element
a_j	View/emissivity coefficients of the instrument components
V_{sh}	View/emissivity coefficient for the shutter
V_{bb}	View/emissivity coefficient for the blackbody

Table 3-7. Symbols

3.3.3.2.5 Evaluation

1. Plot trends in all parameters trended with time. Attempt correlation of trends with measurable parameters (i.e., available PCD temperatures). Flag any trends that cannot be explained by visible system state changes.
2. Fit equations to observed trends in the current data set. Fit curves to accumulated trend parameters to obtain a lifetime behavior model. Test current trend parameters against predicted behavior based on previously generated behavior models. Flag discrepancies.

3.3.3.2.6 References

Lansing, J. Some Thermal Calibration Equations. SBRC Internal Memorandum. PL2807-00870-0-00-1. 20 June 1986.

Lansing, J. ETM Band 6 Calibration Equations. SBRC Internal Memorandum. PL2807-01750-0-00-1. 18 April 1988.

Lansing, J. Band 6 Algorithm Coefficient Refinement. SBRC Internal Memorandum. PL2807-03970-0-00-1. 13 February 1991.

Lansing, J. Band 6 Algorithm Coefficient Alternate. SBRC Internal Memorandum. PL2807-03974-0-00-1. 15 February 1991.

Hughes Santa Barbara Research Center. Enhanced Thematic Mapper Plus (ETM+) Algorithms Document (CDRL 36). DM VP16-0956. June 1995.

Hughes Santa Barbara Research Center. Enhanced Thematic Mapper Plus (ETM+) Hardware Qual and Acceptance Test Procedures (CDRL 118 - Test BL10, Document TP32015-518). DM VP16-1079. October 1995.

3.3.4 PROCESS IC DATA - REFLECTIVE BAND

3.3.4.1 Algorithm Description

3.3.4.1.1 Background

Proper calibration of the reflective bands, using the onboard IC, involves the following steps:

1. Rejecting Shutter Data Outliers and Integrating Valid Data

The purpose of this process is to remove outliers, or data points that contain errors, from the data in the shutter region. This is completed partially by the IN algorithm, which identifies significant departures from "normal" shutter values and flags them in the LM. The task is completed in this algorithm by statistically testing data in the shutter region to determine if it is part of the expected data population. When all outliers are removed, the remaining shutter region values are integrated over 550 samples to determine nominal detector bias for each scan.

2. Ghosting

Recent detailed examinations of L4 and L5 TM IC shutter data have revealed a hitherto undocumented instrument artifact contained in the cal shutter - bias region. A faint secondary image of the cal lamp pulses can be seen in band 5 shutter data from L4, and in bands 5 & 7 data from L5. The secondary image, or "ghost," occurs in advance of a cal pulse on forward scans and after a cal pulse on reverse scans. Preliminary analysis of the observed ghost pulses within a single scan indicates that their magnitudes and pulse shapes can be strongly correlated to corresponding cal pulses. Further, ghost pulse locations (expressed as offset from the edge of a cal pulse) are fixed to within one-tenth mf of cal pulse location. Although ghost pulses are detectable, they are typically of magnitudes on the order of the standard deviation of shutter interval samples from a single scan, and are at times masked by quantization uncertainty. Thus, to accurately characterize the ghost, statistical methods must be employed and a sample space consisting of a large number of scans must be analyzed. Worst case observed ghost amplitudes are on the order of 0.20 DN per mf. Because such pulses span the same number of mf as a cal pulse (about 40), they can introduce errors of up to 0.4 percent in calculations of IC bias when mf's that have not been corrected for ghosting are used. This procedure performs the first logical step in compensating for any ghost pulse existing in ETM+ data. It statistically characterizes the magnitude, shape and location of ghost pulses as a function of lamp state, FWD/REV scan direction, and time. Data provided by this procedure can be used to identify the mf's of shutter data that are corrupted by the ghost pulse, so those mf's may be excluded from the calculation of detector offset. Note that for clarity of explanation, this procedure is described independent of any host algorithm; however, for ease of development, it will be incorporated into the Process IC - Reflective algorithm, because much of the data input to the ghost compensation process is also used in Process IC -

Reflective. Note also that the ghosting in L4 and L5 has been confined to CFP Reflective bands, strongly suggesting that ghosting is an optical characteristic of the aft relay optics. It is recommended that this algorithm be used initially on data from bands 5 and 7 of ETM+. It could be modified to include analysis of the other reflective bands if visual inspection of IC data from those bands shows evidence of significant pulse ghosting.

3. Determining Calibration Lamp State

For ETM+, there are only two identical calibration lamps. It was initially assumed that one lamp would be turned on and left on whenever imagery was being acquired. The second lamp would be held in reserve. However, lifetime test studies by SBRS have indicated that these lamps might actually have less than half of the nominal 40,000 hour expected life, because half of them failed in less than 20,000 hours of testing. With a maximum 30% duty cycle for ETM+ and an expected lifetime of 5 years, this would argue for not using one lamp all the time unless observations of within-orbit stability required accepting that risk. One possible scenario would be to turn on the lamp for three seconds out of every 21 seconds. This would ensure that each scene would include an interval when the lamp was on. It is anticipated that the second lamp might be exercised at a rate of 10% of the use of the primary IC lamp. One task, therefore, will be to determine when the calibration lamp is on for proper location and integration of calibration pulses.

4. Rejecting Lamp Data outliers and Integrating Calibration Pulses

This process is similar to the previous discussion for the shutter region. Calibration Lamp Pulses will be characterized by four parameters: Height, Minima, Width and Location. Only the pulses that have acceptable values for all four parameters will be used for subsequent calibration procedures.

5. Calculating Detector Gains

Detector gains are calculated from integrated pulse values and shutter data to obtain the transfer function from digital numbers to radiance. These values are also corrected for instrument state (i.e., temperature, on time, etc.).

All parameters mentioned above are trended in databases. Using these data, models can be generated to describe the instrument's behavior and predict what the measured values of the parameters ought to be for any scene that is being processed. Examples of parameters that are trended include, but are not limited to, detector bias, all four-pulse parameters, and integrated pulse values.

The following algorithm description applies to all reflective bands in the ETM+, but does not include the thermal band, band 6.

3.3.4.1.2 Inputs

- Artifact-Corrected Shutter Data

- Artifact-Corrected Lamp Data
- Lamp State Data (from PCD?)
- PCD Time (i.e., "ON" Time), and Temp. Data
- Orbit position (row number)
- LM
- Instrument State Coefficients
- Ghost Parameters: Peak and Edge (2) Locations

3.3.4.1.3 Outputs

- Integrated Shutter Values
- Lamp Statistics
- Instrument State Model
- Net Pulse Values
- Detector Gains and Biases
- Updated Ghost Parameters: Peak and Edge (2) Locations

3.3.4.1.4 Algorithm

1. Reject Shutter Data Outliers

This process accepts as input artifact-corrected Level 0R IC shutter data, along with LM information, and calculates the mean and standard deviation of the shutter data on a line-by-line basis for each detector. All shutter region data, except that flagged in the LM and in the Ghost region, will be used (approximately 550 mf's). Location of the 550 mf window will be based on a priori (prelaunch) knowledge of calibration file structure, calibration pulse locations, and any known noise artifacts, and will also be referenced to the nearest 40% of peak value on the cal pulse skirt. If location of the Ghost region is not "known," a Ghost characterization should be performed before this step (see below) in order to obtain the best estimate of the Ghost location. A mean and standard deviation will be calculated for the window. Data will be flagged as "bad" if values are more than 3 sigma from the mean (rounded to the nearest integer value). If 3 sigma results in less than 0.5 DN, then m1 DN will be used. Because no bias value greater than 10 DN should ever exist, that will be used as an upper threshold in addition to the 3-sigma test. For each scene and each detector, the number of outliers per scan will be recorded in a database (along with data, path and row). When the number of outliers/scan rises above 1% (based on L4, L5) of the samples in the scan, a flag will be set. These statistical parameters output to the IAS Local Database (LDB) for use in subsequent processing of the scene.

2. Ghosting Characterization

Experience with L4 and L5 data indicates that the ghost artifacts are extremely stable in magnitude with respect to lamp state, and stationary in position (measured as offset in mf from the nearest edge of the cal pulse). If L7 ETM+ behaves in a

similar fashion, the process of characterizing ghost pulses is one of converging to a "best estimate" of ghost parameters. While it is not possible to predict a priori how quickly the best estimate will be achieved, it is possible to recognize when that point is reached, either by measuring the relative changes in ghost pulse parameters from update to update, or by simply measuring the ratio of standard deviations of input data sets (from the current scene) to the accumulated average data set. This procedure describes and uses the latter method, both because it is computationally more efficient than tracking the incremental changes in 40+ mf of data and because it yields a single "figure of merit" that predicts in advance whether inclusion of any additional data will significantly improve the next estimate.

1. Calculate the current scene (interval) based average IC – shutter regions, and applicable statistics:

- Align FWD scan shutter intervals along leading edges of FWD cal pulses (based on 40% of peak skirt location) and REV scan shutter intervals along trailing edges of REV cal pulses.
- Form scene average shutter intervals by adding all shutter region mf within the scene being processed, per detector, per discrete lamp state, separately for forward and for reverse scans, across all applicable scans (NOT along scan), and dividing by the appropriate number of scans. This yields one scene-based average shutter interval (of approximately 540 mf) per lamp state, per detector. This data set will be maintained as floating-point. (NOTE: This step can be coordinated with the above shutter interval outlier rejection algorithm and the following shutter integration algorithm to minimize computational overhead.)
- Compute mean and standard deviation of all resulting scene average shutter intervals.

2. Compare the current scene average shutter intervals against the cumulative average shutter intervals with the matching lamp states. If the comparison meets reasonableness criteria, update existing cumulative average interval with the results of the new scene average and recomputed cumulative interval statistics:

IF $|MEAN_{cum} - MEAN_{sc}| < t * SIGMA_{sc}$, and (t is TBD confidence factor) if $SIGMA_{sc} / SIGMA_{cum} \leq e$, (i.e., is TBD tolerance value) THEN

- Incorporate the current scene average interval into the updated cumulative shutter interval (also floating point values). Compute the updated mean and standard deviation of cumulative intervals.
- Scan updated cum average intervals to locate ghost pulse. (NOTE: Employ a search technique similar to the EDC Level 1 Prototype System (EL1PS); see EL1PS source code for the documentation of the technique). If the search reveals no pulse detected, report NO GHOST, and skip to next detector.

- Characterize ghost pulse. Locate peak to the nearest mf. Using piecewise linear fit to interpolate between mf values, locate $(0.707 \cdot \text{SIGMAcum} \cdot (\text{peak-offset}))$ points. For each of those points, determine the nearest mf whose value is $\leq (0.707 \cdot \text{SIGMAcum} \cdot (\text{peak-offset}))$. Those mf represent the statistically significant extents of the ghost pulse.
- Store newly updated ghost pulse characteristics (offset of peak and each edge from nearest cal pulse skirt, value in DN of each mf between edges, bias value of cum mean interval computed without ghost mf included) in the database. Do not delete the past pulse information; this will be used for subsequent trend analysis.

ELSE

- Flag scene (interval) as noisy; do not use to update cumulative statistics. Enter scene average shutter mean and standard deviation into the database for subsequent trend analysis.
- If reasonableness criteria (described above) are violated for more than 100 scenes, report BEST ESTIMATE of GHOST OBTAINED. Further operation of Ghost Characterization algorithm is then not required, unless trending of ghost parameters over time is desired.
- NOTE: The "t" and "e" in the above description are parameters that will need to be established only after some "real" ETM+ data have been processed, and they may need to change over the life of the instrument. Thus, they should be incorporated as operator-modifiable parameters, rather than as constant values.

3. Integrate Shutter Data

All valid shutter samples within a "shutter window" are integrated to obtain an "average" shutter value. The nominal size of the window will be 550 samples and will include data from the entire shutter region. The size and position of the window is user-selectable and based initially on a priori (prelaunch) information. A simple averaging operation is used to integrate the data--all valid samples are weighted equally. Concurrently, a sum of the squares of each valid data value will be performed. Data that have been flagged as "bad" are not used in the calculations. An integrated shutter value is obtained for each detector for each scan to be used in subsequent correction processes. The standard deviation is calculated for all values used to calculate the integrated shutter value for each detector and each scan.

On a scan-by-scan basis, the integrated shutter value and the standard deviation is compared with what was predicted for the scene based on the Shutter Value Trending Database. A hypothesis test determines whether the integrated shutter value obtained for each scan is the same as what was predicted from the Shutter Value Trending Database. This will be completed using a standard hypothesis test

with a significance level of TBD. If the Integrated Shutter Value fails the test, it may be replaced with the predicted value or kept; the default will be to replace with the predicted value. In addition, a flag will be set if the Integrated Shutter Value fails the test. A similar hypothesis test will be conducted for the standard deviation for that scan. A flag will be set if the test fails (i.e., the predicted value of standard deviation and the actual value for that scan are not the same).

For each scene, an overall Integrated Shutter Value and Shutter Value Standard Deviation will be sent to the Shutter Value Trending Database. These will be calculated using only data from the scans that passed the two hypothesis tests. An overall Integrated Shutter Value will be calculated by simply averaging all of the Integrated Shutter Values. An overall Shutter Value Standard Deviation value will be calculated using all of the data (i.e., the sum of squares from each scan and average from each scan can be combined efficiently).

For the data sets in which a contiguous swath of data is obtained (i.e., consecutive scenes in a single orbit), Integrated Shutter Value and Shutter Value Standard Deviation will be sent to the Shutter Value trending Database for each scan. Because these data will be studied for short-term variations in detector bias, statistics from all scans will be sent to the Shutter Value Trending Database, including those that fail the hypothesis tests.

4. Shutter Value Trending Database

This database trends the detector bias data at two different time scales: 1) over the lifetime of the instrument; 2) over a contiguous interval (within a single orbit). It also provides predicted values of Integrated Shutter Value and Shutter Value Standard Deviation. These two parameters are recorded for each scene. In addition, the two parameters are recorded scan-by-scan for contiguous scenes.

It is anticipated that little variation will occur in detector bias over the life of the instrument. A linear model will first be used to determine if any changes do occur. A linear regression will be used for each detector to regress Integrated Shutter Value to time (days since launch). This model will be used to predict the Integrated Shutter Value for the scene currently being processed. Adequacy of the model will be checked periodically (particularly during IOC). A hypothesis test will be constructed to determine if the slope of the regression line is nonzero at significance level TBD. If a slope is determined to be nonzero, a flag will notify the operator that a change in detector bias has been detected. As necessary, the model can be modified to reflect the true nature of change in detector bias (higher order polynomial, exponential, spline, etc.).

5. Determine Calibration Lamp State

Starting from the center of each calibration interval, a search will be conducted for a calibration pulse, using data from two detectors. Search direction will be dependent

upon scan direction (i.e., for forward scans, the direction will be to the “right” or in the positive time direction). Because only one calibration lamp level occurs, the search will continue until a threshold value of TBD is reached (12 DN for L4 and L5). To ensure that a calibration pulse is located rather than a noise spike, the threshold will need to be exceeded for five consecutive mf’s. This Pulse Location Estimate will be recorded for each scan to form a two-time series, one for forward scans and one for reverse scans. If a pulse is not detected, the last (first, for reverse scans) mf is used as input to the time series. From knowledge of the calibration pulse width, a derivative operator will be convolved with the Pulse Location Estimate time series. The derivative operator kernel values will be [0 0 0 - 1 1 0 0 0] with the number of 0s TBD. Detecting a peak above a threshold level of TBD will indicate turning on the calibration lamp. Detecting a peak below a threshold level of TBD will indicate turning off the calibration lamp. Agreement between two detectors will make the algorithm more robust. A third detector will be used in a voting arrangement in the event that an agreement is not reached using only two.

6. Reject Lamp Data Outliers

The purpose of this process is to identify outlier lamp data and trends in the statistics of the calibration lamp pulses. Outliers are defined as significant departures from expected data and may be caused by transmission errors (bit flips, etc.). Calibration Lamp Pulses will be characterized by four parameters: 1) Pulse Height; 2) Pulse Minima; 3) Pulse Width; 4) Pulse Location. Each of these parameters will be calculated for individual scenes based on detector, scan, and scan direction (because pulse location will certainly vary with direction, and Pulse Height/Minima may as well). Pulse height will be determined using a simple peak detector. Pulse Width will be determined by finding values on the "skirts" of the pulse that are 40% of the peak. The 40% skirt locations will be found using floating point (not integer) values. The corresponding mf locations will also be determined in floating point, not integer. Linear interpolation between DN’s and mf’s will be incorporated. The distance in mf’s between these locations is Pulse Width (floating point value). Pulse Location will be the interpolated center point between the interpolated mf values just described. Pulse Minima will be the interpolated minimum pulse value within the pulse integration width (exactly 30 (TBD) mf’s) centered in the Pulse Location.

After these values have been determined, they will be evaluated for outlier rejection. Each of these values will be compared to predicted values obtained from the Lamp Statistics Trending Database. Using a hypothesis test at significance level TBD, Pulse Height will be compared to Predicted Pulse Height. If the test shows they are the same value, no flags will be set. If the test shows they are not the same value, that calibration pulse will be designated as an outlier. The remaining three parameters will be tested in a similar fashion. Additionally, Pulse Height will be correlated with Lamp State as determined from PCD information. The

number of failures will be recorded by detector and parameter in the Lamp Statistics Trending Database. A flag will be set at each occurrence.

When individual scenes are being processed, an overall scene statistic will be calculated for the four parameters. Only the data that are free of outliers will be used in the calculation. The mean value for each of the four parameters will be calculated, along with a standard deviation. These two statistics will be stored in the Lamp Statistics Trending Database for each detector (and scan direction).

When a contiguous set of scenes is processed, the four parameters will be calculated on a scan basis and all values (including outliers) will be stored in the Lamp Statistics Trending Database.

7. Lamp Statistics Trending Database

This database tracks four Lamp Statistics: 1) Pulse Height; 2) Pulse Minima; 3) Pulse Width; 4) Pulse Location. The data are tracked at two different time scales: 1) lifetime of the instrument; and 2) contiguous scenes within an orbit. The parameters are normally stored in the database on a scene basis, and on a scan basis for contiguous scenes that are processed. Data stored on a scene basis include parameter values and their standard deviations. Based on the data, a model is developed and fitted to the data. The model is used as a predictor of the four Lamp Statistics for the scene being processed.

Data collected on a scene basis will have the following models. Pulse Height and Pulse Minima are expected to decay exponentially with time. Hence, a three parameter exponential model will be used. Pulse width variations with time are currently unknown. As a first guess, a linear model will be used for this parameter. Pulse location has been observed to shift in a somewhat linear fashion and will use a linear model. All models will be fit through standard regression procedures and updated when new data are available. Adequacy of model fit will be monitored on a regular basis so models can be modified or replaced as needed.

Data collected on a scan basis will be trended using a linear model for all parameters. Linear changes with respect to time have been observed for Pulse Height and Pulse Minima. The other two parameters are not expected to change significantly during this short of an interval. Adequacy of model fit will be monitored on a regular basis so models can be modified or replaced as needed.

8. Calculate Detector Gains

To calculate Detector Gains, four operations are required: 1) Integrate Outlier Corrected Lamp Data; 2) Remove detector bias (Integrated Shutter Values); 3) Adjust Radiances; and 4) Calculate Detector Gain. Each of these operations is discussed in detail below.

1) Outlier Corrected Lamp Data will be integrated (averaged) to determine an Integrated Pulse Value. To ensure the highest degree of repeatability, this will be completed in a continuous, rather than discrete, fashion by averaging the 30 (TBD, based on prelaunch data) mf's centered on the Pulse Location. Every scan with valid (no outliers) data will be used. Pulse center (floating point value) as found in the outlier rejection section will serve as the center of the integration window. The integration window will be of fixed width and necessitate integrating using interpolated pulse values. Trapezoidal integration will be used to increase consistency in pulse values from scan-to-scan. For example, integration may need to be performed from mf 798.4 to mf 829.4

2) Net Pulse Values will be obtained by simply subtracting the Integrated Shutter Value obtained for that scan from the Integrated Pulse Value. Net Pulse Values will be compared to the Predicted Net Pulse Value obtained from the Net Pulse Value Trending Database. A standard hypothesis test will be performed at significance level TBD to determine if the calculated Net Pulse Values are in agreement with the prediction. If not, calculated values will be replaced by predicted values and appropriate flags will be set (optionally, the calculated values can be retained). An overall Net Pulse Value and its associated standard error (TBD) for each scene will be stored in the Net Pulse Value Trending Database. The overall Net Pulse Value will simply be an average of Net Pulse Values for all valid scans. If a set of contiguous scenes is being processed, the Net Pulse Value for each scan will be stored in the Net Pulse Value Trending Database, along with their standard errors (TBD). An exponential model (suggested by Landsat TM, but subject to modification based on ETM+ data) will be regressed to the data for trending and prediction purposes.

3) Radiance levels produced by the internal calibrator, or seen by the detectors, vary as a function of instrument state. Therefore, several parameters affecting instrument state will be tracked and used for correcting this effect. The parameters of particular interest include: instrument "on" time, position in orbit, and temperatures of the internal calibrator components and focal plane arrays. These parameters will be extracted from the PCD for each scene. The model used to correct for these effects will have the following form:

$$(1) DN = a_1 \cdot T_1 + a_2 \cdot T_2 + \dots + a_{15} \cdot t_1 + a_{16} \cdot t_2 + a_{17} \cdot row + b$$

Where:

a and b = model coefficients

T# = PCD temperatures

t# = time since turn-on, and previous acquisition

ROW = WRS row number

The 14 temperatures required for this model include:

1. Cal Shutter Flag Temperature

2. Backup Shutter Flag Temperature
3. Silicon Focal Plane Assembly Temperature
4. CFP Monitor Temperature
5. Cal Lamp Housing Temperature
6. Scan-line corrector Temperature
7. Cal Shutter Hub Temperature
8. Ambient Preamp Temperature (High Channels)
9. Ambient Preamp Temperature (Low Channels)
10. Band 7 Preamp Temperature
11. Band 4 Post Amp Temperature
12. Primary Mirror Temperature
13. Secondary Mirror Temperature
14. Pan Band Post Amp Temperature

NOTE: These temperatures, in degrees Celsius, are converted from engineering units using the conversion coefficients from the CPF. The coefficients will be determined via an off-line procedure using contiguous data from a single orbit collected at regular intervals. A (TBD) model will be developed to correct the radiance levels produced by the lamps, or sensed by the detectors.

Preliminary indications from L5 data indicate the model may be as simple as a linear regression of radiance (or Net Pulse Values) to PFP temperature. However, the initial model will include the capability of a multiple regression of radiance to the above factors. Prelaunch data will be used to refine the model. Further refinement will occur during IOC. When scenes are processed from a contiguous swath, all of the above parameters will be stored in the Instrument State Trending Database.

4) After the pulse values (or the radiance values) have been corrected for instrument state, Detector Gain can be calculated. Detector Gain is determined by dividing the Net Pulse Value in each scan that has a valid scan pulse, by the effective radiance level. If all artifacts have been removed from the calibration data at this point, gain is not expected to change within a time period of one scene. Therefore, all Detector Gain values are averaged to obtain the Detector Gain for that scene. This value, along with its standard deviation, is stored in the Detector Gain Trending Database. After this value is calculated, it will be compared to the Predicted Detector Gain value obtained from the Detector Gain Trending Database. A simple hypothesis test will be performed at significance level TBD to determine if the calculated value is in agreement with the predicted value. If it is not, a flag will be generated. When the obtained value does not agree with the predicted value, it will be replaced by the predicted value (however, an option will be available to use the calculated value). If a contiguous swath of data is being processed, then all Detector Gain values (for each scan, essentially) will be stored in the Detector Gain Trending Database.

9. Net Pulse Value Trending Database

The Net Pulse Value Trending Database will track Net Pulse Value and its standard deviation as a function of time at two time scales: 1) Lifetime of the instrument; and 2) within a single orbit. When single scenes are being processed, a single Net Pulse Value, and standard deviation, will be recorded for each scene. These data will be fitted to an exponential model through a regression operation. This model will be used to predict new Net Pulse Values obtained from the next scene being processed.

When contiguous scenes within an orbit are being processed, Net Pulse Values and standard deviations will be stored for each scan. These samples will be modeled in a linear fashion using regression analysis and results from this operation will be used for modeling instrument state corrections to calibration.

10. Instrument State Trending Database

Data describing the instrument will be stored in this database. These will include time since instrument was turned "on"; position in orbit; and all recorded temperatures. These data will be incorporated in a multiple regression model that describes the state of the instrument as it relates to radiometric calibration of the reflective bands. The model output will be used to correct for instrument state when performing Detector Gain calculations.

11. Detector Gain Trending Database

Detector Gains and their standard deviations are stored in this database. One Detector Gain value is stored per detector per scene when individual scenes are processed. An exponential model will be developed from the data to predict Detector Gain values for new scenes being processed. When contiguous scenes are processed, Detector gain and its standard deviation will be stored for each scan. A linear model will be fitted to these data. This model will indicate how well artifacts are being removed during the detector gain calibration procedure.

3.3.4.1.5 Evaluation

1. All parameters tracked in trending databases should be monitored periodically for significant changes. Shutter region outlier statistics should be monitored for sudden or gradual increases in numbers of outliers as an indication of change in either instrument or algorithm performance. Integrated shutter values should be trended (probably linearly) and evaluated for any nonzero slope in the trend line.
2. Lamp state should be analyzed to ensure that calibration lamps are indeed being used as desired for both adequate calibration and optimal lamp lifetime. Calibration pulse parameters are trended automatically; however, it is imperative to monitor the trends to detect significant departures from predicted behavior and to ensure that pulses are used optimally for calibration purposes.

3. Analysis of Net Pulse Values and detector gains needs to be conducted periodically to ensure that no significant departures from predicted models occur, and also as a check for trending detector bias and Integrated Pulse Values and their corresponding algorithms.
4. Although most of the parameters that are being analyzed and trended have been characterized from TM, it is imperative that a periodic check takes place on these parameters to detect departures from those models. The frequency of these analyses will depend on the instrument performance. Early in instrument life, these analyses (and subsequent reports) should be made on a fairly frequent basis. As confidence is gained in instrument performance, these checks may be made much less frequently. Initially, it will probably be prudent for daily evaluations. Frequency of evaluation may be easily reduced to six months intervals later in instrument life.

3.3.4.1.6 References

J.L Barker. Characterization of Radiometric Calibration of Landsat 4 TM Reflective Bands. NASA Landsat 4 Scientific Characterization Early Results. Vol. 2. Pt. 1. p. 373-474. January 1985.

JL Barker. Relative Radiometric Calibration of Landsat TM Reflective Bands. Proceedings of the Landsat 4 Science Characterization Early Results Symposium, Greenbelt, MD. NASA Conference Publication 2355. Vol. 55. No. 3. Feb. 22-24 1983.

D. Fischel. Validation of the Thematic Mapper Radiometric and Geometric Correction Algorithms. IEEE Transactions on Geoscience and Remote Sensing. Vol. GE-22. No. 3. p. 237-242. May 1984.

D. Helder. A Radiometric Calibration Archive for Landsat TM. SPIE AeroSense. 1996. SPIE Proc. Vol. 2758.

M.D. Metzler and W.A. Malila. Characterization and Comparison of Landsat 4 and Landsat 5 Thematic Mapper Data. Photogrammetric Engineering and Remote Sensing. Vol. 51. No. 9. p. 1315-1330.

D. Helder et al. A Technique for the Reduction of Banding in Landsat Thematic Mapper Images. Photogrammetric Engineering and Remote Sensing. Vol. 58. No. 10. pp. 1425-1431.

D. Helder et al. Short Term Calibration of Landsat TM: Recent Findings and Suggested Techniques. IGARSS '96. May 27-31 1996. Lincoln, Neb.

3.4 Radiometric Correction Algorithms

3.4.1 PRE-1R CORRECTION OF RADIOMETRIC ARTIFACTS

3.4.1.1 COMBINE IMAGE AND IC DATA

3.4.1.2 Algorithm Description

3.4.1.2.1 Background

The instrument produces a constant stream of data, in which the image pixels of a scan line are followed by the IC data for that scan line. The IC is separated from the image line during OR product formatting. For the memory effect and CN correction, the image and IC data must be recombined, with no loss of mf's in between. This algorithm describes how to paste one line of image and IC data together. In reality, a group of lines will probably have to be combined in a block due to the nature of the ME correction (possibly using data from more than one line).

The data stream comes down in the following time order: fwd: fwd img pixels(l to r)->bdc->dc rest->adc->lamp->dark rev: rev img pixels(r to l)->dark->lamp->bdc->dc rest->adc

The OR data product reverses the image pixels and the IC data on reverse scans, and splits the IC data out to a separate file:

Image File	IC File
fwd:fwd img pixels (l to r)	bdc->dc rest->adc->lamp->dark
rev:rev img pixels (l to r)	adc->dc rest->bdc->lamp->dark

NOTE: This assumes the LPS is reversing img AND IC DATA on reverse scans.

The lines should be recombined as such (we want to place the data in time order, so all the reverse pixels must be re-reversed and the IC data tacked on to the end):

fwd img(l to r)->bdc->dc rest->adc->lamp->dark->rev img(r to l)->dark->lamp->bdc->dc rest->adc->fwd img(l to r)->bdc->dc rest->adc->lamp->dark-> rev img(r to l)->dark->lamp->bdc->dc rest->adc...

3.4.1.2.2 Inputs

- 0R Imagery (separate file, spatially oriented)
- IC Data (separate file, reverse scans time-reversed)
- Line number
- Band number

3.4.1.2.3 Outputs

- 0R Image Plus IC (in memory or in temp disk file)
- Direction (fwd or rev) of the line
- Nimg, NIC (number of image and IC pixels, respectively)

3.4.1.2.4 Algorithm

This module should combine ONE line of image and IC into ONE line of time-oriented image + IC data:

1. Get the direction of the line from the band file OR from the IC file (possibly both and check to make sure they agree). In addition, get the Left Hand Side (LHS) and Right Hand Side (RHS) data offset of the actual data from both the band data record & IC data record.
2. For a given band/line number, read the appropriate pixels of image data from the appropriate band file into a buffer, and read the appropriate pixels of IC data from the IC file into a buffer. (Rely on the scan line lengths read from the band file & IC file headers for the number of img & IC pixels to read.)
3. If the line is a reverse scan, copy the image pixels in reverse order into the time-oriented buffer. Then copy the IC pixels in reverse order into the time-oriented buffer.
4. If the line is a forward scan, copy the image pixels directly into the time-oriented buffer, then copy the IC pixels into the time-oriented buffer.

INTEGRATION CONSIDERATIONS

This function will be combined with the ME correction. The implementation should be such that the correction algorithm can run continuously through the data, including crossing the area where one line ends and another begins.

*Example: Combine two lines at a time. Correct the 1st line, then have the program loop to work on the remaining lines in the line 2 buffer (with the previous line available in the line 1 buffer for correcting the pixels at the start of the line). As the processing proceeds, the line 2 buffer is promoted into the line 1 buffer, and the next line is read into the line 2 buffer. Other options available

- Combining ALL the lines for one band into memory.
- Combining one line at a time in memory, and then writing to a temporary disk file for later use by correction algorithms.
- Combining N lines at a time into memory and doing the necessary corrections while rotating through and updating the buffer. The corrected data in the buffer can be written to a temporary file or re-separated in memory before sending it on to the next operation.

LANDSAT 7 CONSIDERATIONS

For L4/L5, IC data is stored in scan, detector, band order, with data from each band having the same record size; L7 is band sequential, with band 6 and 8 different record sizes from bands 1-5, 7. In addition, in L4/L5, IC data is NOT reversed for reverse scans, but is for L7.

3.4.1.2.5 Evaluation

Not applicable

3.4.1.2.6 References

None

3.4.2 CORRECT MEMORY EFFECT

3.4.2.1 Algorithm Description

3.4.2.2 Background

ME is an artifact that has plagued TM data from the beginning. It is manifested in a noise pattern commonly known as banding. It can be observed as alternating lighter and darker horizontal stripes that are 16 pixels wide, in data that has not been geometrically corrected. These stripes are most intense near a significant change in brightness in the horizontal (along scan) direction, such as a cloud/water boundary. Because of this, it was formerly termed “Bright Target Saturation” or “Bright Target Recovery.” Another artifact known as “Scan Line Droop” was originally thought to be a separate phenomenon, but has since been shown to be simply another manifestation of ME. Because of its nature, ME has historically been the cause of significant error in calibration efforts because its affect on IC calibration data is scene dependent. It is present in bands 1 through 4 of the PFP, and nearly absent in the CFP.

ME is caused by circuitry contained in the preamplifiers immediately following the detectors in the instrument electronics. It is primarily due to a portion of a feedback circuit that contains a resistor/capacitor combination with a time constant of approximately 10 ms. This directly corresponds to time constants of approximately 1100 mf’s that have been derived from night scenes. Therefore, ME has been modeled as a simple first order linear system and only three model parameters need to be identified to characterize it (actually one of the three is simply detector bias).

$$(1) \quad g(mf) = b - k(1 - e^{-t/\tau})$$

Where:

$g(mf)$ is the ME pulse response,
 b is detector bias,
 k is ME magnitude,
 τ is the ME time constant

Although the exact approach taken to characterize ME is dependent on data type, response of the detector to some type of pulse is measured and averaged over many scan lines. Because the response will be exponential in form, the data are manipulated by subtracting out the appropriate bias level, linearized via the natural logarithm, and linearly regressed to determine the model parameters.

ME can be corrected by a convolution operation using a filter that performs the appropriate inverse operation. Fortunately, the power spectrum of the ME blurring function contains no zeros. Thus, its inverse function is well behaved and can be implemented directly.

3.4.2.2.1 Inputs

- 0R Image and IC Data from Night Scenes
- 0R Image and IC PASC Data
- 0R Image and IC FASC Data
- LM
- ME magnitude for each detector
- ME time constant for each detector

3.4.2.2.2 Outputs

- ME Corrected Image and IC Data

3.4.2.2.3 Algorithm

1. Correction of ME is completed simply through a convolution operation. To accomplish this, the data must be arranged in a time sequence. Data must be stitched together for each detector in the following fashion: forward scan image data, forward calibration interval, reverse scan image data, reverse calibration interval. If gaps in the data exist (as in L4 and L5 TMACS output), an estimate must be obtained as to how many mf's are missing, and synthetic data must be generated. A simple approach to this is to linearly interpolate across the missing interval.
2. The restoration filter is typically quite long in length due to the long time constant (~1100 mf) of the ME. Typical filters could be from 3000 to 6000 mf's in length. Derivation of the filter is as follows:
 - a. Obtain ME parameters from the database, kME , and tME .
 - b. Impulse response of the restoration filter is given as

$$(2) \quad hr(mf) = \delta(mf) - kME \cdot \exp[-kME + 1 \div tME] \cdot mf)$$

Where:

mf = minor frame number (independent variable)

= Kronecker delta function (unity value at mf=0, 0 elsewhere).

- c. Truncate the filter. Because the filter is of infinite length, it must be truncated to some finite length. A guideline is to use a filter length of from 3 to 6 time ME time constants (on the order of 3000 to 6000 mf).
3. The last step in the algorithm is to simply convolve the filter with the detector time series. After this, the time series for each of the detectors can be rearranged to form image and calibration data.

NOTE: Because of the extreme length of the filters, it may be necessary to replace the restoration filter with an approximation to speed up the compute time. One approach is to divide the filter into equal length intervals, with the exception of the first filter coefficient. In each interval, average the coefficient to find the mean value for that interval. In this manner, the filter can be converted into several boxcar filters so the number of multiplies and adds for each pixel is equal to the number of intervals the filter is divided into.

3.4.2.2.4 Evaluation

Evaluation of this algorithm is best performed through visual inspection and use of the Deband algorithm. Several scene locations should be selected that are known to have features conducive to producing banding. These images can be inspected on a regular basis, using an appropriate contrast enhancement, to determine the extent whereby banding (and therefore ME) is eliminated. Comparison of imagery before and after ME correction is recommended.

The Deband algorithm provides a measure of banding correction that can be calculated on a regular basis and trended to assess the adequacy of this algorithm in conjunction with the Characterize ME algorithm. Visual inspection of Deband output images can also provide a qualitative assessment of banding removal and ME reduction.

3.4.2.2.5 References

J.L. Barker. Characterization of Radiometric Calibration of Landsat 4 TM Reflective Bands. NASA Landsat 4 Scientific Characterization Early Results. Vol. 2. Pt. 1. pp. 373-474. January 1985.

JL Barker. Relative Radiometric Calibration of Landsat TM Reflective Bands. Proceedings of the Landsat 4 Science Characterization Early Results Symposium, Greenbelt, MD. NASA Conference Publication 2355. Vol. 55. No. 3. Feb. 22-24 1983.

D. Fischel. Validation of the Thematic Mapper Radiometric and Geometric Correction Algorithms. IEEE Transactions on Geoscience and Remote Sensing. Vol. GE-22. No. 3. p. 237-242. May 1984.

D. Helder. A Radiometric Calibration Archive for Landsat TM. SPIE AeroSense. 1996. SPIE Proc. Vol. 2758.

M.D. Metzler and W.A. Malila. Characterization and Comparison of Landsat 4 and Landsat 5 Thematic Mapper Data. Photogrammetric Engineering and Remote Sensing. Vol. 51. No. 9. p. 1315-1330.

D. Helder et al. A Technique for the Reduction of Banding in Landsat Thematic Mapper Images. Photogrammetric Engineering and Remote Sensing. Vol. 58. No. 10. p. 1425-1431.

D. Helder et al. Short Term Calibration of Landsat TM: Recent Findings and Suggested Techniques. IGARSS '96. May 27-31, 1996. Lincoln, Neb.

D. Helder et al. An Adaptive Debanding Filter For Thematic Mapper Images, in review for IEEE Transactions on Geoscience and Remote Sensing.

3.4.3 CORRECT SCAN-CORRELATED SHIFT (SCS).

3.4.3.1 Algorithm Description

3.4.3.1.1 Background

SCS is a sudden change in bias that occurs simultaneously in all detectors. The bias level switches between two states (It is assumed that L7 will behave like L5). Not all detectors are in phase--some are 180 degrees out of phase (i.e., when one detector changes from low to high, another may change from high to low). All detectors shift between two states that are constant or slowly (on the order of days to months) time varying.

Estimation of SCS levels occurs in the process "Characterize Scan-Correlated Shift" (See Section 3.2.3). SCS levels are normally determined from analysis of night data. Changes in SCS level normally do not occur (L4 and L5) during the part of a scan when scene information is acquired or when shutter/IC information is acquired. Thus, SCS level is constant during a scan. The SCS level that exists for each detector during each scan is determined via an analysis of shutter data in the process "Characterize Scan-Correlated Shift." This is completed for each scene. The current best estimate of SCS level is also obtained from the same process. However, because these values are estimated only from night scenes, the most current estimate is obtained from the SCS Trending Database.

When detector bias is corrected on a scan line basis, SCS is automatically removed from the data. This process provides a separate and distinct method for dealing with SCS, independent of other calibration operations.

It is assumed that L7 will behave like L4/L5 in that SCS transitions will not occur during active scan periods (i.e., acquisition of image data or IC/shutter data). If this is not the case, and transitions in SCS level occur during active scan periods, corrections will be made based on knowledge of where the transition occurred with the scan (this is determined in the process "Characterize Scan-Correlated Shift."). This correction can only be made if the point of transition from one SCS level to the other SCS level occurs in a predictable and repeatable manner. If this is not the case, the location of the transition will not be determinable from normal daytime data.

SCS correction is arbitrary (i.e., there is no "right" or "wrong" state). All that is needed is a consistent correction. The procedure that will be followed in this process will be to correct each detector to its "high" SCS level. If any detector is near its lower limit in dynamic range, this correction will provide some margin from that limit.

3.4.3.1.2 Inputs

- 0R Image Plus IC
- SCS State Scan Mask

- SCS Levels

3.4.3.1.3 Outputs

- SCS Corrected 0R Image Plus IC

3.4.3.1.4 Algorithm

1. For the scene to be corrected, the SCS state for each scan and the SCS levels for each detector are received from process "Characterize Scan-Related Shift" (See Section 3.2.3). From this information, it can be determined for each detector, and each scan, whether that detector is in its "low" or "high" SCS state. If the SCS state is low, the difference in SCS levels is added to all pixel value in that scan. If the SCS state is high, the data are not altered.
2. If it is determined that SCS transitions occur during active scans, and those transitions occur in a predictable and repeatable manner, the SCS correction will vary within a scan line. That is, before the transition, the detector will be in a different state from after the transition. The low state will again be corrected to the high state as described in the preceding paragraph, but only for a portion of the scan line. SCS Transition Location information will be obtained from "Characterize Scan-Related Shift" in order to perform this correction.

3.4.3.1.5 Evaluation

This algorithm can be evaluated both qualitatively and quantitatively. A qualitative evaluation can be performed by visually inspecting night image and cal files for the presence of SCS level changes. Data must be stretched appropriately.

A quantitative evaluation can be performed by processing SCS corrected data through the SCS characterization algorithm. The algorithm should fail to find SCS level transitions, so the state transition mask should indicate SCS high levels only for each scan.

3.4.3.1.6 References

D. Helder et al. Short Term Calibration of Landsat TM: Recent Findings and Suggested Techniques. IGARSS '96. May 27-31, 1996. Lincoln, Neb.

M.D. Metzler and W.A. Malila. Characterization and Comparison of Landsat 4 and Landsat 5 Thematic Mapper Data. Photogrammetric Engineering and Remote Sensing. Vol. 51. No. 9. p. 1315-1330.

3.4.4 CORRECT COHERENT NOISE

3.4.4.1 Algorithm Description

3.4.4.1.1 Background

CN is a low-level periodic noise pattern present in all Landsat TM imagery. It is most obvious in homogeneous regions such as water and desert areas. The periodic components are generally quite stable in terms of their period or frequency. In some cases, the phase of the component is also stable. These characteristics are described in detail in the Characterize Coherent Noise Algorithm Background section (See Section 3.2.4). Unfortunately, for the most part, the components exhibiting the greatest magnitude are not locked in frequency and phase. There is just enough variation, both within and between scans, that it is very difficult to characterize the noise well enough so a subtractive process can be utilized to remove it from the data. However, because there are indications that this particular type of noise will be more apparent in ETM+ and, thus, perhaps more characterizable, a subtractive correction procedure is included in this algorithm description. A second approach to removing CN is to filter it out with appropriate notch filters. Again, because the noise components are, for the most part, very narrow in bandwidth, notch filters can be derived that remove the noise with little effect on the desired signal components. A wideband component is present in L5 data; however, its bandwidth is still only on the order of 0.003 cycles/mf (one a scale in which 0.5 represents Nyquist).

It needs to be mentioned at this point that this algorithm is based on studies of night TM scenes. These data consist primarily of detector bias information. Because the system is at the end of its dynamic range, there is justification for the data exhibiting some nonlinear (compression) effects. To fully characterize CN, it is highly desirable to apply a steady-state signal to the instrument (such as an integrating sphere) so CN appears on top of a signal that is removed from either end of the dynamic range. When data of this type are available from ETM+, significant improvement can be made on both the characterization and correction algorithms.

3.4.4.1.2 Inputs

- 0R Image Plus IC
- Trended CN parameter values for each detector LM (to avoid using known bad data in the correction process)

3.4.4.1.3 Outputs

- CN corrected 0R Image Plus IC

3.4.4.1.4 Algorithm

This section describes two methods for removing CN: the subtractive method and the filter method. The operator will have the ability to choose the method. However, the

subtractive method can only be used on the components that are locked in frequency, phase, and magnitude to start of scan. All CN components can be removed using the filter method. When the subtractive method is invoked simultaneously with the filter method, the filter method will only be applied to the components that are not removed by the subtractive method.

For both methods, parameters are needed from the Characterize CN Database. These data are available on a scan-by-scan basis. This algorithm will use the data available from the most recently acquired 20 scenes in that database. For each CN component and each detector, the frequency estimates will first be smoothed by a 3-point median filter to remove outlier noise from the estimates. The mean, max, min, and standard deviation of the frequency for each component will be calculated (giving an average frequency estimate for the last 20 characterized scenes). If the difference between max and min for a frequency component is less than 1.5×10^{-5} cycles/mf for a component, the frequency is stable enough for a subtractive operation. The phase for that component is then also processed in a similar manner. If the difference between min and max is less than $\pi/20$ radians, the phase is also stable enough for subtraction across scans. Finally, the same procedure is applied to the magnitude component. If the range of the magnitude variation is less than 10% of the peak value, it is stable enough for subtraction across scans.

1) Subtractive Method

1.1) For the CN components that meet the criteria given above for all three parameters, the subtractive method may be used for noise removal. This is completed by simply constructing a sinusoidal waveform with the average frequency, phase, and magnitude calculated above. This waveform is then subtracted from the scene data. Because it is assumed that the gap (if any exists) between scene and calibration data is known, this knowledge can be used to correct the calibration data as well. This is completed by simply inserting the proper amount of phase shift into the sinusoidal function and then subtracting it from the cal data. Data flagged by the LM should not be corrected.

1.2) Situations will most likely also occur in which CN components are frequency locked to start of scan, but are not locked in phase or magnitude. For these situations, it will be impossible to use the subtractive method of correction on normal day scenes unless phase and magnitude can be estimated on a scan-by-scan basis from the calibration shutter interval. This procedure has not been successfully applied to L4 or L5 data due to the small magnitude of the CN and consequential low SNRs.

For band 8, the Pan band, which is known to exhibit a severe (later [1998] reduced significantly with a power supply rework) CN problem at the sampling frequency, the subtractive method can be simplified for this component. Because the frequency is known, only the phase and amplitude need to be determined. Because the noise is at the Nyquist rate, only 0 or 180 degrees phase shifts are possible. Unfortunately, phase and amplitude vary scan by scan and, therefore, need to be calculated for each scan.

The shutter region is used to do this. Using the approx. 500 mf bias window (as in Process IC Refl.), calculate the average values of the odd and even mf's separately. Whichever result is less will determine the mf's that are to be corrected. The difference between the averages indicates the peak-to-peak amplitude of the noise and the amount of correction to be applied. For example, if the odd mf values are lower than the even mf values by 11.7 DN, all odd mf values are increased by 11.7 DN. If this increase causes a DN value to exceed 255, that value should be limited to 255.

1.3) FASC scenes provide an almost ideal data type for characterization of CN. Estimates of frequency, phase, and magnitude can be made for each scan. Thus, the subtractive approach is a viable alternative for removal of CN from these data sets.

1.4) PASC scenes will provide another alternative for the characterization of CN. These scenes will have sharp transitions that may corrupt the FFT estimation procedure. However, it is anticipated that these scenes are also candidates for the subtractive method of CN removal.

2) Filtering method

2.1) By far, the majority of the CN components are not locked in frequency, phase, or magnitude. Because these parameters are impossible to measure on a scan-by-scan basis for normal day scenes, an alternative method of CN correction must be available. This approach uses a notch filter to remove CN from data. Fortunately, CN components are all narrowband, nearly sinusoidal. Therefore, the notches employed in this method can be quite narrow so a minimum amount of desired information is rejected. When the subtractive approach is used in conjunction with the filtering approach, the filtering approach will only notch the CN components that are not addressed by the subtractive approach. The notches used are Gaussian in shape. This is completed to minimize any artifacts possibly generated by the filtering approach and allows design of the filter using only two parameters.

2.2) The Fourier domain filter is designed in the following manner. As described above, data from the CN archive that have been median filtered are used. The estimated average frequency of the CN component defines the center frequency of the notch. The notch width is determined by the standard deviation of the frequency of the CN component. If the standard deviation of the frequency is greater than frequency resolution of the discrete Fourier transform for one scan of data, that standard deviation defines the standard deviation of the Gaussian notch. If the standard deviation of the CN frequency component is less than the frequency resolution of the discrete Fourier transform (which will be the case for many CN components), the standard deviation of the filter is given as a function of the distance the frequency of the CN component is from a discrete frequency calculated by the discrete Fourier transform. To elaborate further, the discrete Fourier transform calculates the energy present in the waveform at discrete locations in the continuous frequency spectrum. If a frequency component in the waveform is located exactly at one of the calculated frequencies, the transform works well. However, if the exact frequency location is between two adjacent

frequencies calculated by the transform, its energy will leak into those two components and several additional neighboring components. As a result, energy that is in reality located at only one frequency is perceived to be spread over a number of frequencies. The algorithm takes this into account by calculating the width of the notch according to the following formula, which is a function of the distance the actual frequency component is from a frequency value calculated by the discrete Fourier transform.

$$(1) \quad \text{SIGMA} = 2 * \text{DELTA F}$$

where

SIGMA = the width of the notch

DELTA F = normalized absolute distance from FFT frequency (range 0 to 0.5)

When DELTA F = 0, the CN component frequency is exactly one of those calculated by the FFT, and only that frequency is notched out. For all other cases, the notch becomes wider than only one calculated FFT value.

As implied in the above discussion, the implementation of this method is completed in the Fourier domain. The notch filter is simply of vector with unity value everywhere except near the notches. At these locations, the Gaussian functions defining notches (which are also normalized to unity amplitude at the center frequencies) are subtracted from unity to define the notch filter. A separate filter is defined for each detector. A scan line of data is transformed via an appropriate FFT algorithm, is multiplied by the filter vector, and then inverse transformed to obtain the desired result. Because gaps will exist in the data stream from ETM+ (and do, indeed, also exist in L4 and L5 TM), the filter is applied to individual scan lines and to individual calibration intervals. Unfortunately, the lengths of these intervals are not powers of two and so do not lend themselves to the most efficient FFT algorithms.

This algorithm may be applied to any type of data, including day, night, PASC, and FASC data.

Figure of Merit

3.4.4.1.5 Evaluation

1. Because CN has a small magnitude and is difficult to observe, evaluation of the algorithm performance is best implemented on data sets that have very homogeneous regions: night, PASC, and FASC data. A qualitative appraisal of performance can be made through a visual inspection of such imagery. The data should be stretched significantly so the CN artifacts can be observed. A more optimal approach would be to perform a side-by-side comparison of stretched data before and after CN correction. Additionally, a difference image can be obtained from the before and after data and evaluated for the presence of CN (which, ideally, is all that it should contain).

2. A quantitative evaluation of algorithm performance can be obtained in the following manner. Again, using a homogeneous image (night, PASC, FASC), extract a smooth portion of the scene. For night and FASC, this could be the entire scene. For PASC, extract the sun region. For each detector, average all the scan lines to compress all the data into one scan line. Calculate the FFT of the scan line. Median filter the magnitude of the FFT using a window width twice as wide as the 3-sigma width of the broadest CN frequency component to obtain a baseline spectra. Subtract the baseline spectra from the original magnitude spectra. Any peaks in this result that are more than 3 sigma above the standard deviation of the spectrum can be flagged and a database can be established to trend these frequency and magnitude values with time.
3. The above procedure can be repeated in a slightly modified fashion. This time, calculate the FFT of each scan line for each detector, and then average all of the spectra to obtain one average spectrum for that detector. The above procedure isolates the components with little phase variation from scan to scan, while this approach captures all periodic components. The resulting average spectra can then be processed in a manner as outlined above and the residual peaks can be tracked in a database over time.
4. Results in the quantitative evaluation outlined above can be compared with those obtained in the Characterize Coherent Noise algorithm (Section 3.2.4).

3.4.4.1.6 References

None

3.4.5 SEPARATE IMAGE AND IC DATA

3.4.5.1 Algorithm Description

3.4.5.1.1 Background

The image pixels and IC must be re-separated after corrections (e.g. ME) are complete. When we combined the two, we reversed (time oriented) the pixels on reverse scans. Therefore, when they are split, we must re-reverse (spatially orient) the pixels on reverse scans, and place the IC data (in the same order) into a separate file.

On input, the lines have been combined as such (in time order; all the reverse pixels are in forward time/reverse spatial order, and the IC data is in forward time/reverse spatial order and tacked on to the end):

```
fwd img(l to r)->bdc->dc rest->adc->lamp->dark->rev img(r to l)->
dark->lamp-> bdc->dc rest->adc->fwd img(l to r)->bdc->dc rest->
adc->lamp->dark-> rev img(r to l)->dark->lamp->bdc->dc rest->adc...
```

To get back to the OR data product format, we have to re-reverse the image pixels and the IC data on reverse scans, and split the IC data back out:

Image	IC
fwd:fwd img pixels (l to r)	bdc->dc rest->adc->lamp->dark
rev:rev img pixels (l to r)	adc->dc rest->bdc->lamp->dark

3.4.5.1.2 Inputs

- OR Image Plus IC (in memory, after corrections; reverse scans are time-ordered)
- Direction (of the line, fwd or rev)
- Nimg, NIC (number of image & IC pixels in the buffer)

3.4.5.1.3 Outputs

- Image Line (in memory or to a file, spatially oriented)
- IC Line (in memory or to a file, reverse scans are time-reversed)

3.4.5.1.4 Algorithm

Following are the steps to split up ONE line of image + IC:

- For a forward scan, copy Nimg pixels from OR Image Plus IC into Image Line, and read the next NIC pixels from OR Image Plus IC into IC Line.
- For a reverse scan, copy Nimg pixels BACKWARD from OR Image Plus IC into Image Line, and copy pixels Nimg+1 to Nimg+NIC+1 BACKWARD from OR Image Plus IC into IC Line.

INTEGRATION CONSIDERATIONS

If more corrections are to be completed, keep the spatially-oriented data in memory; otherwise, write in to an intermediate file.

LANDSAT 7 CONSIDERATIONS

For L4/L5, IC data of reverse scans is NOT reversed, but for L7 it is.

3.4.5.1.5 Evaluation

Not applicable

3.4.5.1.6 References

None

3.4.6 APPLICATION OF RADIOMETRIC CALIBRATIONS

APPLY CORRECTION CURVE EQUATION /CONVERT DATA TO ABSOLUTE RADIANCE VALUES

3.4.6.1 Algorithm Description

3.4.6.1.1 Background

This section describes the application of the radiometric gains and biases to the image data. This process converts the raw or artifact corrected image data (in DN) to radiance (in W/m² sr mm). The operator has the ability to select the source of the gains and biases as well as to decide whether any relative gain or temperature sensitivity corrections are performed. The absolute detector-by-detector gains within the CPF are the source of the relative gain information used in the relative gain correction. Temperature sensitivity coefficients and reference temperatures, also in the CPF, are available to adjust the absolute gains if the operating temperature of the instrument during the acquisition being processed is different from the operating temperature to which the absolute gains apply.

3.4.6.1.2 Inputs

- ORc image and shutter data (floating point, DN).
- Operator Switches:
 - Gains to be used for processing
 - GAIN_SOURCE (CPF, IC, ...)
 - If CPF is selected, then which set of CPF gains:
 - CAL_PARM_SEL (CURRENT, POSTLAUNCH, PRELAUNCH)
 - Biases to be used for processing
 - BIAS_SOURCE (IC, CPF, ...)
 - Apply relative gain correction?
 - APPLY_RELGAINS (None, Band Average, Reference Detector)
 - Apply temperature sensitivity correction?
 - APPLY_TEMPCORR (Yes, No)
 - Instrument Bias (floating point, DN)
- Instrument Gains (floating point, DN/(W/(m²sr mm)))

3.4.6.1.3 Outputs

1R intermediate data (floating point, W/m² sr mm).

3.4.6.1.4 Algorithm

1. Apply basic equation:

(1)

$$L_{\lambda,d,b,l,s} = \frac{(Q_{d,b,l,s} - B_{d,b,l})}{G_{d,b}}$$

where:

$L_{\lambda,d,b,l,s}$ = the spectral radiance (in W/m² sr mm) for detector d in band b for line l pixel s

$Q_{d,b,l,s}$ = the level 0Rc quantized voltage (in DN) for detector d in band b for line l pixel s

$B_{d,b,l}$ = the Bias (in DN) for detector d in band b for image line l (constant across line)

$G_{d,b}$ = the Gain or Responsivity (in DN/(W/m² sr mm)) for detector d in band b (constant across scene)

2. Bias selection

BIAS_SOURCE = IC,

Use line-by-line, detector-by-detector "Process IC Data" algorithm provided biases.

BIAS_SOURCE= CPF,

Use detector-by-detector CPF biases (GROUP=Automated Cloud Cover Assessment (ACCA)_BIASES). The same bias value is used for every scan line for a given detector (i.e., the l subscript on B in the basic equation is removed).

BIAS_SOURCE = PASC,

Use detector-by-detector "PASC" algorithm-provided biases from the database for the nearest in time PASC scene. The same bias value is used for every scan line for a given detector, (i.e., the l subscript on B in the basic equation is removed, not implemented)

3. Gain selection

GAIN_SOURCE=CPF,

Use detector-by-detector gains contained in the current CPF (GROUP=DETECTOR_GAINS). Use "Current," "Postlaunch" or "Prelaunch" gains based on selection of "CAL_PARM_SEL."

GAIN_SOURCE = IC,

Use scene average detector-by-detector "Process IC data" algorithm-provided gains.

GAIN_SOURCE = PASC Facet 1, Facet 2, Facet 3 or Facet 4,

Use detector-by-detector gains based on evaluation of PASC fitting equations for the acquisition time of the scene being processed. (Valid only if fitting equation exists)

GAIN_SOURCE = FASC,

Use detector-by-detector gains based on evaluation of FASC fitting equations for the acquisition time of the scene being processed. (Valid only if fitting equation exists)

GAIN_SOURCE = IC Lamp 1 or IC Lamp 2,

Use detector-by-detector gains based on evaluation of IC fitting equations for the acquisition time of the scene being processed. (Valid only if fitting equation exists)

GAIN_SOURCE = GLC

Use detector-by-detector gains based on evaluation of GLC fitting equations for the acquisition time of the scene being processed. (Valid only if fitting equation exists)

4. Gain Corrections:

Two gain corrections are available: a relative gain correction and a temperature sensitivity correction. Section 3.5.1 describes temperature sensitivity correction. If the temperature correction is applied, the Temperature corrected Gains (GCOR) from Section 3.5.1 is substituted for G in the basic equation above.

Relative Gain Correction: The detector-by-detector relative gains are extracted from the current CPF gain values and the selected gains are adjusted to obtain the same relative gains as the current gains in the CPF.

- a. For the selected gain ($G_{sel,b,d}$), the detector-by-detector relative gains are calculated by ratioing them to the band average gain ($GBAR_{sel,b}$) or to the reference detector gain ($G_{REF_{sel,b}}$), depending on the operator selection of APPLY_RELGAINS. These are the observed gain ratios: $GR_{OBS,b,d} = G_{sel,b,d}/GBAR_{sel,b}$ or $G_{sel,b,d}/G_{REF_{sel,b}}$. The reference detectors are defined in the CPF in (GROUP=REFERENCE_DETECTORS).
- b. The desired relative gains ($GR_{DES,b,d}$) are calculated by the same method using the current CPF gains: $GR_{DES,b,d} = G_{CPF,b,d}/GBAR_{CPF,b}$ or $G_{CPF,b,d}/G_{REF_{CPF,b}}$.
- c. The selected gains are adjusted to have the desired relative gains: $G_{ADJ,b,d} = (GR_{DES,b,d}/GR_{OBS,b,d}) * G_{sel,b,d}$.
- d. These adjusted gains are used in the basic equation above.

3.4.6.1.5 Evaluation

None

3.4.6.1.6 References

None

3.4.7 RESCALE RADIANCE TO SCALED 8-BIT INTEGERS

3.4.7.1 Background

Historically, L1 Landsat TM products have been provided as 8-bit integer values. For L7 ETM+, this practice was continued for the fully processed level 1G data products, but the Level 1R products are provided in 16-bit integer format. In order to use the number of bits available for each data product effectively, the calibrated radiances (32-bit floating point) generated by Level 1R or Level 1G processing need to be rescaled. This algorithm performs that rescaling. The level 1R product rescaling occurs after the radiometric processing flow; the level 1G product rescaling occurs after the geometric processing is complete.

3.4.7.2 Inputs

For Level 1R:

- Floating point Level 1R intermediary product

For Level 1G:

- LMIN and LMAX values per band (from CPF)
- QCALMIN and QCALMAX (1 and 255, respectively)
- Floating point Level 1G intermediary product

3.4.7.3 Output

For Level 1R:

- 16-bit product

For Level 1G:

- 8-bit product

3.4.7.4 Algorithm

For Level 1R:

$$(1) \quad QCAL_{1R} = ROUND(L_{\lambda} \cdot 100)$$

Where:

$QCAL_{1R}$ = 16-bit integer radiance output value (DN)

$L_{i,1R}$ = Level 1R floating point radiance value (W/m^2 sr mm)

For Level 1G:

(2)

$$QCAL_{1G} = ROUND \left(\frac{(L_{\lambda,1G} - LMIN) \cdot (QCALMAX - QCALMIN)}{(LMAX - LMIN)} + QCALMIN \right)$$

Where:

QCAL_{1G} = 8-bit integer scaled radiance output value (DN)

L_{λ,1G} = Level 1G floating point radiance value (W/m² sr mm)

LMIN = radiance corresponding to QCALMIN (W/m² sr mm)

LMAX = radiance corresponding to QCALMAX (W/m² sr mm)

QCALMIN = DN value corresponding to LMIN (1 DN)

QCALMAX = DN value corresponding to LMAX (255 DN)

NOTE: QCAL=0 is reserved for fill pixels.

The rounded value is bounded (i.e., it cannot be greater than QCALMAX, or less than QCALMIN). If the band has a gain change in the scene, the low gain LMIN and LMAX values are used. If a pixel is saturated and flagged in the original Level 0R product, it is set to LMAX value in the level 1R processing.

3.4.7.5 Evaluation

None

3.4.7.6 References

None

3.4.8 POST-1R CORRECTION OF RADIOMETRIC CHARACTERISTICS

3.4.8.1 DROPPED LINES AND INOPERABLE DETECTORS

3.4.8.2 Algorithm Description

3.4.8.2.1 Background

Certain image artifacts, such as those due to dropped lines or inoperable detectors, cannot be minimized effectively until after radiometric calibration (Level 1R) takes place. Each "Post L-1 Correction" should be selectable based on how the current scene is to be further processed/analyzed. The selectable options include substituting an interpolated value for the corrupt data (the "pretty picture" method), marking bad data with a predetermined synthetic pattern in the image (to observe how corrupt data propagates through later modules), or allowing the bad data to pass through unchanged. If selected for substitution or replacement, corrections can be handled in the scene's image file at the same time, reducing processing Input/Output (I/O) overhead.

In general, these corrections will be applied to the image data only. Calibration data that have been corrupted will not be changed; those Cal data mf's marked as "bad" by the Characterize Dropped Lines, Characterize Saturation Effects, or Characterize Inoperable Detectors modules will simply be identified in a report for later evaluation and trend analysis.

3.4.8.2.2 Inputs

For both artifacts:

- Intermediate 1R Calibrated Image Data (floating point)
- Fill Value for substitution correction (radiance; from work order parameters)

For Dropped Lines:

- Dropped Line locations and extents in Image (from LM)

For Inoperable Detectors:

- Inoperable Detector list (from the CPF)

3.4.8.2.3 Outputs

- Post-Calibration Corrected 1R Image Data (scaled 16-bit integer)

3.4.8.2.4 Algorithm

1. Load Intermediate 1R Image.

2. IF: Perform Dropped Line Correction = Y,
 THEN: Load Dropped Line Locations and Extents,
 FOR: Every dropped line segment in the scan
 IF: An entire Mf is dropped, THEN:
 IF: Substitute/Interpolate = S, THEN:
 Substitute Dropped Line fill values in Dropped Line Locations, for appropriate extents.
 ELSE IF: Substitute/Interpolate = I, THEN:
 Search through previous scans until a good scan line is found.
 Search through next scans until a good scan line is found.
 Substitute DN resulting from cross-scan linear interpolation between the previous and next good scan line.
 ELSE IF: A Minor Frame is dropped, THEN:
 IF: Substitute/Interpolate = S, THEN:
 Substitute Dropped Line fill values in Dropped Line Locations, for appropriate extents.
 ELSE IF: Substitute/Interpolate = I, THEN:
 For Detector, i, in the segment, i from 1 to 16:
 Avg_Prior(i) = Average of Detector i's DN values from three mf's before dropout.
 Avg_Post(i) = Average of Detector i's DN values from three mf's after dropout.

Perform Linear interpolation between Avg_Prior(i) and Avg_Post(i). Fill dropped mf with appropriate interpolated values. /* NOTE: This approximation, while not computationally intensive, will result in dropped line edges that allow resampling of the region to occur without incorporating artificially sharp transitions. */
 If the segment is on the left edge of the image, just fill with Avg_Post; if on the right, fill with Avg_Prior.

NOTE: The default state for bch uncorrected errors (which result in blocks of mf's corrupted that are generally less than a full scan) is Perform Correction = Yes. The default state for full lines lost (through Major Frame (MF) sync loss) is also Perform Correction = Yes.

3. IF: Perform Inoperable Detector Correction = Y,
 THEN: Load Inop. Detector Locations and Extents.
 IF: Substitute/Interpolate = S, THEN:
 Substitute Inop Detector fill values in Inop Detector Locations, for appropriate extents.
 ELSE: For each Inop Detector:
 IF: Detector = 1 or 16, THEN: Substitute DN of adjacent cross-scan detector

(i.e., 2 for 1, or 15 for 16) within same scan line
ELSE: Substitute DN resulting from cross-scan adjacent detector linear interpolation.

NOTE: Lines from adjacent detectors must not be flagged as dropped, saturated, or inoperable.

3.4.8.2.5 Evaluation

Not applicable

3.4.8.2.6 References

None

3.4.9 STRIPING

3.4.9.1 Algorithm Description

3.4.9.1.1 Background

This function is intended to remove residual striping (detector-to-detector gain and offset variations within a band) from ETM+ level 1R data. The application of the radiometric calibration to the ETM+ data (i.e., the generation of the level 1R data) is intended to remove the detector-to-detector variations in gain and offset, effectively de-striping the data. As Detector-to-detector variations are already taken into account explicitly through the generation of relative gains and bias from histograms, and these are included in the process of generating the applied gains and biases, this function should not be required in routine processing.

In this algorithm, the 1R data are linearly adjusted to match the means and standard deviations of each detector to a reference detector, or average of the detectors.

3.4.9.1.2 Inputs

- Scene Data
 - Normal Earth scenes (1R) - (Long Integer)
- Correction relative gains (Real, unitless) and bias (Real, DN) from histogram analysis performed on 1R data. (For relative gains, use band average or reference detector for normalization).

Parameters to set

- Normalization method -- Band Avg or Reference detector

3.4.9.1.3 Outputs

- Destriped 1R data (Long Integer)

3.4.9.1.4 Algorithm

This algorithm applies the relative gains and relative bias calculated by the histogram analysis procedure. The relative gains are calculated by ratioing the standard deviations. The application procedure is similar to the standard destriping Land Analysis System Software (LAS) algorithm, "DESTRIPE," although the correction gains and bias are calculated slightly differently. (NOTE: "DESTRIPE" calculates and applies correction factors). The application of these gains and biases, per detector per band, is expressed as follows:

$$(1) \quad Q_{cor} = (1 / GAIN_{rel}) * Q_{uncor} + BIAS_{ref}$$

Where:

Qcor= the corrected quantized radiance in DN

GAINrel = the relative gain factor per detector, from the histogram analysis program based on the ratios of the individual detector standard deviations to the standard deviation of either the band average or reference detector.

Quncorr = the uncorrected quantized radiance in DN

BIASrel = the relative bias per detector, determined by the histogram analysis program relative to either the average or reference detector

3.4.9.1.5 Evaluation

Not applicable

3.4.9.1.6 References

None

3.4.10 BANDING

3.4.10.1 Algorithm Description

3.4.10.1.1 Background

Banding, or "scan-to-scan striping," is a noise pattern that is sometimes visible in TM imagery due to ME. After scanning past a bright target such as clouds or snow, detector response is reduced due to ME. Thus, if the region past the bright target is uniform, data values obtained from the sensor will be slightly lower than corresponding values obtained on the following scan (because the following scan is in the opposite direction and therefore has yet to encounter the bright target.) As a result, scans in one direction will be noticeably darker than adjacent scans in the opposite direction. The banding pattern is very small in intensity, typically on the order of 1 to 2 DN.

The IAS will implement algorithms to correct for ME. If these algorithms prove ineffective, or it is desirable to evaluate the effectiveness of the correction, a correction for banding can be applied. Such a banding algorithm is described herein, and is based on the "Deband" process available in LAS.

The approach used in this algorithm is to apply a filter that has been optimized for detecting the banding pattern. Because of the small amplitude inherent to banding, the filter is adaptive so it only operates on the portions of the image where banding is detectable (i.e., in homogeneous, or "smooth" image regions.) The filtering operation produces an output image in which banding has been removed, as well as a difference image that gives an indication of where banding was detected, and its amplitude. An overall figure of merit is also calculated. The filtering operation is separable and computationally efficient.

3.4.10.1.2 Inputs

- 1R or 1Rc Image data

3.4.10.1.3 Output

- 1Rc data
- Global Figure of Merit (GBFOM)
- Corrected image (Difference Image (DIFFIM))

3.4.10.1.4 Algorithm

The filter implementation is outlined below. The pixel being filtered is given as $P1R(x,y)$, (i.e., x and y are the horizontal and vertical coordinates, respectively).

1. Find the Upper Data Point (UDP)

FOR (ALL x,y) DO

```

IF ( ABS((P1R(x,y)-P1R(x,y-16)) LE T ) THEN
  UDP = P1R((x,y-16) WHERE (4 LE T LE 8). Nominally, T=5
ELSE
  ; find valid data for correction when UDP corrupted by image data
  FOR n= -2, -1, 1, 2 DO
    IF ( ABS(P1R(x+10n,y-16) - P1R(x,y)) LE T ) THEN
      UDP = AVERAGE( P1R(x+10n,y-16))
    ENDFOR
  ENDIF

```

```

; If both conditions fail, do not use UDP to calculate Initial
; Correction Factor (ICF)

```

2. Find lower data point (LDP).

```

; Repeat Step 1, using P1R(x,y+16).

```

3. Calculate ICF.

```

; Create a mask as large as the image to use for calculating a GBFOM

```

```

FOR (all x,y) DO
  MASK(x,y) = 1
ENDFOR

```

```

IF (UDP and LDP) THEN BEGIN
  ICF(x,y) = .5*( P1R(x,y)-.5*(UDP+LDP) )
  ELSE IF UDP THEN
    ICF(x,y) = .5*(P1R(x,y)-UDP)
  ELSE IF LDP THEN
    ICF(x,y) = .5*(P1R(x,y)-LDP)
  ELSE PRINT, "No ICF at this point"
  PRINT, "Zero-out mask where no ICF exists"
  MASK(x,y) = 0

```

4. Obtain final correction factors, (CF(x,y)).

```

FOR all n=-25,25 DO
  IF ICF(x+n,y) THEN CF(x,y) = AVERAGE (ICF(x+n,y))

```

5. Subtract to obtain corrected image.

```

P1Rcorr(x,y) = P1R(x,y) - CF(x,y)

```

ENDFOR

6. Calculate localized measure of banding and GBFM.

$$\text{DIFFIM}(x,y) = \text{P1R}(x,y) - \text{P1Rcorr}(x,y)$$

IF (MASK(*,*) EQ 1) THEN GBFOM = STDEV (DIFFIM(*,*))

Thresholding is used in the algorithm as a method to ensure that correction factors are calculated from subregions of the image that have no significant edge component present. Due to the amplitude level of banding, a range of values from four to eight is suggested. Experimental analysis has shown T=5 to work well. Offsets of 16 are used to obtain data from the same detector in either the preceding or following scan.

For trending purposes, the GBFOM should be stored in a database for each image processed. A WRS scene that has known image structure that causes banding should be identified so on a periodic basis (perhaps 1 to 6 months) a DIFFIM can be saved for visual evaluation and comparison.

3.4.10.1.5 Evaluation

Because banding is not expected to be present due to improvements in ME characterization and correction, the primary use of this algorithm is to serve as an independent check on the accuracy of those algorithms. The GBFOM should be tracked for each scene processed by this algorithm. That trend should be observed for flatness (i.e., no change with time) and magnitude. Expected values for GBFOM should be less than 0.5 DN. If larger values occur, a flag should be set and the operator should be notified. Difference images should be stored, as mentioned previously, to serve as a baseline for algorithm performance. Periodic inspection of imagery with known structure that is conducive to producing banding should be performed on a periodic basis (perhaps once per month). Output images should also be inspected at that time for presence/absence of banding.

3.4.10.1.6 References

Helder D., Hood J., Krause D. An Adaptive Debanding Filter for Thematic Mapper Images. In-review for IEEE Transactions on Geoscience and Remote Sensing.

LAS "Deband" Processes. LAS Software. EROS Data Center.

D.Helder, B.Quirk, J.Hood. A Technique for the Reduction of Banding in Landsat TM Images. Photogrammetric Engineering and Remote Sensing. Vol 58. p 1425-1431. Oct 1992.

3.5 Miscellaneous Radiometric Processing Algorithms

Though not used in standard IAS processing, these algorithms could be implemented as the need arises.

3.5.1 CORRECT DETECTOR TEMPERATURE SENSITIVITY

3.5.1.1 Algorithm Description

3.5.1.1.1 Background

The temperature of the PFP Assembly (PFPA) of the ETM+ is not controlled. The detectors for bands 1-4 and 8 (pan) are on the PFPA, and as the instrument operates, the PFPA warms. The temperature of the CFP Array (CFPA) is actively controlled and has several temperature set points. Bands 5-7 are on the CFPA. Although it is intended for the ETM+ CFPA to operate at only its primary set point (91.4 K), this cannot be guaranteed for the life of the mission. Degradation of the radiative cooler could require changing to one of the warmer set points (95 K or 105K). Most detectors show some dependency of responsivity (gain) on temperature. This algorithm provides a linear correction for any observed temperature dependency. The correction can be applied to any gain used for processing ETM+ data, with the exception of the IC gains derived from the specific scene being processed.

3.5.1.1.2 Inputs

- Reference gains by detector, GREF, from CPF (GROUP = DETECTOR_GAINS) or alternate gain sources, e.g., gain fitting or CRaM, if available (DN/(W/(m² sr mm))).
- Reference temperatures by band, T₀, i.e., the focal plane temperature at which the reference gain applies, from CPF (GROUP = REFERENCE_TEMPERATURES) (°C)
- Temperature sensitivity coefficient by detector, R, from the CPF (GROUP = SENSITIVITY_TEMPERATURES)
- PFPA(°C) temperature and CFPA(K), T, from IAS Database (TEMP_SILICON_FP_ASSEMBLY and TEMP_CFPA_MONITOR)

3.5.1.1.3 Outputs

- Corrected gains, GCOR, (by detector)

3.5.1.1.4 Algorithm

1. For the scene being processed, average the focal plane temperature readings in the IAS Database that occur within the scene. The Silicon/PFP Temperature telemetry point (TEMP_SILICON_FP_ASSEMBLY) is used for bands 1-4 and 8; the CFP Monitor Temperature telemetry point (TEMP_CFPA_MONITOR) is used for bands 5 and 7.

2. Extract the reference gains, GREF, and reference gain temperatures, T0, to be applied to the scene being processed. The reference gains and reference gain temperatures currently only come from the CPF ((GROUP = DETECTOR_GAINS) and (GROUP = REFERENCE_TEMPERATURES)).
3. Extract the temperature sensitivity coefficients, R, from the CPF (GROUP = SENSITIVITY_TEMPERATURES).
4. Adjust each detector gain to the actual operating temperatures as follows:

$$(1) \quad GCOR = GREF * (1 + R * T) / (1 + R * T0)$$

Where:

R = band and detector dependent temperature sensitivity coefficient in °C-1 or K-1 (This is the inverse of the sensitivity coefficient as used by Jackson et al, 1985.)

T0 = band dependent reference temperature in °C for PFPA, K for CFPA*

T = band dependent current focal plane temperature in °C for PFPA, K for CFPA*

GREF = provided gain by band and detector at the reference temperature

GCOR = gain by band and detector corrected to the current focal plane temperature.

Note that an R = 0 translates to no temperature correction.

5. Output the adjusted gains for application to the scene being processed.

3.5.1.1.5 Evaluation

None required

3.5.1.1.6 References

Jackson, R.D. and B. F. Robinson. 1985. Field Evaluation of the Temperature Stability of a Multispectral Radiometer. Remote Sensing of Environment. 17:103-108.

3.5.2 GAIN FITTING FUNCTION

3.5.2.1 Algorithm Description

3.5.2.1.1 Background

The output of each of the calibration algorithms (Process IC, Process FASC, and Process PASC) is a time-tagged series of gains $g[t]$ (DN/radiance) and uncertainties in these gains $u[t]$ for each calibrator or segment thereof (e.g., lamp on the IC or facet on the PASC). This procedure takes these gain-time series and uncertainties, fits an equation to them to provide a continuous function giving the gain versus time, and evaluates the confidence intervals for this functional fit. The modeling process is intended to be semi-automated in that it will fit functions of increasing complexity to the data and flag possible outliers, discontinuities and poor fits to the data for the analyst to examine.

The gain-fitting Evaluation and Analysis (E&A) function will be performed at periodic intervals (perhaps once a week for IC data and PASC data and once a month for FASC data). Thus, typically, each time the function is run, there will be more than one data point added, perhaps 35 for the IC (7 days times 5 scenes/day) or 7 for PASC (7 days times 1 scene per day).

For a particular calibrator, the initial run of gain fitting will occur after the tweaking of the calibration algorithm has been completed and a number of calibrations (minimum of 5) have been performed with a "stable" algorithm--this will not be expected to occur before the second half of the Activation and Evaluation phase of the mission for the IC, and later for the new calibrators.

3.5.2.1.2 Inputs

- The gain values $g[t]$ by detector by band for a particular calibrator for all time points (or a subset) up to the present.
- The uncertainties $u[t]$ (if available) for each gain value by detector by band for all time points (or a subset) up to the present.

3.5.2.1.3 Outputs

- Gain equations $g(t)$ by detector by band for a particular calibrator for all time points (or a subset) up to the present.
- Confidence intervals for the gain equation by detector by band for a particular calibrator, evaluated at all time points (or a subset) up to the present.

Intermediate outputs to analyst:

- Outliers
- Possible discontinuities

3.5.2.1.4 Algorithm

Overall Strategy

Before gain versus time fitting, any temperature-dependent and icing-dependent gain effects need to be removed from the calibrator output or the instrument response data. Temperature sensitivity of the instrument response is a true gain effect and as such is incorporated into the gain values actually applied to the data. Calibrator temperature sensitivity effects, if present, need to be removed and not reincorporated into the gain values applied to the data. Historically, icing of one of the windows in front of the CFP has caused a diminution of the gain of band 6 with time, which is reversed by periodically heating up and outgassing the CFP. This icing has also caused an oscillation of the CFP band gains due to 1/4 wave interference effects. If present, this is a real gain effect and needs to be reincorporated into the gain values actually applied to the ETM+ data.

The initial step of gain fitting should be to display the data for the analyst-- a plot of each channel's gain versus time and the average of all of the operational detectors. This will allow the analyst to flag/remove outliers and possible discontinuities and determine how to proceed with the gain fittings. Examples: (1) if one detector behaves very different from the rest, it can be removed at this stage, (2) if an outlier is located, it can be removed and (3) if there is an obvious discontinuity in the data, the procedures to fit simple continuous functions to the data can be skipped. "Change point" detection tools are provided to aid the analyst in determining outliers and locating discontinuities in this initial screening operation. If the fitting run is not the initial run, the previous fit to the data should be overlaid with the old and new data at this point.

On initial use, go through the complete sequence of functions to fit and test. On subsequent runs, once a model has been established, the new point(s) will be tested for consistency with the current model (i.e., ensure the point(s) fall within the 95% confidence limits for an observation from the existing model). If the point "fits" the current model, the model will be refitted with the current form of the equation. If the point does not fit the current model, the current model and parameters will be kept, and the operator will be flagged for possible refitting of the model with a more complicated function or rejection of the outlier.

The type of model to start fitting the data with is a function of the data itself (e.g., for data without apparent discontinuities, start with a continuous function). Begin with a simple linear model and progress to exponential and combined exponential and linear models. At each stage, test the significance of regression, significance of parameters, and randomness of residuals. If residuals are non-random, refit with the next most-complicated function. NOTE: For the exponential functions, nonlinear model fitting is used, which is subject to converging on local minima. Routines have been developed to estimate and test a range of initial parameters to achieve convergence to the "best model."

The spline routine developed allows treating an entire series of data with or without discontinuities. This obviates the need to break up the data sets, and simplifies the gain-fitting procedure. In addition to fitting discontinuities in the data, this routine can be used if single continuous functions fail to fit the time series. This routine requires an estimate as to the location of any jumps (discontinuities), which will be provided by the prescreening algorithm. The "knot" locations will be determined through linear regression iterations. This routine allows using a second order polynomial spline or a decaying exponential function splined to second order polynomial splines. The conditions for using these two fitting functions are as follows.

Strictly Polynomial spline:

- For gain fitting when discontinuities are present
- As a last resort when no other function will fit, even if no discontinuities are present

Exponential to polynomial spline:

For gain fitting when a exponential function is initially present and has been fitted individually, then 1) a discontinuity appears, or 2) the function begins to deviate from an exponential or exponential plus a linear function. This function requires the equation for the previous exponential fit.

Detailed Flow: (5 steps)

1. Remove any temperature dependence of instrument responsivity (determined by characterize detector temperature sensitivity) and calibrator radiances (determined by evaluation of IC gains).

If the detectors have a temperature sensitivity, a linear correction is:

$$(1) \quad G(T_0) = G(T) \left\{ \frac{(1+R \cdot T_0)}{(1+R \cdot T)} \right\}$$

Where

R = temperature sensitivity coefficient in 1/ degrees C. (This is the inverse of the sensitivity coefficient as used by Jackson et al, 1985.)

T₀ = reference temperature in C,

T = temperature in C

G(T₀) = gain at the reference temperature

G(T) = gain determined at an arbitrary temperature T.

2. Remove icing-related gain dependence for bands 5 and 7, if any.

NOTE: L4 and L5 TMs showed this effect; an additional window was added to the ETM+ in an attempt to reduce it.

It is expected that if the effect is present in L7 ETM+ data, it will be at a reduced magnitude from L4/L5. This function is designed to handle the situation in which band 6 internal gain is solely dependent upon ice thickness; if the band 6 gain varies due to other reasons, this relationship will need to be updated with time.

NOTE: This gain dependence is a true instrument effect and although it is removed for gain fitting, it must be remodeled to provide the real instrument gain.

The gain dependence of band 5 and 7 is first determined by analyses of the bands 5 and 7 gains versus the band 6 gain within an outgassing cycle of the ETM+. The ratio of the observed band 6 gain to the initial band 6 gain (band 6 gain max) is an estimate of the transmission(T) of the ice in band 6. The thickness of the ice (d) is estimated as:

$$(2) \quad d = -\ln(T)/\alpha$$

Where

alpha = the attenuation coefficient of ice for band 6 wavelengths (~ 0.45/um).

This ice thickness is fitted as a linear function of time within the outgassing interval. The gain function for bands 5 and 7 is then fit to an equation of the form of:

For no absorption (band 5):

$$\text{Fit:} \quad \bar{G} = G + M \cos(ad + \theta)$$

yielding \bar{G} , M, a, θ

$$\text{Calculate:} \quad \bar{G}(0) = G + M \cos(\theta)$$

$$\text{i.e., } G(d) = G(0) - M \cos(\theta) + M \cos(ad + \theta)$$

$$\text{Correct: } G(0) = G_{\text{corr}} \quad \text{from } G(d) = G_{\text{act}}$$

i.e., the Correction Equation is:

$$G_{\text{corr}} = G_{\text{actual}} + M \cos(\theta) - M \cos(ad + \theta)$$

With absorption (band 7):

Fit: $\bar{G} = G + M \cos(ad + \theta) + bd$

yielding \bar{G} , M , a , θ , b

Calculate: $\bar{G}(0) = G + M \cos(\theta)$

i.e., $G(d) = G(0) - M \cos(\theta) + M \cos(ad + \theta) + bd$

Correct: $G(0) = G_{\text{corr}}$ from $G(d) = G_{\text{act}}$

i.e., the Correction Equation is:

$$G_{\text{corr}} = G_{\text{actual}} + M \cos(\theta) - [M \cos(ad + \theta) + bd]$$

In these equations,

$G(0)$ = gain at zero ice thickness

d = fitted ice thickness

$G(d)$ = gain at ice thickness d

\bar{G} = average of gain (bias of cosine)

M = amplitude of cosine

a = frequency of cosine

b = linear term added to cosine

θ = phase of cosine

NOTE: A more correct characterization of the icing effect correction has been developed and will be implemented here if time allows.

3. Compute band average gain

- a. Average gains across all detectors in a band (weighting by uncertainties of individual detector gain values) per time sample per band.
- b. Display data from all 16 detectors (plus average) in the band with previous fit (if available).
- c. Run prescreen routines to determine outlier and discontinuity locations.
- d. Remove outliers.
- e. Reaverage across all detectors without any identified outlier detectors.

4. Determine functional form of gain versus time equation.

NOTE: In the following description “discontinuity” refers to an immediate jump in the data, and “knot” refers to a functional change point in the data.

- a. Determine function to best model data.
 - * IF No Discontinuities and not previously fit with a spline, "simplefit.pro" will automatically execute the following steps:
 - o If previous fit is not available
 - + Start with linear fit
 - o If previous fit is available,
 - + test whether new points agree with previous fit, (evaluate previous fit and 95% confidence intervals for a single response at all new time locations)
 - + if new points fall within confidence interval
 - + start with previous fit
 - + if new points do not fall within confidence interval
 - + start with the next most complicated function, in order of complexity (i.e., linear, exponential, exp+linear, exp+spline)
 - * If discontinuities are present or previous fit was a spline
 - o start with a spline
- b. Model data with the chosen starting function

NOTE: Although the curve fitting routines will automatically calculate curve fits in order of complexity, the operator can override the final result if an intermediate result is desired instead.

- * If not starting with a spline, "simple_fit.pro" will calculate model by automatically executing the following steps:
 - o If starting function is linear
 - + Call "iaslinfit.pro" to calculate coefficients. This is the IDL function linfit modified by adding the calculation of confidence intervals and standard error of coefficients
 - o If starting function is exponential or exp+linear
 - + If latest fit was with same function
 - + use latest coefficients for starting values
 - + If not previously fit with starting function
 - + estimate starting values (with "estimate_exp.pro" and "findstartvals.pro")
 - + Call "iascurvefit.pro" to calculate coefficients. This is the IDL function curvefit modified by adding the calculation of confidence intervals and standard error of coefficients.
 - o Evaluate randomness of residuals
 - + If residuals are random, accept fit
 - + If residuals non-random
 - + go back to step 4b), and repeat with the next most complex function
- * If starting with spline, "parabola_spline_fit.pro" will calculate model by automatically executing the following steps:

- o Create the X array for the regression
 - + If not previously successfully fit with an exponential or spline
 - + create a linear column and 2 more columns: linear and parabolic before knot 1, and 0 after knot 1
 - + If beginning segment of data has previously been successfully modeled with an exponential
 - + create one column with the successful exponential fit evaluated at all time locations
 - + If data have been successfully modeled previously with a spline
 - + recreate the xarray from the previous fit, evaluated at all time locations of old and new gain data.
 - + Add a column for each discontinuity
 - + Add 2 more columns; linear and parabolic after knot 1, and 0 before knot 1
 - o Iterate on the location of knot 1 ranging from minknot to n-3. (Minknot is 3 for parabolic splines, minknot is the location of the end of the pure exponential fit for exponential+parabolic splines.)
 - + For each iteration, perform a linear regression with the X array as the independent variable and gain values as the dependent variable. Choose the knot 1 location that minimizes the residuals.
 - o Evaluate significance of coefficients, and remove columns of the X array that correspond to insignificant coef's.
 - o Repeat the previous 3 steps for every additional knot. Stop when a satisfactory fit is achieved.
 - o Calculate confidence intervals for the final fit
5. Fit each detector gain history with selected functional form using band average values as initial parameter estimates. Compute goodness of fit and uncertainties in parameters. Test if appropriate parameters are significantly different from 0. Compute residuals and evaluate randomness of residuals. Detectors with poor fits to selected model should be deleted from band average and the band avg refitted. Compute uncertainty functions in predicted values and mean value of gain function. Output to LDB gain function, and intermediate results necessary for calculating confidence intervals for each detector.

3.5.3 COMBINED RADIOMETRIC MODEL (CRaM)

3.5.3.1 Algorithm Description

3.5.3.1.1 Background

The CRaM is a method for combining and comparing the results from the various reflective band calibration sources for the ETM+. It generates a function that converts ETM+ data to absolute radiometric units. This function can also be used to recalibrate one calibration source relative to another (e.g., postlaunch recalibration of the PASC relative to the IC). For the ETM+, these sources include the three on-board reflective band calibration devices: IC, PASC and FASC. The IC has two lamps, a primary and a redundant. The primary lamp will be used predominantly; the redundant lamp will be used at 5-10% of the primary's duty cycle. The PASC has four separate facets. The bulk of the PASC acquisitions will be completed with two of the facets, with a third being illuminated only at certain times of the year. In addition, prelaunch calibration data and ground look calibration (GLC) data are available.

The CRaM will be used three different ways in processing: (1) to recalibrate one calibrator relative to another, (2) to combine the calibration results of each subcalibrator (e.g., lamp or facet) into a gain history for each calibrator assembly and (3) to combine the calibrations results of each calibrator into overall gain history.

In each case, the inputs to CRaM are gain time history functions $G(t)$ for a calibration device or subdevice. For a recalibration, inputs are the gain functions for the reference calibrator (e.g., internal calibrator and the destination calibrator, PASC facet 2 and the reference time for the recalibration.) For a combination CRaM, run input are the gain and uncertainty functions for all of the applicable calibration devices. These gain functions are generated by the gain fitting algorithm, which takes the discrete time outputs from each calibrator and fits a continuous function to them (with the possible exception of discontinuities).

When CRaM is run in the recalibration mode, the output is a multiplicative calibration factor (CF) determined at time t_0 to be applied to all calibrations from a given device. When run in the combination mode, the output is a discrete time series $G[t]$ of gain values. This discrete time gain series is fitted by the gain-fitting algorithm to obtain a continuous time function.

Part of the CRaM is an estimation of the accuracy of the radiometric calibration coefficients being supplied for the ETM+. The first order accuracy assessment will be based upon the consistency of the calibration achieved with the different sources.

3.5.3.1.2 Inputs

Recalibration mode:

Fitted gain functions and gain uncertainty functions from the reference calibrator and the target calibrator, per detector

- Time for recalibration (day since launch, Real)

Combination mode:

Fitted gain functions($g(t)$) and gain uncertainty functions for applicable calibrators(IC, FASC, PASC, GLC, and prelaunch data) or subcalibrators (the individual lamps of the IC or facets of the PASC)

3.5.3.1.3 Outputs

Recalibration mode:

Multiplicative calibration factors at time t for target calibrator, per detector; one per detector to be recalibrated (Unitless, Real)

Combination mode:

- Combined gain time series ($g[t]$) and uncertainties
- Degradation factor time series $DF[t]$ for calibrators
Flags indicating calibrators that failed to agree with majority and/or failure of all calibrators to agree

3.5.3.1.4 Algorithm

Recalibration mode:

1. Input externally fitted gain functions and uncertainty functions from reference and destination (to be recalibrated) calibrators (one gain function per detector).
2. Exercise gain and uncertainty functions for times $t=t_0$ in which each t_0 represents the day of data acquisition, since launch, for which the recalibration is desired.
3. Ratio reference gain at t_0 to destination gain at t_0 to obtain calibration factor. Compute uncertainty in calibration based on standard error propagation.
4. Output the calibration factors and uncertainties to a database.

Combination mode:

1. Input externally fitted gain functions and uncertainty functions for the calibrator or subcalibrators to be combined.
2. Exercise gain and uncertainty functions for times $t=t_0, t_1, t_2, t_3, \text{ etc.}$ in which each t represents the day since launch of the satellite. Compute correlation coefficients (r^2) between discrete gain values from each calibration source.
3. Test equivalency of predicted values from each calibration method, at each output t . Pairwise test whether the 95% confidence intervals for the predicted values overlap.
4. Majority rules:
10-dec-97
(a) If majority of measures agree to within uncertainties, calculate the best estimate of gain ($x\text{-best}$) as the weighted average of values for given t i.e.,

$$(1) \quad x - \text{best} = \sum_{i=1, N} w_i \cdot X_i$$

Where:

$$w_i = 1 \div u_i^2$$

and u is the uncertainty associated with an individual measurement i .

The uncertainty in x -best is,

$$u = 1 \div \sqrt{\sum_{i=1, n} w_i}$$

This formulation is valid if the multiple measurements agree within their uncertainties, and their fitting uncertainties represent the true uncertainties. If this is not the case, the uncertainty in the average value, weighted or unweighted, is less well-defined. If the values do not agree to within their fitting uncertainties, a flag should be set and the standard deviation of the mean of the values should be reported as the estimate of the uncertainty. (Taylor, J.R. 1982) 10-dec-97 (b) If no majority, calculate unweighted average of values.

5. If 4(a) occurs for the minority value, calculate the ratio of the majority average gain value to the minority value. This can be used to update this calibrators' effective radiances. If there is no agreement between all sources, set a flag so indicating, requiring examination of calibrators' results and possible normalization.

6. Store output array of CRaM gains and uncertainties, nominally one per detector per day since launch.

3.5.3.1.5 Evaluation

1. The output CRaM gain values are examined by the analyst and fitted with the gain-fitting algorithm.

2. The correlations between gain functions from the different calibrators are examined to identify calibrators with different behaviors.

3. The degradation factors are examined by the analyst, evaluated as to whether they describe a "reasonable" degradation behavior. If so, they are fitted and input to the appropriate calibration algorithm to adjust the output of that calibrator's gain calibrations.

3.5.3.1.6 References

None

Section 4 Processing Flows and Descriptions

The following process flows illustrate the algorithmic implementations for producing level 1R data products, performing radiometric characterizations with night scenes, and calibrations with FASC and PASC scenes.

Each process distinguishes the processing of IC data (in the upper half of the flow diagram) from the imagery (in the lower half of the flow diagram).

The symbols and terms in

Figure 4-1 are common to all flows.

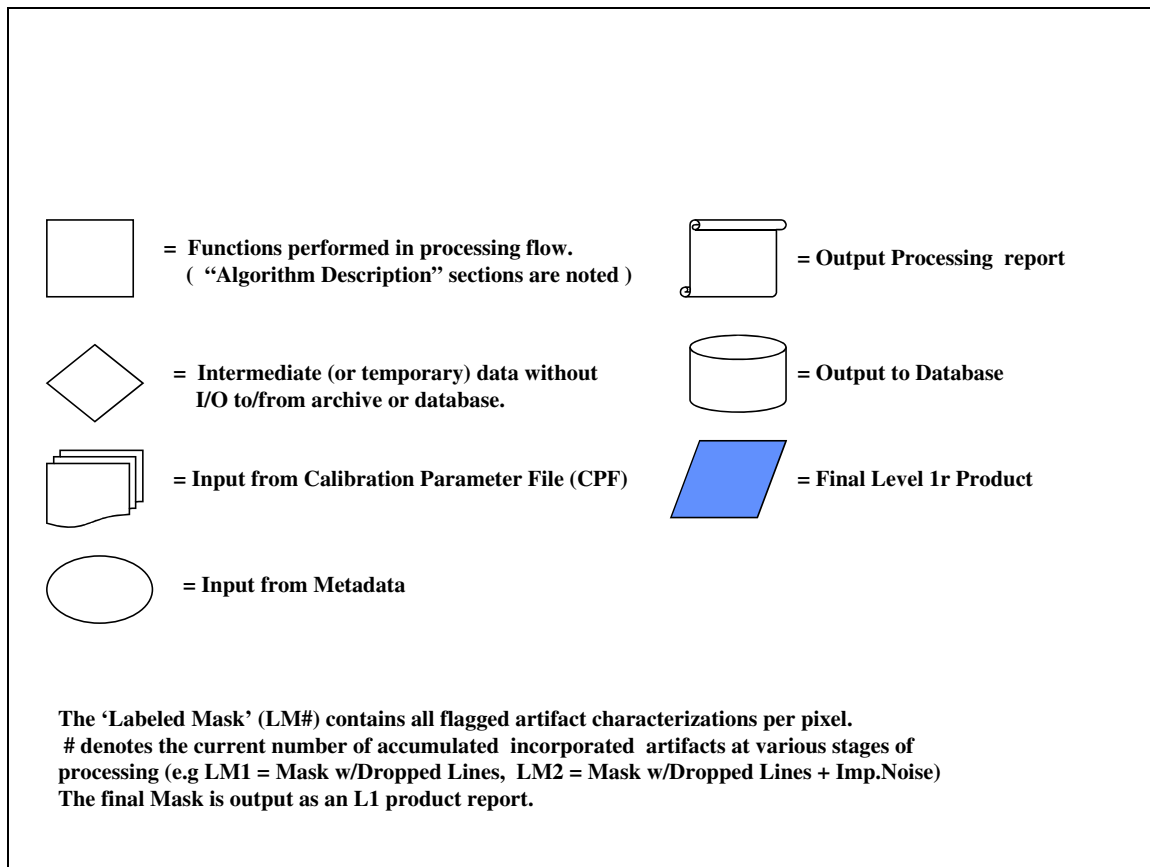


Figure 4-1. Symbols and Terms

4.1 Level 1R Processing (Day Scenes)

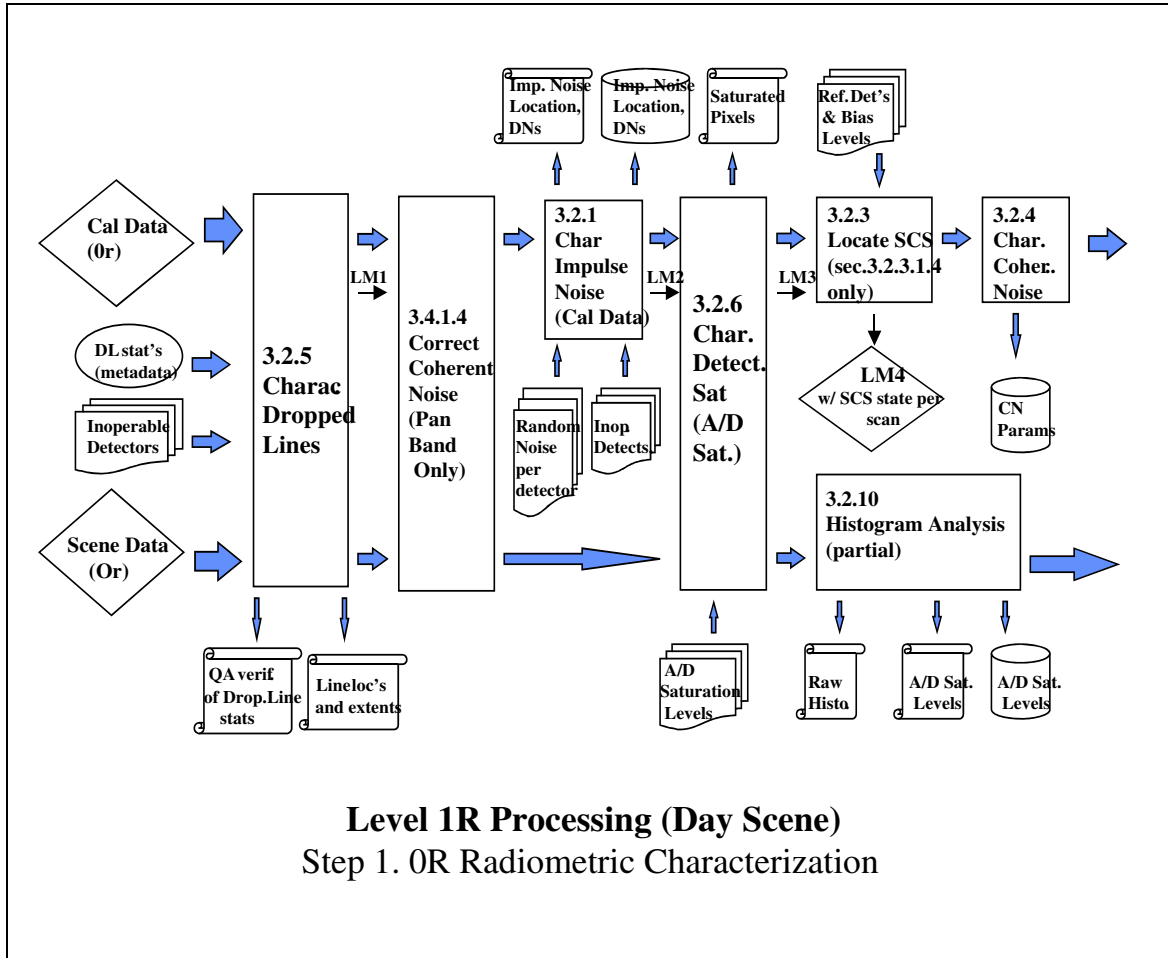


Figure 4-2. Step 1. 0R Radiometric Characterization

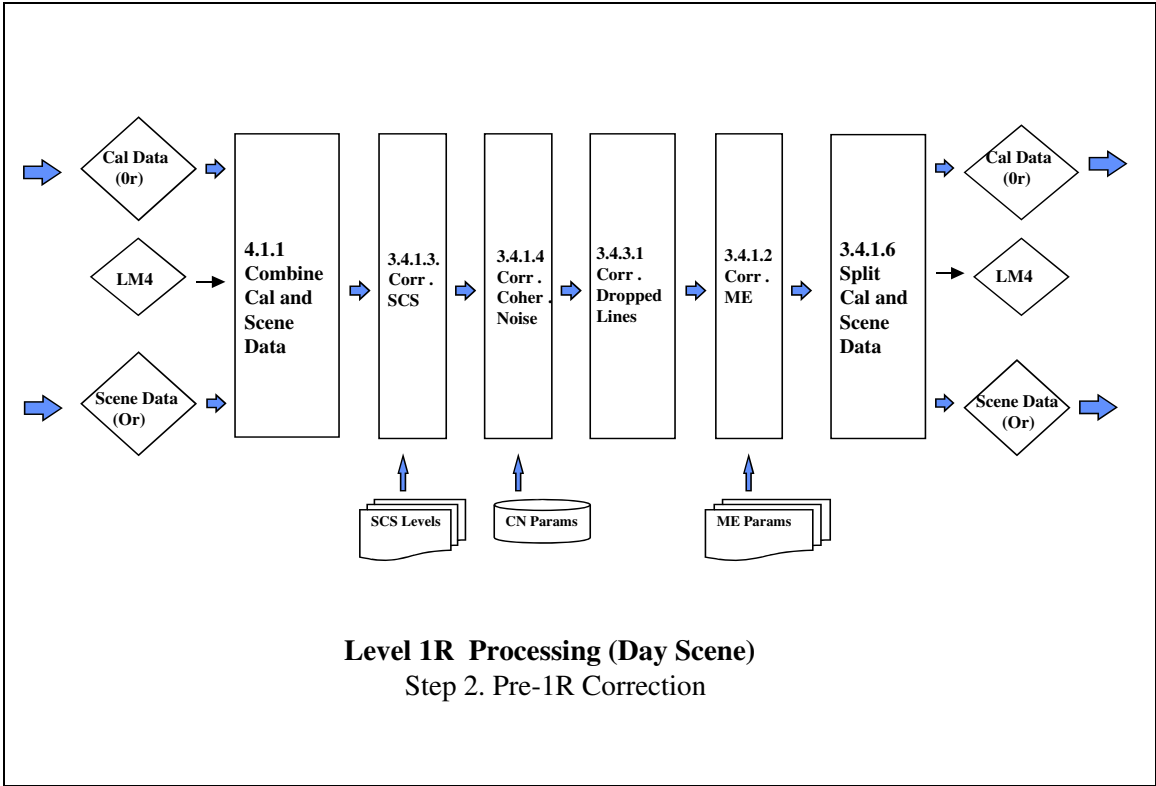


Figure 4-3. Step 2. Pre-1R Correction

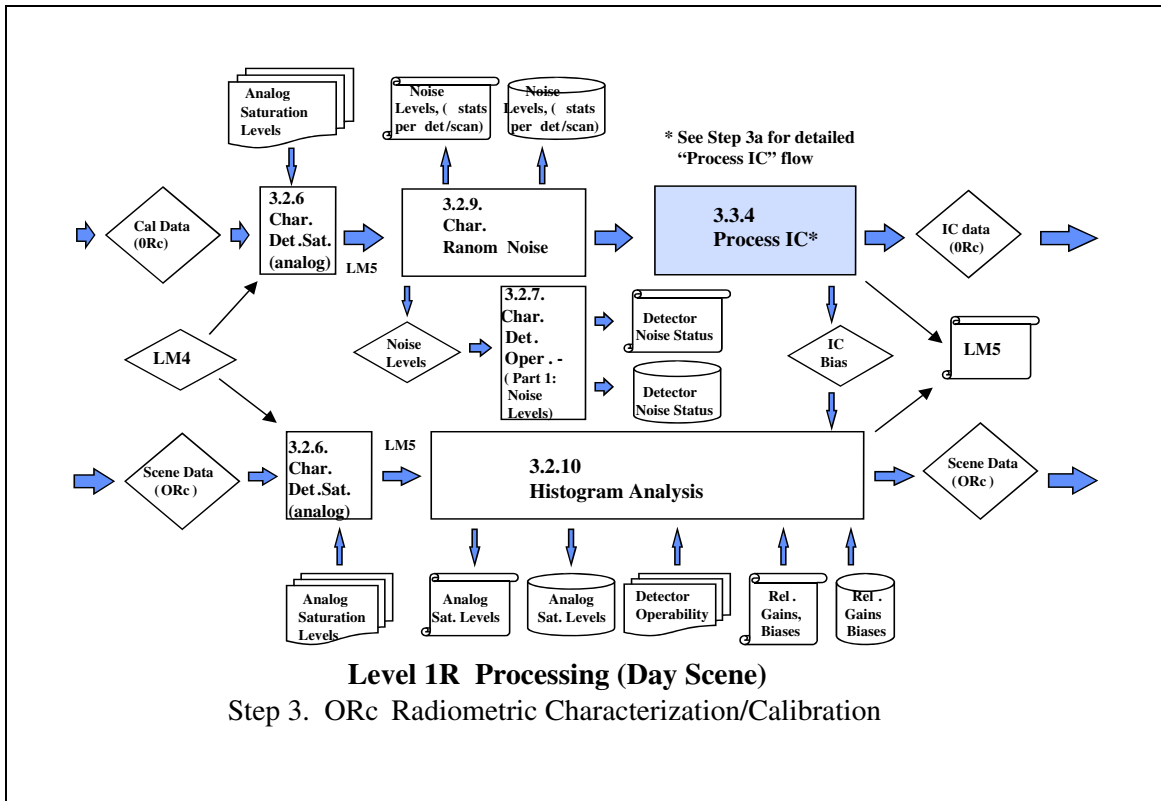


Figure 4-4. Step 3. ORc Radiometric Characterization/Calibration

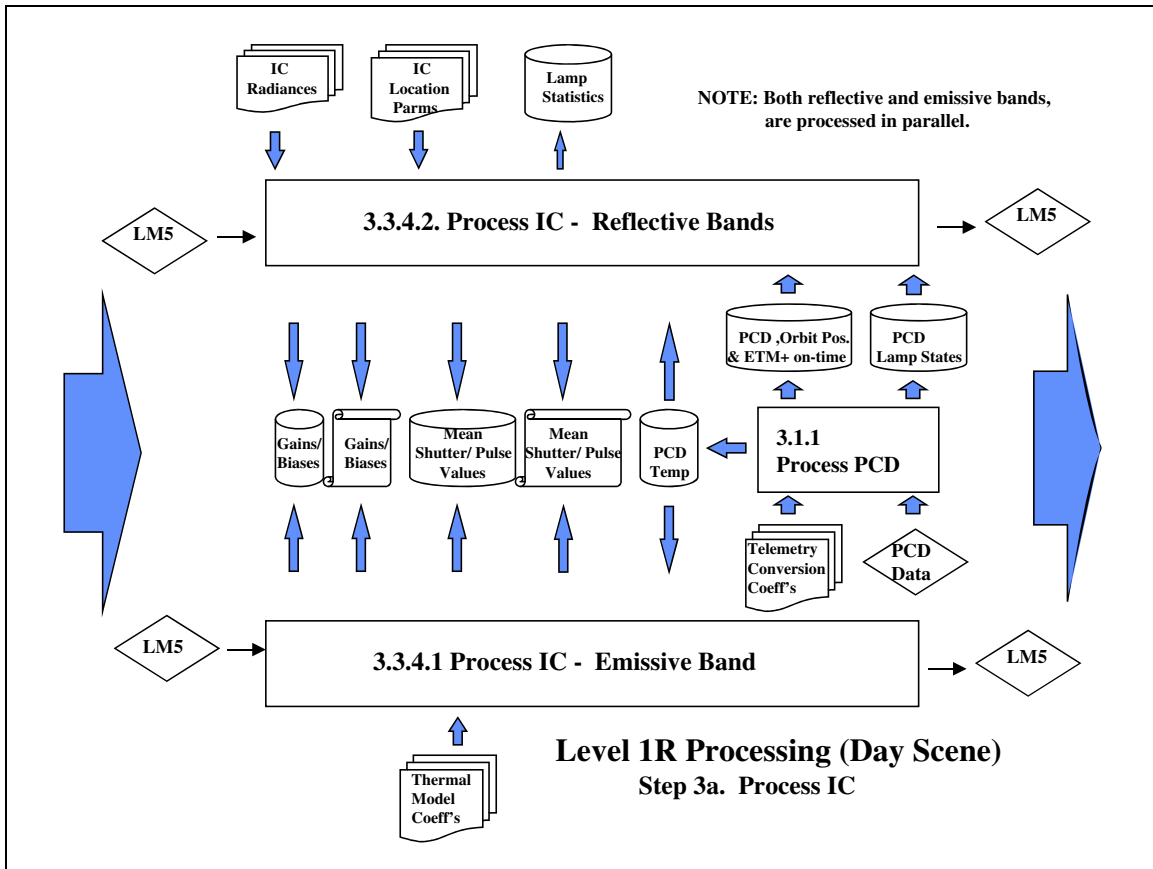


Figure 4-5. Step 3a. Process IC

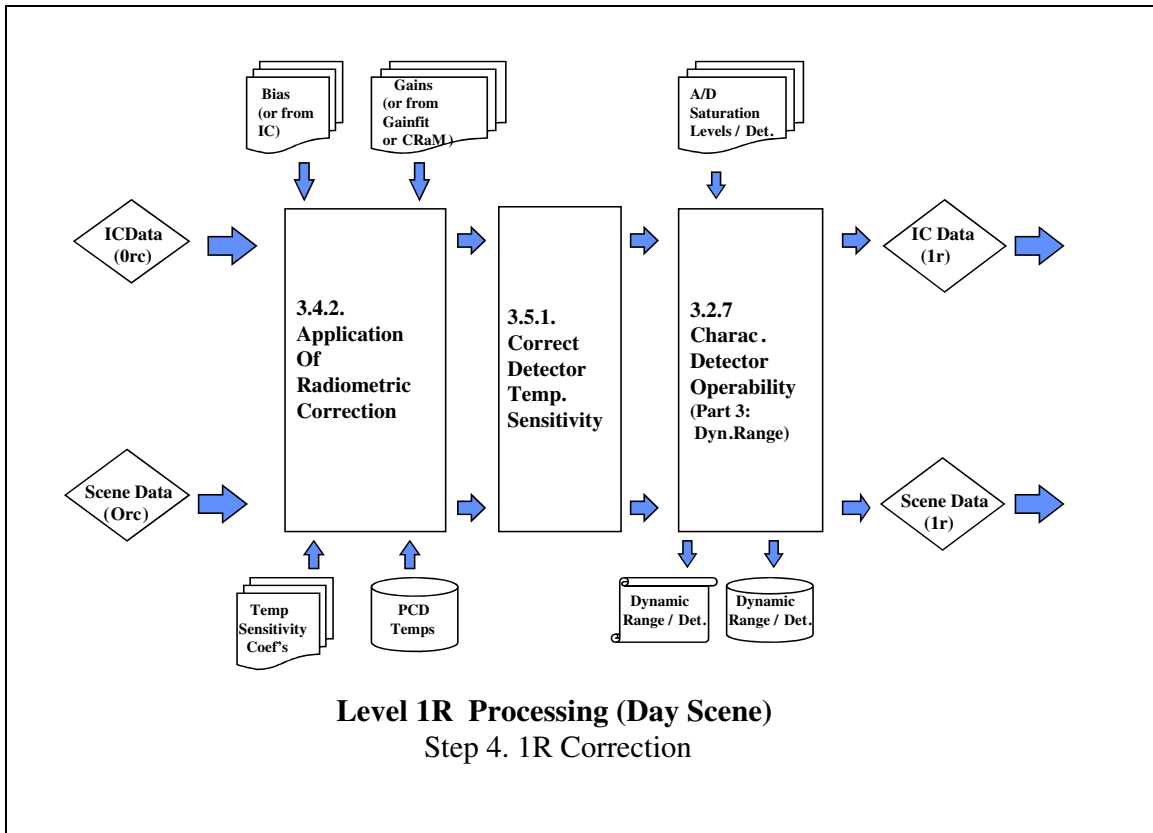


Figure 4-6. Step 4. 1R Correction

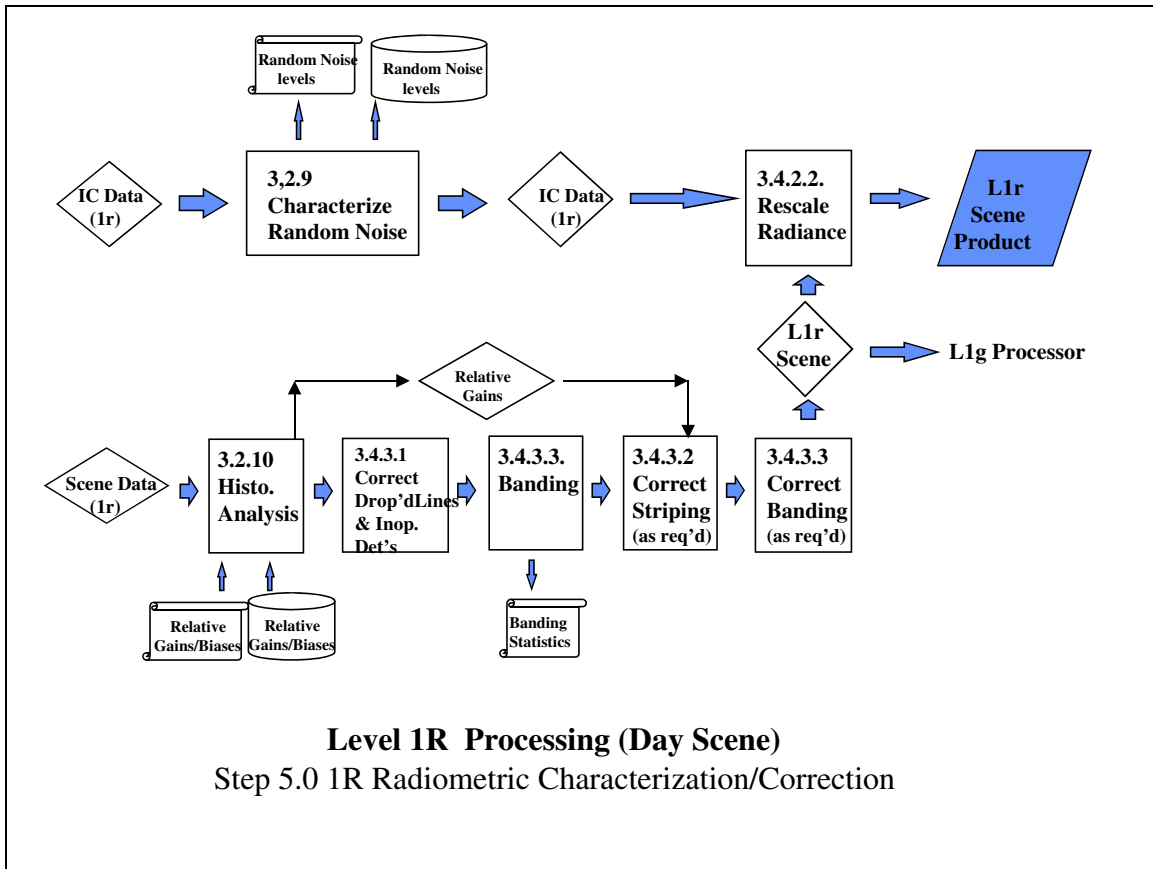


Figure 4-7. Step 5. 1R Radiometric Characterization/Correction

4.2 Night Scene Processing/Characterization

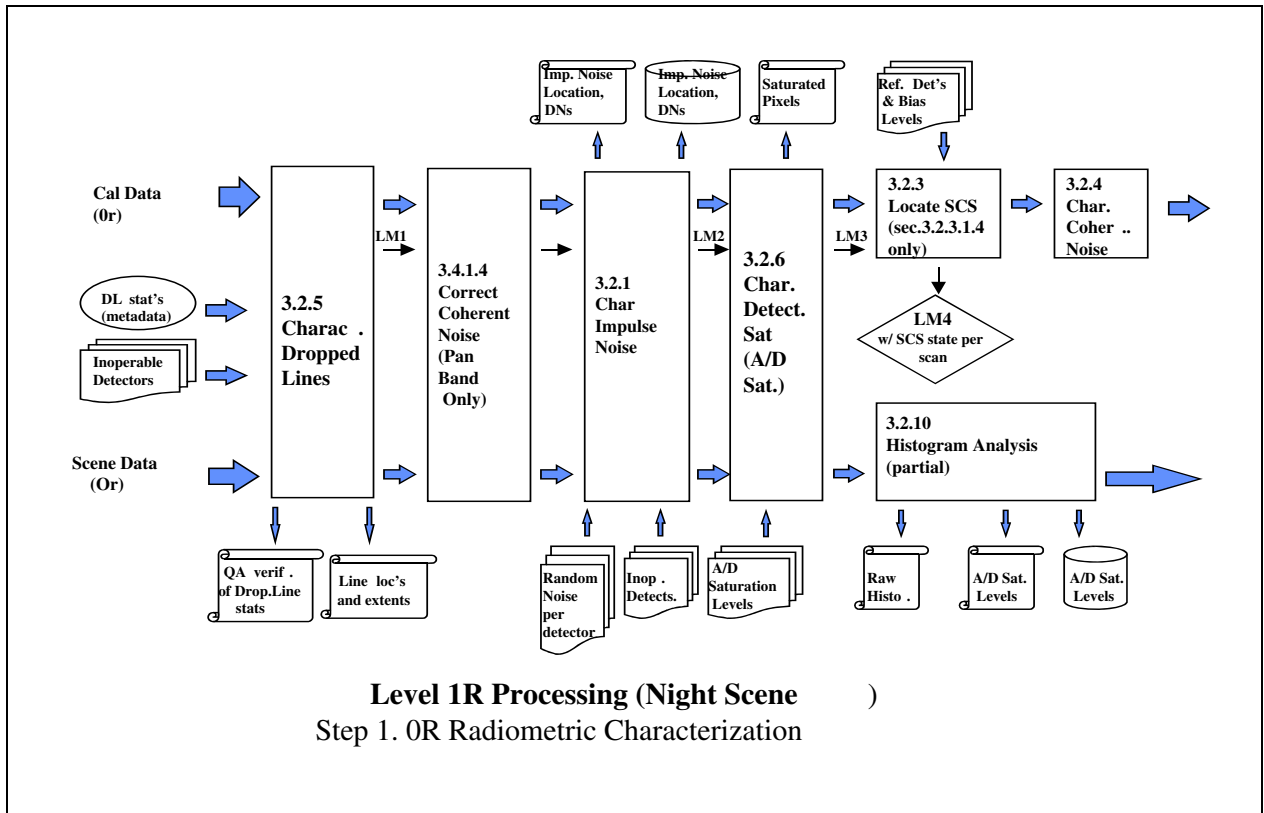


Figure 4-8. Step 1. 0R Radiometric Characterization

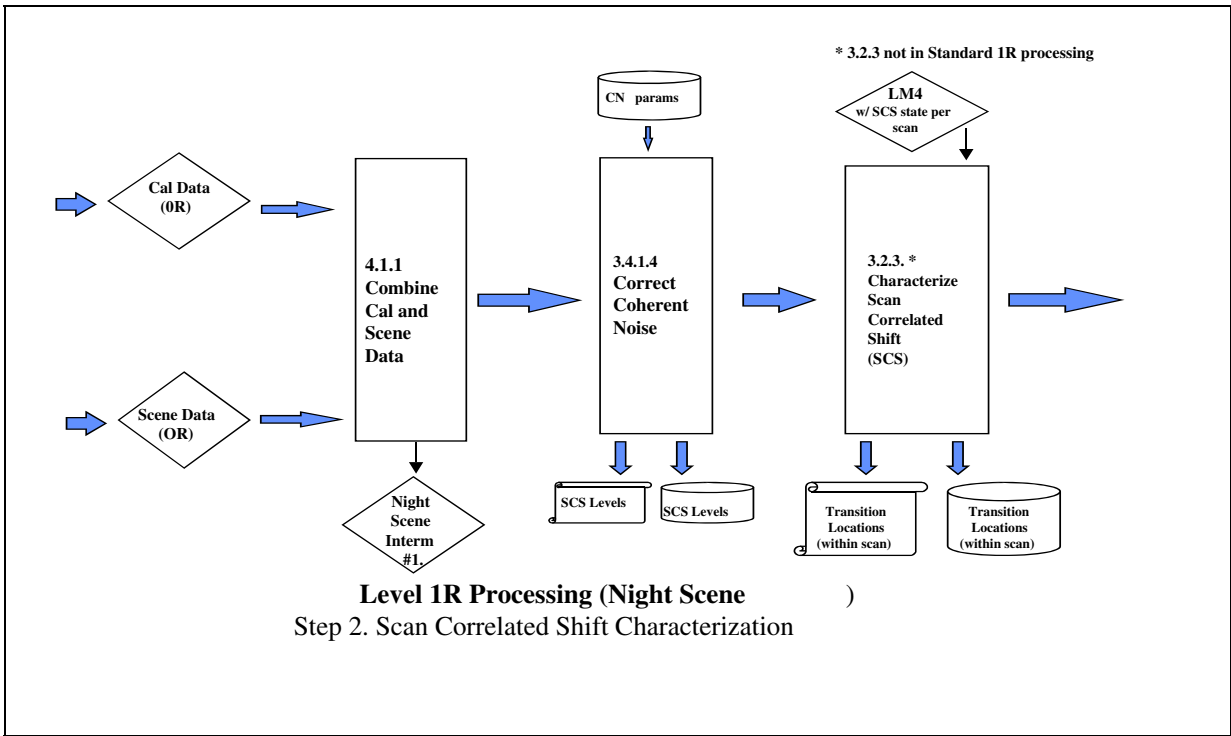


Figure 4-9. Step 2. Scan Correlated Shift Characterization

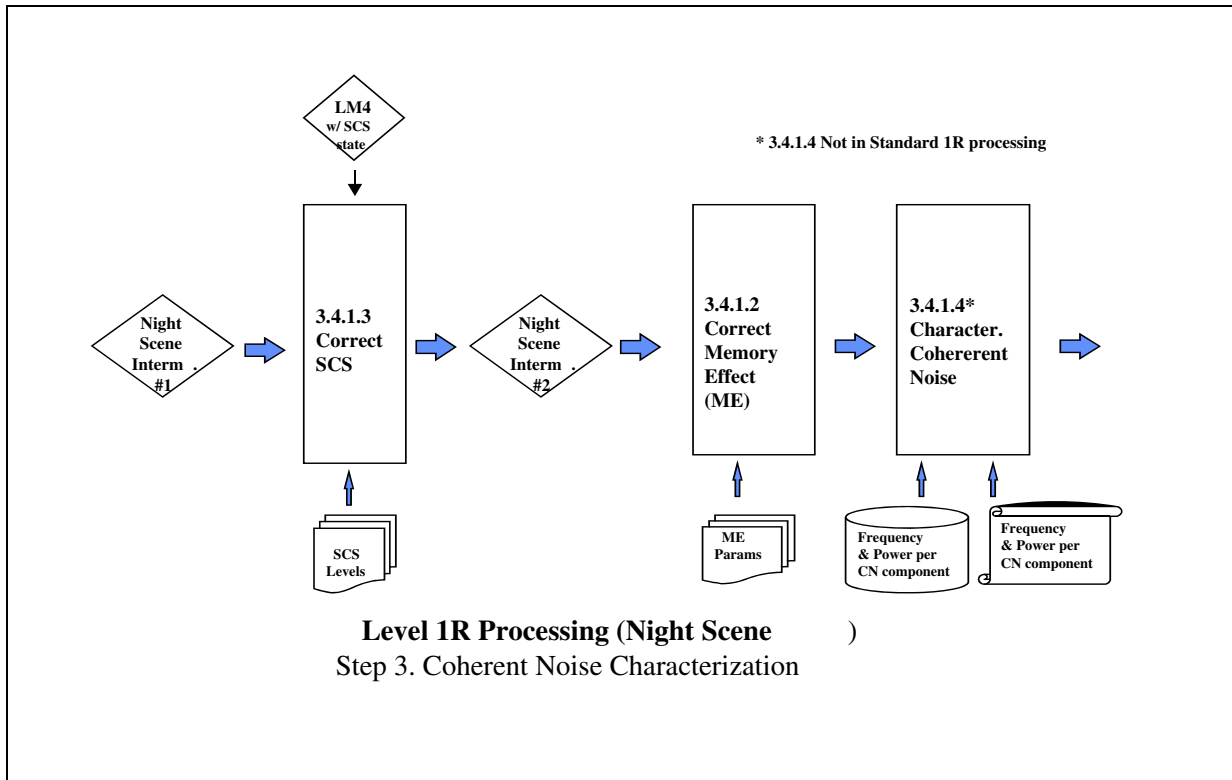


Figure 4-10. Step 3. Coherent Noise Characterization

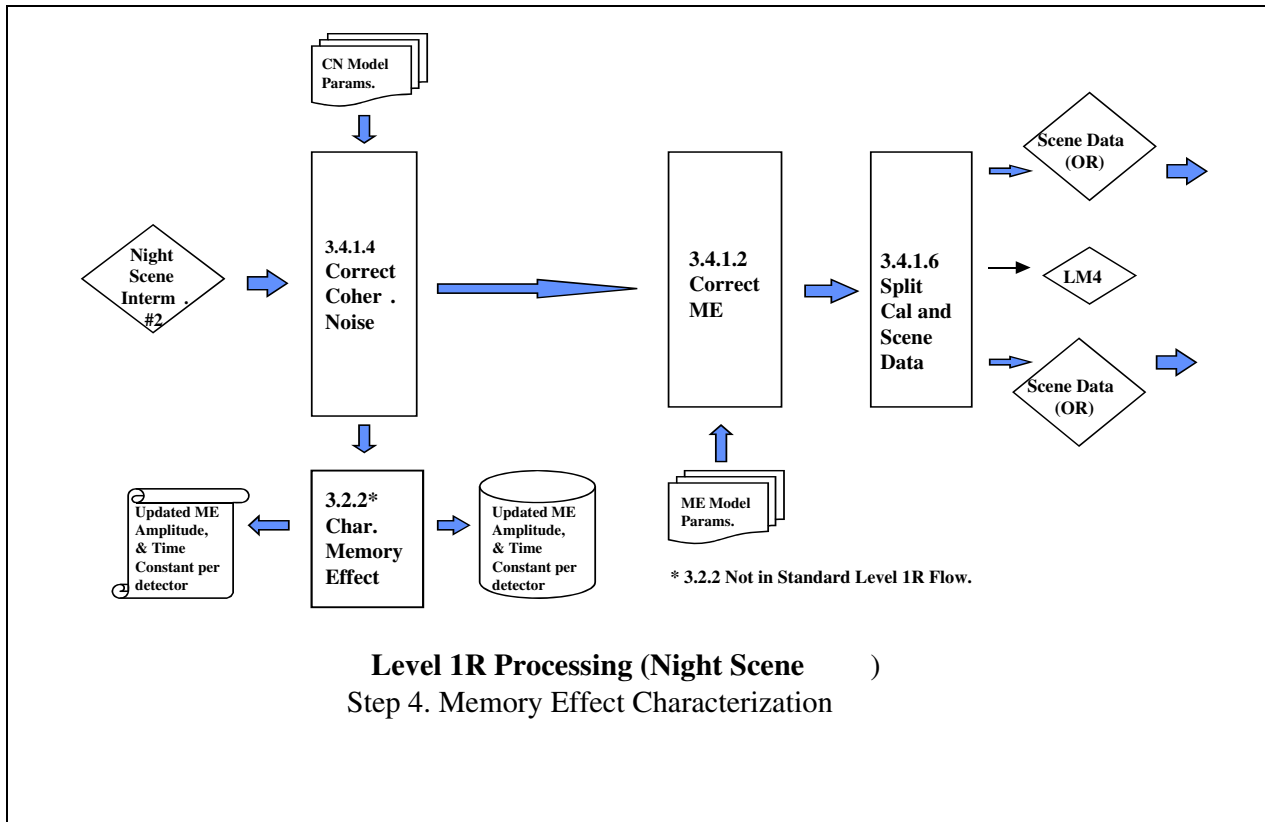


Figure 4-11. Step 4. Memory Effect Characterization

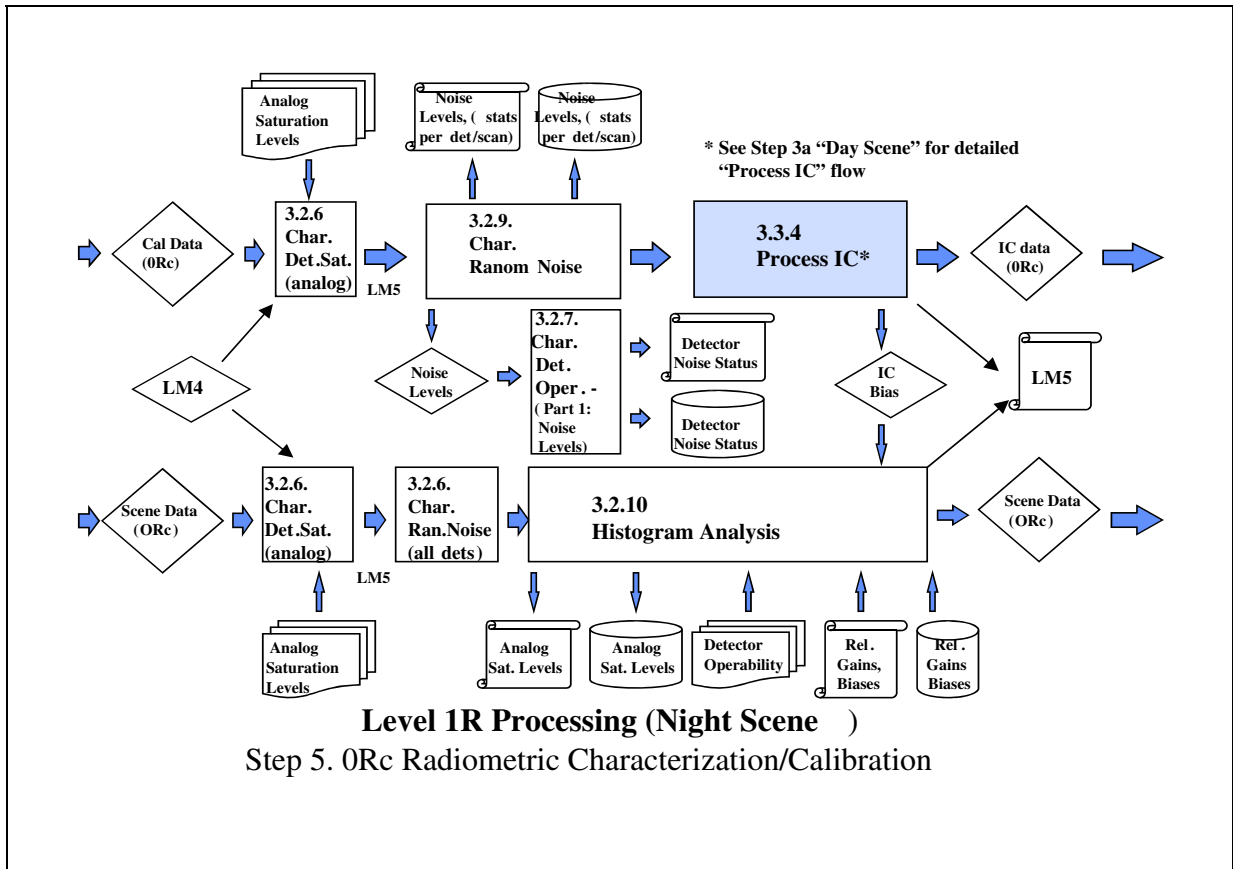


Figure 4-12. Step 5. 0Rc Radiometric Characterization/Calibration

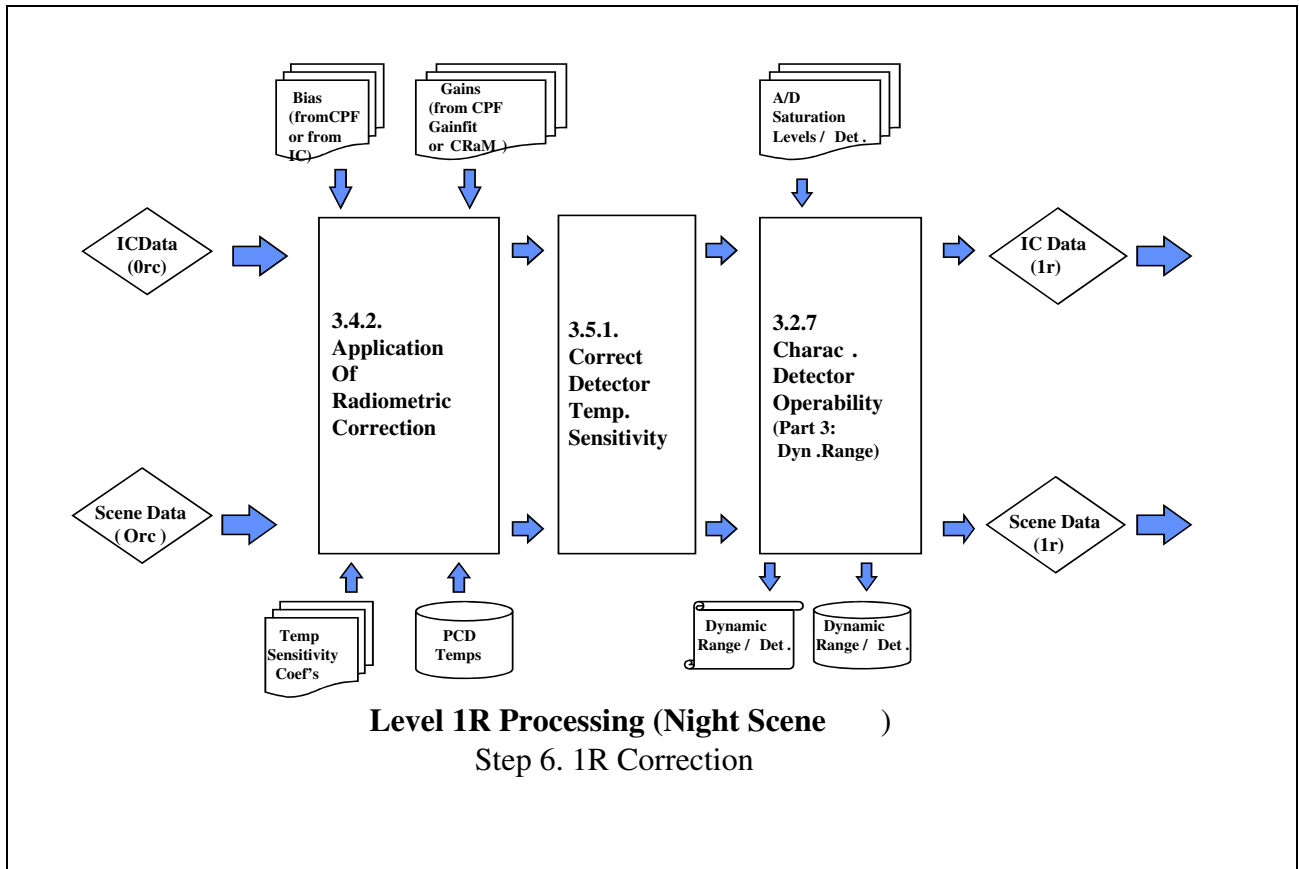


Figure 4-13. Step 6. 1R Correction

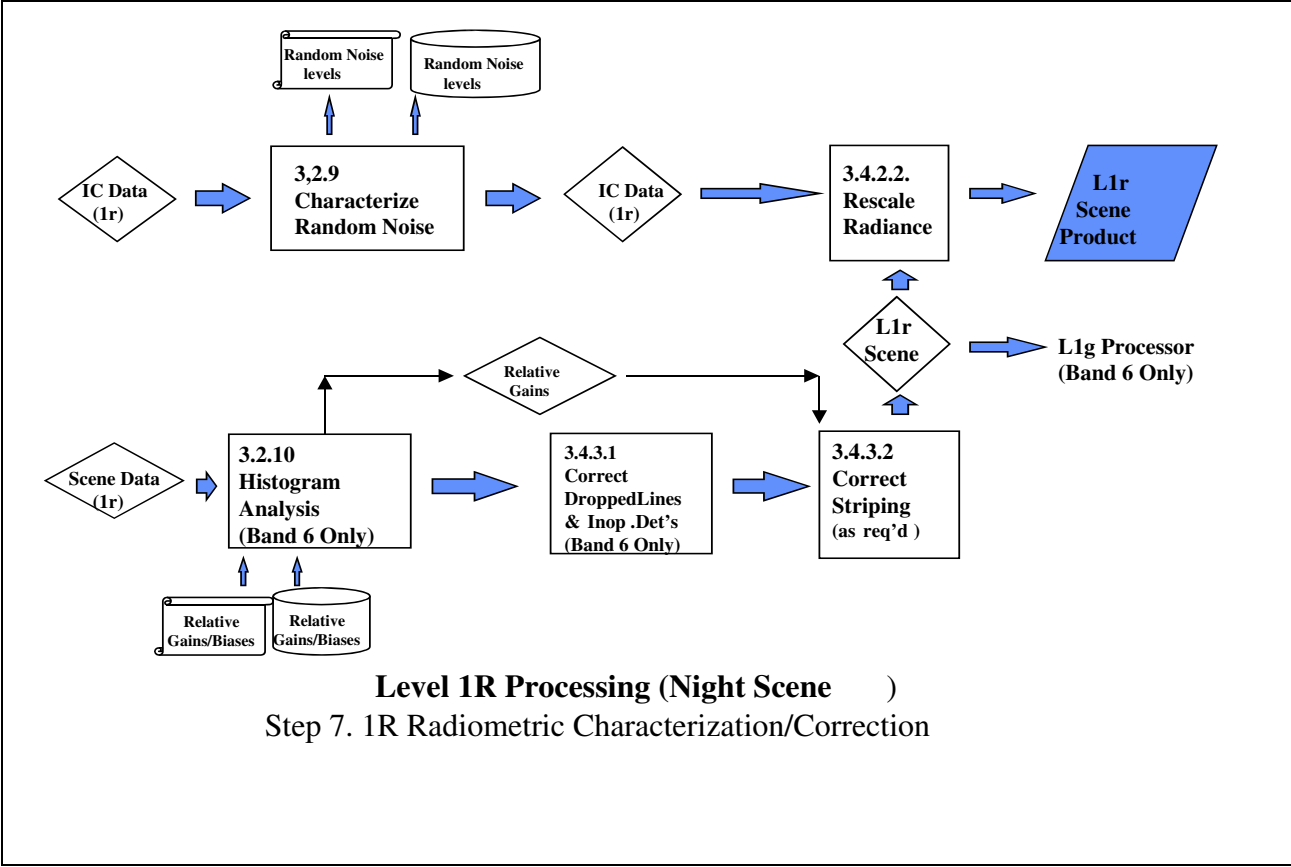


Figure 4-14. Step 7. 1R Radiometric Characterization/Correction

4.3 FASC Scene Processing/Characterization

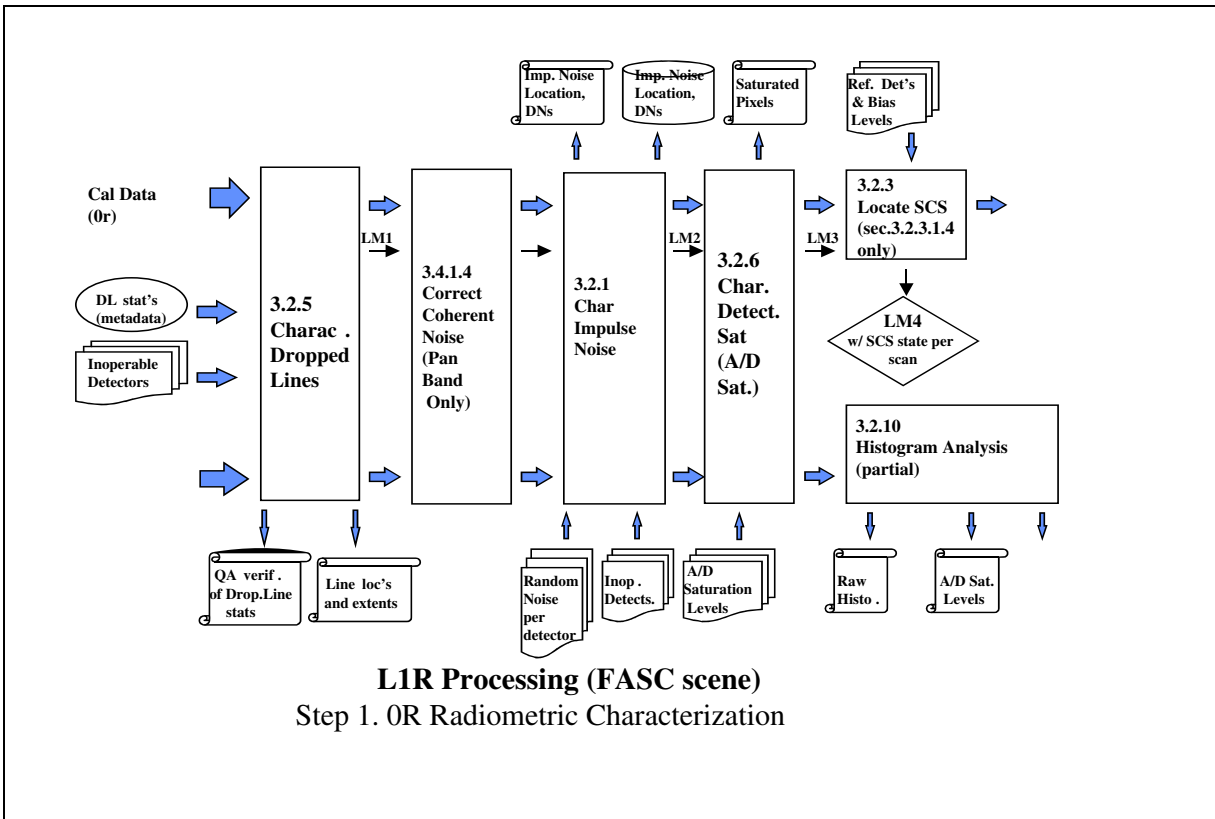


Figure 4-15. Step 1. 0R Radiometric Characterization

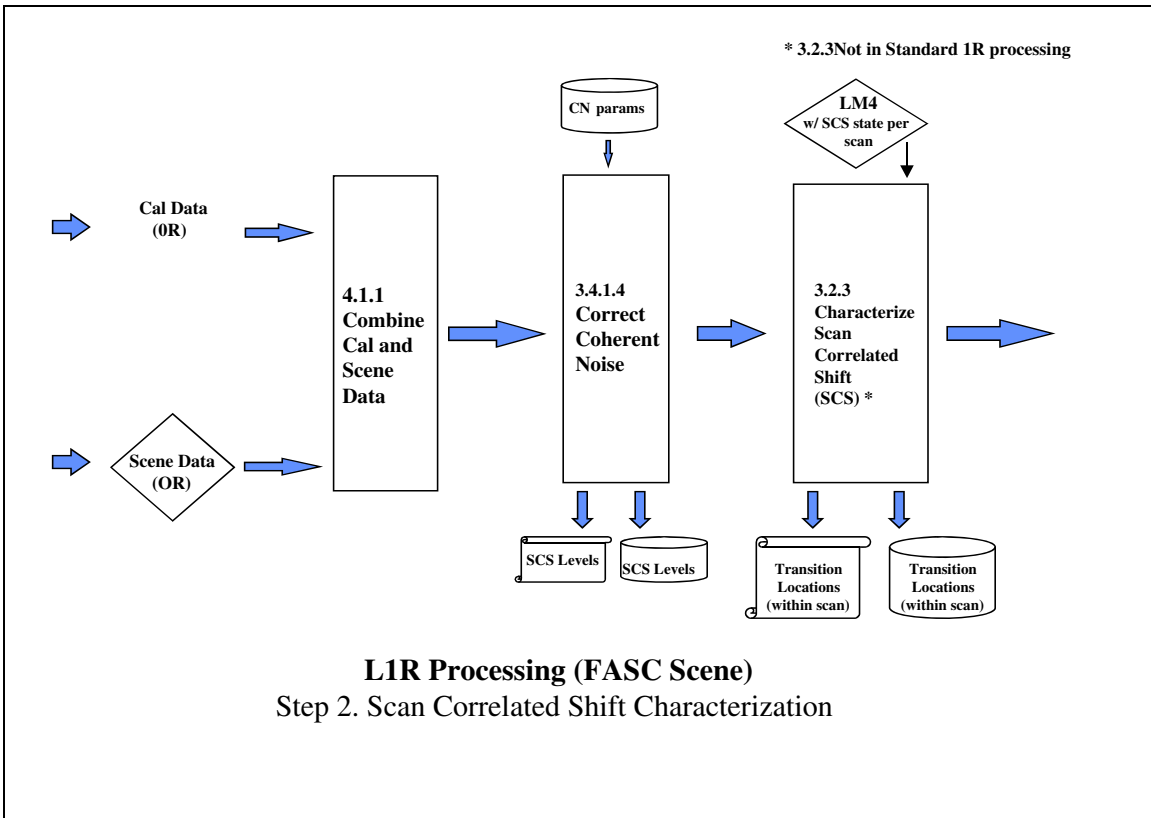


Figure 4-16. Step 2. Scan Correlated Shift Characterization

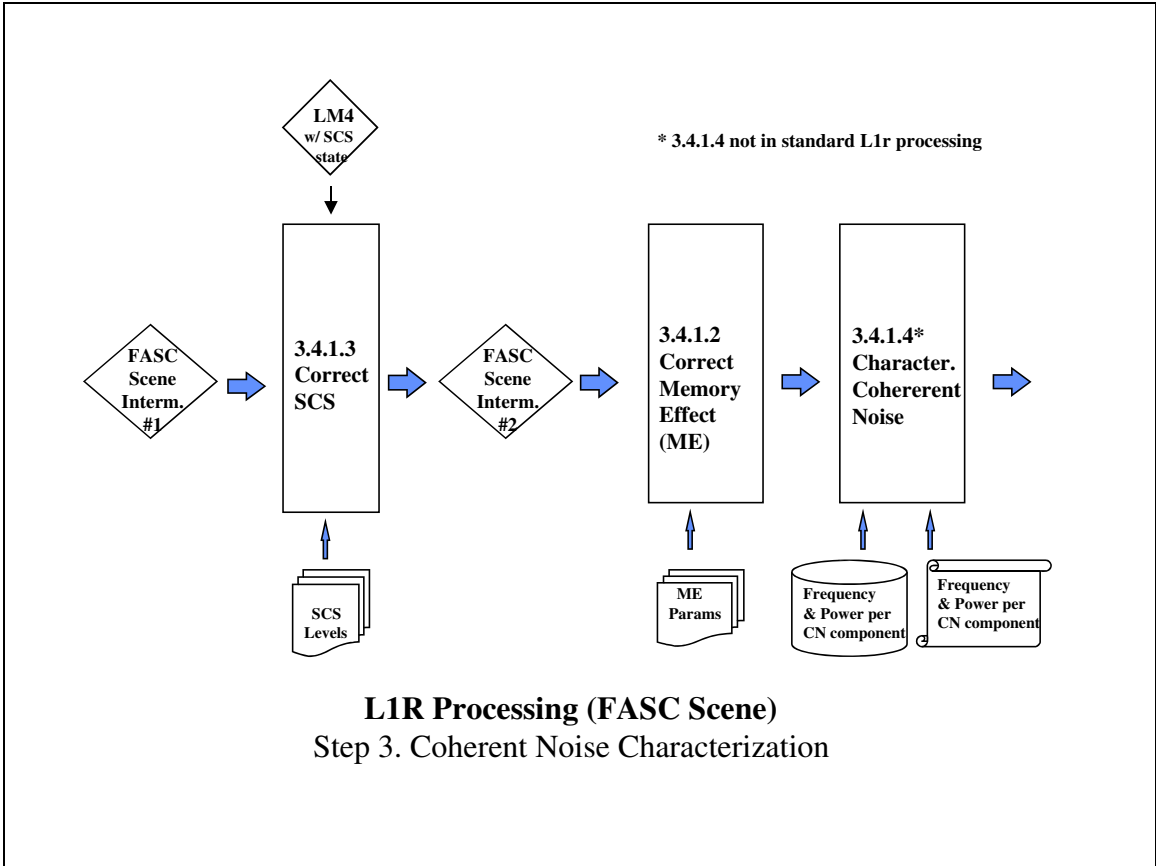


Figure 4-17. Step 3. Coherent Noise Characterization

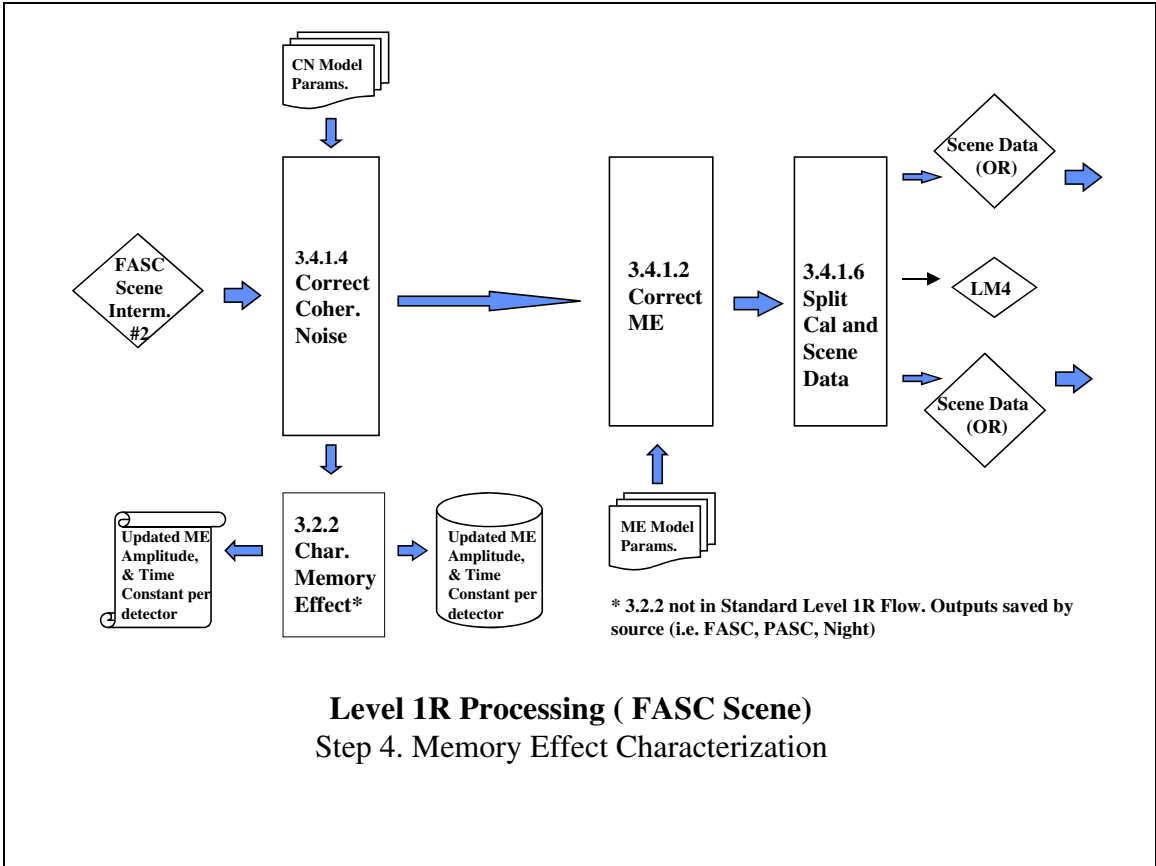


Figure 4-18. Step 4. Memory Effect Characterization

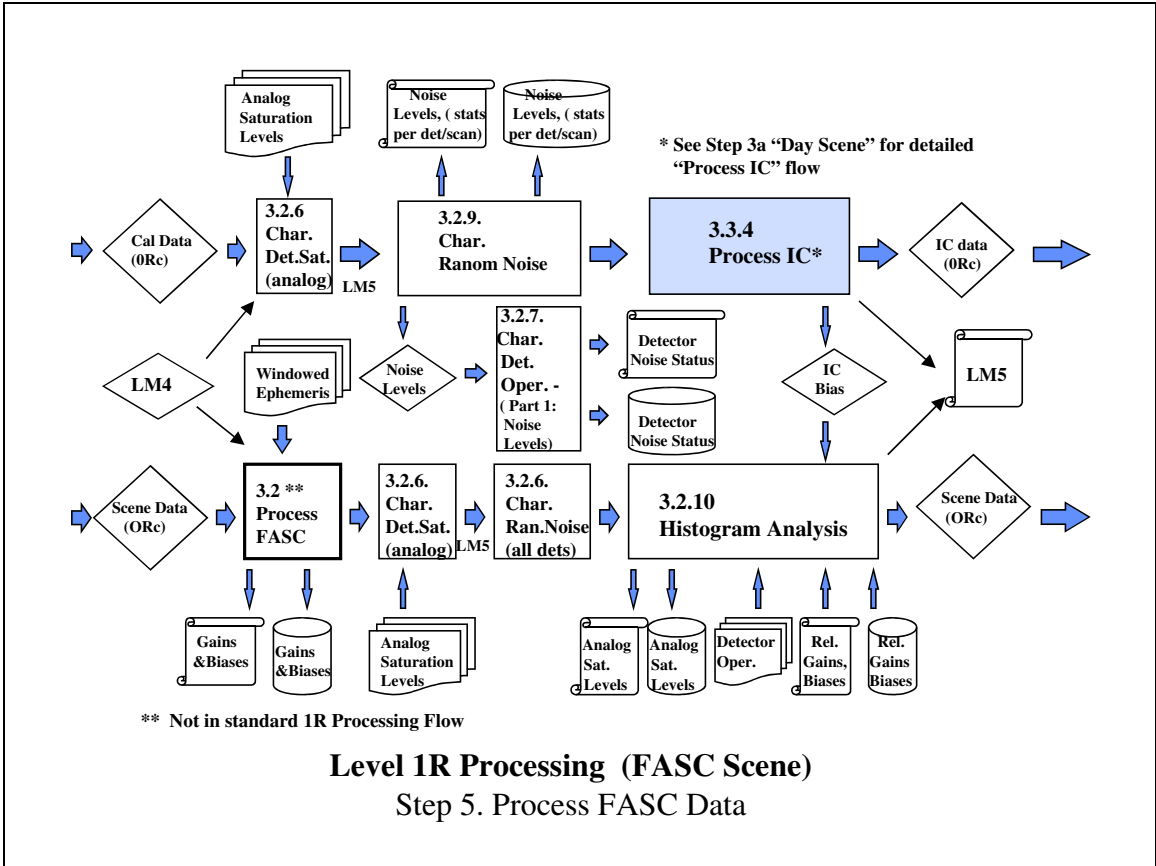


Figure 4-19. Step 5. Process FASC Data

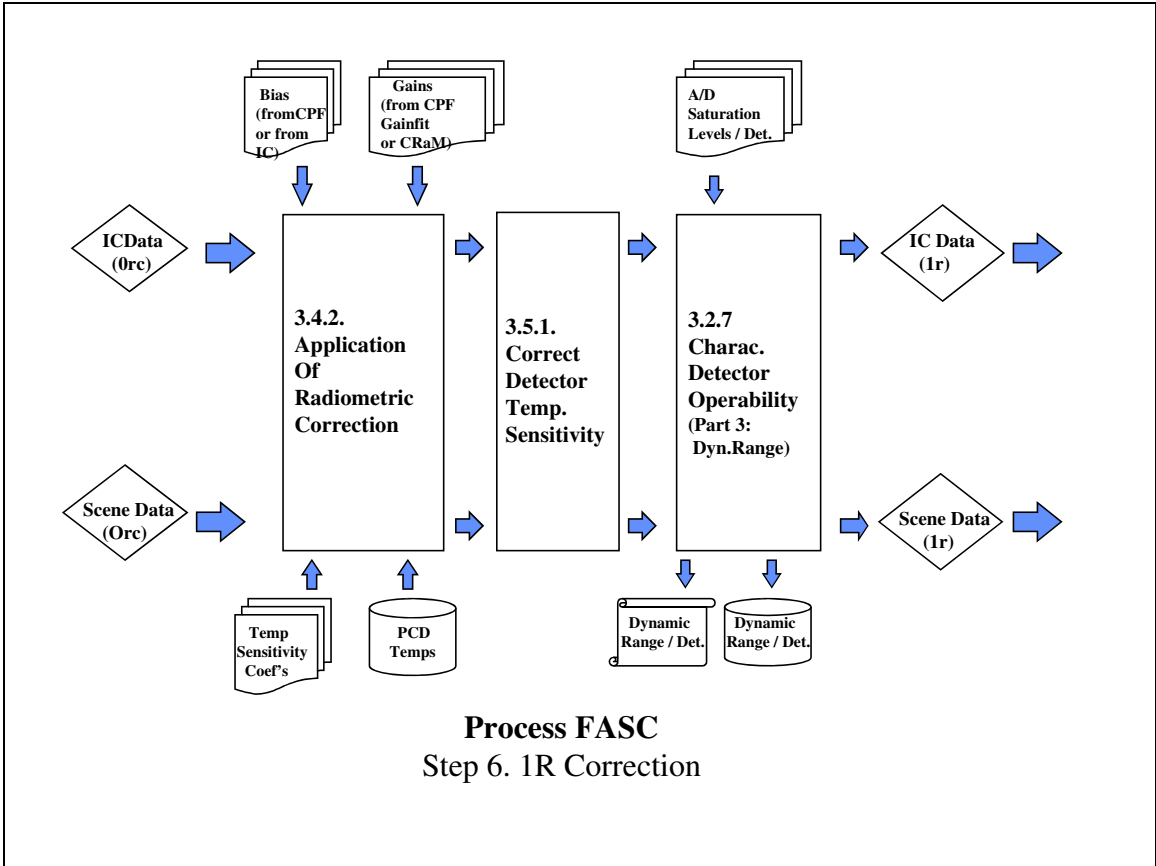


Figure 4-20. Step 6. 1R Correction

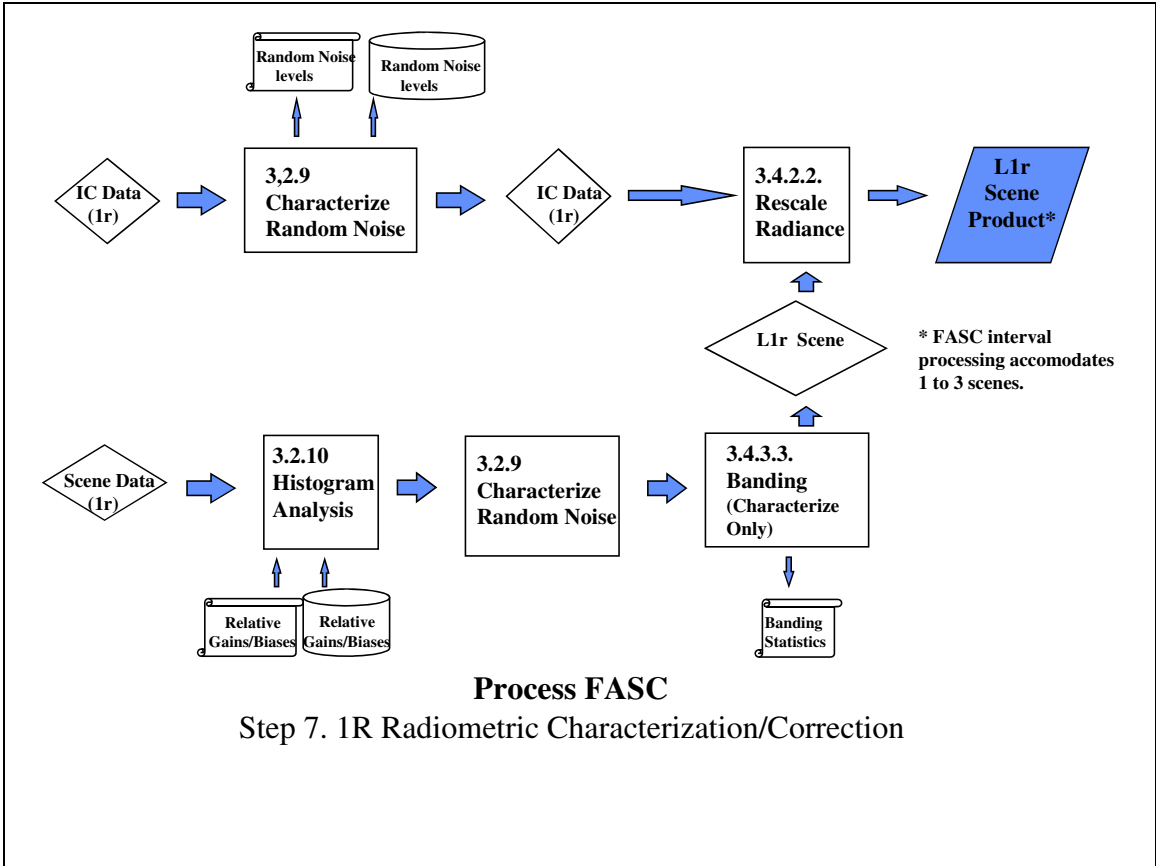


Figure 4-21. Step 7. Radiometric Characterization/Correction

4.4 PASC Scene Processing/Characterization

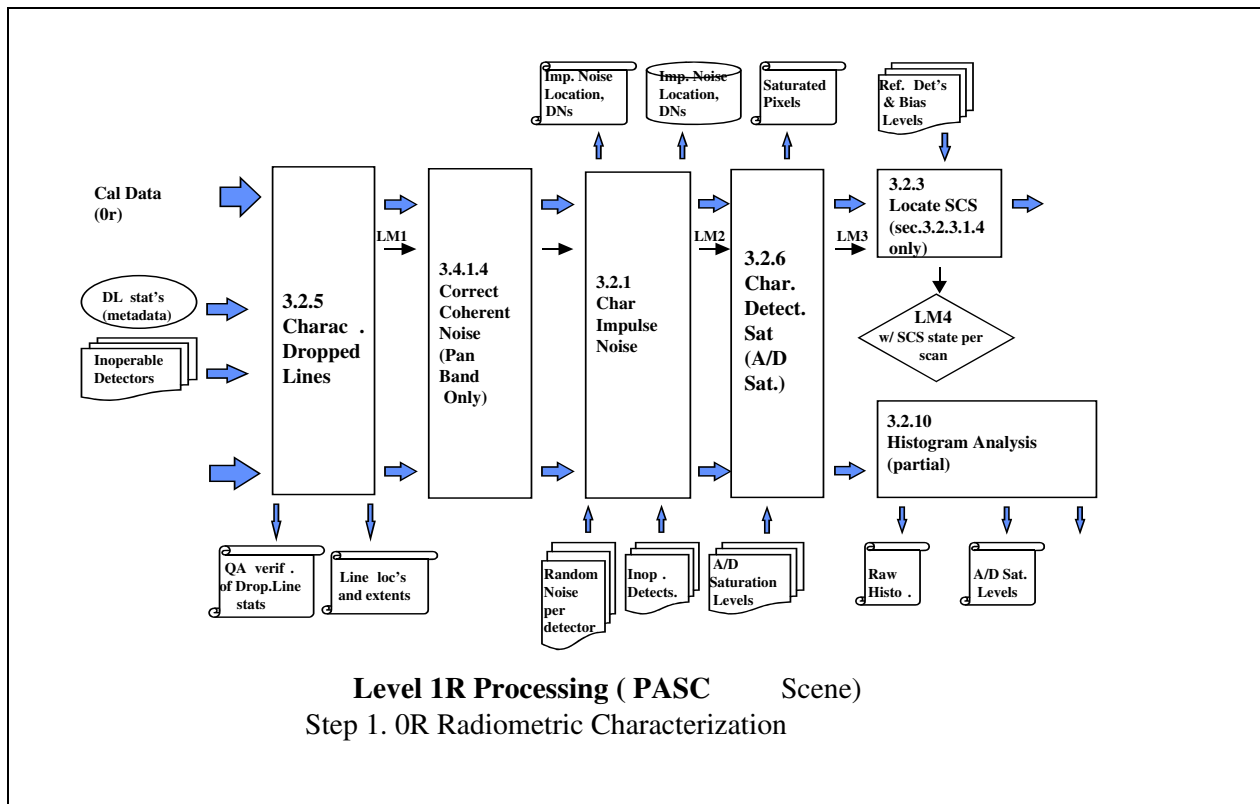


Figure 4-22. Step 1.0R Radiometric Characterization

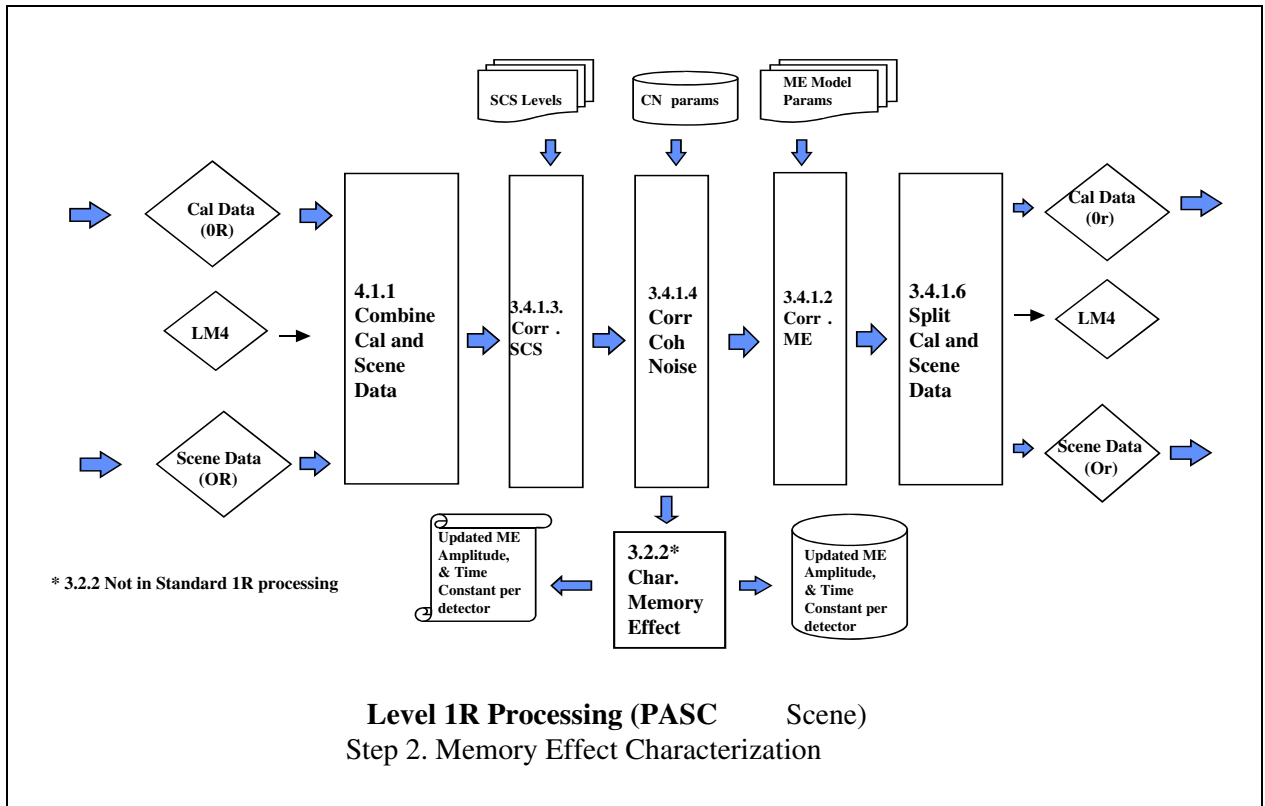


Figure 4-23. Step 2. Memory Effect Characterization

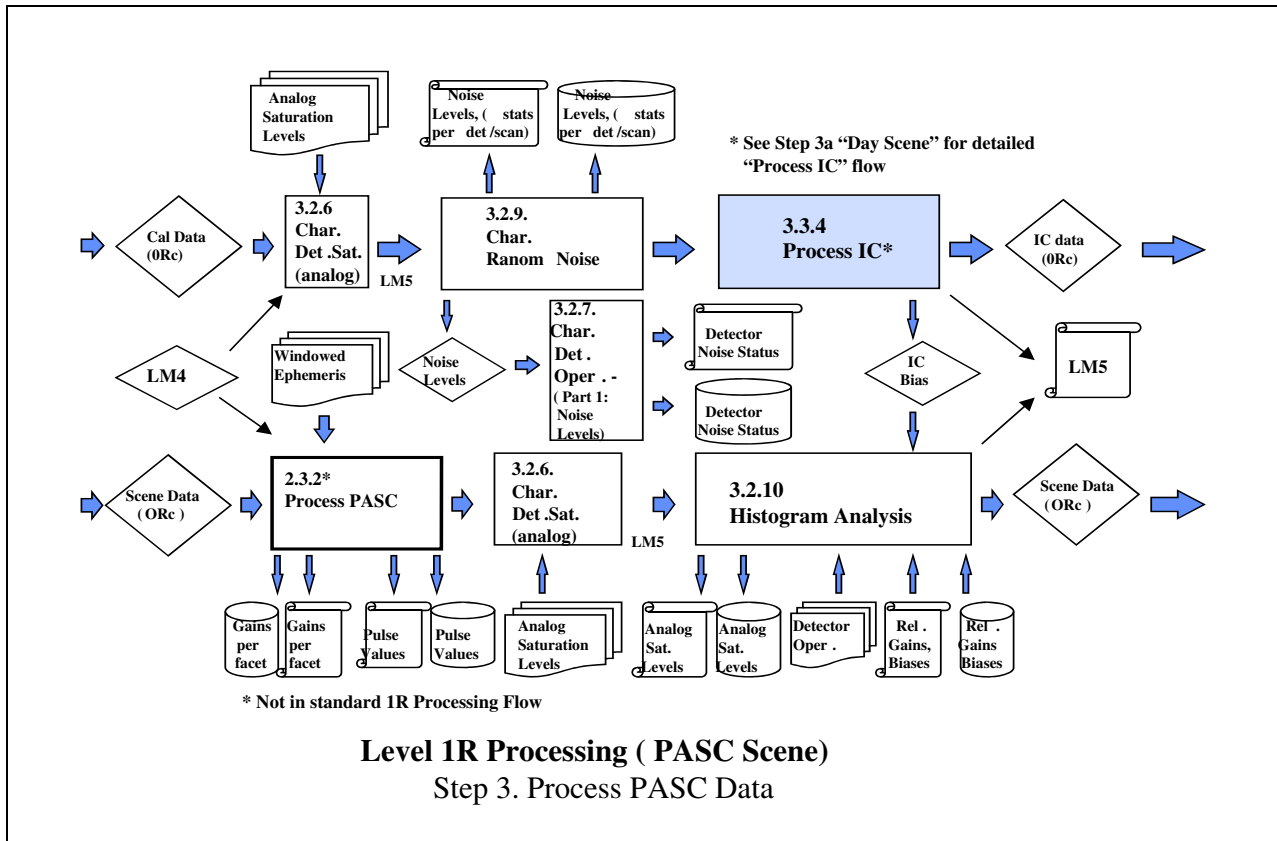


Figure 4-24. Step 3. Process PASC Data

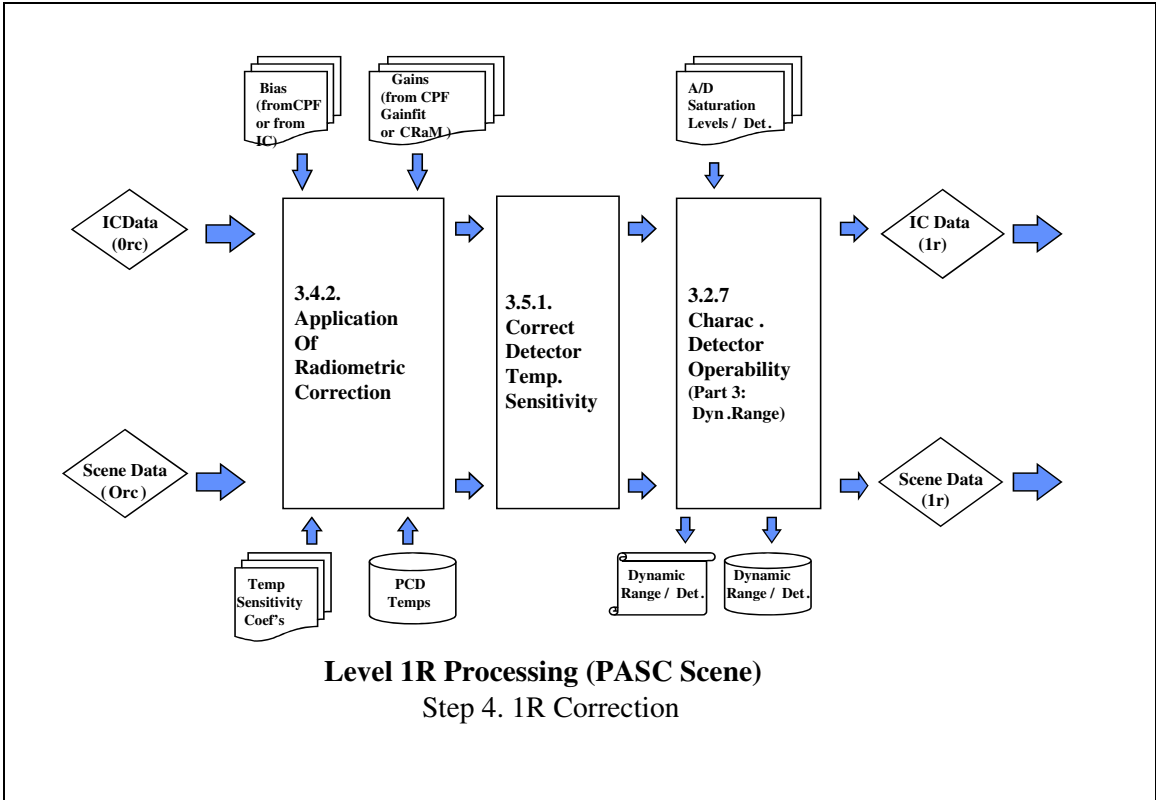


Figure 4-25. Step 4. 1R Correction

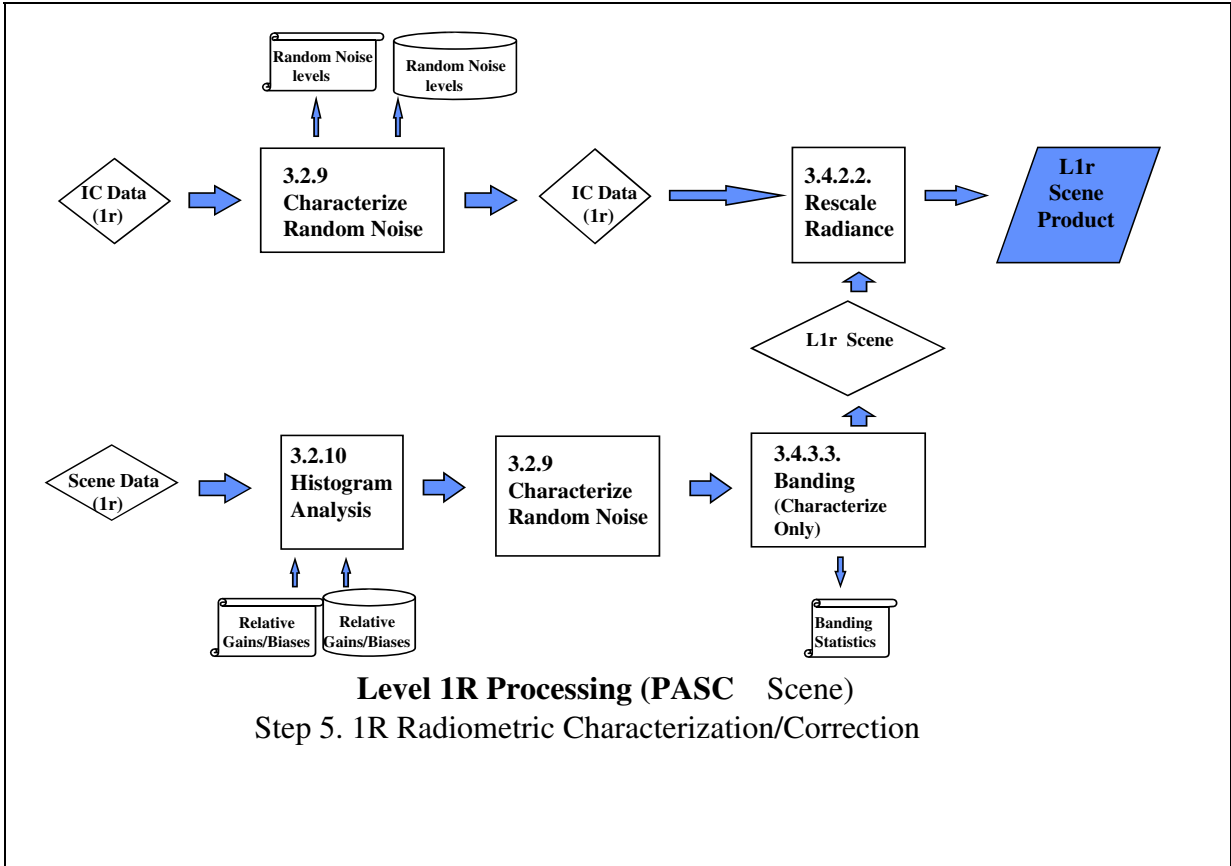


Figure 4-26. Step 5. 1R Radiometric Characterization/Correction

Appendix A Acronyms

A/D	Analog/Digital
μm	Micrometer (also called a micron); measurement of spectral wavelength.
0R	Zero-R data product. 0R products have gone through subinterval processing but no corrections have been performed on them.
1G	1G data product; a product that has gone through both radiometric and geometric corrections.
1R	1R data product; a product that has gone through radiometric correction processing.
ACCA	Automated Cloud Cover Assessment
ADC	After DC Restore
aj	View/emissivity coefficients of the instrument components
ASTER	Advanced Spaceborne Thermal Emission and Reflection Radiometer
ATBD	Algorithm Theoretical Basis Document
B	Detector Bias or Background Response (DN)
b0	Detector Bias (DN)
BDC	Before DC Restore
BN	Background Noise
BRDF	Bi-directional Reflectance Distribution Function
BRDF-n	Normalized Bi-directional Reflectance Distribution Function
BRDF-s	Spectral Bi-directional Reflectance Distribution Function
C	Celsius
CFP	Cold Focal Plane
CFPA	Cold Focal Plane Array
CH	Horizontal/Azimuthal angle of the PASC facets
CHV	Facet Horizontal/Azimuthal View Angle
cm	Centimeter
CN	Coherent Noise
cos	Cosine
CPF	Calibration Parameter File
CRaM	Combined Radiometric Model
CV	Vertical angle of the PASC facets

CVV	Facet Vertical/Zenith View Angle
DB	Database
DC	Direct Current, also used to denote the DC Restore circuit.
DCORR	Corrective factor used to refine the Earth-Sun distance measurement
deg	Degree
DELTA F	Normalized absolute distance from FFT frequency
Det	Detector
DF[t]	Degradation factor time series for calibrators
DIFFIM	Difference Image
DN	Digital Number
DNsun	DN value from an observation of the sun (via PASC glints)
E&A	Evaluation and Analysis
ECS	EOS Core System
EL1PS	EDC Level 1 Prototype System
EOS	Earth Observatory System
Eqs	Equations
EROS	Earth Resources Observation System
ESUN	Solar Spectral Irradiance (also written "Esun")
ETM	Enhanced Thematic Mapper
ETM+	Enhanced Thematic Mapper Plus
EVS	Earth-Vehicle-Sun angle
exp	exponent
FASC	Full Aperture Solar Calibrator
FDF	Flight Dynamics Facility
FFT	Fast Fourier Transform
FOV	Field of View
frv	Integrated instrument view factor
F-test	Statistical hypothesis test
FW	Full Width
G	Detector Gain or Responsivity ($DN/(W/(m^2 - sr -))$)

G(d)	Gain at ice thickness d
G(O)	Gain at zero ice thickness
GBAR _{sel}	Band Average Detector Gain, User Selected
GBFOM	Global Band Figure of Merit
GCOR	Temperature corrected Gains
G _{CPF}	Gain from the Calibration Parameter File
Gd	Average detector gain (counts/spectral radiance) per scene
GR _{DES}	Relative Gain, Desired
GREF	Detector Gains at Reference Temperature
GREF _{sel}	Detector Gains at Reference Temperature, User Selected
GR _{OBS}	Relative Gain, Observed
G _{sd}	Detector gain (counts/spectral radiance) per scan
G _{sel}	Detector gain, User Selected
I/O	Input/Output
IAD	Ion-Assisted Deposition
IAS	Image Assessment System
IC	Internal Calibrator
ICe	Internal Calibrator processing for Emissive bands
ICF	Initial Correction Factor
IEEE	Institute of Electrical and Electronics Engineers
IFOV	Instrument/Instantaneous ? Field of View
IMF	inverse minor frames
IN	Impulse Noise
IOC	Initial On-orbit Checkout
JPL	Jet Propulsion Laboratory
K	Kelvin
km	kilometer
kME	ME unit pulse response magnitude
L	Spectral Radiance (W/(m ² - sr -)) = (Q-B)/G
L1	Level 1

L1	Level 1
L4	Landsat 4
L5	Landsat 5
L6	Landsat 6
L7	Landsat 7
La	ETM+ structure aft of the shutter
LAS	Land Analysis System Software
Lbb	Spectral radiance of the Thermal Blackbody
LDB	IAS Local Database
Lesh	Equivalent shutter spectral radiance of a scene element
L _f	ETM+ forward of the shutter
LHS	Left-hand Side or Left-hand SLO
L _j	Spectral radiance of ETM+ component j
LM	Labeled Mask
LMAX	MAXimum Spectral Radiance Response Corresponding to a Data Product QCALMAX
LMIN	MINimum Spectral Radiance Response Corresponding to a Data Product QCALMIN
LOS	Line-of-Sight
LPGS	Level 1 Product Generation System
LPS	Landsat Processing System
LSATH	High Saturation Radiance
LSATL	Low Saturation Radiance
Lsc	Spectral radiance of the scene element
LSF	Linespread function
Lsh	Spectral radiance of the shutter
m	S/C mass (constant)
M	Meter
ME	Memory Effect
mf	Minor Frame
Mf	Major Frame
mi	Mean Deviation

MISR	Multiangle Imaging SpectroRadiometer
mm	millimeter
MODIS	Moderate Resolution Imaging Spectroradiometer
MODTRAN	Moderate Resolution Transmittance atmospheric modeling software
MSCD	Mirror Scan Correction Data
msec	Millisecond
MSS	MultiSpectral Scanner
MTF	Modulation Transfer Function
mu	micron
mW	megawatt
N	Number of samples
NASA	National Aeronautics and Space Administration
NEDL	Noise Equivalent Detector Radiance
NEDT	Noise Equivalent Detector Temperature
NIC	Number of IC pixels
Nimg	Number of image pixels
nm	Nanometer
ORc	ORc data product; a product that has gone through partial radiometric correction processing
OTF	Optical Transfer Function
P	Average net pulse height
PAPH	Pseudo Average Pulse Height
PASC	Partial Aperture Solar Calibrator
PCD	Payload Correction Data
PFP	Primary Focal Plane
PFPA	Primary Focal Plane Assembly
Phiv	Variation in view azimuth
PSD	Power Spectral Density
Pw	Integrated pulse value
Q	Raw Quantized Voltage or Response (DN) = $G * L + B$

Q0	Digital Counts, response of a detector to an input radiance of zero (the offset DN)
QA	Quality Assurance
Q _{bb}	Digital Counts, response of a detector to radiance from the blackbody
QCAL	Quantized CALibrated Response (DN)
QCALMAX	MAXimum Quantized CALibrated Response Corresponding to a Data Product LMAX
QCALMIN	MINimum Quantized CALibrated Response Corresponding to a Data Product LMIN
QSATH	High Saturation Signal
QSATHL	Low Saturation Signal
Qsc	Digital Counts, response of a detector to the scene input radiance
Qsh	Digital Counts, response of a detector to radiance from the IC Shutter Flag
r	
RA	Right Ascension
RF	Radio Frequency
rho	Product of spectral reflectances
RHS	Right-hand Side or Right-hand SLO
RMS	Root-Mean-Square
RN	Random Noise
RSR	Relative Spectral Responses
S/C	Spacecraft
SAIC	Science Applications International Corporation
SBRS	Santa Barbara Remote Sensing Inc
SCS	Scan-Related Shift
Secs	Seconds
SEV	Sun-Earth-Vehicle angle
si	Standard Deviation
SIGMA	Width of the notch
Sinc	Sine Cardinal sampling function
SNR	Signal-to-Noise Ratio

SQRT	Square Root
Sr	Steradian
STDEV	Standard Deviation
SVN	Sun-Vehicle-Normal angle
SWIR	Short Wavelength Infrared
SZA	Solar Zenith Angle
T	Temperature
tau	Memory Effect time constant
Thetav	Variation in view zenith
THR	Threshold value
TM	Thematic Mapper
TMACS	TMMSS Archive Conversion System ?
Tmax	Maximum width of the PASC pulse
tME	Memory Effect time constant parameter from the database
Tr	
Tsc	Scan Mirror Temperature ?
Tsec	Secondary Mirror temperature?
T-test	Statistical hypothesis test; a specialized form of the F-test
u	Spatial Frequency
UDP	Upper Data Point
USGS	U.S. Geological Survey
Vbb	View/emissivity coefficient for the blackbody
VNIR	Visible & Near Infrared
Vsh	View/emissivity coefficient for the shutter
WRS	Worldwide Reference System
wrt	“With Respect To”
X	X-axis position
Z	Z-axis position

Appendix B SBRS Algorithm Documents

SBRs_ALL.pdf
SBRs_IC.pdf
SBRs_PASC.pdf
SBRs_PASCI1.pdf

Appendix C Sample IAS Output Reports

3.2.5 Dropped Lines Summary

Landsat 7 Image Assessment System 02/21/2003 14:51:12
Dropped Lines Characterization tightrope

Product: L72EDC149915317010 Processing Level: R0R

Band 2 Scene 1 -- DAY data

Scan Dropped minor frames Entirely
Number MSCD Image+IC Dropped?

Landsat 7 Image Assessment System 02/21/2003 14:52:35
Dropped Lines Characterization tightrope

Product: L72EDC149915317010 Processing Level: R0R

Band 61 Scene 1 -- DAY data

Scan Dropped minor frames Entirely
Number MSCD Image+IC Dropped?

Landsat 7 Image Assessment System 02/21/2003 14:52:44
Dropped Lines Characterization tightrope

Product: L72EDC149915317010 Processing Level: R0R

Band 62 Scene 1 -- DAY data

Scan Dropped minor frames Entirely
Number MSCD Image+IC Dropped?

3.2.6 A/D Saturation Summary (Band 2):

Landsat 7 Image Assessment System 02/21/2003 14:51:17
A/D Detector Saturation Characterization tightrope

Product : L72EDC149915317010 Processing Level: /u04/ias/ias_sys/oper/bin/R0R

Band B2 Scene 1 Gain H -- DAY data

Detector Total SP/Det Rel SP Avg/Det

1 45 1.60356
2 56 1.99555
3 35 1.24722
4 50 1.78174
5 32 1.14031
6 34 1.21158
7 26 0.92650
8 21 0.74833
9 12 0.42762
10 23 0.81960
11 11 0.39198
12 18 0.64143
13 15 0.53452
14 20 0.71269
15 26 0.92650
16 25 0.89087

Grand total number of SP for this band for both IC and IMAGE is 449
The avg # of SP/Det for this band is 28.062500.

3.2.6 Analog Saturation Summary (Band 2):

Landsat 7 Image Assessment System 02/21/2003 14:56:28

Analog Detector Saturation Characterization tightrope

Product : L72EDC149915317010 Processing Level: /u04/ias/ias_sys/oper/bin/R0C

Band B2 Scene 1 Gain H -- DAY data

The scene average is 0.

No saturated pixels in scene number 1.

Grand total number of SP for this band for both IC and IMAGE is 0
The avg # of SP/Det for this band is 0.000000.

3.2.7 Detector Operability Summary :

Landsat 7 Image Assessment System 02/21/2003 14:55:02
Detector Operability Characterization tightrope

Product: L72EDC149915317010 Processing Level: R0C

Band B2 Scene 1 Gain H -- DAY IC data

DYNAMIC RANGE CHECK

Min Saturated Spectral Radiance (Hi) = 193.7 Lo Spec = 135.6 Hi spec = 387.4
Min Saturated Spectral Radiance (Lo) = 0.0 (0.7 * SatSpecRad) (2.0 *
SatSpecRad)

DET #	STATUS STATE	RANGE-L	RANGE-H	SATURATION		SATURATION		DYNAMIC RANGE		RANGE	
				LEVEL GAIN	BIAS	RADIANCES HI	LO	HI	LO		
1	0	0	0	1.197	14.914	255.0	0.0	200.635	-12.464	213.098	0
2	0	0	0	1.194	15.190	255.0	0.0	200.826	-12.721	213.546	0
3	0	0	0	1.182	14.911	255.0	0.0	203.200	-12.620	215.820	0
4	0	0	0	1.200	15.149	255.0	0.0	199.809	-12.620	212.429	0

Product: L72EDC149915317010 Processing Level: R0C

Band B62 Scene 1 Gain H -- DAY IC data

DYNAMIC RANGE CHECK

Min Saturated Spectral Radiance (Hi) = 12.2 Lo Spec = 5.1 Hi spec = 14.7
Min Saturated Spectral Radiance (Lo) = 4.9 (0.7 * SatSpecRad) (2.0 *
SatSpecRad)

DET #	STATUS	SATURATION		SATURATION		DYNAMIC RANGE		
		RANGE-L	RANGE-H	LEVEL GAIN	BIAS	RADIANCES HI	LO	HI

FLAG

1	0	0	0	24.240	-69.304	255.0	0.0	13.379	2.859	10.520	0
2	0	0	0	24.689	-72.358	255.0	0.0	13.259	2.931	10.328	0
3	0	0	0	26.085	-82.149	255.0	0.0	12.925	3.149	9.776	0
4	0	0	0	24.776	-72.825	255.0	0.0	13.231	2.939	10.292	0
5	0	0	0	25.212	-75.798	255.0	0.0	13.120	3.006	10.114	0
6	0	0	0	25.244	-75.705	255.0	0.0	13.100	2.999	10.101	0
7	0	0	0	25.862	-80.112	255.0	0.0	12.958	3.098	9.860	0
8	0	0	0	25.460	-77.253	255.0	0.0	13.050	3.034	10.016	0

Landsat 7 Image Assessment System 02/21/2003 15:02:32
Detector Operability Characterization tightrope

Product: L72EDC149915317010 Processing Level: R0C

3.2.9 Random Noise Summary:

Landsat 7 Image Assessment System 02/12/2003 18:39:37
Random Noise Characterization tightrope

Product: L72EDC110222815020 Processing Level: R0C

Band B2 Scene 1 Gain L -- DAY IC data

SCENE AVERAGES AND STANDARD DEVIATIONS BY DETECTOR (COUNTS)
det mean mean mean mean stdev stdev stdev stdev

of A of B of C all of A of B of C all

All Scans

1	9.91	9.92	9.92	9.92	0.60	0.59	0.59	0.59
2	10.11	10.11	10.11	10.11	0.57	0.56	0.57	0.56
3	9.87	9.87	9.87	9.87	0.58	0.57	0.58	0.58
4	10.04	10.04	10.04	10.04	0.57	0.56	0.57	0.56
5	9.82	9.82	9.82	9.82	0.59	0.58	0.59	0.59
6	10.03	10.03	10.03	10.03	0.59	0.58	0.59	0.59
7	9.94	9.94	9.94	9.94	0.58	0.57	0.58	0.58
8	10.08	10.08	10.08	10.08	0.60	0.59	0.60	0.60
9	9.82	9.81	9.82	9.82	0.62	0.61	0.62	0.62
10	10.08	10.07	10.07	10.07	0.61	0.60	0.61	0.60
11	9.85	9.85	9.85	9.85	0.61	0.60	0.61	0.61
12	10.13	10.12	10.11	10.12	0.58	0.57	0.58	0.58
13	9.79	9.78	9.78	9.78	0.61	0.60	0.61	0.61
14	10.08	10.08	10.07	10.08	0.58	0.57	0.59	0.58
15	9.83	9.82	9.82	9.82	0.60	0.59	0.59	0.60
16	10.13	10.12	10.12	10.12	0.58	0.57	0.58	0.58

Forward Scans

1	9.91	9.92	9.92	9.92	0.60	0.59	0.59	0.59
2	10.11	10.11	10.11	10.11	0.57	0.56	0.57	0.57
3	9.87	9.88	9.87	9.87	0.58	0.57	0.58	0.58
4	10.05	10.05	10.04	10.04	0.57	0.56	0.57	0.56
5	9.82	9.83	9.82	9.82	0.59	0.58	0.59	0.59
6	10.03	10.03	10.02	10.03	0.59	0.58	0.58	0.59
7	9.93	9.94	9.93	9.94	0.58	0.57	0.58	0.58
8	10.08	10.08	10.08	10.08	0.61	0.59	0.60	0.60
9	9.82	9.81	9.82	9.82	0.62	0.61	0.62	0.62
10	10.09	10.06	10.07	10.07	0.61	0.60	0.60	0.61
11	9.86	9.84	9.85	9.85	0.62	0.60	0.60	0.61
12	10.14	10.11	10.12	10.12	0.58	0.57	0.57	0.57
13	9.80	9.77	9.78	9.78	0.62	0.60	0.61	0.61
14	10.08	10.07	10.07	10.07	0.58	0.57	0.58	0.58
15	9.83	9.82	9.83	9.83	0.60	0.59	0.59	0.60
16	10.13	10.11	10.12	10.12	0.59	0.58	0.58	0.58

Reverse Scans

1	9.92	9.91	9.92	9.92	0.60	0.59	0.59	0.59
2	10.11	10.11	10.11	10.11	0.57	0.56	0.56	0.56
3	9.88	9.87	9.88	9.87	0.58	0.57	0.58	0.57
4	10.04	10.04	10.05	10.05	0.56	0.56	0.57	0.56
5	9.82	9.82	9.82	9.82	0.59	0.58	0.59	0.59
6	10.03	10.03	10.04	10.03	0.59	0.58	0.60	0.59
7	9.94	9.93	9.94	9.94	0.57	0.57	0.58	0.58

8	10.08	10.09	10.09	10.09	0.60	0.59	0.60	0.60
9	9.82	9.82	9.81	9.82	0.62	0.61	0.62	0.62
10	10.08	10.07	10.07	10.07	0.61	0.60	0.61	0.60
11	9.85	9.85	9.84	9.85	0.61	0.60	0.61	0.61
12	10.12	10.12	10.11	10.12	0.57	0.57	0.58	0.58
13	9.78	9.78	9.77	9.78	0.61	0.60	0.62	0.61
14	10.08	10.08	10.07	10.08	0.58	0.57	0.59	0.58
15	9.83	9.83	9.82	9.82	0.60	0.59	0.60	0.60
16	10.12	10.13	10.11	10.12	0.58	0.57	0.58	0.58

TESTS OF EQUIVALENCE OF SECTION MEANS AND STANDARD DEVIATIONS
(TEST FOR RESIDUAL MEMORY EFFECT; NOISE VARIATION ACROSS IMAGE)
Number of lines that failed t or f test (alpha < 0.05)

TTEST FOR MEANS FTEST FOR VARIANCE #lines TTEST FTEST #scans
det A-B B-C A-C A-B B-C A-C tested for-rev for-rev tested

All Scans

1	6	2	4	41	43	51	375	17	30	187
2	2	3	7	40	48	57	375	12	32	187
3	5	8	3	40	46	52	375	11	31	187
4	3	2	3	53	49	58	375	10	31	187
5	2	3	9	30	25	38	375	18	22	187
6	1	2	2	37	41	45	375	7	28	187
7	3	7	1	36	39	56	375	13	23	187
8	1	3	5	45	38	49	375	13	28	187
9	4	3	3	34	38	45	375	9	21	187
10	4	1	2	34	41	57	375	26	32	187
11	1	2	5	46	39	49	375	4	27	187
12	2	4	6	47	56	56	375	9	27	187
13	8	4	7	29	20	36	375	18	22	187
14	3	0	2	55	50	55	375	6	28	187
15	1	0	2	34	39	29	375	3	23	187
16	4	0	3	52	43	52	375	10	30	187

Forward Scans

1	4	0	4	23	18	24	188
2	1	1	2	21	21	32	188
3	2	1	0	18	20	20	188
4	1	2	3	29	18	30	188
5	0	1	6	14	12	17	188
6	1	1	1	21	18	27	188
7	1	4	0	20	16	26	188
8	0	1	3	23	19	26	188

9	2	1	2	15	12	23	188
10	1	0	0	21	19	25	188
11	1	1	0	21	23	21	188
12	2	3	6	27	27	32	188
13	5	3	3	16	6	19	188
14	1	0	1	31	24	29	188
15	1	0	1	17	20	11	188
16	3	0	2	28	20	28	188

Reverse Scans

1	2	2	0	18	25	27	187
2	1	2	5	19	27	25	187
3	3	7	3	22	26	32	187
4	2	0	0	24	31	28	187
5	2	2	3	16	13	21	187
6	0	1	1	16	23	18	187
7	2	3	1	16	23	30	187
8	1	2	2	22	19	23	187
9	2	2	1	19	26	22	187
10	3	1	2	13	22	32	187
11	0	1	5	25	16	28	187
12	0	1	0	20	29	24	187
13	3	1	4	13	14	17	187
14	2	0	1	24	26	26	187
15	0	0	1	17	19	18	187
16	1	0	1	24	23	24	187

 AVERAGE OF LINE BY LINE STANDARD DEVIATIONS AND RANDOMNESS CHECK
 (alpha level of < 0.05 for randomness tests indicates rejection of
 null hypothesis of randomness of sequence of line means or stdevs)

det	Averaged Standard Deviations of Lines				Randomness Test	
	A	B	C	All	MEAN	STDEV
	(counts)	(counts)	(counts)	(counts)	(alpha)	(alpha)

All Scans

1	0.59	0.59	0.59	0.59	0.376	0.060
2	0.57	0.56	0.57	0.56	0.029	0.398
3	0.58	0.57	0.58	0.57	0.136	0.106
4	0.56	0.56	0.57	0.56	0.376	0.284
5	0.59	0.58	0.59	0.58	0.267	0.418
6	0.59	0.58	0.59	0.59	0.020	0.339
7	0.58	0.57	0.58	0.57	0.340	0.378
8	0.60	0.59	0.60	0.60	0.002	0.378

9	0.62	0.61	0.62	0.62	0.259	0.127
10	0.61	0.60	0.60	0.60	0.416	0.438
11	0.61	0.60	0.61	0.61	0.078	0.150
12	0.58	0.57	0.57	0.57	0.374	0.189
13	0.61	0.60	0.61	0.61	0.020	0.302
14	0.58	0.57	0.59	0.58	0.122	0.250
15	0.60	0.59	0.59	0.59	0.249	0.302
16	0.58	0.57	0.58	0.58	0.217	0.479

Forward Scans

1	0.59	0.59	0.59	0.59	0.187	0.279
2	0.57	0.56	0.57	0.56	0.119	0.153
3	0.58	0.57	0.58	0.58	0.355	0.020
4	0.57	0.56	0.57	0.56	0.060	0.385
5	0.59	0.58	0.58	0.58	0.386	0.029
6	0.59	0.58	0.58	0.59	0.150	0.040
7	0.58	0.57	0.57	0.57	0.016	0.385
8	0.60	0.59	0.60	0.60	0.230	0.385
9	0.62	0.61	0.61	0.62	0.229	0.190
10	0.61	0.60	0.60	0.60	0.089	0.330
11	0.62	0.60	0.60	0.61	0.412	0.153
12	0.58	0.57	0.57	0.57	0.270	0.190
13	0.61	0.60	0.61	0.61	0.474	0.385
14	0.58	0.57	0.58	0.58	0.470	0.385
15	0.60	0.59	0.59	0.60	0.209	0.279
16	0.58	0.58	0.58	0.58	0.071	0.442

Reverse Scans

1	0.59	0.59	0.59	0.59	0.037	0.278
2	0.57	0.56	0.56	0.56	0.037	0.231
3	0.57	0.57	0.57	0.57	0.050	0.356
4	0.56	0.56	0.57	0.56	0.439	0.330
5	0.59	0.58	0.59	0.59	0.184	0.231
6	0.59	0.58	0.59	0.59	0.499	0.442
7	0.57	0.57	0.58	0.57	0.013	0.231
8	0.59	0.59	0.60	0.59	0.494	0.330
9	0.62	0.61	0.62	0.62	0.303	0.442
10	0.60	0.60	0.61	0.60	0.228	0.330
11	0.61	0.60	0.61	0.61	0.169	0.152
12	0.57	0.57	0.58	0.57	0.411	0.009
13	0.61	0.60	0.62	0.61	0.099	0.020
14	0.58	0.57	0.59	0.58	0.076	0.053
15	0.60	0.59	0.59	0.59	0.031	0.189
16	0.58	0.57	0.58	0.58	0.471	0.442

CORRELATION OF LINE-BY-LINE MEANS BETWEEN DETECTORS: All SCANS

Pearson correlation coefficient (r)

	1	2	3	4	5	6	7	8	9	10	11	12	13	14	15	16
1	0.00	0.00	0.00	0.00	0.00	0.00	0.00	0.00	0.00	0.00	0.00	0.00	0.00	0.00	0.00	0.00
2	0.18	0.00	0.00	0.00	0.00	0.00	0.00	0.00	0.00	0.00	0.00	0.00	0.00	0.00	0.00	0.00
3	0.13	-0.17	0.00	0.00	0.00	0.00	0.00	0.00	0.00	0.00	0.00	0.00	0.00	0.00	0.00	0.00
4	-0.25	0.03	0.00	0.00	0.00	0.00	0.00	0.00	0.00	0.00	0.00	0.00	0.00	0.00	0.00	0.00
5	0.01	-0.29	0.25	-0.02	0.00	0.00	0.00	0.00	0.00	0.00	0.00	0.00	0.00	0.00	0.00	0.00
6	-0.46	-0.14	-0.06	0.42	-0.04	0.00	0.00	0.00	0.00	0.00	0.00	0.00	0.00	0.00	0.00	0.00
7	-0.13	-0.35	0.21	0.12	0.45	0.24	0.00	0.00	0.00	0.00	0.00	0.00	0.00	0.00	0.00	0.00
8	-0.47	-0.19	-0.05	0.34	0.12	0.61	0.37	0.00	0.00	0.00	0.00	0.00	0.00	0.00	0.00	0.00
9	0.21	-0.03	0.27	-0.15	0.19	-0.30	0.08	-0.21	0.00	0.00	0.00	0.00	0.00	0.00	0.00	0.00
10	0.07	0.16	-0.12	-0.03	-0.21	-0.02	-0.26	-0.08	-0.23	0.00	0.00	0.00	0.00	0.00	0.00	0.00
11	0.18	-0.09	0.18	-0.17	0.25	-0.20	0.26	-0.11	0.38	-0.32	0.00	0.00	0.00	0.00	0.00	0.00
12	-0.21	-0.01	-0.03	0.19	-0.10	0.30	0.04	0.25	-0.26	0.25	-0.23	0.00	0.00	0.00	0.00	0.00
13	-0.14	-0.34	0.19	0.04	0.32	0.13	0.37	0.21	0.25	-0.32	0.36	-0.08	0.00	0.00	0.00	0.00
14	-0.29	-0.18	0.08	0.23	0.02	0.39	0.21	0.39	-0.27	0.10	-0.15	0.39	-0.02	0.00	0.00	0.00
15	-0.10	-0.29	0.26	-0.03	0.44	0.06	0.34	0.15	0.28	-0.30	0.36	-0.13	0.47	-0.06	0.00	0.00
16	-0.20	-0.18	0.04	0.21	0.03	0.37	0.24	0.36	-0.21	0.09	-0.13	0.34	0.04	0.44	0.01	0.00

Percentage of unexplained variance (100*[1-r^2])

	1	2	3	4	5	6	7	8	9	10	11	12	13	14	15	16
1	0	0	0	0	0	0	0	0	0	0	0	0	0	0	0	0
2	97	0	0	0	0	0	0	0	0	0	0	0	0	0	0	0
3	98	97	0	0	0	0	0	0	0	0	0	0	0	0	0	0
4	94	100	100	0	0	0	0	0	0	0	0	0	0	0	0	0
5	100	92	94	100	0	0	0	0	0	0	0	0	0	0	0	0
6	79	98	100	83	100	0	0	0	0	0	0	0	0	0	0	0
7	98	88	96	99	80	94	0	0	0	0	0	0	0	0	0	0
8	77	96	100	88	98	63	86	0	0	0	0	0	0	0	0	0
9	96	100	93	98	96	91	99	96	0	0	0	0	0	0	0	0
10	99	98	99	100	96	100	93	99	95	0	0	0	0	0	0	0
11	97	99	97	97	94	96	93	99	86	90	0	0	0	0	0	0
12	95	100	100	96	99	91	100	94	93	94	95	0	0	0	0	0
13	98	89	96	100	90	98	86	95	94	89	87	99	0	0	0	0
14	92	97	99	95	100	85	96	85	93	99	98	84	100	0	0	0
15	99	92	93	100	81	100	88	98	92	91	87	98	78	100	0	0
16	96	97	100	96	100	86	94	87	96	99	98	88	100	81	100	0

Significance of regression (Reject hypothesis if alpha < 0.05)

	1	2	3	4	5	6	7	8	9	10	11	12	13	14	15	16
1	0.00	0.00	0.00	0.00	0.00	0.00	0.00	0.00	0.00	0.00	0.00	0.00	0.00	0.00	0.00	0.00
2	0.00	0.00	0.00	0.00	0.00	0.00	0.00	0.00	0.00	0.00	0.00	0.00	0.00	0.00	0.00	0.00
3	0.00	0.03	0.00	0.00	0.00	0.00	0.00	0.00	0.00	0.00	0.00	0.00	0.00	0.00	0.00	0.00
4	0.00	0.06	1.00	0.00	0.00	0.00	0.00	0.00	0.00	0.00	0.00	0.00	0.00	0.00	0.00	0.00

5	0.27	0.00	0.00	0.66	0.00	0.00	0.00	0.00	0.00	0.00	0.00	0.00	0.00	0.00	0.00	0.00
6	0.00	0.16	0.20	0.00	0.87	0.00	0.00	0.00	0.00	0.00	0.00	0.00	0.00	0.00	0.00	0.00
7	0.13	0.00	0.00	0.02	0.00	0.00	0.00	0.00	0.00	0.00	0.00	0.00	0.00	0.00	0.00	0.00
8	0.00	0.01	0.28	0.00	0.01	0.00	0.00	0.00	0.00	0.00	0.00	0.00	0.00	0.00	0.00	0.00
9	0.00	0.50	0.00	0.00	0.00	0.00	0.33	0.00	0.00	0.00	0.00	0.00	0.00	0.00	0.00	0.00
10	0.03	0.00	0.02	0.62	0.00	0.19	0.00	0.03	0.00	0.00	0.00	0.00	0.00	0.00	0.00	0.00
11	0.00	0.69	0.00	0.00	0.00	0.00	0.00	0.00	0.00	0.00	0.00	0.00	0.00	0.00	0.00	0.00
12	0.00	0.27	0.54	0.00	0.23	0.00	0.76	0.00	0.00	0.00	0.00	0.00	0.00	0.00	0.00	0.00
13	0.05	0.00	0.00	0.45	0.00	0.10	0.00	0.00	0.00	0.00	0.00	0.25	0.00	0.00	0.00	0.00
14	0.00	0.03	0.12	0.00	0.28	0.00	0.00	0.00	0.00	0.02	0.04	0.00	0.50	0.00	0.00	0.00
15	0.36	0.00	0.00	0.65	0.00	1.00	0.00	0.04	0.00	0.00	0.00	0.05	0.00	0.14	0.00	0.00
16	0.00	0.02	0.46	0.00	0.23	0.00	0.00	0.00	0.00	0.03	0.08	0.00	0.60	0.00	0.73	0.00

CORRELATION OF LINE-BY-LINE MEANS BETWEEN DETECTORS: Forward SCANS

Pearson correlation coefficient (r)

	1	2	3	4	5	6	7	8	9	10	11	12	13	14	15	16
1	0.00	0.00	0.00	0.00	0.00	0.00	0.00	0.00	0.00	0.00	0.00	0.00	0.00	0.00	0.00	0.00
2	0.18	0.00	0.00	0.00	0.00	0.00	0.00	0.00	0.00	0.00	0.00	0.00	0.00	0.00	0.00	0.00
3	0.08	-0.16	0.00	0.00	0.00	0.00	0.00	0.00	0.00	0.00	0.00	0.00	0.00	0.00	0.00	0.00
4	-0.27	-0.02	0.09	0.00	0.00	0.00	0.00	0.00	0.00	0.00	0.00	0.00	0.00	0.00	0.00	0.00
5	0.03	-0.37	0.32	0.01	0.00	0.00	0.00	0.00	0.00	0.00	0.00	0.00	0.00	0.00	0.00	0.00
6	-0.46	-0.15	-0.01	0.37	-0.03	0.00	0.00	0.00	0.00	0.00	0.00	0.00	0.00	0.00	0.00	0.00
7	-0.13	-0.40	0.22	0.14	0.46	0.27	0.00	0.00	0.00	0.00	0.00	0.00	0.00	0.00	0.00	0.00
8	-0.48	-0.24	-0.06	0.31	0.06	0.63	0.38	0.00	0.00	0.00	0.00	0.00	0.00	0.00	0.00	0.00
9	0.23	-0.03	0.29	-0.13	0.15	-0.32	0.07	-0.23	0.00	0.00	0.00	0.00	0.00	0.00	0.00	0.00
10	0.15	0.23	-0.13	-0.07	-0.17	-0.09	-0.29	-0.17	-0.23	0.00	0.00	0.00	0.00	0.00	0.00	0.00
11	0.16	-0.09	0.12	-0.06	0.26	-0.17	0.24	-0.04	0.40	-0.33	0.00	0.00	0.00	0.00	0.00	0.00
12	-0.21	-0.03	0.04	0.19	-0.05	0.34	0.12	0.26	-0.28	0.19	-0.23	0.00	0.00	0.00	0.00	0.00
13	-0.15	-0.44	0.21	0.08	0.29	0.13	0.41	0.24	0.32	-0.34	0.36	-0.08	0.00	0.00	0.00	0.00
14	-0.32	-0.19	0.08	0.20	0.06	0.39	0.22	0.36	-0.32	0.09	-0.14	0.42	-0.01	0.00	0.00	0.00
15	-0.15	-0.31	0.32	0.00	0.43	0.10	0.34	0.14	0.27	-0.30	0.30	-0.09	0.46	-0.06	0.00	0.00
16	-0.13	-0.17	0.09	0.18	0.04	0.34	0.29	0.32	-0.20	0.02	-0.06	0.35	0.07	0.41	0.01	0.00

Percentage of unexplained variance ($100*[1-r^2]$)

	1	2	3	4	5	6	7	8	9	10	11	12	13	14	15	16
1	0	0	0	0	0	0	0	0	0	0	0	0	0	0	0	0
2	97	0	0	0	0	0	0	0	0	0	0	0	0	0	0	0
3	99	97	0	0	0	0	0	0	0	0	0	0	0	0	0	0
4	93	100	99	0	0	0	0	0	0	0	0	0	0	0	0	0
5	100	86	89	100	0	0	0	0	0	0	0	0	0	0	0	0
6	79	98	100	86	100	0	0	0	0	0	0	0	0	0	0	0
7	98	84	95	98	79	93	0	0	0	0	0	0	0	0	0	0

8	77	94	100	90	100	60	86	0	0	0	0	0	0	0	0	0
9	95	100	92	98	98	90	100	95	0	0	0	0	0	0	0	0
10	98	95	98	100	97	99	91	97	95	0	0	0	0	0	0	0
11	98	99	98	100	93	97	94	100	84	89	0	0	0	0	0	0
12	95	100	100	97	100	88	98	93	92	96	95	0	0	0	0	0
13	98	81	95	99	92	98	84	94	90	89	87	99	0	0	0	0
14	90	96	99	96	100	85	95	87	90	99	98	83	100	0	0	0
15	98	91	90	100	82	99	89	98	93	91	91	99	79	100	0	0
16	98	97	99	97	100	89	92	90	96	100	100	87	99	83	100	0

Significance of regression (Reject hypothesis if alpha < 0.05)

	1	2	3	4	5	6	7	8	9	10	11	12	13	14	15	16
1	0.00	0.00	0.00	0.00	0.00	0.00	0.00	0.00	0.00	0.00	0.00	0.00	0.00	0.00	0.00	0.00
2	0.01	0.00	0.00	0.00	0.00	0.00	0.00	0.00	0.00	0.00	0.00	0.00	0.00	0.00	0.00	0.00
3	0.24	0.02	0.00	0.00	0.00	0.00	0.00	0.00	0.00	0.00	0.00	0.00	0.00	0.00	0.00	0.00
4	0.00	0.70	0.24	0.00	0.00	0.00	0.00	0.00	0.00	0.00	0.00	0.00	0.00	0.00	0.00	0.00
5	0.64	0.00	0.00	0.62	0.00	0.00	0.00	0.00	0.00	0.00	0.00	0.00	0.00	0.00	0.00	0.00
6	0.00	0.03	0.79	0.00	0.51	0.00	0.00	0.00	0.00	0.00	0.00	0.00	0.00	0.00	0.00	0.00
7	0.09	0.00	0.01	0.02	0.00	0.00	0.00	0.00	0.00	0.00	0.00	0.00	0.00	0.00	0.00	0.00
8	0.00	0.00	0.35	0.00	0.50	0.00	0.00	0.00	0.00	0.00	0.00	0.00	0.00	0.00	0.00	0.00
9	0.00	0.54	0.00	0.16	0.06	0.00	0.24	0.00	0.00	0.00	0.00	0.00	0.00	0.00	0.00	0.00
10	0.04	0.00	0.06	0.58	0.01	0.27	0.00	0.03	0.00	0.00	0.00	0.00	0.00	0.00	0.00	0.00
11	0.03	0.16	0.13	0.71	0.00	0.02	0.00	0.69	0.00	0.00	0.00	0.00	0.00	0.00	0.00	0.00
12	0.01	0.56	0.73	0.00	0.38	0.00	0.05	0.00	0.00	0.00	0.01	0.00	0.00	0.00	0.00	0.00
13	0.05	0.00	0.01	0.15	0.00	0.06	0.00	0.00	0.00	0.00	0.00	0.61	0.00	0.00	0.00	0.00
14	0.00	0.01	0.37	0.00	0.54	0.00	0.00	0.00	0.00	0.07	0.12	0.00	0.90	0.00	0.00	0.00
15	0.05	0.00	0.00	0.68	0.00	0.14	0.00	0.04	0.00	0.00	0.00	0.69	0.00	0.23	0.00	0.00
16	0.09	0.01	0.28	0.01	0.77	0.00	0.00	0.00	0.01	0.35	0.67	0.00	0.24	0.00	0.70	0.00

CORRELATION OF LINE-BY-LINE MEANS BETWEEN DETECTORS: Reverse SCANS

Pearson correlation coefficient (r)

	1	2	3	4	5	6	7	8	9	10	11	12	13	14	15	16
1	0.00	0.00	0.00	0.00	0.00	0.00	0.00	0.00	0.00	0.00	0.00	0.00	0.00	0.00	0.00	0.00
2	0.18	0.00	0.00	0.00	0.00	0.00	0.00	0.00	0.00	0.00	0.00	0.00	0.00	0.00	0.00	0.00
3	0.19	-0.19	0.00	0.00	0.00	0.00	0.00	0.00	0.00	0.00	0.00	0.00	0.00	0.00	0.00	0.00
4	-0.23	0.08	-0.09	0.00	0.00	0.00	0.00	0.00	0.00	0.00	0.00	0.00	0.00	0.00	0.00	0.00
5	0.00	-0.20	0.17	-0.06	0.00	0.00	0.00	0.00	0.00	0.00	0.00	0.00	0.00	0.00	0.00	0.00
6	-0.47	-0.13	-0.13	0.45	-0.05	0.00	0.00	0.00	0.00	0.00	0.00	0.00	0.00	0.00	0.00	0.00
7	-0.13	-0.30	0.20	0.09	0.45	0.19	0.00	0.00	0.00	0.00	0.00	0.00	0.00	0.00	0.00	0.00
8	-0.48	-0.15	-0.06	0.36	0.20	0.59	0.36	0.00	0.00	0.00	0.00	0.00	0.00	0.00	0.00	0.00
9	0.19	-0.02	0.25	-0.17	0.23	-0.27	0.09	-0.18	0.00	0.00	0.00	0.00	0.00	0.00	0.00	0.00
10	0.00	0.09	-0.11	0.01	-0.25	0.04	-0.23	0.01	-0.23	0.00	0.00	0.00	0.00	0.00	0.00	0.00

11 0.21-0.09 0.25-0.27 0.23-0.22 0.29-0.16 0.35-0.31 0.00 0.00 0.00 0.00 0.00 0.00
 12 -0.21 0.02-0.08 0.21-0.16 0.27-0.03 0.27-0.26 0.30-0.25 0.00 0.00 0.00 0.00 0.00
 13 -0.14-0.22 0.17 0.00 0.36 0.14 0.35 0.20 0.17-0.32 0.35-0.10 0.00 0.00 0.00 0.00
 14 -0.26-0.17 0.08 0.24-0.01 0.38 0.19 0.40-0.22 0.12-0.15 0.41-0.02 0.00 0.00 0.00
 15 -0.05-0.27 0.21-0.04 0.45 0.02 0.36 0.16 0.29-0.30 0.41-0.18 0.48-0.04 0.00 0.00
 16 -0.27-0.20 0.00 0.24 0.02 0.40 0.21 0.40-0.22 0.15-0.20 0.34 0.02 0.47 0.00 0.00

Percentage of unexplained variance (100*[1-r^2])

	1	2	3	4	5	6	7	8	9	10	11	12	13	14	15	16
1	0	0	0	0	0	0	0	0	0	0	0	0	0	0	0	0
2	97	0	0	0	0	0	0	0	0	0	0	0	0	0	0	0
3	96	96	0	0	0	0	0	0	0	0	0	0	0	0	0	0
4	95	99	99	0	0	0	0	0	0	0	0	0	0	0	0	0
5	100	96	97	100	0	0	0	0	0	0	0	0	0	0	0	0
6	78	98	98	79	100	0	0	0	0	0	0	0	0	0	0	0
7	98	91	96	99	80	96	0	0	0	0	0	0	0	0	0	0
8	77	98	100	87	96	66	87	0	0	0	0	0	0	0	0	0
9	97	100	94	97	94	93	99	97	0	0	0	0	0	0	0	0
10	100	99	99	100	94	100	95	100	95	0	0	0	0	0	0	0
11	96	99	94	92	95	95	92	97	88	91	0	0	0	0	0	0
12	96	100	99	96	97	93	100	93	93	91	94	0	0	0	0	0
13	98	95	97	100	87	98	88	96	97	90	88	99	0	0	0	0
14	93	97	99	94	100	86	96	84	95	99	98	83	100	0	0	0
15	100	93	96	100	80	100	87	97	91	91	83	97	77	100	0	0
16	93	96	100	94	100	84	96	84	95	98	96	88	100	78	100	0

Significance of regression (Reject hypothesis if alpha < 0.05)

	1	2	3	4	5	6	7	8	9	10	11	12	13	14	15	16
1	0.00	0.00	0.00	0.00	0.00	0.00	0.00	0.00	0.00	0.00	0.00	0.00	0.00	0.00	0.00	0.00
2	0.11	0.00	0.00	0.00	0.00	0.00	0.00	0.00	0.00	0.00	0.00	0.00	0.00	0.00	0.00	0.00
3	0.09	0.01	0.00	0.00	0.00	0.00	0.00	0.00	0.00	0.00	0.00	0.00	0.00	0.00	0.00	0.00
4	0.00	0.24	0.09	0.00	0.00	0.00	0.00	0.00	0.00	0.00	0.00	0.00	0.00	0.00	0.00	0.00
5	0.41	0.01	0.05	1.00	0.00	0.00	0.00	0.00	0.00	0.00	0.00	0.00	0.00	0.00	0.00	0.00
6	0.00	0.11	0.03	0.00	0.65	0.00	0.00	0.00	0.00	0.00	0.00	0.00	0.00	0.00	0.00	0.00
7	0.01	0.00	0.02	0.05	0.00	0.01	0.00	0.00	0.00	0.00	0.00	0.00	0.00	0.00	0.00	0.00
8	0.00	0.05	0.26	0.00	0.01	0.00	0.00	0.00	0.00	0.00	0.00	0.00	0.00	0.00	0.00	0.00
9	0.11	0.89	0.00	0.13	0.00	0.00	0.32	0.02	0.00	0.00	0.00	0.00	0.00	0.00	0.00	0.00
10	0.47	0.20	0.06	0.45	0.00	0.51	0.00	0.79	0.00	0.00	0.00	0.00	0.00	0.00	0.00	0.00
11	0.07	0.28	0.01	0.01	0.00	0.01	0.00	0.05	0.00	0.00	0.00	0.00	0.00	0.00	0.00	0.00
12	0.00	0.65	0.12	0.00	0.04	0.00	0.58	0.00	0.00	0.00	0.00	0.00	0.00	0.00	0.00	0.00
13	0.01	0.01	0.06	0.51	0.00	0.04	0.00	0.00	0.07	0.00	0.00	0.08	0.00	0.00	0.00	0.00
14	0.00	0.03	0.50	0.00	1.00	0.00	0.02	0.00	0.00	0.15	0.02	0.00	0.68	0.00	0.00	0.00
15	0.12	0.00	0.02	0.82	0.00	0.63	0.00	0.02	0.00	0.00	0.00	0.01	0.00	0.65	0.00	0.00
16	0.00	0.01	0.72	0.00	0.66	0.00	0.01	0.00	0.00	0.05	0.00	0.00	1.00	0.00	0.58	0.00

RANDOM NOISE SUMMARY REPORT

det	Scene mean data value (counts)	Scene mean noise level (counts)	Line mean noise level (counts)	Scene/line noise ratio
-----	--------------------------------------	---------------------------------------	--------------------------------------	---------------------------

All Scans

1	9.917	0.592	0.591	1.002
2	10.111	0.565	0.563	1.002
3	9.873	0.575	0.574	1.002
4	10.044	0.564	0.563	1.003
5	9.821	0.586	0.585	1.002
6	10.030	0.588	0.587	1.002
7	9.938	0.576	0.574	1.003
8	10.084	0.597	0.596	1.002
9	9.817	0.616	0.616	1.001
10	10.074	0.605	0.603	1.002
11	9.849	0.607	0.606	1.001
12	10.119	0.575	0.574	1.002
13	9.782	0.609	0.608	1.003
14	10.076	0.581	0.579	1.002
15	9.824	0.596	0.595	1.002
16	10.121	0.580	0.578	1.003

Forward Scans

1	9.916	0.593	0.591	1.002
2	10.110	0.565	0.564	1.003
3	9.872	0.577	0.575	1.002
4	10.043	0.565	0.563	1.003
5	9.822	0.585	0.584	1.003
6	10.028	0.587	0.586	1.002
7	9.936	0.576	0.575	1.003
8	10.080	0.598	0.597	1.002
9	9.817	0.616	0.615	1.001
10	10.075	0.605	0.604	1.002
11	9.850	0.607	0.606	1.002
12	10.122	0.575	0.573	1.002
13	9.784	0.609	0.607	1.003
14	10.073	0.580	0.579	1.002
15	9.826	0.596	0.595	1.002
16	10.121	0.580	0.578	1.003

Reverse Scans

1	9.918	0.592	0.591	1.002
2	10.113	0.564	0.563	1.002

3	9.874	0.574	0.572	1.003
4	10.046	0.564	0.562	1.003
5	9.820	0.587	0.585	1.002
6	10.032	0.588	0.587	1.002
7	9.939	0.575	0.574	1.002
8	10.087	0.596	0.595	1.002
9	9.816	0.617	0.616	1.001
10	10.074	0.604	0.603	1.002
11	9.847	0.608	0.607	1.001
12	10.116	0.576	0.574	1.002
13	9.780	0.610	0.609	1.002
14	10.079	0.581	0.580	1.003
15	9.823	0.596	0.595	1.002
16	10.121	0.580	0.578	1.003

Landsat 7 Image Assessment System
Random Noise Characterization

02/12/2003 18:50:37
tightrope

Product: L72EDC110222815020 Processing Level: R0C

Band B2 Scene 1 Gain L -- DAY IC data

SCENE AVERAGES AND STANDARD DEVIATIONS BY DETECTOR (COUNTS)

det	mean	mean	mean	mean	stdev	stdev	stdev	stdev
	of A	of B	of C	all	of A	of B	of C	all

All Scans

1	9.91	9.92	9.92	9.92	0.60	0.59	0.59	0.59
2	10.11	10.11	10.11	10.11	0.57	0.56	0.57	0.56
3	9.87	9.87	9.87	9.87	0.58	0.57	0.58	0.58
4	10.04	10.04	10.04	10.04	0.57	0.56	0.57	0.56
5	9.82	9.82	9.82	9.82	0.59	0.58	0.59	0.59
6	10.03	10.03	10.03	10.03	0.59	0.58	0.59	0.59
7	9.94	9.94	9.94	9.94	0.58	0.57	0.58	0.58
8	10.08	10.08	10.08	10.08	0.60	0.59	0.60	0.60
9	9.82	9.81	9.82	9.82	0.62	0.61	0.62	0.62
10	10.08	10.07	10.07	10.07	0.61	0.60	0.61	0.60
11	9.85	9.85	9.85	9.85	0.61	0.60	0.61	0.61
12	10.13	10.12	10.11	10.12	0.58	0.57	0.58	0.58
13	9.79	9.78	9.78	9.78	0.61	0.60	0.61	0.61
14	10.08	10.08	10.07	10.08	0.58	0.57	0.59	0.58
15	9.83	9.82	9.82	9.82	0.60	0.59	0.59	0.60
16	10.13	10.12	10.12	10.12	0.58	0.57	0.58	0.58

Forward Scans

1	9.91	9.92	9.92	9.92	0.60	0.59	0.59	0.59
2	10.11	10.11	10.11	10.11	0.57	0.56	0.57	0.57
3	9.87	9.88	9.87	9.87	0.58	0.57	0.58	0.58
4	10.05	10.05	10.04	10.04	0.57	0.56	0.57	0.56
5	9.82	9.83	9.82	9.82	0.59	0.58	0.59	0.59
6	10.03	10.03	10.02	10.03	0.59	0.58	0.58	0.59
7	9.93	9.94	9.93	9.94	0.58	0.57	0.58	0.58
8	10.08	10.08	10.08	10.08	0.61	0.59	0.60	0.60
9	9.82	9.81	9.82	9.82	0.62	0.61	0.62	0.62
10	10.09	10.06	10.07	10.07	0.61	0.60	0.60	0.61
11	9.86	9.84	9.85	9.85	0.62	0.60	0.60	0.61
12	10.14	10.11	10.12	10.12	0.58	0.57	0.57	0.57
13	9.80	9.77	9.78	9.78	0.62	0.60	0.61	0.61
14	10.08	10.07	10.07	10.07	0.58	0.57	0.58	0.58
15	9.83	9.82	9.83	9.83	0.60	0.59	0.59	0.60
16	10.13	10.11	10.12	10.12	0.59	0.58	0.58	0.58

Reverse Scans

1	9.92	9.91	9.92	9.92	0.60	0.59	0.59	0.59
2	10.11	10.11	10.11	10.11	0.57	0.56	0.56	0.56
3	9.88	9.87	9.88	9.87	0.58	0.57	0.58	0.57
4	10.04	10.04	10.05	10.05	0.56	0.56	0.57	0.56
5	9.82	9.82	9.82	9.82	0.59	0.58	0.59	0.59
6	10.03	10.03	10.04	10.03	0.59	0.58	0.60	0.59
7	9.94	9.93	9.94	9.94	0.57	0.57	0.58	0.58
8	10.08	10.09	10.09	10.09	0.60	0.59	0.60	0.60
9	9.82	9.82	9.81	9.82	0.62	0.61	0.62	0.62
10	10.08	10.07	10.07	10.07	0.61	0.60	0.61	0.60
11	9.85	9.85	9.84	9.85	0.61	0.60	0.61	0.61
12	10.12	10.12	10.11	10.12	0.57	0.57	0.58	0.58
13	9.78	9.78	9.77	9.78	0.61	0.60	0.62	0.61
14	10.08	10.08	10.07	10.08	0.58	0.57	0.59	0.58
15	9.83	9.83	9.82	9.82	0.60	0.59	0.60	0.60
16	10.12	10.13	10.11	10.12	0.58	0.57	0.58	0.58

 TESTS OF EQUIVALENCE OF SECTION MEANS AND STANDARD DEVIATIONS
 (TEST FOR RESIDUAL MEMORY EFFECT; NOISE VARIATION ACROSS IMAGE)
 Number of lines that failed t or f test (alpha < 0.05)

TTEST FOR MEANS FTEST FOR VARIANCE #lines TTEST FTEST #scans
 det A-B B-C A-C A-B B-C A-C tested for-rev for-rev tested

All Scans

1	6	2	4	41	43	51	375	17	30	187
---	---	---	---	----	----	----	-----	----	----	-----

2	2	3	7	40	48	57	375	12	32	187
3	5	8	3	40	46	52	375	11	31	187
4	3	2	3	53	49	58	375	10	31	187
5	2	3	9	30	25	38	375	18	22	187
6	1	2	2	37	41	45	375	7	28	187
7	3	7	1	36	39	56	375	13	23	187
8	1	3	5	45	38	49	375	13	28	187
9	4	3	3	34	38	45	375	9	21	187
10	4	1	2	34	41	57	375	26	32	187
11	1	2	5	46	39	49	375	4	27	187
12	2	4	6	47	56	56	375	9	27	187
13	8	4	7	29	20	36	375	18	22	187
14	3	0	2	55	50	55	375	6	28	187
15	1	0	2	34	39	29	375	3	23	187
16	4	0	3	52	43	52	375	10	30	187

Forward Scans

1	4	0	4	23	18	24	188
2	1	1	2	21	21	32	188
3	2	1	0	18	20	20	188
4	1	2	3	29	18	30	188
5	0	1	6	14	12	17	188
6	1	1	1	21	18	27	188
7	1	4	0	20	16	26	188
8	0	1	3	23	19	26	188
9	2	1	2	15	12	23	188
10	1	0	0	21	19	25	188
11	1	1	0	21	23	21	188
12	2	3	6	27	27	32	188
13	5	3	3	16	6	19	188
14	1	0	1	31	24	29	188
15	1	0	1	17	20	11	188
16	3	0	2	28	20	28	188

Reverse Scans

1	2	2	0	18	25	27	187
2	1	2	5	19	27	25	187
3	3	7	3	22	26	32	187
4	2	0	0	24	31	28	187
5	2	2	3	16	13	21	187
6	0	1	1	16	23	18	187
7	2	3	1	16	23	30	187
8	1	2	2	22	19	23	187
9	2	2	1	19	26	22	187
10	3	1	2	13	22	32	187
11	0	1	5	25	16	28	187

12	0	1	0	20	29	24	187
13	3	1	4	13	14	17	187
14	2	0	1	24	26	26	187
15	0	0	1	17	19	18	187
16	1	0	1	24	23	24	187

AVERAGE OF LINE BY LINE STANDARD DEVIATIONS AND RANDOMNESS CHECK
(alpha level of < 0.05 for randomness tests indicates rejection of
null hypothesis of randomness of sequence of line means or stdevs)

det	Averaged Standard Deviations of Lines				Randomness Test	
	A	B	C	All	MEAN	STDEV
	(counts)	(counts)	(counts)	(counts)	(alpha)	(alpha)

All Scans

1	0.59	0.59	0.59	0.59	0.376	0.060
2	0.57	0.56	0.57	0.56	0.029	0.398
3	0.58	0.57	0.58	0.57	0.136	0.106
4	0.56	0.56	0.57	0.56	0.376	0.284
5	0.59	0.58	0.59	0.58	0.267	0.418
6	0.59	0.58	0.59	0.59	0.020	0.339
7	0.58	0.57	0.58	0.57	0.340	0.378
8	0.60	0.59	0.60	0.60	0.002	0.378
9	0.62	0.61	0.62	0.62	0.259	0.127
10	0.61	0.60	0.60	0.60	0.416	0.438
11	0.61	0.60	0.61	0.61	0.078	0.150
12	0.58	0.57	0.57	0.57	0.374	0.189
13	0.61	0.60	0.61	0.61	0.020	0.302
14	0.58	0.57	0.59	0.58	0.122	0.250
15	0.60	0.59	0.59	0.59	0.249	0.302
16	0.58	0.57	0.58	0.58	0.217	0.479

Forward Scans

1	0.59	0.59	0.59	0.59	0.187	0.279
2	0.57	0.56	0.57	0.56	0.119	0.153
3	0.58	0.57	0.58	0.58	0.355	0.020
4	0.57	0.56	0.57	0.56	0.060	0.385
5	0.59	0.58	0.58	0.58	0.386	0.029
6	0.59	0.58	0.58	0.59	0.150	0.040
7	0.58	0.57	0.57	0.57	0.016	0.385
8	0.60	0.59	0.60	0.60	0.230	0.385
9	0.62	0.61	0.61	0.62	0.229	0.190
10	0.61	0.60	0.60	0.60	0.089	0.330
11	0.62	0.60	0.60	0.61	0.412	0.153
12	0.58	0.57	0.57	0.57	0.270	0.190

13	0.61	0.60	0.61	0.61	0.474	0.385
14	0.58	0.57	0.58	0.58	0.470	0.385
15	0.60	0.59	0.59	0.60	0.209	0.279
16	0.58	0.58	0.58	0.58	0.071	0.442

Reverse Scans

1	0.59	0.59	0.59	0.59	0.037	0.278
2	0.57	0.56	0.56	0.56	0.037	0.231
3	0.57	0.57	0.57	0.57	0.050	0.356
4	0.56	0.56	0.57	0.56	0.439	0.330
5	0.59	0.58	0.59	0.59	0.184	0.231
6	0.59	0.58	0.59	0.59	0.499	0.442
7	0.57	0.57	0.58	0.57	0.013	0.231
8	0.59	0.59	0.60	0.59	0.494	0.330
9	0.62	0.61	0.62	0.62	0.303	0.442
10	0.60	0.60	0.61	0.60	0.228	0.330
11	0.61	0.60	0.61	0.61	0.169	0.152
12	0.57	0.57	0.58	0.57	0.411	0.009
13	0.61	0.60	0.62	0.61	0.099	0.020
14	0.58	0.57	0.59	0.58	0.076	0.053
15	0.60	0.59	0.59	0.59	0.031	0.189
16	0.58	0.57	0.58	0.58	0.471	0.442

CORRELATION OF LINE-BY-LINE MEANS BETWEEN DETECTORS: All SCANS

Pearson correlation coefficient (r)

	1	2	3	4	5	6	7	8	9	10	11	12	13	14	15	16
1	0.00	0.00	0.00	0.00	0.00	0.00	0.00	0.00	0.00	0.00	0.00	0.00	0.00	0.00	0.00	0.00
2	0.18	0.00	0.00	0.00	0.00	0.00	0.00	0.00	0.00	0.00	0.00	0.00	0.00	0.00	0.00	0.00
3	0.13-0.17	0.00	0.00	0.00	0.00	0.00	0.00	0.00	0.00	0.00	0.00	0.00	0.00	0.00	0.00	0.00
4	-0.25	0.03	0.00	0.00	0.00	0.00	0.00	0.00	0.00	0.00	0.00	0.00	0.00	0.00	0.00	0.00
5	0.01-0.29	0.25-0.02	0.00	0.00	0.00	0.00	0.00	0.00	0.00	0.00	0.00	0.00	0.00	0.00	0.00	0.00
6	-0.46-0.14-0.06	0.42-0.04	0.00	0.00	0.00	0.00	0.00	0.00	0.00	0.00	0.00	0.00	0.00	0.00	0.00	0.00
7	-0.13-0.35	0.21	0.12	0.45	0.24	0.00	0.00	0.00	0.00	0.00	0.00	0.00	0.00	0.00	0.00	0.00
8	-0.47-0.19-0.05	0.34	0.12	0.61	0.37	0.00	0.00	0.00	0.00	0.00	0.00	0.00	0.00	0.00	0.00	0.00
9	0.21-0.03	0.27-0.15	0.19-0.30	0.08-0.21	0.00	0.00	0.00	0.00	0.00	0.00	0.00	0.00	0.00	0.00	0.00	0.00
10	0.07	0.16-0.12-0.03-0.21-0.02-0.26-0.08-0.23	0.00	0.00	0.00	0.00	0.00	0.00	0.00	0.00	0.00	0.00	0.00	0.00	0.00	0.00
11	0.18-0.09	0.18-0.17	0.25-0.20	0.26-0.11	0.38-0.32	0.00	0.00	0.00	0.00	0.00	0.00	0.00	0.00	0.00	0.00	0.00
12	-0.21-0.01-0.03	0.19-0.10	0.30	0.04	0.25-0.26	0.25-0.23	0.00	0.00	0.00	0.00	0.00	0.00	0.00	0.00	0.00	0.00
13	-0.14-0.34	0.19	0.04	0.32	0.13	0.37	0.21	0.25-0.32	0.36-0.08	0.00	0.00	0.00	0.00	0.00	0.00	0.00
14	-0.29-0.18	0.08	0.23	0.02	0.39	0.21	0.39-0.27	0.10-0.15	0.39-0.02	0.00	0.00	0.00	0.00	0.00	0.00	0.00
15	-0.10-0.29	0.26-0.03	0.44	0.06	0.34	0.15	0.28-0.30	0.36-0.13	0.47-0.06	0.00	0.00	0.00	0.00	0.00	0.00	0.00
16	-0.20-0.18	0.04	0.21	0.03	0.37	0.24	0.36-0.21	0.09-0.13	0.34	0.04	0.44	0.01	0.00	0.00	0.00	0.00

Percentage of unexplained variance ($100*[1-r^2]$)

	1	2	3	4	5	6	7	8	9	10	11	12	13	14	15	16
--	---	---	---	---	---	---	---	---	---	----	----	----	----	----	----	----

1	0	0	0	0	0	0	0	0	0	0	0	0	0	0	0	0
2	97	0	0	0	0	0	0	0	0	0	0	0	0	0	0	0
3	98	97	0	0	0	0	0	0	0	0	0	0	0	0	0	0
4	94	100	100	0	0	0	0	0	0	0	0	0	0	0	0	0
5	100	92	94	100	0	0	0	0	0	0	0	0	0	0	0	0
6	79	98	100	83	100	0	0	0	0	0	0	0	0	0	0	0
7	98	88	96	99	80	94	0	0	0	0	0	0	0	0	0	0
8	77	96	100	88	98	63	86	0	0	0	0	0	0	0	0	0
9	96	100	93	98	96	91	99	96	0	0	0	0	0	0	0	0
10	99	98	99	100	96	100	93	99	95	0	0	0	0	0	0	0
11	97	99	97	97	94	96	93	99	86	90	0	0	0	0	0	0
12	95	100	100	96	99	91	100	94	93	94	95	0	0	0	0	0
13	98	89	96	100	90	98	86	95	94	89	87	99	0	0	0	0
14	92	97	99	95	100	85	96	85	93	99	98	84	100	0	0	0
15	99	92	93	100	81	100	88	98	92	91	87	98	78	100	0	0
16	96	97	100	96	100	86	94	87	96	99	98	88	100	81	100	0

Significance of regression (Reject hypothesis if alpha < 0.05)

	1	2	3	4	5	6	7	8	9	10	11	12	13	14	15	16
1	0.00	0.00	0.00	0.00	0.00	0.00	0.00	0.00	0.00	0.00	0.00	0.00	0.00	0.00	0.00	0.00
2	0.00	0.00	0.00	0.00	0.00	0.00	0.00	0.00	0.00	0.00	0.00	0.00	0.00	0.00	0.00	0.00
3	0.00	0.03	0.00	0.00	0.00	0.00	0.00	0.00	0.00	0.00	0.00	0.00	0.00	0.00	0.00	0.00
4	0.00	0.06	1.00	0.00	0.00	0.00	0.00	0.00	0.00	0.00	0.00	0.00	0.00	0.00	0.00	0.00
5	0.27	0.00	0.00	0.66	0.00	0.00	0.00	0.00	0.00	0.00	0.00	0.00	0.00	0.00	0.00	0.00
6	0.00	0.16	0.20	0.00	0.87	0.00	0.00	0.00	0.00	0.00	0.00	0.00	0.00	0.00	0.00	0.00
7	0.13	0.00	0.00	0.02	0.00	0.00	0.00	0.00	0.00	0.00	0.00	0.00	0.00	0.00	0.00	0.00
8	0.00	0.01	0.28	0.00	0.01	0.00	0.00	0.00	0.00	0.00	0.00	0.00	0.00	0.00	0.00	0.00
9	0.00	0.50	0.00	0.00	0.00	0.00	0.33	0.00	0.00	0.00	0.00	0.00	0.00	0.00	0.00	0.00
10	0.03	0.00	0.02	0.62	0.00	0.19	0.00	0.03	0.00	0.00	0.00	0.00	0.00	0.00	0.00	0.00
11	0.00	0.69	0.00	0.00	0.00	0.00	0.00	0.00	0.00	0.00	0.00	0.00	0.00	0.00	0.00	0.00
12	0.00	0.27	0.54	0.00	0.23	0.00	0.76	0.00	0.00	0.00	0.00	0.00	0.00	0.00	0.00	0.00
13	0.05	0.00	0.00	0.45	0.00	0.10	0.00	0.00	0.00	0.00	0.00	0.25	0.00	0.00	0.00	0.00
14	0.00	0.03	0.12	0.00	0.28	0.00	0.00	0.00	0.00	0.02	0.04	0.00	0.50	0.00	0.00	0.00
15	0.36	0.00	0.00	0.65	0.00	1.00	0.00	0.04	0.00	0.00	0.00	0.05	0.00	0.14	0.00	0.00
16	0.00	0.02	0.46	0.00	0.23	0.00	0.00	0.00	0.00	0.03	0.08	0.00	0.60	0.00	0.73	0.00

CORRELATION OF LINE-BY-LINE MEANS BETWEEN DETECTORS: Forward SCANS

Pearson correlation coefficient (r)

	1	2	3	4	5	6	7	8	9	10	11	12	13	14	15	16
1	0.00	0.00	0.00	0.00	0.00	0.00	0.00	0.00	0.00	0.00	0.00	0.00	0.00	0.00	0.00	0.00
2	0.18	0.00	0.00	0.00	0.00	0.00	0.00	0.00	0.00	0.00	0.00	0.00	0.00	0.00	0.00	0.00
3	0.08-0.16	0.00	0.00	0.00	0.00	0.00	0.00	0.00	0.00	0.00	0.00	0.00	0.00	0.00	0.00	0.00

4 -0.27-0.02 0.09 0.00 0.00 0.00 0.00 0.00 0.00 0.00 0.00 0.00 0.00 0.00 0.00 0.00
5 0.03-0.37 0.32 0.01 0.00 0.00 0.00 0.00 0.00 0.00 0.00 0.00 0.00 0.00 0.00 0.00
6 -0.46-0.15-0.01 0.37-0.03 0.00 0.00 0.00 0.00 0.00 0.00 0.00 0.00 0.00 0.00 0.00
7 -0.13-0.40 0.22 0.14 0.46 0.27 0.00 0.00 0.00 0.00 0.00 0.00 0.00 0.00 0.00 0.00
8 -0.48-0.24-0.06 0.31 0.06 0.63 0.38 0.00 0.00 0.00 0.00 0.00 0.00 0.00 0.00 0.00
9 0.23-0.03 0.29-0.13 0.15-0.32 0.07-0.23 0.00 0.00 0.00 0.00 0.00 0.00 0.00 0.00 0.00
10 0.15 0.23-0.13-0.07-0.17-0.09-0.29-0.17-0.23 0.00 0.00 0.00 0.00 0.00 0.00 0.00
11 0.16-0.09 0.12-0.06 0.26-0.17 0.24-0.04 0.40-0.33 0.00 0.00 0.00 0.00 0.00 0.00 0.00
12 -0.21-0.03 0.04 0.19-0.05 0.34 0.12 0.26-0.28 0.19-0.23 0.00 0.00 0.00 0.00 0.00
13 -0.15-0.44 0.21 0.08 0.29 0.13 0.41 0.24 0.32-0.34 0.36-0.08 0.00 0.00 0.00 0.00
14 -0.32-0.19 0.08 0.20 0.06 0.39 0.22 0.36-0.32 0.09-0.14 0.42-0.01 0.00 0.00 0.00
15 -0.15-0.31 0.32 0.00 0.43 0.10 0.34 0.14 0.27-0.30 0.30-0.09 0.46-0.06 0.00 0.00
16 -0.13-0.17 0.09 0.18 0.04 0.34 0.29 0.32-0.20 0.02-0.06 0.35 0.07 0.41 0.01 0.00

Percentage of unexplained variance ($100*[1-r^2]$)

	1	2	3	4	5	6	7	8	9	10	11	12	13	14	15	16
1	0	0	0	0	0	0	0	0	0	0	0	0	0	0	0	0
2	97	0	0	0	0	0	0	0	0	0	0	0	0	0	0	0
3	99	97	0	0	0	0	0	0	0	0	0	0	0	0	0	0
4	93	100	99	0	0	0	0	0	0	0	0	0	0	0	0	0
5	100	86	89	100	0	0	0	0	0	0	0	0	0	0	0	0
6	79	98	100	86	100	0	0	0	0	0	0	0	0	0	0	0
7	98	84	95	98	79	93	0	0	0	0	0	0	0	0	0	0
8	77	94	100	90	100	60	86	0	0	0	0	0	0	0	0	0
9	95	100	92	98	98	90	100	95	0	0	0	0	0	0	0	0
10	98	95	98	100	97	99	91	97	95	0	0	0	0	0	0	0
11	98	99	98	100	93	97	94	100	84	89	0	0	0	0	0	0
12	95	100	100	97	100	88	98	93	92	96	95	0	0	0	0	0
13	98	81	95	99	92	98	84	94	90	89	87	99	0	0	0	0
14	90	96	99	96	100	85	95	87	90	99	98	83	100	0	0	0
15	98	91	90	100	82	99	89	98	93	91	91	99	79	100	0	0
16	98	97	99	97	100	89	92	90	96	100	100	87	99	83	100	0

Significance of regression (Reject hypothesis if $\alpha < 0.05$)

	1	2	3	4	5	6	7	8	9	10	11	12	13	14	15	16
1	0.00	0.00	0.00	0.00	0.00	0.00	0.00	0.00	0.00	0.00	0.00	0.00	0.00	0.00	0.00	0.00
2	0.01	0.00	0.00	0.00	0.00	0.00	0.00	0.00	0.00	0.00	0.00	0.00	0.00	0.00	0.00	0.00
3	0.24	0.02	0.00	0.00	0.00	0.00	0.00	0.00	0.00	0.00	0.00	0.00	0.00	0.00	0.00	0.00
4	0.00	0.70	0.24	0.00	0.00	0.00	0.00	0.00	0.00	0.00	0.00	0.00	0.00	0.00	0.00	0.00
5	0.64	0.00	0.00	0.62	0.00	0.00	0.00	0.00	0.00	0.00	0.00	0.00	0.00	0.00	0.00	0.00
6	0.00	0.03	0.79	0.00	0.51	0.00	0.00	0.00	0.00	0.00	0.00	0.00	0.00	0.00	0.00	0.00
7	0.09	0.00	0.01	0.02	0.00	0.00	0.00	0.00	0.00	0.00	0.00	0.00	0.00	0.00	0.00	0.00
8	0.00	0.00	0.35	0.00	0.50	0.00	0.00	0.00	0.00	0.00	0.00	0.00	0.00	0.00	0.00	0.00
9	0.00	0.54	0.00	0.16	0.06	0.00	0.24	0.00	0.00	0.00	0.00	0.00	0.00	0.00	0.00	0.00
10	0.04	0.00	0.06	0.58	0.01	0.27	0.00	0.03	0.00	0.00	0.00	0.00	0.00	0.00	0.00	0.00
11	0.03	0.16	0.13	0.71	0.00	0.02	0.00	0.69	0.00	0.00	0.00	0.00	0.00	0.00	0.00	0.00

12	0.01	0.56	0.73	0.00	0.38	0.00	0.05	0.00	0.00	0.00	0.01	0.00	0.00	0.00	0.00	0.00
13	0.05	0.00	0.01	0.15	0.00	0.06	0.00	0.00	0.00	0.00	0.00	0.61	0.00	0.00	0.00	0.00
14	0.00	0.01	0.37	0.00	0.54	0.00	0.00	0.00	0.00	0.07	0.12	0.00	0.90	0.00	0.00	0.00
15	0.05	0.00	0.00	0.68	0.00	0.14	0.00	0.04	0.00	0.00	0.00	0.69	0.00	0.23	0.00	0.00
16	0.09	0.01	0.28	0.01	0.77	0.00	0.00	0.00	0.01	0.35	0.67	0.00	0.24	0.00	0.70	0.00

CORRELATION OF LINE-BY-LINE MEANS BETWEEN DETECTORS: Reverse SCANS

Pearson correlation coefficient (r)

	1	2	3	4	5	6	7	8	9	10	11	12	13	14	15	16
1	0.00	0.00	0.00	0.00	0.00	0.00	0.00	0.00	0.00	0.00	0.00	0.00	0.00	0.00	0.00	0.00
2	0.18	0.00	0.00	0.00	0.00	0.00	0.00	0.00	0.00	0.00	0.00	0.00	0.00	0.00	0.00	0.00
3	0.19	-0.19	0.00	0.00	0.00	0.00	0.00	0.00	0.00	0.00	0.00	0.00	0.00	0.00	0.00	0.00
4	-0.23	0.08	-0.09	0.00	0.00	0.00	0.00	0.00	0.00	0.00	0.00	0.00	0.00	0.00	0.00	0.00
5	0.00	-0.20	0.17	-0.06	0.00	0.00	0.00	0.00	0.00	0.00	0.00	0.00	0.00	0.00	0.00	0.00
6	-0.47	-0.13	-0.13	0.45	-0.05	0.00	0.00	0.00	0.00	0.00	0.00	0.00	0.00	0.00	0.00	0.00
7	-0.13	-0.30	0.20	0.09	0.45	0.19	0.00	0.00	0.00	0.00	0.00	0.00	0.00	0.00	0.00	0.00
8	-0.48	-0.15	-0.06	0.36	0.20	0.59	0.36	0.00	0.00	0.00	0.00	0.00	0.00	0.00	0.00	0.00
9	0.19	-0.02	0.25	-0.17	0.23	-0.27	0.09	-0.18	0.00	0.00	0.00	0.00	0.00	0.00	0.00	0.00
10	0.00	0.09	-0.11	0.01	-0.25	0.04	-0.23	0.01	-0.23	0.00	0.00	0.00	0.00	0.00	0.00	0.00
11	0.21	-0.09	0.25	-0.27	0.23	-0.22	0.29	-0.16	0.35	-0.31	0.00	0.00	0.00	0.00	0.00	0.00
12	-0.21	0.02	-0.08	0.21	-0.16	0.27	-0.03	0.27	-0.26	0.30	-0.25	0.00	0.00	0.00	0.00	0.00
13	-0.14	-0.22	0.17	0.00	0.36	0.14	0.35	0.20	0.17	-0.32	0.35	-0.10	0.00	0.00	0.00	0.00
14	-0.26	-0.17	0.08	0.24	-0.01	0.38	0.19	0.40	-0.22	0.12	-0.15	0.41	-0.02	0.00	0.00	0.00
15	-0.05	-0.27	0.21	-0.04	0.45	0.02	0.36	0.16	0.29	-0.30	0.41	-0.18	0.48	-0.04	0.00	0.00
16	-0.27	-0.20	0.00	0.24	0.02	0.40	0.21	0.40	-0.22	0.15	-0.20	0.34	0.02	0.47	0.00	0.00

Percentage of unexplained variance (100*[1-r^2])

	1	2	3	4	5	6	7	8	9	10	11	12	13	14	15	16
1	0	0	0	0	0	0	0	0	0	0	0	0	0	0	0	0
2	97	0	0	0	0	0	0	0	0	0	0	0	0	0	0	0
3	96	96	0	0	0	0	0	0	0	0	0	0	0	0	0	0
4	95	99	99	0	0	0	0	0	0	0	0	0	0	0	0	0
5	100	96	97	100	0	0	0	0	0	0	0	0	0	0	0	0
6	78	98	98	79	100	0	0	0	0	0	0	0	0	0	0	0
7	98	91	96	99	80	96	0	0	0	0	0	0	0	0	0	0
8	77	98	100	87	96	66	87	0	0	0	0	0	0	0	0	0
9	97	100	94	97	94	93	99	97	0	0	0	0	0	0	0	0
10	100	99	99	100	94	100	95	100	95	0	0	0	0	0	0	0
11	96	99	94	92	95	95	92	97	88	91	0	0	0	0	0	0
12	96	100	99	96	97	93	100	93	93	91	94	0	0	0	0	0
13	98	95	97	100	87	98	88	96	97	90	88	99	0	0	0	0
14	93	97	99	94	100	86	96	84	95	99	98	83	100	0	0	0

15 100 93 96 100 80 100 87 97 91 91 83 97 77 100 0 0
 16 93 96 100 94 100 84 96 84 95 98 96 88 100 78 100 0

Significance of regression (Reject hypothesis if alpha < 0.05)

	1	2	3	4	5	6	7	8	9	10	11	12	13	14	15	16
1	0.00	0.00	0.00	0.00	0.00	0.00	0.00	0.00	0.00	0.00	0.00	0.00	0.00	0.00	0.00	0.00
2	0.11	0.00	0.00	0.00	0.00	0.00	0.00	0.00	0.00	0.00	0.00	0.00	0.00	0.00	0.00	0.00
3	0.09	0.01	0.00	0.00	0.00	0.00	0.00	0.00	0.00	0.00	0.00	0.00	0.00	0.00	0.00	0.00
4	0.00	0.24	0.09	0.00	0.00	0.00	0.00	0.00	0.00	0.00	0.00	0.00	0.00	0.00	0.00	0.00
5	0.41	0.01	0.05	1.00	0.00	0.00	0.00	0.00	0.00	0.00	0.00	0.00	0.00	0.00	0.00	0.00
6	0.00	0.11	0.03	0.00	0.65	0.00	0.00	0.00	0.00	0.00	0.00	0.00	0.00	0.00	0.00	0.00
7	0.01	0.00	0.02	0.05	0.00	0.01	0.00	0.00	0.00	0.00	0.00	0.00	0.00	0.00	0.00	0.00
8	0.00	0.05	0.26	0.00	0.01	0.00	0.00	0.00	0.00	0.00	0.00	0.00	0.00	0.00	0.00	0.00
9	0.11	0.89	0.00	0.13	0.00	0.00	0.32	0.02	0.00	0.00	0.00	0.00	0.00	0.00	0.00	0.00
10	0.47	0.20	0.06	0.45	0.00	0.51	0.00	0.79	0.00	0.00	0.00	0.00	0.00	0.00	0.00	0.00
11	0.07	0.28	0.01	0.01	0.00	0.01	0.00	0.05	0.00	0.00	0.00	0.00	0.00	0.00	0.00	0.00
12	0.00	0.65	0.12	0.00	0.04	0.00	0.58	0.00	0.00	0.00	0.00	0.00	0.00	0.00	0.00	0.00
13	0.01	0.01	0.06	0.51	0.00	0.04	0.00	0.00	0.07	0.00	0.00	0.08	0.00	0.00	0.00	0.00
14	0.00	0.03	0.50	0.00	1.00	0.00	0.02	0.00	0.00	0.15	0.02	0.00	0.68	0.00	0.00	0.00
15	0.12	0.00	0.02	0.82	0.00	0.63	0.00	0.02	0.00	0.00	0.00	0.01	0.00	0.65	0.00	0.00
16	0.00	0.01	0.72	0.00	0.66	0.00	0.01	0.00	0.00	0.05	0.00	0.00	1.00	0.00	0.58	0.00

 RANDOM NOISE SUMMARY REPORT

det Scene mean Scene mean Line mean Scene/line
 data value noise level noise level noise ratio
 (counts) (counts) (counts)

All Scans

1	9.917	0.592	0.591	1.002
2	10.111	0.565	0.563	1.002
3	9.873	0.575	0.574	1.002
4	10.044	0.564	0.563	1.003
5	9.821	0.586	0.585	1.002
6	10.030	0.588	0.587	1.002
7	9.938	0.576	0.574	1.003
8	10.084	0.597	0.596	1.002
9	9.817	0.616	0.616	1.001
10	10.074	0.605	0.603	1.002
11	9.849	0.607	0.606	1.001
12	10.119	0.575	0.574	1.002
13	9.782	0.609	0.608	1.003
14	10.076	0.581	0.579	1.002
15	9.824	0.596	0.595	1.002

16	10.121	0.580	0.578	1.003
----	--------	-------	-------	-------

Forward Scans

1	9.916	0.593	0.591	1.002
2	10.110	0.565	0.564	1.003
3	9.872	0.577	0.575	1.002
4	10.043	0.565	0.563	1.003
5	9.822	0.585	0.584	1.003
6	10.028	0.587	0.586	1.002
7	9.936	0.576	0.575	1.003
8	10.080	0.598	0.597	1.002
9	9.817	0.616	0.615	1.001
10	10.075	0.605	0.604	1.002
11	9.850	0.607	0.606	1.002
12	10.122	0.575	0.573	1.002
13	9.784	0.609	0.607	1.003
14	10.073	0.580	0.579	1.002
15	9.826	0.596	0.595	1.002
16	10.121	0.580	0.578	1.003

Reverse Scans

1	9.918	0.592	0.591	1.002
2	10.113	0.564	0.563	1.002
3	9.874	0.574	0.572	1.003
4	10.046	0.564	0.562	1.003
5	9.820	0.587	0.585	1.002
6	10.032	0.588	0.587	1.002
7	9.939	0.575	0.574	1.002
8	10.087	0.596	0.595	1.002
9	9.816	0.617	0.616	1.001
10	10.074	0.604	0.603	1.002
11	9.847	0.608	0.607	1.001
12	10.116	0.576	0.574	1.002
13	9.780	0.610	0.609	1.002
14	10.079	0.581	0.580	1.003
15	9.823	0.596	0.595	1.002
16	10.121	0.580	0.578	1.003

Landsat 7 Image Assessment System
Random Noise Characterization

02/12/2003 18:55:57
tightrope

Product: L72EDC110222815020 Processing Level: R1R

Band B2 Scene 1 Gain L -- DAY IC data

 SCENE AVERAGES AND STANDARD DEVIATIONS BY DETECTOR (COUNTS)

det	mean of A	mean of B	mean of C	mean all	stdev of A	stdev of B	stdev of C	stdev all
-----	--------------	--------------	--------------	-------------	---------------	---------------	---------------	--------------

All Scans

1	0.31	0.31	0.31	0.31	0.48	0.47	0.48	0.48
2	1.13	1.12	1.13	1.13	0.23	0.14	0.22	0.20
3	0.33	0.33	0.33	0.33	0.45	0.44	0.45	0.44
4	0.38	0.38	0.38	0.38	0.58	0.56	0.60	0.58
5	0.38	0.38	0.37	0.38	0.43	0.42	0.43	0.43
6	0.39	0.38	0.38	0.38	0.58	0.57	0.58	0.58
7	0.28	0.28	0.28	0.28	0.48	0.47	0.48	0.47
8	1.14	1.13	1.13	1.13	0.29	0.26	0.31	0.28
9	0.42	0.42	0.42	0.42	0.46	0.45	0.46	0.46
10	1.01	0.99	1.00	1.00	0.45	0.43	0.45	0.44
11	0.38	0.37	0.38	0.38	0.47	0.45	0.46	0.46
12	1.13	1.12	1.13	1.13	0.20	0.13	0.21	0.19
13	0.44	0.43	0.43	0.43	0.44	0.42	0.43	0.43
14	1.08	1.07	1.08	1.07	0.36	0.36	0.41	0.38
15	0.39	0.38	0.38	0.38	0.45	0.43	0.43	0.44
16	1.13	1.13	1.13	1.13	0.21	0.14	0.22	0.20

Forward Scans

1	0.31	0.32	0.31	0.31	0.48	0.48	0.47	0.48
2	1.13	1.12	1.13	1.13	0.29	0.14	0.17	0.21
3	0.33	0.33	0.33	0.33	0.45	0.44	0.44	0.45
4	0.40	0.38	0.39	0.39	0.61	0.56	0.56	0.58
5	0.38	0.37	0.37	0.38	0.44	0.42	0.42	0.43
6	0.37	0.36	0.36	0.36	0.58	0.56	0.56	0.57
7	0.28	0.29	0.28	0.28	0.48	0.47	0.47	0.48
8	1.13	1.12	1.12	1.13	0.35	0.29	0.29	0.31
9	0.42	0.41	0.42	0.42	0.47	0.45	0.46	0.46
10	1.01	0.99	1.00	1.00	0.48	0.43	0.44	0.45
11	0.39	0.37	0.37	0.38	0.48	0.45	0.46	0.46
12	1.13	1.12	1.12	1.12	0.25	0.13	0.15	0.19
13	0.44	0.42	0.43	0.43	0.46	0.42	0.43	0.43
14	1.06	1.06	1.07	1.06	0.40	0.36	0.36	0.37
15	0.39	0.38	0.38	0.38	0.46	0.43	0.43	0.44
16	1.13	1.13	1.13	1.13	0.26	0.13	0.15	0.19

Reverse Scans

1	0.31	0.30	0.31	0.31	0.48	0.47	0.48	0.48
2	1.12	1.12	1.13	1.12	0.14	0.14	0.27	0.19
3	0.33	0.32	0.32	0.32	0.44	0.43	0.45	0.44
4	0.37	0.37	0.38	0.37	0.56	0.56	0.63	0.58

5	0.38	0.38	0.37	0.38	0.43	0.42	0.43	0.43
6	0.41	0.40	0.41	0.41	0.58	0.58	0.61	0.59
7	0.28	0.28	0.29	0.28	0.47	0.47	0.48	0.47
8	1.14	1.14	1.14	1.14	0.21	0.22	0.32	0.26
9	0.42	0.42	0.42	0.42	0.46	0.46	0.46	0.46
10	1.00	1.00	1.00	1.00	0.42	0.42	0.46	0.44
11	0.38	0.38	0.38	0.38	0.46	0.45	0.47	0.46
12	1.13	1.12	1.13	1.13	0.14	0.13	0.26	0.19
13	0.44	0.43	0.43	0.43	0.43	0.42	0.44	0.43
14	1.09	1.08	1.08	1.08	0.33	0.35	0.44	0.38
15	0.39	0.38	0.37	0.38	0.44	0.43	0.43	0.43
16	1.12	1.13	1.13	1.13	0.14	0.16	0.28	0.20

TESTS OF EQUIVALENCE OF SECTION MEANS AND STANDARD DEVIATIONS
(TEST FOR RESIDUAL MEMORY EFFECT; NOISE VARIATION ACROSS IMAGE)
Number of lines that failed t or f test (alpha < 0.05)

TTEST FOR MEANS FTEST FOR VARIANCE #lines TTEST FTEST #scans
det A-B B-C A-C A-B B-C A-C tested for-rev for-rev tested

All Scans

1	4	2	1	42	45	45	375	0	31	187
2	3	2	4	11	10	8	126	0	19	140
3	8	5	1	48	43	44	375	0	31	187
4	0	0	0	7	3	10	42	0	11	37
5	4	4	12	29	29	36	375	0	25	187
6	0	0	0	16	12	12	107	0	17	73
7	2	8	2	36	48	60	375	0	24	187
8	0	1	2	10	10	17	129	0	19	147
9	2	5	4	46	40	45	375	0	21	187
10	3	1	1	13	9	15	135	0	18	132
11	2	4	1	35	35	49	375	0	24	187
12	1	0	2	14	16	20	176	0	27	162
13	8	5	5	28	22	38	375	0	22	187
14	0	0	0	6	9	6	60	0	12	118
15	2	2	3	41	40	40	375	0	23	187
16	2	0	1	14	13	12	202	0	27	155

Forward Scans

1	3	1	1	20	19	22	188
2	2	0	1	5	4	6	64
3	2	0	0	19	19	20	188
4	0	0	0	5	0	5	18
5	1	2	5	15	16	18	188
6	0	0	0	8	5	7	61

7	1	4	1	17	23	31	188
8	0	1	2	3	6	8	62
9	2	1	4	22	17	16	188
10	0	1	0	8	4	6	67
11	1	4	0	15	19	19	188
12	0	0	1	5	3	8	89
13	5	3	2	14	9	19	188
14	0	0	0	1	4	4	30
15	2	1	3	21	19	19	188
16	2	0	1	10	7	7	105

Reverse Scans

1	1	1	0	22	26	23	187
2	1	2	3	6	6	2	62
3	6	5	1	29	24	24	187
4	0	0	0	2	3	5	24
5	3	2	7	14	13	18	187
6	0	0	0	8	7	5	46
7	1	4	1	19	25	29	187
8	0	0	0	7	4	9	67
9	0	4	0	24	23	29	187
10	3	0	1	5	5	9	68
11	1	0	1	20	16	30	187
12	1	0	1	9	13	12	87
13	3	2	3	14	13	19	187
14	0	0	0	5	5	2	30
15	0	1	0	20	21	21	187
16	0	0	0	4	6	5	97

 AVERAGE OF LINE BY LINE STANDARD DEVIATIONS AND RANDOMNESS CHECK
 (alpha level of < 0.05 for randomness tests indicates rejection of
 null hypothesis of randomness of sequence of line means or stdevs)

det	Averaged Standard Deviations of Lines				Randomness Test	
	A	B	C	All	MEAN	STDEV
	(counts)	(counts)	(counts)	(counts)	(alpha)	(alpha)

All Scans

1	0.48	0.47	0.48	0.47	0.378	0.001
2	0.10	0.08	0.11	0.10	0.167	0.216
3	0.44	0.43	0.44	0.44	0.459	0.039
4	0.32	0.30	0.32	0.31	0.235	0.315
5	0.43	0.41	0.42	0.42	0.025	0.339
6	0.36	0.34	0.37	0.36	0.027	0.130
7	0.47	0.47	0.47	0.47	0.302	0.074

8	0.11	0.10	0.13	0.11	0.037	0.406
9	0.46	0.45	0.45	0.45	0.107	0.025
10	0.15	0.12	0.15	0.14	0.116	0.405
11	0.47	0.45	0.46	0.46	0.127	0.438
12	0.09	0.07	0.10	0.09	0.255	0.174
13	0.44	0.41	0.42	0.42	0.039	0.234
14	0.11	0.10	0.11	0.11	0.168	0.290
15	0.44	0.42	0.43	0.43	0.127	0.459
16	0.09	0.09	0.10	0.09	0.456	0.099

Forward Scans

1	0.48	0.47	0.47	0.47	0.121	0.330
2	0.12	0.08	0.10	0.10	0.500	0.043
3	0.45	0.44	0.44	0.44	0.385	0.072
4	0.33	0.30	0.28	0.30	0.140	0.075
5	0.43	0.41	0.42	0.42	0.153	0.029
6	0.40	0.36	0.38	0.38	0.187	0.500
7	0.48	0.47	0.47	0.47	0.040	0.442
8	0.14	0.11	0.12	0.12	0.432	0.365
9	0.46	0.45	0.46	0.46	0.232	0.119
10	0.18	0.12	0.13	0.14	0.057	0.434
11	0.48	0.45	0.46	0.46	0.500	0.040
12	0.11	0.08	0.09	0.09	0.439	0.070
13	0.44	0.41	0.42	0.43	0.020	0.121
14	0.11	0.09	0.10	0.10	0.339	0.102
15	0.44	0.42	0.43	0.43	0.500	0.279
16	0.10	0.08	0.09	0.09	0.079	0.407

Reverse Scans

1	0.48	0.47	0.48	0.47	0.231	0.189
2	0.08	0.08	0.13	0.10	0.305	0.466
3	0.44	0.43	0.44	0.44	0.189	0.020
4	0.30	0.30	0.36	0.32	0.162	0.094
5	0.43	0.42	0.42	0.42	0.023	0.093
6	0.31	0.31	0.37	0.33	0.016	0.118
7	0.47	0.46	0.48	0.47	0.231	0.039
8	0.09	0.09	0.13	0.11	0.203	0.467
9	0.45	0.45	0.45	0.45	0.384	0.330
10	0.13	0.12	0.17	0.14	0.500	0.363
11	0.46	0.45	0.46	0.46	0.231	0.330
12	0.08	0.07	0.11	0.09	0.236	0.374
13	0.43	0.41	0.43	0.42	0.120	0.189
14	0.11	0.12	0.13	0.12	0.048	0.147
15	0.44	0.43	0.43	0.43	0.384	0.189
16	0.07	0.10	0.12	0.10	0.054	0.468

CORRELATION OF LINE-BY-LINE MEANS BETWEEN DETECTORS: All SCANS

Pearson correlation coefficient (r)

	1	2	3	4	5	6	7	8	9	10	11	12	13	14	15	16
1	0.00	0.00	0.00	0.00	0.00	0.00	0.00	0.00	0.00	0.00	0.00	0.00	0.00	0.00	0.00	0.00
2	0.00	0.00	0.00	0.00	0.00	0.00	0.00	0.00	0.00	0.00	0.00	0.00	0.00	0.00	0.00	0.00
3	0.08	0.05	0.00	0.00	0.00	0.00	0.00	0.00	0.00	0.00	0.00	0.00	0.00	0.00	0.00	0.00
4	0.08	0.00	0.02	0.00	0.00	0.00	0.00	0.00	0.00	0.00	0.00	0.00	0.00	0.00	0.00	0.00
5	0.09	-0.06	0.12	-0.13	0.00	0.00	0.00	0.00	0.00	0.00	0.00	0.00	0.00	0.00	0.00	0.00
6	0.11	-0.09	0.01	0.05	0.00	0.00	0.00	0.00	0.00	0.00	0.00	0.00	0.00	0.00	0.00	0.00
7	0.07	-0.02	0.08	-0.09	0.24	-0.05	0.00	0.00	0.00	0.00	0.00	0.00	0.00	0.00	0.00	0.00
8	-0.05	-0.02	-0.01	-0.05	-0.07	0.03	-0.01	0.00	0.00	0.00	0.00	0.00	0.00	0.00	0.00	0.00
9	0.08	-0.10	0.19	-0.13	0.23	0.04	0.21	0.07	0.00	0.00	0.00	0.00	0.00	0.00	0.00	0.00
10	-0.05	0.08	0.02	-0.13	-0.12	0.01	-0.10	-0.04	-0.02	0.00	0.00	0.00	0.00	0.00	0.00	0.00
11	0.15	-0.05	0.09	-0.15	0.15	-0.01	0.13	-0.01	0.23	-0.08	0.00	0.00	0.00	0.00	0.00	0.00
12	-0.06	0.01	0.09	-0.03	-0.02	0.05	-0.01	0.06	-0.03	0.09	-0.12	0.00	0.00	0.00	0.00	0.00
13	-0.02	0.07	0.08	-0.13	0.10	0.04	0.28	0.00	0.27	0.01	0.11	0.02	0.00	0.00	0.00	0.00
14	-0.03	-0.08	0.03	-0.15	-0.06	0.03	-0.03	-0.04	-0.04	0.11	0.07	0.02	-0.01	0.00	0.00	0.00
15	0.12	-0.14	0.10	0.09	0.21	0.19	0.09	0.00	0.15	-0.06	0.16	-0.02	0.16	0.00	0.00	0.00
16	0.01	0.06	0.02	-0.12	-0.01	0.12	0.00	-0.02	0.05	0.05	-0.05	-0.02	0.06	-0.13	0.06	0.00

Percentage of unexplained variance (100*[1-r^2])

	1	2	3	4	5	6	7	8	9	10	11	12	13	14	15	16
1	0	0	0	0	0	0	0	0	0	0	0	0	0	0	0	0
2	100	0	0	0	0	0	0	0	0	0	0	0	0	0	0	0
3	99	100	0	0	0	0	0	0	0	0	0	0	0	0	0	0
4	99	100	100	0	0	0	0	0	0	0	0	0	0	0	0	0
5	99	100	98	98	0	0	0	0	0	0	0	0	0	0	0	0
6	99	99	100	100	100	0	0	0	0	0	0	0	0	0	0	0
7	100	100	99	99	94	100	0	0	0	0	0	0	0	0	0	0
8	100	100	100	100	99	100	100	0	0	0	0	0	0	0	0	0
9	99	99	96	98	95	100	95	99	0	0	0	0	0	0	0	0
10	100	99	100	98	99	100	99	100	100	0	0	0	0	0	0	0
11	98	100	99	98	98	100	98	100	95	99	0	0	0	0	0	0
12	100	100	99	100	100	100	100	100	100	99	99	0	0	0	0	0
13	100	100	99	98	99	100	92	100	93	100	99	100	0	0	0	0
14	100	99	100	98	100	100	100	100	100	99	100	100	100	0	0	0
15	99	98	99	99	96	96	99	100	98	100	98	100	97	100	0	0
16	100	100	100	99	100	99	100	100	100	100	100	100	100	98	100	0

Significance of regression (Reject hypothesis if alpha < 0.05)

	1	2	3	4	5	6	7	8	9	10	11	12	13	14	15	16
1	0.00	0.00	0.00	0.00	0.00	0.00	0.00	0.00	0.00	0.00	0.00	0.00	0.00	0.00	0.00	0.00
2	1.00	0.00	0.00	0.00	0.00	0.00	0.00	0.00	0.00	0.00	0.00	0.00	0.00	0.00	0.00	0.00
3	0.12	0.41	0.00	0.00	0.00	0.00	0.00	0.00	0.00	0.00	0.00	0.00	0.00	0.00	0.00	0.00
4	0.51	1.00	0.87	0.00	0.00	0.00	0.00	0.00	0.00	0.00	0.00	0.00	0.00	0.00	0.00	0.00

5	0.09	0.34	0.02	0.29	0.00	0.00	0.00	0.00	0.00	0.00	0.00	0.00	0.00	0.00	0.00	0.00
6	0.17	0.27	1.00	0.70	1.00	0.00	0.00	0.00	0.00	0.00	0.00	0.00	0.00	0.00	0.00	0.00
7	0.18	0.80	0.14	0.46	0.00	0.53	0.00	0.00	0.00	0.00	0.00	0.00	0.00	0.00	0.00	0.00
8	0.42	0.69	1.00	0.66	0.21	0.67	1.00	0.00	0.00	0.00	0.00	0.00	0.00	0.00	0.00	0.00
9	0.11	0.09	0.00	0.27	0.00	0.66	0.00	0.22	0.00	0.00	0.00	0.00	0.00	0.00	0.00	0.00
10	0.37	0.17	0.71	0.27	0.05	0.87	0.10	0.49	0.68	0.00	0.00	0.00	0.00	0.00	0.00	0.00
11	0.01	0.44	0.08	0.20	0.01	0.86	0.01	0.81	0.00	0.20	0.00	0.00	0.00	0.00	0.00	0.00
12	0.28	0.88	0.10	0.78	0.68	0.58	0.85	0.29	0.59	0.15	0.03	0.00	0.00	0.00	0.00	0.00
13	0.64	0.27	0.13	0.27	0.05	0.58	0.00	1.00	0.00	0.80	0.04	0.67	0.00	0.00	0.00	0.00
14	0.67	0.27	0.68	0.22	0.41	0.70	0.62	0.60	0.53	0.13	0.32	0.76	0.85	0.00	0.00	0.00
15	0.02	0.02	0.06	0.44	0.00	0.02	0.08	1.00	0.01	0.29	0.00	0.73	0.00	1.00	0.00	0.00
16	0.87	0.36	0.79	0.31	0.89	0.16	1.00	0.77	0.39	0.38	0.38	0.78	0.32	0.06	0.30	0.00

CORRELATION OF LINE-BY-LINE MEANS BETWEEN DETECTORS: Forward SCANS

Pearson correlation coefficient (r)

	1	2	3	4	5	6	7	8	9	10	11	12	13	14	15	16
1	0.00	0.00	0.00	0.00	0.00	0.00	0.00	0.00	0.00	0.00	0.00	0.00	0.00	0.00	0.00	0.00
2	-0.07	0.00	0.00	0.00	0.00	0.00	0.00	0.00	0.00	0.00	0.00	0.00	0.00	0.00	0.00	0.00
3	0.03	-0.13	0.00	0.00	0.00	0.00	0.00	0.00	0.00	0.00	0.00	0.00	0.00	0.00	0.00	0.00
4	0.34	0.07	0.01	0.00	0.00	0.00	0.00	0.00	0.00	0.00	0.00	0.00	0.00	0.00	0.00	0.00
5	0.05	0.01	0.18	-0.07	0.00	0.00	0.00	0.00	0.00	0.00	0.00	0.00	0.00	0.00	0.00	0.00
6	-0.12	-0.01	0.04	-0.32	0.12	0.00	0.00	0.00	0.00	0.00	0.00	0.00	0.00	0.00	0.00	0.00
7	0.06	0.02	0.08	-0.21	0.26	-0.07	0.00	0.00	0.00	0.00	0.00	0.00	0.00	0.00	0.00	0.00
8	0.01	-0.13	-0.01	-0.06	0.14	-0.03	-0.01	0.00	0.00	0.00	0.00	0.00	0.00	0.00	0.00	0.00
9	0.11	-0.10	0.27	0.12	0.26	-0.13	0.20	0.06	0.00	0.00	0.00	0.00	0.00	0.00	0.00	0.00
10	-0.09	-0.06	0.16	-0.23	0.01	0.14	-0.05	-0.04	0.01	0.00	0.00	0.00	0.00	0.00	0.00	0.00
11	0.11	-0.01	0.05	0.02	0.11	-0.07	0.07	0.06	0.26	-0.04	0.00	0.00	0.00	0.00	0.00	0.00
12	-0.02	-0.01	-0.14	0.15	0.02	-0.11	-0.07	0.10	-0.03	0.00	-0.18	0.00	0.00	0.00	0.00	0.00
13	0.04	0.01	0.14	-0.23	0.10	0.11	0.37	-0.08	0.26	0.03	0.09	-0.08	0.00	0.00	0.00	0.00
14	-0.13	0.09	0.00	-0.25	-0.07	0.10	-0.08	0.00	-0.13	-0.04	0.00	-0.13	-0.12	0.00	0.00	0.00
15	0.11	0.00	0.11	0.08	0.16	-0.06	0.05	0.10	0.14	0.01	0.13	0.06	0.10	-0.08	0.00	0.00
16	-0.13	-0.03	-0.07	-0.29	-0.11	-0.06	0.04	0.07	-0.03	-0.05	0.03	0.02	-0.03	0.08	0.05	0.00

Percentage of unexplained variance ($100*[1-r^2]$)

	1	2	3	4	5	6	7	8	9	10	11	12	13	14	15	16
1	0	0	0	0	0	0	0	0	0	0	0	0	0	0	0	0
2	99	0	0	0	0	0	0	0	0	0	0	0	0	0	0	0
3	100	98	0	0	0	0	0	0	0	0	0	0	0	0	0	0
4	89	100	100	0	0	0	0	0	0	0	0	0	0	0	0	0
5	100	100	97	100	0	0	0	0	0	0	0	0	0	0	0	0
6	99	100	100	90	99	0	0	0	0	0	0	0	0	0	0	0
7	100	100	99	95	93	100	0	0	0	0	0	0	0	0	0	0

8	100	98	100	100	98	100	100	0	0	0	0	0	0	0	0	0
9	99	99	93	99	93	98	96	100	0	0	0	0	0	0	0	0
10	99	100	97	95	100	98	100	100	100	0	0	0	0	0	0	0
11	99	100	100	100	99	100	99	100	93	100	0	0	0	0	0	0
12	100	100	98	98	100	99	100	99	100	100	97	0	0	0	0	0
13	100	100	98	95	99	99	87	99	93	100	99	99	0	0	0	0
14	98	99	100	94	99	99	99	100	98	100	100	98	98	0	0	0
15	99	100	99	99	97	100	100	99	98	100	98	100	99	99	0	0
16	98	100	100	92	99	100	100	100	100	100	100	100	100	99	100	0

Significance of regression (Reject hypothesis if alpha < 0.05)

	1	2	3	4	5	6	7	8	9	10	11	12	13	14	15	16
1	0.00	0.00	0.00	0.00	0.00	0.00	0.00	0.00	0.00	0.00	0.00	0.00	0.00	0.00	0.00	0.00
2	0.40	0.00	0.00	0.00	0.00	0.00	0.00	0.00	0.00	0.00	0.00	0.00	0.00	0.00	0.00	0.00
3	0.68	0.12	0.00	0.00	0.00	0.00	0.00	0.00	0.00	0.00	0.00	0.00	0.00	0.00	0.00	0.00
4	0.05	0.71	1.00	0.00	0.00	0.00	0.00	0.00	0.00	0.00	0.00	0.00	0.00	0.00	0.00	0.00
5	0.54	1.00	0.02	0.71	0.00	0.00	0.00	0.00	0.00	0.00	0.00	0.00	0.00	0.00	0.00	0.00
6	0.28	1.00	0.69	0.06	0.27	0.00	0.00	0.00	0.00	0.00	0.00	0.00	0.00	0.00	0.00	0.00
7	0.41	0.82	0.29	0.23	0.00	0.53	0.00	0.00	0.00	0.00	0.00	0.00	0.00	0.00	0.00	0.00
8	0.90	0.15	1.00	0.73	0.11	0.77	0.88	0.00	0.00	0.00	0.00	0.00	0.00	0.00	0.00	0.00
9	0.15	0.27	0.00	0.51	0.00	0.24	0.01	0.46	0.00	0.00	0.00	0.00	0.00	0.00	0.00	0.00
10	0.30	0.51	0.05	0.20	0.88	0.22	0.58	0.68	0.88	0.00	0.00	0.00	0.00	0.00	0.00	0.00
11	0.15	1.00	0.53	1.00	0.13	0.55	0.33	0.48	0.00	0.65	0.00	0.00	0.00	0.00	0.00	0.00
12	0.83	1.00	0.08	0.42	0.76	0.31	0.37	0.23	0.75	1.00	0.02	0.00	0.00	0.00	0.00	0.00
13	0.63	0.88	0.05	0.20	0.18	0.31	0.00	0.37	0.00	0.69	0.20	0.32	0.00	0.00	0.00	0.00
14	0.22	0.39	1.00	0.15	0.49	0.35	0.45	1.00	0.20	0.68	1.00	0.19	0.23	0.00	0.00	0.00
15	0.14	1.00	0.15	0.67	0.03	0.62	0.46	0.27	0.05	1.00	0.08	0.43	0.19	0.44	0.00	0.00
16	0.11	0.74	0.40	0.10	0.17	0.60	0.61	0.42	0.69	0.56	0.68	0.77	0.75	0.42	0.54	0.00

CORRELATION OF LINE-BY-LINE MEANS BETWEEN DETECTORS: Reverse SCANS

Pearson correlation coefficient (r)

	1	2	3	4	5	6	7	8	9	10	11	12	13	14	15	16
1	0.00	0.00	0.00	0.00	0.00	0.00	0.00	0.00	0.00	0.00	0.00	0.00	0.00	0.00	0.00	0.00
2	0.12	0.00	0.00	0.00	0.00	0.00	0.00	0.00	0.00	0.00	0.00	0.00	0.00	0.00	0.00	0.00
3	0.13	-0.12	0.00	0.00	0.00	0.00	0.00	0.00	0.00	0.00	0.00	0.00	0.00	0.00	0.00	0.00
4	0.21	-0.12	0.02	0.00	0.00	0.00	0.00	0.00	0.00	0.00	0.00	0.00	0.00	0.00	0.00	0.00
5	0.14	-0.02	0.08	-0.08	0.00	0.00	0.00	0.00	0.00	0.00	0.00	0.00	0.00	0.00	0.00	0.00
6	0.18	-0.15	0.20	0.16	0.26	0.00	0.00	0.00	0.00	0.00	0.00	0.00	0.00	0.00	0.00	0.00
7	0.08	0.05	0.07	0.14	0.22	0.10	0.00	0.00	0.00	0.00	0.00	0.00	0.00	0.00	0.00	0.00
8	0.23	0.11	0.01	0.18	-0.11	-0.19	0.11	0.00	0.00	0.00	0.00	0.00	0.00	0.00	0.00	0.00
9	0.06	-0.11	0.12	0.11	0.20	0.09	0.23	0.04	0.00	0.00	0.00	0.00	0.00	0.00	0.00	0.00
10	0.00	-0.01	0.07	-0.24	0.02	-0.24	0.05	-0.05	0.06	0.00	0.00	0.00	0.00	0.00	0.00	0.00

11 0.20-0.11 0.15 0.12 0.19 0.26 0.21-0.02 0.20-0.04 0.00 0.00 0.00 0.00 0.00 0.00
 12 -0.02 0.16-0.08-0.22-0.02-0.09 0.10-0.01-0.09 0.04-0.16 0.00 0.00 0.00 0.00 0.00
 13 -0.09-0.17 0.02 0.21 0.11 0.03 0.17 0.06 0.29-0.07 0.12 0.08 0.00 0.00 0.00
 14 -0.09 0.00-0.05-0.28 0.12 0.08 0.01-0.10-0.10 0.00 0.05 0.03-0.01 0.00 0.00
 15 0.13-0.06 0.09-0.09 0.27-0.12 0.14-0.06 0.15 0.08 0.18 0.01 0.24-0.05 0.00 0.00
 16 0.09-0.07-0.04-0.14 0.06 0.01 0.07 0.10 0.07-0.05-0.02 0.08 0.02-0.02 0.04 0.00

Percentage of unexplained variance ($100*[1-r^2]$)

	1	2	3	4	5	6	7	8	9	10	11	12	13	14	15	16
1	0	0	0	0	0	0	0	0	0	0	0	0	0	0	0	0
2	98	0	0	0	0	0	0	0	0	0	0	0	0	0	0	0
3	98	99	0	0	0	0	0	0	0	0	0	0	0	0	0	0
4	96	99	100	0	0	0	0	0	0	0	0	0	0	0	0	0
5	98	100	99	99	0	0	0	0	0	0	0	0	0	0	0	0
6	97	98	96	97	93	0	0	0	0	0	0	0	0	0	0	0
7	99	100	100	98	95	99	0	0	0	0	0	0	0	0	0	0
8	95	99	100	97	99	96	99	0	0	0	0	0	0	0	0	0
9	100	99	98	99	96	99	95	100	0	0	0	0	0	0	0	0
10	100	100	99	94	100	94	100	100	100	0	0	0	0	0	0	0
11	96	99	98	99	96	93	96	100	96	100	0	0	0	0	0	0
12	100	97	99	95	100	99	99	100	99	100	97	0	0	0	0	0
13	99	97	100	96	99	100	97	100	91	100	98	99	0	0	0	0
14	99	100	100	92	99	99	100	99	99	100	100	100	100	100	0	0
15	98	100	99	99	93	98	98	100	98	99	97	100	94	100	0	0
16	99	100	100	98	100	100	99	99	99	100	100	99	100	100	100	0

Significance of regression (Reject hypothesis if $\alpha < 0.05$)

	1	2	3	4	5	6	7	8	9	10	11	12	13	14	15	16
1	0.00	0.00	0.00	0.00	0.00	0.00	0.00	0.00	0.00	0.00	0.00	0.00	0.00	0.00	0.00	0.00
2	0.15	0.00	0.00	0.00	0.00	0.00	0.00	0.00	0.00	0.00	0.00	0.00	0.00	0.00	0.00	0.00
3	0.09	0.18	0.00	0.00	0.00	0.00	0.00	0.00	0.00	0.00	0.00	0.00	0.00	0.00	0.00	0.00
4	0.21	0.47	1.00	0.00	0.00	0.00	0.00	0.00	0.00	0.00	0.00	0.00	0.00	0.00	0.00	0.00
5	0.05	0.79	0.30	0.61	0.00	0.00	0.00	0.00	0.00	0.00	0.00	0.00	0.00	0.00	0.00	0.00
6	0.14	0.20	0.09	0.33	0.03	0.00	0.00	0.00	0.00	0.00	0.00	0.00	0.00	0.00	0.00	0.00
7	0.29	0.54	0.37	0.40	0.00	0.40	0.00	0.00	0.00	0.00	0.00	0.00	0.00	0.00	0.00	0.00
8	0.01	0.20	1.00	0.29	0.19	0.11	0.17	0.00	0.00	0.00	0.00	0.00	0.00	0.00	0.00	0.00
9	0.43	0.21	0.09	0.52	0.01	0.47	0.00	0.60	0.00	0.00	0.00	0.00	0.00	0.00	0.00	0.00
10	1.00	0.89	0.42	0.15	0.79	0.04	0.58	0.55	0.47	0.00	0.00	0.00	0.00	0.00	0.00	0.00
11	0.01	0.22	0.04	0.46	0.01	0.03	0.01	0.83	0.01	0.64	0.00	0.00	0.00	0.00	0.00	0.00
12	0.79	0.06	0.30	0.18	0.78	0.45	0.20	1.00	0.25	0.64	0.04	0.00	0.00	0.00	0.00	0.00
13	0.23	0.04	0.83	0.21	0.15	0.81	0.02	0.50	0.00	0.45	0.09	0.32	0.00	0.00	0.00	0.00
14	0.33	1.00	0.58	0.08	0.20	0.48	0.88	0.29	0.29	1.00	0.58	0.74	0.87	0.00	0.00	0.00
15	0.08	0.50	0.21	0.61	0.00	0.30	0.07	0.50	0.04	0.36	0.01	1.00	0.00	0.61	0.00	0.00
16	0.24	0.44	0.62	0.39	0.49	1.00	0.36	0.22	0.37	0.56	0.79	0.31	0.78	0.87	0.58	0.00

 RANDOM NOISE SUMMARY REPORT

det	Scene mean data value (counts)	Scene mean noise level (counts)	Line mean noise level (counts)	Scene/line noise ratio
-----	--------------------------------------	---------------------------------------	--------------------------------------	---------------------------

All Scans

1	0.310	0.477	0.474	1.007
2	1.126	0.200	0.099	2.014
3	0.327	0.443	0.439	1.009
4	0.380	0.582	0.312	1.862
5	0.377	0.426	0.421	1.013
6	0.382	0.579	0.357	1.623
7	0.283	0.474	0.471	1.007
8	1.134	0.284	0.114	2.495
9	0.417	0.459	0.454	1.009
10	1.001	0.443	0.141	3.134
11	0.378	0.463	0.459	1.009
12	1.125	0.187	0.088	2.116
13	0.432	0.431	0.425	1.015
14	1.075	0.376	0.109	3.458
15	0.382	0.436	0.431	1.013
16	1.129	0.195	0.093	2.088

Forward Scans

1	0.311	0.478	0.474	1.008
2	1.127	0.207	0.100	2.063
3	0.331	0.446	0.441	1.010
4	0.389	0.580	0.302	1.916
5	0.375	0.426	0.420	1.014
6	0.360	0.569	0.379	1.503
7	0.284	0.475	0.471	1.008
8	1.125	0.311	0.122	2.540
9	0.417	0.460	0.455	1.010
10	1.002	0.450	0.143	3.151
11	0.377	0.465	0.460	1.011
12	1.124	0.186	0.091	2.055
13	0.431	0.434	0.426	1.018
14	1.065	0.374	0.098	3.811
15	0.382	0.439	0.433	1.014
16	1.129	0.190	0.088	2.154

Reverse Scans

1	0.309	0.476	0.473	1.006
2	1.124	0.194	0.099	1.963

3	0.323	0.440	0.436	1.008
4	0.373	0.583	0.321	1.817
5	0.379	0.426	0.421	1.011
6	0.410	0.590	0.332	1.778
7	0.281	0.474	0.471	1.006
8	1.143	0.256	0.106	2.414
9	0.418	0.458	0.454	1.009
10	1.001	0.435	0.140	3.114
11	0.380	0.462	0.458	1.008
12	1.127	0.188	0.086	2.183
13	0.434	0.429	0.423	1.013
14	1.083	0.377	0.117	3.221
15	0.382	0.434	0.429	1.011
16	1.129	0.200	0.099	2.025

3.3.4 IC Emissive Summary

Using CPF gains to determine B61 bias

 Landsat 7 Image Assessment System 02/21/2003 15:01:06
 IC Emissive Host = tightrope

Product: L72EDC149915317010 Processing Level: R0C

Band B61 Scene 1 Gain L -- DAY IC data

 Work Order IAS_MODE_FLAG = 1
 Work Order rxx_DDR.PutTrendToDB = 0
 Work Order writeLogFile = 0
 r0c_ProcessICEmissive started

 ---- ICEM DDR Parameters ----

 currentSceneNum = 1; firstScanDir = R
 gainState = L; currentBandNum = 5
 numdet = 8; numSceneLines = 3000; numscans = 375
 sceneStartTime = 202497405.789841; sceneStopTime = 202497432.665090

 ---- End DDR Parameters ----

 ---- ICEM Cal Parm File Parameters ----

 Gains (detector 1,2,...):

12.426 12.614 13.270 12.625 12.899 12.893 13.217 12.969
 Biases (detector 1,2,...):
 29.82 28.78 24.29 28.68 26.77 26.94 24.68 26.46
 Status (detector 1,2,...):
 0 0 0 0 0 0
 View Factors (detector 1,2,...):
 0.223 0.182 0.023 0.023 0.007 0.000 0.000 0.000 0.000 0.000 0.000 0.000
 0.706 1.000 0.997
 0.196 0.178 0.023 0.023 0.007 0.000 0.000 0.000 0.000 0.000 0.000 0.000
 0.711 1.000 0.985
 0.207 0.182 0.024 0.024 0.007 0.000 0.000 0.000 0.000 0.000 0.000 0.000
 0.710 1.000 0.996
 0.188 0.181 0.024 0.024 0.007 0.000 0.000 0.000 0.000 0.000 0.000 0.000
 0.710 1.000 0.984
 0.207 0.181 0.025 0.025 0.008 0.000 0.000 0.000 0.000 0.000 0.000 0.000
 0.711 1.000 0.999
 0.199 0.178 0.025 0.025 0.007 0.000 0.000 0.000 0.000 0.000 0.000 0.000
 0.709 1.000 0.989
 0.212 0.177 0.026 0.026 0.008 0.000 0.000 0.000 0.000 0.000 0.000 0.000
 0.711 1.000 1.000
 0.206 0.177 0.022 0.022 0.007 0.000 0.000 0.000 0.000 0.000 0.000 0.000
 0.709 1.000 0.986
 bb/sh/tot_viewfac[0] = 1.000000/0.997189/0.706144
 bb/sh/tot_viewfac[1] = 1.000000/0.985386/0.710532
 bb/sh/tot_viewfac[2] = 1.000000/0.995997/0.710184
 bb/sh/tot_viewfac[3] = 1.000000/0.983917/0.710184
 bb/sh/tot_viewfac[4] = 1.000000/0.998771/0.711379
 bb/sh/tot_viewfac[5] = 1.000000/0.988932/0.709158
 bb/sh/tot_viewfac[6] = 1.000000/1.000250/0.711234
 bb/sh/tot_viewfac[7] = 1.000000/0.986347/0.708862
 Scan mirror temp modeling coefficients: 1.017800 0.000000 0.000000 0.000000
 0.000000 0.000000

 ---- End Cal Parm File Parameters ----

 ---- ICEM PCD Parm File Parameters ----

 bblsoTemp = 317.442017 bbCtlTemp = 319.720001
 baffleHtrTemp = 301.261993 cfpaCtlTemp = 91.473000
 baffleTubeTemp = 296.321014 cfpaMonTemp = 91.501999
 baffleSupTemp = 295.049011 slcTemp = 279.873260
 priMirrorTemp = 284.989990, secMirrorTemp = 289.687988
 teleHouseTemp = 288.747009
 scanMirrorTemp = 294.844421
 bbTemp = 317.442017, shTemp = 284.450439

---- End PCD Parm File Parameters ----

-- Scene average --

DetNo	Bias	StdDev	NumPts	Outliers
1	30.093	0.10	375/375	416
2	28.803	0.10	375/375	411
3	24.366	0.09	374/375	417
4	28.831	0.10	374/375	410
5	26.857	0.10	375/375	420
6	27.119	0.12	375/375	406
7	24.847	0.07	375/375	417
8	26.692	0.09	375/375	405

-- Scene average --

DetNo	Gain	StdDev	NumPts
1	12.492	0.02	292/375
2	12.697	0.02	374/375
3	13.358	0.04	375/375
4	12.700	0.02	374/375
5	12.976	0.02	374/375
6	12.956	0.03	375/375
7	13.296	0.02	370/375
8	13.044	0.03	374/375

--- Outlier Report ---

Pulse_Ave = 0; Pulse_Ht = 0; Pulse_Width = 81; Pulse_Loc = 0
Pulse_RelMin = 0
Temperatures out of range = 0

r0c_ProcessICEmissive ended successfully

3.3.4 IC Reflective Summary (Band2):

Landsat 7 Image Assessment System
Process IC Data - Reflective Band

02/26/2003 15:50:49
tightrope

L0R Product ID: L0I644 Processing Level: R0C

Band B2 Scene 1 Gain: H -- Scene Type: DAY Data Type: IC

IC Reflective, Band B2 Scene 1

Lamp state: 1 Scans: 0 - 374

DAM: 16 negative CIs for IC_PULSEWIDTH

DAM: 16 negative CIs for IC_PULSEHEIGHT

DAM: 16 negative CIs for IC_PULSELOC

DAM: 16 negative CIs for IC_PULSEMINIMA

DAM: 16 negative CIs for IC_SHUTTERAVE

DAM: 16 negative CIs for IC_SHUTTERSTDV

DAM: 16 negative CIs for IC_INTEGPULSEVAL

Band number = B2 Scene Number = 1 Lamp State = 1

Det N Gain Gain Std. Dev. NetPulseValue

1	187	1.222	0.002	113.434
2	372	1.229	0.002	106.407
3	300	1.223	0.002	113.945
4	375	1.231	0.002	107.764
5	375	1.223	0.002	115.846
6	375	1.231	0.002	106.972
7	375	1.221	0.002	116.443
8	375	1.231	0.002	106.395
9	375	1.223	0.002	116.242
10	375	1.233	0.002	108.782
11	375	1.224	0.002	116.164
12	375	1.229	0.002	106.560
13	375	1.227	0.002	116.029
14	375	1.226	0.002	106.474
15	375	1.223	0.002	114.564
16	375	1.223	0.002	104.932

Det	N	Bias	Bias Std. Dev	Number of Shutter Outliers
1	375	14.919	0.045	316
2	375	15.194	0.045	253
3	375	14.916	0.038	201
4	375	15.156	0.047	214
5	375	14.723	0.043	374
6	375	15.022	0.036	238
7	375	14.903	0.036	159
8	375	15.101	0.038	257
9	375	14.824	0.047	346
10	375	15.193	0.048	331
11	375	14.775	0.032	384
12	375	15.168	0.033	191
13	375	14.715	0.043	456
14	375	15.147	0.039	266
15	375	14.750	0.039	374
16	375	15.182	0.039	225

IC Reflective completed

2.3.2 PASC Processing Summary:

Landsat-7 Image Assessment System
PASC Scene Characterization

Tue Jun 26 12:24:13
tightrope

Product: L0I360 Processing Level: R0C

Band 1, 2, 3, 4, 5, 7, 8 Scene 1 Gain LLLLLL_LL -- PASC IMAGE data

(Report 2.0)

SUMMARY REPORT FOR PASC CALIBRATION Report Date: Tue Jun 26 12:24:13 2001

START ACQUISITION: 2000.210 12:03:45.000

STOP ACQUISITION: 2000.210 12:04:12.000

TOTAL ACQUISITION (secs) : 26.9078

Sun to PASC Angles (degs)

MIN Incident Dip(CV) : 23.24

MAX Incident Dip(CV) : 24.68

MIN Azimuth (CH) : 28.08

MAX Azimuth (CH) : 28.43

Spectral Radiances for Illuminated Facet:2

	Band Center Wavelength (nm)	Radiance (W / m ² -mu-ster)
Band B10	485.000	275.103:
Band B20	575.000	244.247:
Band B30	660.000	195.851:
Band B40	830.000	125.508:
Band B50	1663.00	27.5155:
Band B61		
Band B62		

Band B70 2193.00 9.47626:
 Band B80 705.000 172.965:

PASC Image and Gain Statistics:

PASC PULSE STATISTICS

Definitions:

AFCP = Adjustment Factor for mean Center Pulse
 PixLoc = Mean pixel location of per scan center pulse
 StdErr = Standard Error of Peak Pulse Fit

BAND B20:

INTEG PULSE				CENTER PULSE				PEAK PULSE			BACKGROUND		
Center													
===== PulseLoc													
Scans				Scans				PerScan					
Det	Mean	Good	Bad	Mean	Sigma	AFCP	Good	Bad	Value	Sigma	Mean		
Sigma		Average											
1	212.39	142	6	245.03	0.02	1.0177	22	0	245.04	0.014	9.98	0.58	1066.61
2	214.10	142	6	244.86	0.02	1.0177	20	0	244.88	0.009	10.14	0.56	1068.76
3	213.57	141	5	245.06	0.02	1.0179	20	0	245.07	0.010	9.95	0.56	1066.28
4	211.95	141	5	244.92	0.02	1.0178	22	0	244.92	0.004	10.09	0.55	1068.40
5	213.95	142	6	245.15	0.02	1.0177	20	0	245.15	0.011	9.87	0.57	1065.61
6	213.50	142	6	244.97	0.02	1.0180	20	0	244.97	0.004	10.04	0.58	1068.03
7	211.96	142	4	245.00	0.02	1.0175	22	0	245.02	0.012	10.01	0.56	1065.27
8	213.35	142	6	244.87	0.03	1.0178	20	0	244.87	0.005	10.14	0.58	1067.37
9	213.58	142	6	245.10	0.02	1.0178	20	0	245.10	0.011	9.90	0.60	1064.88
10	212.08	142	4	244.87	0.02	1.0177	22	0	244.88	0.010	10.13	0.59	1067.09
11	207.34	142	6	245.11	0.02	1.0177	22	0	245.11	0.004	9.89	0.59	1064.27
12	213.36	142	6	244.86	0.02	1.0180	20	0	244.87	0.010	10.14	0.56	1066.69
13	213.79	142	4	245.16	0.03	1.0177	20	0	245.17	0.005	9.84	0.59	1064.06
14	206.87	142	6	244.89	0.02	1.0178	22	0	244.89	0.004	10.12	0.57	1066.19
15	213.85	142	6	245.11	0.02	1.0177	20	0	245.11	0.004	9.90	0.58	1063.65
16	213.35	142	4	244.84	0.02	1.0178	20	0	244.84	0.004	10.17	0.56	1066.02

ABSOLUTE GAINS

INTEGRATED PULSE CENTER PULSE wrt PEAK PULSE wrt

wrt XCal Rad PASC Rad Sigma Xcal Rad Sigma PASC Rad Sigma Xcal
 Rad Sigma

 Band B20: Det

1	-1.000	1.003	0.000	-1.000	-1.000	1.003	0.000	-1.000	-1.000
2	-1.000	1.003	0.000	-1.000	-1.000	1.003	0.000	-1.000	-1.000
3	-1.000	1.003	0.000	-1.000	-1.000	1.003	0.000	-1.000	-1.000
4	-1.000	1.003	0.000	-1.000	-1.000	1.003	0.000	-1.000	-1.000
5	-1.000	1.004	0.000	-1.000	-1.000	1.004	0.000	-1.000	-1.000
6	-1.000	1.003	0.000	-1.000	-1.000	1.003	0.000	-1.000	-1.000
7	-1.000	1.003	0.000	-1.000	-1.000	1.003	0.000	-1.000	-1.000
8	-1.000	1.003	0.000	-1.000	-1.000	1.003	0.000	-1.000	-1.000
9	-1.000	1.003	0.000	-1.000	-1.000	1.003	0.000	-1.000	-1.000
10	-1.000	1.003	0.000	-1.000	-1.000	1.003	0.000	-1.000	-1.000
11	-1.000	1.004	0.000	-1.000	-1.000	1.004	0.000	-1.000	-1.000
12	-1.000	1.003	0.000	-1.000	-1.000	1.003	0.000	-1.000	-1.000
13	-1.000	1.004	0.000	-1.000	-1.000	1.004	0.000	-1.000	-1.000
14	-1.000	1.003	0.000	-1.000	-1.000	1.003	0.000	-1.000	-1.000
15	-1.000	1.004	0.000	-1.000	-1.000	1.004	0.000	-1.000	-1.000
16	-1.000	1.002	0.000	-1.000	-1.000	1.002	0.000	-1.000	-1.000

RELATIVE GAINS WRT DETECTOR 8

INTEGRATED PULSE CENTER PULSE wrt PEAK PULSE wrt
 wrt XCal Rad PASC Rad Xcal Rad PASC Rad Xcal Rad

 Band B20: Det

1	-1.000	1.000	-1.000	1.000	-1.000
2	-1.000	0.999	-1.000	0.999	-1.000
3	-1.000	1.000	-1.000	1.000	-1.000
4	-1.000	0.999	-1.000	0.999	-1.000
5	-1.000	1.000	-1.000	1.000	-1.000
6	-1.000	0.999	-1.000	0.999	-1.000
7	-1.000	1.000	-1.000	1.000	-1.000
8	-1.000	0.999	-1.000	0.999	-1.000
9	-1.000	1.000	-1.000	1.000	-1.000
10	-1.000	0.999	-1.000	0.999	-1.000
11	-1.000	1.000	-1.000	1.000	-1.000
12	-1.000	0.999	-1.000	0.999	-1.000
13	-1.000	1.000	-1.000	1.000	-1.000
14	-1.000	0.999	-1.000	0.999	-1.000
15	-1.000	1.000	-1.000	1.000	-1.000

16 -1.000 0.999 -1.000 0.999 -1.000

RELATIVE BAND GAINS

Center Pulse wrt PASC Rad

	Band1	Band2	Band3	Band4	Band5	Band7	Band8
Band1	1.000	0.888	0.712	0.559	0.158	0.056	0.313
Band2	1.126	1.000	0.802	0.630	0.178	0.063	0.353
Band3	1.405	1.247	1.000	0.786	0.222	0.079	0.440
Band4	1.788	1.587	1.272	1.000	0.283	0.101	0.560
Band5	6.322	5.612	4.499	3.536	1.000	0.356	1.980
Band7	17.778	15.782	12.653	9.944	2.812	1.000	5.569
Band8	3.192	2.834	2.272	1.785	0.505	0.180	1.000

Center Pulse wrt XCal Rad

	Band1	Band2	Band3	Band4	Band5	Band7	Band8
Band1	-1.000	-1.000	-1.000	-1.000	-1.000	-1.000	-1.000
Band2	-1.000	-1.000	-1.000	-1.000	-1.000	-1.000	-1.000
Band3	-1.000	-1.000	-1.000	-1.000	-1.000	-1.000	-1.000
Band4	-1.000	-1.000	-1.000	-1.000	-1.000	-1.000	-1.000
Band5	-1.000	-1.000	-1.000	-1.000	-1.000	-1.000	-1.000
Band7	-1.000	-1.000	-1.000	-1.000	-1.000	-1.000	-1.000
Band8	-1.000	-1.000	-1.000	-1.000	-1.000	-1.000	-1.000

Peak Pulse wrt PASC Rad

	Band1	Band2	Band3	Band4	Band5	Band7	Band8
Band1	1.000	0.888	0.712	0.558	0.158	0.056	0.313
Band2	1.126	1.000	0.802	0.629	0.178	0.063	0.353
Band3	1.405	1.247	1.000	0.785	0.222	0.079	0.440
Band4	1.791	1.590	1.275	1.000	0.283	0.101	0.561
Band5	6.327	5.617	4.503	3.533	1.000	0.356	1.982
Band7	17.793	15.796	12.664	9.935	2.812	1.000	5.574
Band8	3.192	2.834	2.272	1.783	0.505	0.179	1.000

Peak Pulse wrt XCal Rad

	Band1	Band2	Band3	Band4	Band5	Band7	Band8
Band1	-1.000	-1.000	-1.000	-1.000	-1.000	-1.000	-1.000
Band2	-1.000	-1.000	-1.000	-1.000	-1.000	-1.000	-1.000
Band3	-1.000	-1.000	-1.000	-1.000	-1.000	-1.000	-1.000
Band4	-1.000	-1.000	-1.000	-1.000	-1.000	-1.000	-1.000
Band5	-1.000	-1.000	-1.000	-1.000	-1.000	-1.000	-1.000
Band7	-1.000	-1.000	-1.000	-1.000	-1.000	-1.000	-1.000
Band8	-1.000	-1.000	-1.000	-1.000	-1.000	-1.000	-1.000

Plot files generated:

pasc_angles.ps (L7 Orbit track, vs pasc sun angles)
pasc_bandav_plot.ps (Band Avg Rads vs Band Center Wave.)
pasc_peak_resids.ps (Residuals of polyfit to pulse peak)

Data files generated:

pasc_header_page.txt (ASCII, Summary page for pasc run)
pasc_sunangles.txt (ASCII, Sun and Orbit Parameters)
pasc_pulse.txt (ASCII, Pulse integration stats)
pasc_summary_report.txt (ASCII, Summary of all results)

2.3.3 FASC Processing Summary:

Landsat 7 Image Assessment System
FASC INTERVAL Characterization

Fri Sep 8 16:29:06
tightrope

Product: N/A Processing Level: R0C

Band xxx45__xx Scene N/A Gain L -- FASC IMAGE data

(Report 2.0)

SUMMARY REPORT FOR FASC CALIBRATION Report Date: Fri Sep 8 16:29:06 2000

START ACQUISITION: 2000.236 17:46:50.000

STOP ACQUISITION: 2000.236 17:47:41.000

TOTAL ACQUISITION (secs) : 53.824871

Orbit Angles (degrees)	Min	Max
Not available for FASC interval	n/a	n/a

Sun to FASC Panel Angles (degrees) :	Min	Max
Solar Zenith for Gain Calc (IN):	68.00	70.00
Azimuthal Scatter For Acq (AZ):	29.35	29.95

FASC Panel Spectral Radiances (W/m²-mu-ster):

	Avg	Sigma
Band B10:	N/A	N/A
Band B20:	N/A	N/A
Band B30:	N/A	N/A
Band B40:	110.16	2.888
Band B50:	21.05	0.551
Band B61:	N/A	N/A
Band B62:	N/A	N/A
Band B70:	N/A	N/A
Band B80:	N/A	N/A

FASC Image Statistics (DN):

Image w/ Bias		Image w/o Bias	
Avg	Sigma	Avg	Sigma

Band B10:
*** Band not processed. ***

FASC Image Statistics (DN):

Image w/ Bias		Image w/o Bias	
Avg	Sigma	Avg	Sigma
Band B20: *** Band not processed. ***			

FASC Image Statistics (DN):

Image w/ Bias		Image w/o Bias	
Avg	Sigma	Avg	Sigma
Band B30: *** Band not processed. ***			

FASC Image Statistics (DN):

Image w/ Bias		Image w/o Bias		
Avg	Sigma	Avg	Sigma	
Band B40:				
Det 1:	111.730	2.836	101.693	2.836
Det 2:	111.418	2.829	101.450	2.828
Det 3:	111.739	2.843	101.802	2.843
Det 4:	109.878	2.794	100.028	2.795
Det 5:	111.590	2.846	101.606	2.846
Det 6:	111.321	2.844	101.442	2.845
Det 7:	111.180	2.834	101.175	2.834
Det 8:	111.756	2.854	101.862	2.853
Det 9:	110.543	2.820	100.551	2.820
Det 10:	110.991	2.829	101.064	2.831
Det 11:	109.860	2.804	100.114	2.803
Det 12:	110.793	2.829	101.087	2.831
Det 13:	110.563	2.809	100.751	2.808
Det 14:	110.945	2.821	101.172	2.823
Det 15:	110.225	2.798	100.263	2.796
Det 16:	111.987	2.849	102.065	2.848
Mean:	111.032	2.828	101.133	2.828

FASC Gain Statistics

Absolute Gains		Regression Stats		Relative Gain Ratios	
Avg	Sigma	Slope	Sigma	Prob	ABS/<Det> ABS/(Det9)

Band B40:

Det 1:	0.92311	0.00157	0.98169	0.00046	1.00000	1.00554	1.01136
Det 2:	0.92091	0.00155	0.97894	0.00038	1.00000	1.00314	1.00895
Det 3:	0.92410	0.00160	0.98402	0.00040	1.00000	1.00662	1.01245
Det 4:	0.90799	0.00159	0.96752	0.00043	1.00000	0.98907	0.99480
Det 5:	0.92232	0.00167	0.98518	0.00041	1.00000	1.00468	1.01050
Det 6:	0.92082	0.00170	0.98486	0.00039	1.00000	1.00305	1.00886
Det 7:	0.91840	0.00167	0.98092	0.00041	1.00000	1.00041	1.00621
Det 8:	0.92464	0.00168	0.98763	0.00042	1.00000	1.00721	1.01304
Det 9:	0.91274	0.00169	0.97602	0.00050	1.00000	0.99424	1.00000
Det 10:	0.91740	0.00166	0.97968	0.00046	1.00000	0.99932	1.00511
Det 11:	0.90878	0.00164	0.97026	0.00044	1.00000	0.98993	0.99566
Det 12:	0.91761	0.00166	0.97968	0.00043	1.00000	0.99955	1.00534
Det 13:	0.91456	0.00153	0.97195	0.00039	1.00000	0.99622	1.00199
Det 14:	0.91838	0.00157	0.97702	0.00041	1.00000	1.00039	1.00618
Det 15:	0.91013	0.00154	0.96782	0.00040	1.00000	0.99140	0.99714
Det 16:	0.92649	0.00158	0.98566	0.00046	1.00000	1.00922	1.01507

Mean: 0.91802 0.00162 0.97868 0.00043 1.00000 1.00000 1.00579

FASC Image Statistics (DN):

	Image w/ Bias		Image w/o Bias	
	Avg	Sigma	Avg	Sigma
Band B50:				
Det 1:	114.420	2.940	104.396	2.940
Det 2:	115.181	2.955	105.147	2.953
Det 3:	115.127	2.959	105.151	2.960
Det 4:	114.728	2.954	104.751	2.954
Det 5:	115.533	2.966	105.493	2.967
Det 6:	114.183	2.921	104.131	2.920
Det 7:	114.582	2.943	104.565	2.941
Det 8:	115.260	2.962	105.180	2.961
Det 9:	115.169	2.951	105.032	2.951
Det 10:	115.690	2.962	105.577	2.961
Det 11:	114.358	2.948	104.461	2.949
Det 12:	113.999	2.940	104.014	2.939
Det 13:	114.124	2.919	104.038	2.921
Det 14:	114.613	2.938	104.528	2.939
Det 15:	114.258	2.931	104.217	2.932
Det 16:	115.201	2.958	105.147	2.958
Mean:	114.777	2.947	104.739	2.947

FASC Gain Statistics

	Absolute Gains		Regression Stats		Relative Gain Ratios		
	Avg	Sigma	Slope	Sigma	Prob	ABS/<Det>	ABS/(Det9)
Band B50:							
Det 1:	4.95899	0.01001	5.33745	0.00224	1.00000	0.99672	0.99394
Det 2:	4.99467	0.00971	5.36112	0.00224	1.00000	1.00389	1.00109
Det 3:	4.99484	0.01004	5.37429	0.00234	1.00000	1.00393	1.00113
Det 4:	4.97586	0.01022	5.36298	0.00227	1.00000	1.00011	0.99732
Det 5:	5.01112	0.00995	5.38721	0.00261	1.00000	1.00720	1.00439
Det 6:	4.94643	0.00938	5.30082	0.00246	1.00000	0.99420	0.99142
Det 7:	4.96703	0.00988	5.33997	0.00256	1.00000	0.99834	0.99555
Det 8:	4.99624	0.01005	5.37613	0.00244	1.00000	1.00421	1.00141
Det 9:	4.98922	0.00979	5.35781	0.00257	1.00000	1.00280	1.00000
Det 10:	5.01509	0.00955	5.37515	0.00240	1.00000	1.00800	1.00518
Det 11:	4.96208	0.01035	5.35367	0.00226	1.00000	0.99734	0.99456
Det 12:	4.94084	0.01044	5.33618	0.00226	1.00000	0.99307	0.99030
Det 13:	4.94201	0.00958	5.30354	0.00254	1.00000	0.99331	0.99054
Det 14:	4.96526	0.00981	5.33570	0.00256	1.00000	0.99798	0.99520
Det 15:	4.95050	0.00986	5.32254	0.00257	1.00000	0.99501	0.99224
Det 16:	4.99470	0.00996	5.37101	0.00242	1.00000	1.00390	1.00110
Mean:	4.97531	0.00991	5.34972	0.00242	1.00000	1.00000	0.99721

FASC Image Statistics (DN):

	Image w/ Bias		Image w/o Bias	
	Avg	Sigma	Avg	Sigma
Band B61:				
*** Band not processed. ***				

FASC Image Statistics (DN):

	Image w/ Bias		Image w/o Bias	
	Avg	Sigma	Avg	Sigma
Band B62:				
*** Band not processed. ***				

FASC Image Statistics (DN):

	Image w/ Bias		Image w/o Bias	
	Avg	Sigma	Avg	Sigma
Band B70:				
*** Band not processed. ***				

FASC Image Statistics (DN):

Image w/ Bias		Image w/o Bias	

2	87	24.32	44.02	108	25.82	43.31
3	130	24.20	43.79	144	25.52	42.96
4	106	24.77	44.01	123	25.89	43.22
5	97	24.72	43.77	117	25.73	42.91
6	97	25.12	43.96	123	26.03	43.07
7	101	25.16	43.77	129	26.07	42.77
8	113	25.31	43.92	134	26.11	43.17
9	100	25.48	43.69	122	26.20	43.01
10	114	25.64	44.02	118	26.29	43.19
11	126	25.31	43.83	132	25.99	42.78
12	83	25.38	43.95	113	25.96	43.01
13	98	25.17	43.81	113	25.82	42.96
14	98	25.23	43.90	116	25.78	43.10
15	90	25.20	43.77	113	25.77	42.94
16	106	25.47	43.97	117	25.97	43.15

 Landsat-7 Image Assessment System
 Memory Effect Characterization

02/12/2003 21:33:26
 tightrope

Product: L72EDC110222815020 Scene start time: 08/16/2002 08:43:06

Band 2, Scene 1, Gain L, NIGHT

Number of scans: 375 First Scan: Forward

Det	Magnitude (DN)	Std Dev 95% CI	Within (Minor Frames)	Time Constant	Std Dev 95% CI	Within
1	10.403099	0.019249	???	1291.38	59.0638	???
2	8.604730	0.022345	???	1270.18	50.7173	???
3	11.978750	0.017826	???	1408.86	58.2639	???
4	14.772645	0.035423	???	534.97	50.6714	???
5	29.288288	0.050969	???	227.34	50.7891	???
6	8.517014	0.021892	???	1357.22	48.7884	???
7	8.004892	0.023420	???	1165.11	53.3304	???
8	8.784361	0.021513	???	1376.84	49.1380	???
9	52.781136	0.055475	???	151.04	52.2265	???
10	10.473116	0.020356	???	1267.94	56.3904	???
11	13.481622	0.017656	???	1396.45	59.0441	???
12	13.761214	0.030333	???	707.52	51.9145	???
13	9.671200	0.021919	???	1361.39	48.6393	???
14	11.765102	0.020267	???	1154.27	62.2790	???
15	15.532531	0.030755	???	707.43	51.3965	???
16	12.662707	0.019852	???	1298.78	56.5087	???

Det	FORWARD	Mean pulse	REVERSE	Mean pulse
-----	---------	------------	---------	------------

	Num scans	height	width	Num scans	height	width
1	13	59.12	47.15	37	60.80	46.59
2	10	56.18	47.30	26	57.61	46.65
3	22	59.34	47.45	28	60.98	46.36
4	15	56.09	47.67	25	57.47	46.60
5	14	60.42	47.50	26	62.05	46.42
6	23	56.77	47.43	30	58.01	46.63
7	23	60.82	47.52	29	62.46	46.62
8	19	56.45	47.37	29	57.73	46.69
9	15	60.71	47.47	27	62.45	46.44
10	21	57.53	47.67	31	59.04	46.58
11	24	60.51	47.62	32	62.41	46.62
12	28	56.14	47.75	44	57.85	46.48
13	18	60.57	47.44	30	62.53	46.60
14	16	56.39	47.44	41	57.86	46.56
15	17	59.83	47.59	34	62.01	46.38
16	14	55.70	47.36	31	57.25	46.29

3.2.3 Scan Correlated Shift Summary:

Landsat-7 Image Assessment System 02/12/2003 20:58:45
Scan Correlated Shift Characterization tightrope

Product : L72EDC110222815020 Processing Level: R0R
Band B1 Scene 1 Gain L -- NIGHT IMAGE data

Dataline	Transition Location	Previous Pixel Value	Current Pixel Value
1855	98	12.00000	11.00000
1871	101	119.00000	120.00000
3535	101	120.00000	122.00000
3551	98	10.00000	10.00000
3999	98	11.00000	11.00000
4015	101	117.00000	120.00000
4335	101	124.00000	124.00000
4351	98	12.00000	10.00000
4543	98	11.00000	11.00000
4559	101	125.00000	127.00000
4575	98	11.00000	11.00000

Landsat-7 Image Assessment System
Scan Correlated Shift Characterization

02/12/2003 21:18:19
tightrope

Product : L72EDC110222815020 Processing Level: R0R

Band B2 Scene 1 Gain L -- NIGHT IMAGE data

Dataline Transition Previous Pixel Current Pixel
 Location Value Value
----- ----- ----- -----

No SCS transition locations were found.

3.2.4 Coherent Noise Characterization Summary

Landsat-7 Image Assessment System
Coherent Noise Characterization

02/12/2003 21:33:08
tightrope

Product: Processing Level: R0R

Band 2 Scene 1 375 scans, 2 SCS states

Image size: (6600 pixels, 6000 lines) 151.06 Mbytes

Number of unused scans: 0

Number of CN components: 2

Total processing time: 498.4 sec

Average time per scan: 1.3 sec

Continuum fit to 4th-order Legendre Polynomial

Det SCS Noise Floor Coefficients

Num State and Standard Deviations

1	0	-1.782E+00	-9.324E-01	2.412E-01	-1.414E-02	4.028E-02	6.702E-02	1.557E-01	2.174E-01	2.304E-01	2.232E-01
2	0	-1.777E+00	-9.126E-01	2.373E-01	-2.885E-02	4.354E-02	6.870E-02	1.558E-01	2.268E-01	2.304E-01	2.369E-01
3	0	-1.800E+00	-9.321E-01	2.481E-01	-1.142E-02	5.005E-02					

7.599E-02 1.564E-01 2.632E-01 2.327E-01 2.787E-01

4 0 -1.789E+00 -9.399E-01 2.373E-01 -2.056E-02 4.311E-02
6.678E-02 1.557E-01 2.161E-01 2.304E-01 2.210E-01

5 0 -1.783E+00 -9.411E-01 2.337E-01 -1.899E-02 5.074E-02
7.266E-02 1.559E-01 2.472E-01 2.312E-01 2.620E-01

6 0 -1.795E+00 -9.289E-01 2.430E-01 -2.429E-02 4.838E-02
6.870E-02 1.558E-01 2.268E-01 2.304E-01 2.369E-01

7 0 -1.797E+00 -9.301E-01 2.458E-01 -1.338E-02 4.274E-02
6.678E-02 1.557E-01 2.161E-01 2.304E-01 2.210E-01

8 0 -1.804E+00 -9.246E-01 2.611E-01 -1.428E-02 4.259E-02
7.129E-02 1.558E-01 2.404E-01 2.308E-01 2.542E-01

9 0 -1.787E+00 -9.088E-01 2.733E-01 -1.409E-02 4.706E-02
7.087E-02 1.558E-01 2.382E-01 2.307E-01 2.516E-01

10 0 -1.781E+00 -9.419E-01 2.532E-01 -2.142E-02 5.628E-02
6.972E-02 1.558E-01 2.322E-01 2.305E-01 2.441E-01

11 0 -1.791E+00 -9.181E-01 2.617E-01 -2.111E-02 4.782E-02
6.903E-02 1.558E-01 2.285E-01 2.305E-01 2.392E-01

12 0 -1.830E+00 -9.433E-01 2.429E-01 -1.809E-02 4.934E-02
6.754E-02 1.558E-01 2.203E-01 2.304E-01 2.276E-01

13 0 -1.788E+00 -9.526E-01 2.345E-01 -1.046E-02 5.840E-02
7.315E-02 1.559E-01 2.497E-01 2.313E-01 2.647E-01

14 0 -1.798E+00 -9.349E-01 2.431E-01 -1.611E-02 4.629E-02
6.678E-02 1.557E-01 2.161E-01 2.304E-01 2.210E-01

15 0 -1.793E+00 -9.587E-01 2.444E-01 -1.580E-02 5.032E-02
6.972E-02 1.558E-01 2.322E-01 2.305E-01 2.441E-01

16 0 -1.799E+00 -9.616E-01 2.413E-01 -1.996E-02 5.124E-02
6.702E-02 1.557E-01 2.174E-01 2.304E-01 2.232E-01

Det SCS Noise Floor Coefficients

Num State and Standard Deviations

1 1 -1.788E+00 -9.365E-01 2.453E-01 -7.130E-03 4.120E-02
7.135E-02 1.523E-01 2.421E-01 2.274E-01 2.594E-01

2 1 -1.785E+00 -9.157E-01 2.410E-01 -2.024E-02 4.151E-02
6.689E-02 1.522E-01 2.187E-01 2.265E-01 2.299E-01

3 1 -1.809E+00 -9.377E-01 2.492E-01 -1.488E-02 4.833E-02
6.748E-02 1.522E-01 2.219E-01 2.266E-01 2.345E-01

4 1 -1.795E+00 -9.403E-01 2.418E-01 -1.938E-02 4.602E-02
7.266E-02 1.559E-01 2.472E-01 2.312E-01 2.620E-01

5 1 -1.790E+00 -9.426E-01 2.336E-01 -1.466E-02 5.109E-02
6.972E-02 1.558E-01 2.322E-01 2.305E-01 2.441E-01

6 1 -1.802E+00 -9.305E-01 2.496E-01 -1.964E-02 5.224E-02
6.810E-02 1.558E-01 2.234E-01 2.304E-01 2.322E-01

7 1 -1.803E+00 -9.373E-01 2.520E-01 -1.489E-02 5.109E-02
7.173E-02 1.558E-01 2.426E-01 2.309E-01 2.568E-01

8 1 -1.811E+00 -9.242E-01 2.536E-01 -1.135E-02 3.551E-02
6.678E-02 1.557E-01 2.161E-01 2.304E-01 2.210E-01

9 1 -1.792E+00 -9.034E-01 2.768E-01 -7.803E-03 4.853E-02
8.123E-02 1.556E-01 2.880E-01 2.334E-01 3.030E-01

10 1 -1.793E+00 -9.343E-01 2.444E-01 -2.403E-03 3.896E-02
7.044E-02 1.523E-01 2.375E-01 2.271E-01 2.542E-01

11 1 -1.801E+00 -9.140E-01 2.592E-01 -6.073E-03 3.558E-02
7.587E-02 1.532E-01 2.639E-01 2.296E-01 2.816E-01

12 1 -1.839E+00 -9.431E-01 2.412E-01 -6.340E-03 3.966E-02
7.135E-02 1.523E-01 2.421E-01 2.274E-01 2.594E-01

13 1 -1.800E+00 -9.506E-01 2.280E-01 2.445E-04 4.060E-02
6.910E-02 1.558E-01 2.285E-01 2.307E-01 2.393E-01

14 1 -1.806E+00 -9.344E-01 2.452E-01 -8.597E-03 4.876E-02
7.596E-02 1.533E-01 2.639E-01 2.296E-01 2.820E-01

15 1 -1.799E+00 -9.567E-01 2.409E-01 -8.835E-03 4.507E-02
6.813E-02 1.522E-01 2.254E-01 2.266E-01 2.393E-01

16 1 -1.807E+00 -9.560E-01 2.456E-01 -9.488E-03 4.710E-02
7.088E-02 1.523E-01 2.398E-01 2.273E-01 2.568E-01

Lower and upper bound frequencies

Cmp	Det	Lower bound	Upper bound	Integrated
Num	Num	Frequency	Frequency	Power
1	1	-0.000488	0.056152	23.874273

2 7 0.056152 0.060059 0.034281

Coherent Noise Ratios and Total Power

SCS State: Low

Det	CN Ratio	Total Power
1	0.563282	45.245708
2	0.564702	44.689911
3	0.561962	43.538284
4	0.560947	44.765800
5	0.549411	44.227970
6	0.559621	43.584457
7	0.561002	43.435776
8	0.558824	42.769707
9	0.548692	43.002674
10	0.545119	44.909306
11	0.550465	43.025375
12	0.570536	42.103619
13	0.547035	44.169983
14	0.558603	43.400826
15	0.545884	44.381622
16	0.540508	43.371502

SCS State: High

Det	CN Ratio	Total Power
1	0.534781	42.133217
2	0.537248	41.459827
3	0.530277	40.211456
4	0.529240	41.397789
5	0.520151	40.914715
6	0.527732	40.331036
7	0.523175	40.207237
8	0.535369	39.628635
9	0.521633	39.786690
10	0.534235	41.386692
11	0.531559	39.700706
12	0.548666	38.833427
13	0.529182	40.662830
14	0.529105	39.883835
15	0.518306	40.841301
16	0.513786	39.872578

Scan-level Statistics

Scan 1 SCS state: Low

Det	Cmp	Magnitude	Frequency	Phase
Num	Num	(DN)	(cycles/mf)	(radians)
1	1	250.700562	0.000000	0.000000
1	2	0.374922	0.058540	-0.285116
2	1	251.676056	0.000000	0.000000
2	2	0.418336	0.058540	-0.808439
3	1	249.491867	0.000000	0.000000
3	2	0.584674	0.058540	-0.008310
4	1	257.223511	0.000000	0.000000
4	2	0.652589	0.058540	-0.476421
5	1	251.416534	0.000000	0.000000
5	2	0.934119	0.058540	-0.034727
6	1	249.229675	0.000000	0.000000
6	2	1.302815	0.058540	-0.747806
7	1	253.451447	0.000000	0.000000
7	2	0.876098	0.058540	-0.280240
8	1	256.027954	0.000000	0.000000
8	2	0.613181	0.058540	-1.096268
9	1	252.878952	0.000000	0.000000
9	2	0.646222	0.058540	-0.722403
10	1	259.477417	0.000000	0.000000
10	2	1.060756	0.058540	-1.369157
11	1	249.243988	0.000000	0.000000
11	2	1.021209	0.058540	-1.033600
12	1	249.265930	0.000000	0.000000
12	2	0.885658	0.058540	-1.539271
13	1	256.917297	0.000000	0.000000
13	2	0.813767	0.058540	-0.846539
14	1	258.811249	0.000000	0.000000
14	2	0.674313	0.058540	-1.529600
15	1	265.527710	0.000000	0.000000
15	2	0.539269	0.058540	-1.125355
16	1	257.163025	0.000000	0.000000
16	2	0.836163	0.058540	-1.418667

. (Similar statistics for all scans)

Scan 375 SCS state: Low

Det	Cmp	Magnitude	Frequency	Phase
Num	Num	(DN)	(cycles/mf)	(radians)
1	1	42.227600	0.000000	0.000000
1	2	0.088177	0.056648	-1.342185
2	1	41.284695	0.000000	0.000000
2	2	0.068142	0.056648	-1.396358

3	1	40.993896	0.000000	0.000000
3	2	-0.022543	0.056648	-1.092133
4	1	41.948959	0.000000	0.000000
4	2	0.016935	0.056648	-1.236468
5	1	40.402252	0.000000	0.000000
5	2	-0.022748	0.056648	-1.315503
6	1	40.642883	0.000000	0.000000
6	2	-0.079904	0.056648	-1.737076
7	1	40.793102	0.000000	0.000000
7	2	-0.141135	0.056648	-1.479323
8	1	40.072769	0.000000	0.000000
8	2	-0.090624	0.056648	-2.096399
9	1	39.036751	0.000000	0.000000
9	2	-0.006646	0.056648	-1.532894
10	1	40.549541	0.000000	0.000000
10	2	0.035766	0.056648	-1.832620
11	1	39.793537	0.000000	0.000000
11	2	0.022536	0.056648	-1.063128
12	1	40.253353	0.000000	0.000000
12	2	0.006058	0.056648	-1.299285
13	1	39.902954	0.000000	0.000000
13	2	-0.023300	0.056648	-0.877688
14	1	39.956951	0.000000	0.000000
14	2	-0.015291	0.056648	-1.211875
15	1	39.536713	0.000000	0.000000
15	2	-0.024079	0.056648	-0.950581
16	1	38.361526	0.000000	0.000000
16	2	0.023988	0.056648	-1.396520

3.2.10 Histogram Analysis Summary:

HISTOGRAM ANALYSIS REPORT- HEADER PAGE

INPUT DATA: SCENE, byte data

DATE OF ACQUISITION: 07/28/2000 12:03:45

TIME: 06/26/2001 14:51:25

SATELLITE: LANDSAT 7
PATH: 202
ROW: 210
BAND: B2
REFERENCE DETECTOR: 12
PROCESSING LEVEL: R0R
NUMBER OF SCANS ANALYZED: 374
GAIN STATE: L

TOTAL # PIXELS USED PER DET: 2178750

PIXELS TAKEN OFF LOW END PER DETECTOR

FORWARD SCANS 0
REVERSE SCANS 0
ALL SCANS 0

PIXELS TAKEN OFF HIGH END PER DETECTOR

FORWARD SCANS 9115
REVERSE SCANS 9037
ALL SCANS 18126

NOTE: BIAS WAS CALCULATED FROM THE IC DATA

TEMPERATURES IN DEGREES C:

MEAN

AMBIENT_PREAMP_LOW_CH	0.0000
BACKUP_SHUTTER_FLAG	0.0000
BAFFLE_HEATER	0.0000
BAFFLE_SUPPORT	0.0000
BAFFLE_TUBE	0.0000
BAND4_POSTAMP	0.0000
BAND7_PREAMP	0.0000
BLACKBODY_CTL	0.0000
BLACKBODY_ISO	0.0000
CAL_LAMP_HOUSING	0.0000
CAL_SHUTTER_FLAG	0.0000
CAL_SHUTTER_HUB	0.0000
CFPA_CTL	0.0000
CFPA_MONITOR	0.0000
MEM_HEAT_SINK_PS1	0.0000
MEM_HEAT_SINK_PS2	0.0000
MUX_ELECTRONICS	0.0000
MUX_POWER_SUPPLY	0.0000
PANBAND_POSTAMP	0.0000
PRIMARY_MIRROR	0.0000
PRIMARY_MIRROR_MASK	0.0000
SCAN_LINE_CORRECTOR	0.0000
SECONDARY_MIRROR	0.0000
SECONDARY_MIRROR_MASK	0.0000
SILICON_FP_ASSEMBLY	0.0000
TELESCOPE_BASEPLATE	0.0000

TELESCOPE_HOUSING 0.0000

LAMP CURRENTS IN MILLIAMPS:

MEAN

TEC_LAMP_1I -1.0000

TEC_LAMP_2I -1.0000

Landsat-7 Image Assessment System

06/26/2001 14:51:25

Histogram Analysis

tightrope

Product: L71EDC110021017040 Processing Level: R0R

Band B2 Scene 1 Gain L -- PASC IMAGE data

HISTOGRAM ANALYSIS REPORT- SUMMARY PAGE

INPUT DATA: SCENE, byte data

REFERENCE DETECTOR = 12

DETECTOR SATURATION LEVEL FIND RESULTS

DetNo	High Sat	Low Sat
01	255.0000	0.0000
02	255.0000	0.0000
03	255.0000	0.0000
04	255.0000	0.0000
05	255.0000	0.0000
06	255.0000	0.0000
07	255.0000	0.0000
08	255.0000	0.0000
09	255.0000	0.0000
10	255.0000	0.0000
11	255.0000	0.0000
12	255.0000	0.0000
13	255.0000	0.0000
14	255.0000	0.0000
15	255.0000	0.0000
16	255.0000	0.0000

FOR ALL SCANS:

TOTAL # PIXELS USED PER DET: 2178750
PIXELS TAKEN OFF LOW END (BIN 0) PER DETECTOR: 0
PIXELS TAKEN OFF HIGH END (BIN 255) PER DETECTOR: 18126

	unweighted	weighted	reference
	detector		
scene mean (counts)	10.5256	10.5279	10.6436
scene stdev (counts)	8.9284	8.9284	8.9210
scene mean for/rev ratio	0.9983	0.9983	0.9977
scene stdev for/rev ratio	0.9730	0.9728	0.9648
scene mean for/all ratio	0.9989	0.9989	0.9986
scene stdev for/all ratio	0.9820	0.9819	0.9779

PEAKS IN FFT

frequency (lines/cycle)	FFT magnitude	magnitude- background
32.0000	0.0225	-0.0579
16.0000	0.0237	-0.0465
8.0000	0.0277	-0.0105
5.3333	0.0154	-0.0124
4.0000	0.0168	-0.0062
3.2000	0.0131	-0.0074

2.6667	0.0111	-0.0079
2.2857	0.0202	0.0016
2.0000	0.1014	0.0793

RESULTS FOR ALL SCANS

Note: weighted means and standard deviations are based on detector noise level

det	scene	scene	detector
	mean,md	stdev,sd	noise lev
	(counts)	(counts)	(counts)
1	10.487	9.021	0.601
2	10.651	9.014	0.576
3	10.457	8.863	0.579
4	10.598	8.968	0.573
5	10.374	8.923	0.588
6	10.546	8.896	0.591
7	10.519	8.957	0.578
8	10.646	8.874	0.597
9	10.412	8.878	0.612
10	10.641	9.015	0.600
11	10.397	8.945	0.602
12	10.644	8.921 (sr)	0.572
13	10.349	8.907	0.606
14	10.618	8.877	0.589
15	10.404	8.936	0.586

16	10.668	8.860	0.575
mean	10.526	8.928 (sa)	0.589
stdev	0.115	0.055	0.013
coef of var	1.088	0.612	2.178
minimum	10.349	8.860	0.572
maximum	10.668	9.021	0.612
wgt mean	10.528	8.928	0.588

RESULTS FOR FWD SCANS

Note: weighted means and standard deviations are based on detector noise level

det	scene mean,md (counts)	scene stdev,sd (counts)	detector noise lev (counts)
1	10.480	8.916	0.601
2	10.642	8.875	0.576
3	10.447	8.673	0.579
4	10.587	8.814	0.573
5	10.364	8.746	0.588
6	10.534	8.726	0.591
7	10.508	8.749	0.578
8	10.632	8.667	0.597
9	10.407	8.812	0.612
10	10.630	8.873	0.600

11	10.387	8.785	0.602
12	10.629	8.723 (sr)	0.572
13	10.339	8.765	0.606
14	10.606	8.749	0.589
15	10.385	8.745	0.586
16	10.648	8.669	0.575

mean	10.514	8.768 (sa)	0.589
stdev	0.113	0.074	0.013
coef of var	1.075	0.849	2.178
minimum	10.339	8.667	0.572
maximum	10.648	8.916	0.612
wgt mean	10.516	8.767	0.588

RESULTS FOR REV SCANS

Note: weighted means and standard deviations are based on detector noise level

det	scene mean,md (counts)	scene stdev,sd (counts)	detector noise lev (counts)
1	10.488	9.047	0.601
2	10.654	9.073	0.576
3	10.462	8.975	0.579
4	10.604	9.043	0.573
5	10.378	9.022	0.588

6	10.553	8.988	0.591
7	10.525	9.088	0.578
8	10.654	9.006	0.597
9	10.411	8.868	0.612
10	10.647	9.077	0.600
11	10.401	9.026	0.602
12	10.653	9.042 (sr)	0.572
13	10.353	8.970	0.606
14	10.624	8.926	0.589
15	10.417	9.050	0.586
16	10.683	8.974	0.575
mean	10.532	9.011 (sa)	0.589
stdev	0.116	0.059	0.013
coef of var	1.102	0.653	2.178
minimum	10.353	8.868	0.572
maximum	10.683	9.088	0.612
wgt mean	10.534	9.012	0.588

COMPARISON OF FORWARD AND REVERSE RESULTS

Note: weighted means and standard deviations are based on detector noise level

det	scene mean,md (for/rev)	scene stdev,sd (for/rev)
1	0.99931	0.98545
2	0.99882	0.97813
3	0.99857	0.96631
4	0.99842	0.97462
5	0.99865	0.96936
6	0.99823	0.97087
7	0.99840	0.96268
8	0.99788	0.96237
9	0.99969	0.99367
10	0.99840	0.97751
11	0.99865	0.97323
12	0.99774	0.96482 (sr)
13	0.99863	0.97722
14	0.99829	0.98017
15	0.99696	0.96633
16	0.99674	0.96599
mean	0.99834	0.97304 (sa)

stdev	0.00074	0.00873
coef of var	0.07454	0.89718
minimum	0.99674	0.96237
maximum	0.99969	0.99367
wgt mean	0.99832	0.97283

HISTOGRAM ANALYSIS REPORT- HEADER PAGE

INPUT DATA: SCENE, float data

DATE OF ACQUISITION: 07/28/2000 12:03:45

TIME: 06/26/2001 15:20:43

SATELLITE: LANDSAT 7

PATH: 202

ROW: 210

BAND: B2

REFERENCE DETECTOR: 12

PROCESSING LEVEL: R0C

NUMBER OF SCANS ANALYZED: 374

GAIN STATE: L

TOTAL # PIXELS USED PER DET: 2178750

PIXELS TAKEN OFF LOW END PER DETECTOR

FORWARD SCANS 0

REVERSE SCANS 0

ALL SCANS 0

PIXELS TAKEN OFF HIGH END PER DETECTOR

FORWARD SCANS 9115

REVERSE SCANS 9037

ALL SCANS

18126

NOTE: BIAS WAS CALCULATED FROM THE IC DATA

TEMPERATURES IN DEGREES C:

MEAN

AMBIENT_PREAMP_LOW_CH	11.5170
BACKUP_SHUTTER_FLAG	11.5150
BAFFLE_HEATER	28.0875
BAFFLE_SUPPORT	22.2060
BAFFLE_TUBE	23.1610
BAND4_POSTAMP	19.0430
BAND7_PREAMP	-4.5240
BLACKBODY_CTL	46.5600
BLACKBODY_ISO	44.3967
CAL_LAMP_HOUSING	10.5760
CAL_SHUTTER_FLAG	11.7056
CAL_SHUTTER_HUB	11.2030
CFPA_CTL	91.4730
CFPA_MONITOR	91.5020
MEM_HEAT_SINK_PS1	14.0210
MEM_HEAT_SINK_PS2	14.3340
MUX_ELECTRONICS	11.0950
MUX_POWER_SUPPLY	8.1720
PANBAND_POSTAMP	18.4130

PRIMARY_MIRROR	12.1430
PRIMARY_MIRROR_MASK	12.1430
SCAN_LINE_CORRECTOR	6.4590
SECONDARY_MIRROR	16.5280
SECONDARY_MIRROR_MASK	15.9010
SILICON_FP_ASSEMBLY	12.4845
TELESCOPE_BASEPLATE	9.9480
TELESCOPE_HOUSING	15.2740

LAMP CURRENTS IN MILLIAMPS:

	MEAN
TEC_LAMP_1I	95.2430
TEC_LAMP_2I	94.2335

Landsat-7 Image Assessment System 06/26/2001 15:20:43

Histogram Analysis tightrope

Product: L71EDC110021017040 Processing Level: R0C

Band B2 Scene 1 Gain L -- PASC IMAGE data

HISTOGRAM ANALYSIS REPORT- SUMMARY PAGE

INPUT DATA: SCENE, float data

REFERENCE DETECTOR = 12

DETECTOR SATURATION LEVEL FIND RESULTS

DetNo	High Sat	Low Sat
01	255.0000	8.0000
02	255.0000	0.0000
03	255.0000	8.0000
04	255.0000	8.0000
05	255.0000	8.0000
06	255.0000	8.0000
07	255.0000	8.0000
08	255.0000	8.0000
09	255.0000	8.0000
10	255.0000	8.0000
11	255.0000	8.0000
12	255.0000	0.0000
13	255.0000	8.0000
14	255.0000	8.0000
15	255.0000	8.0000
16	255.0000	0.0000

FOR ALL SCANS:

TOTAL # PIXELS USED PER DET: 2178750
 # PIXELS TAKEN OFF LOW END (BIN 0) PER DETECTOR: 0
 # PIXELS TAKEN OFF HIGH END (BIN 255) PER DETECTOR: 18126

	unweighted	weighted	reference
	detector		
scene mean (counts)	10.5256	10.5279	10.6436
net scene mean (counts)	0.5361	0.5361	0.5389
scene stdev (counts)	8.9284	8.9284	8.9210
net scene stdev (counts)	8.9284	8.9284	8.9208
net scene mean for/rev ratio	0.9653	0.9651	0.9565
scene stdev for/rev ratio	0.9730	0.9728	0.9648
net scene mean for/all ratio	0.9771	0.9770	0.9727
scene stdev for/all ratio	0.9820	0.9819	0.9779

det	nmd/nma	sd/sa	b(avg)	b(ref)	nmd/nma	sd/sa	b(avg)	b(ref)
			(for/rev)	for/rev	(for-rev)	(for-rev)	b(ref)	
1 0.20242	1.00774	1.01038	0.14869	0.27293	1.01745	1.01299	0.12337	
2 0.13269	1.01680	1.00956	-0.02192	0.10246	1.01070	1.00546	0.05217	
3 0.00718	0.99526	0.99266	-0.00650	0.11787	1.00731	0.99331	-0.07333	

4 0.09907	1.01526	1.00444	-0.02354	0.10084	1.00448	1.00186	0.01851
5 0.03860	0.99161	0.99939	0.14785	0.27209	1.01006	0.99645	-0.04060
6 0.06083	0.99843	0.99640	-0.05662	0.06780	1.00959	0.99801	-0.02005
7 0.03055	1.00234	1.00320	0.04215	0.16648	0.99829	0.98958	-0.11069 -
8 0.02859	1.00323	0.99391	-0.18291	-0.05839	0.99621	0.98926	-0.11057 -
9 0.28727	0.99576	0.99433	0.05681	0.18113	1.01461	1.02144	0.20754
10 0.13044	1.01358	1.00968	-0.01134	0.11304	1.00253	1.00483	0.05000
11 0.07981	0.99548	1.00184	0.15015	0.27439	1.00721	1.00042	0.00066
12 0.00000	1.00511	0.99917	-0.12447	0.00000	0.99108	0.99179	-0.08148
13 0.12247	0.99851	0.99760	0.15427	0.27850	1.00186	1.00453	0.04339
14 0.16258	0.99657	0.99423	-0.15127	-0.02678	0.99003	1.00756	0.08102
15 0.02370	0.98367	1.00086	0.13306	0.25731	0.97183	0.99333	-0.05564
16 0.02398	0.98026	0.99235	-0.22227	-0.09771	0.97048	0.99299	-0.05829
mean 0.08199	0.99998	1.00000	0.00201	0.12637	1.00023	1.00024	0.00163
stdev 0.08805	0.01035	0.00612	0.12612	0.12602	0.01371	0.00897	0.08843
coef of var 107.39045	1.03461	0.61178	6279.72998	99.71741	1.37117	0.89727	5438.92334
minimum 0.03055	0.98026	0.99235	-0.22227	-0.09771	0.97048	0.98926	-0.11069 -

maximum	1.01680	1.01038	0.15427	0.27850	1.01745	1.02144	0.20754
0.28727							
wgt mean	1.00000	1.00000	-0.00031	0.12406	1.00001	1.00002	-0.00046
0.07992							

PEAKS IN FFT

frequency (lines/cycle)	FFT magnitude	magnitude- background
32.0000	0.0225	-0.0579
16.0000	0.0237	-0.0465
8.0000	0.0277	-0.0105
5.3333	0.0154	-0.0124
4.0000	0.0168	-0.0062
3.2000	0.0131	-0.0074
2.6667	0.0111	-0.0079
2.2857	0.0202	0.0016
2.0000	0.1014	0.0793

RESULTS FOR ALL SCANS

Note: weighted means and standard deviations are based on detector noise level

det	scene mean,md (counts)	scene stdev,sd (counts)	detector noise lev (counts)	net scene mean,nmd (counts)	net scene stdev,nsd (counts)
1	10.487	9.021	0.601	0.540	9.021
2	10.651	9.014	0.576	0.545	9.014
3	10.457	8.863	0.579	0.534	8.863
4	10.598	8.968	0.573	0.544	8.968
5	10.374	8.923	0.588	0.532	8.923
6	10.546	8.896	0.591	0.535	8.896
7	10.519	8.957	0.578	0.537	8.957
8	10.646	8.874	0.597	0.538	8.874
9	10.412	8.878	0.612	0.534	8.878
10	10.641	9.015	0.600	0.543	9.015
11	10.397	8.945	0.602	0.534	8.945
12	10.644	8.921 (sr)	0.572	0.539 (nmr)	8.921
13	10.349	8.907	0.606	0.535	8.907
14	10.618	8.877	0.589	0.534	8.877
15	10.404	8.936	0.586	0.527	8.936
16	10.668	8.860	0.575	0.526	8.860
mean	10.526	8.928 (sa)	0.589	0.536 (nma)	8.928

stdev	0.115	0.055	0.013	0.006	0.055
coef of var	1.088	0.612	2.178	1.035	0.611
minimum	10.349	8.860	0.572	0.526	8.860
maximum	10.668	9.021	0.612	0.545	9.021
wgt mean	10.528	8.928	0.588	0.536	8.928

Calculated gain and bias corrections

det b(ref)	nmd/nma	% diff		% diff		sd/sr	nmd/nmr	b(avg)
		sd/sa	nmd/nma	nmd/nmr	& sd/sr			
1 0.27293	1.00774	1.01038	-0.26213	1.00262	1.01122	-0.85486	0.14869	
2 0.10246	1.01680	1.00956	0.71532	1.01164	1.01040	0.12258	-0.02192	
3 0.11787	0.99526	0.99266	0.26161	0.99020	0.99348	-0.33114	-0.00650	
4 0.10084	1.01526	1.00444	1.07204	1.01010	1.00527	0.47930	-0.02354	
5 0.27209	0.99161	0.99939	-0.78072	0.98657	1.00022	-1.37344	0.14785	
6 0.06780	0.99843	0.99640	0.20297	0.99335	0.99723	-0.38976	-0.05662	
7 0.16648	1.00234	1.00320	-0.08550	0.99725	1.00403	-0.67823	0.04215	
8 0.05839	1.00323	0.99391	0.93401	0.99814	0.99474	0.34128	-0.18291 -	

9 0.18113	0.99576	0.99433	0.14336	0.99070	0.99516	-0.44938	0.05681
10 0.11304	1.01358	1.00968	0.38561	1.00843	1.01052	-0.20713	-0.01134
11 0.27439	0.99548	1.00184	-0.63736	0.99042	1.00268	-1.23008	0.15015
12 0.00000	1.00511	0.99917	0.59273	1.00000	1.00000	0.00000	-0.12447
13 0.27850	0.99851	0.99760	0.09101	0.99343	0.99843	-0.50172	0.15427
14 0.02678	0.99657	0.99423	0.23584	0.99151	0.99505	-0.35689	-0.15127 -
15 0.25731	0.98367	1.00086	-1.73277	0.97867	1.00169	-2.32544	0.13306
16 0.09771	0.98026	0.99235	-1.22558	0.97528	0.99318	-1.81828	-0.22227 -
mean 0.12637	0.99998	1.00000	-0.00560	0.99489	1.00083	-0.59832	0.00201
stdev 0.12602	0.01035	0.00612	0.76695	0.01029	0.00612	0.76694	0.12612
coef of var 6279.72998	1.03461 99.71741	0.61178	-13703.55957	1.03461	0.61187	-128.18115	
minimum 0.09771	0.98026	0.99235	-1.73277	0.97528	0.99318	-2.32544	-0.22227 -
maximum 0.27850	1.01680	1.01038	1.07204	1.01164	1.01122	0.47930	0.15427
wgt mean 0.12406	1.00000	1.00000	-0.00337	0.99492	1.00083	-0.59610	-0.00031

RESULTS FOR FWD SCANS

Note: weighted means and standard deviations are based on detector noise level

det	scene mean,md (counts)	scene stdev,sd (counts)	detector noise lev (counts)	net scene mean,nmd (counts)	net scene stdev,nsd (counts)
1	10.480	8.916	0.601	0.532	8.916
2	10.642	8.875	0.576	0.535	8.875
3	10.447	8.673	0.579	0.523	8.673
4	10.587	8.814	0.573	0.533	8.814
5	10.364	8.746	0.588	0.522	8.746
6	10.534	8.726	0.591	0.526	8.726
7	10.508	8.749	0.578	0.525	8.749
8	10.632	8.667	0.597	0.525	8.667
9	10.407	8.812	0.612	0.525	8.812
10	10.630	8.873	0.600	0.532	8.873
11	10.387	8.785	0.602	0.523	8.785
12	10.629	8.723 (sr)	0.572	0.524 (nmr)	8.723
13	10.339	8.765	0.606	0.523	8.766
14	10.606	8.749	0.589	0.519	8.749
15	10.385	8.745	0.586	0.508	8.745
16	10.648	8.669	0.575	0.506	8.669
mean	10.514	8.768 (sa)	0.589	0.524 (nma)	8.768

stdev	0.113	0.074	0.013	0.008	0.074
coef of var	1.075	0.849	2.178	1.540	0.849
minimum	10.339	8.667	0.572	0.506	8.667
maximum	10.648	8.916	0.612	0.535	8.916
wgt mean	10.516	8.767	0.588	0.524	8.767

Calculated gain and bias corrections

det b(ref)	nmd/nma	% diff		% diff		sd/sr	nmd/nmr	b(avg)
		sd/sa	nmd/nma	nmd/nmr	& sd/sr			
1 0.37436	1.01654	1.01698	-0.04304	1.01591	1.02205	-0.60263	0.21074	
2 0.16858	1.02229	1.01229	0.98314	1.02166	1.01734	0.42354	0.00393	
3 0.12112	0.99899	0.98928	0.97618	0.99836	0.99421	0.41658	-0.04376	
4 0.15010	1.01759	1.00533	1.21152	1.01696	1.01035	0.65193	-0.01464	
5 0.29141	0.99664	0.99760	-0.09606	0.99602	1.00257	-0.65567	0.12738	
6 0.09773	1.00326	0.99535	0.79175	1.00264	1.00031	0.23215	-0.06727	
7 0.15126	1.00156	0.99795	0.36078	1.00093	1.00293	-0.19883	-0.01347	
8 0.07225	1.00146	0.98858	1.29436	1.00084	0.99351	0.73477	-0.23809	-

9 0.32600	1.00313	1.00514	-0.20066	1.00250	1.01015	-0.76026	0.16214
10 0.17797	1.01484	1.01209	0.27172	1.01421	1.01713	-0.28790	0.01337
11 0.31411	0.99906	1.00203	-0.29697	0.99843	1.00702	-0.85658	0.15020
12 0.00000	1.00062	0.99504	0.55961	1.00000	1.00000	0.00000	-0.16549
13 0.33939	0.99939	0.99982	-0.04309	0.99877	1.00481	-0.60270	0.17560
14 0.05431	0.99144	0.99797	-0.65653	0.99083	1.00295	-1.21612	-0.11091
15 0.26932	0.96933	0.99751	-2.86589	0.96873	1.00249	-3.42535	0.10518
16 0.08652	0.96526	0.98877	-2.40609	0.96466	0.99370	-2.96559	-0.25243 -
mean 0.16731	1.00009	1.00011	-0.00995	0.99947	1.00510	-0.56954	0.00265
stdev 0.14497	0.01540	0.00849	1.17700	0.01539	0.00854	1.17697	0.14569
coef of var 5488.44238	1.54029 86.64988	0.84934	-11824.25488	1.54027	0.84940	-206.65248	
minimum 0.08652	0.96526	0.98858	-2.86589	0.96466	0.99351	-3.42535	-0.25243 -
maximum 0.37436	1.02229	1.01698	1.29436	1.02166	1.02205	0.73477	0.21074
wgt mean 0.16395	1.00000	1.00000	-0.00812	0.99938	1.00499	-0.56770	-0.00072

RESULTS FOR REV SCANS

Note: weighted means and standard deviations are based on detector noise level

det	scene mean,md (counts)	scene stdev,sd (counts)	detector noise lev (counts)	net scene mean,nmd (counts)	net scene stdev,nsd (counts)
1	10.488	9.047	0.601	0.542	9.047
2	10.654	9.073	0.576	0.549	9.073
3	10.462	8.975	0.579	0.538	8.975
4	10.604	9.043	0.573	0.550	9.043
5	10.378	9.022	0.588	0.536	9.022
6	10.553	8.988	0.591	0.539	8.988
7	10.525	9.088	0.578	0.545	9.088
8	10.654	9.006	0.597	0.546	9.006
9	10.411	8.868	0.612	0.537	8.868
10	10.647	9.077	0.600	0.549	9.077
11	10.401	9.026	0.602	0.538	9.027
12	10.653	9.042 (sr)	0.572	0.548 (nmr)	9.041
13	10.353	8.970	0.606	0.541	8.970
14	10.624	8.926	0.589	0.544	8.926
15	10.417	9.050	0.586	0.541	9.050
16	10.683	8.974	0.575	0.540	8.974
mean	10.532	9.011 (sa)	0.589	0.543 (nma)	9.011

stdev	0.116	0.059	0.013	0.005	0.059
coef of var	1.102	0.653	2.178	0.859	0.652
minimum	10.353	8.868	0.572	0.536	8.868
maximum	10.683	9.088	0.612	0.550	9.088
wgt mean	10.534	9.012	0.588	0.543	9.012

Calculated gain and bias corrections

det b(ref)	nmd/nma	% diff		% diff		sd/sr	nmd/nmr	b(avg)
		sd/sa	nmd/nma	nmd/nmr	& sd/sr			
1 0.17194	0.99910	1.00394	-0.48303	0.98958	1.00066	-1.11363	0.08737	
2 0.03588	1.01147	1.00679	0.46320	1.00182	1.00350	-0.16741	-0.04824	
3 0.11395	0.99174	0.99594	-0.42296	0.98228	0.99269	-1.05354	0.02957	
4 0.05103	1.01305	1.00347	0.94988	1.00339	1.00019	0.31929	-0.03315	
5 0.25281	0.98671	1.00115	-1.45214	0.97731	0.99788	-2.08269	0.16798	
6 0.03690	0.99373	0.99734	-0.36177	0.98426	0.99408	-0.99236	-0.04723	
7 0.18182	1.00328	1.00845	-0.51491	0.99371	1.00516	-1.14549	0.09722	
8 0.04366	1.00527	0.99931	0.59488	0.99569	0.99605	-0.03571	-0.12752	-

9 0.03873	0.98868	0.98405	0.47012	0.97926	0.98083	-0.16049	-0.04540
10 0.04753	1.01228	1.00722	0.50135	1.00263	1.00393	-0.12924	-0.03663
11 0.23431	0.99191	1.00160	-0.97275	0.98245	0.99833	-1.60333	0.14954
12 0.00000	1.00962	1.00328	0.63060	1.00000	1.00000	0.00000	-0.08401
13 0.21692	0.99754	0.99531	0.22376	0.98803	0.99206	-0.40683	0.13221
14 0.10827	1.00142	0.99048	1.09874	0.99188	0.98725	0.46816	-0.19192 -
15 0.24563	0.99743	1.00421	-0.67731	0.98792	1.00093	-1.30789	0.16082
16 0.11050	0.99462	0.99576	-0.11399	0.98514	0.99250	-0.74458	-0.19415 -
mean 0.08531	0.99987	0.99989	-0.00415	0.99033	0.99663	-0.63473	0.00103
stdev 0.12116	0.00858	0.00652	0.72722	0.00850	0.00650	0.72721	0.12077
coef of var 11740.15430	0.85853 142.02005	0.65255	-17542.24609	0.85860	0.65249	-114.56892	
minimum 0.11050	0.98671	0.98405	-1.45214	0.97731	0.98083	-2.08269	-0.19415 -
maximum 0.25281	1.01305	1.00845	1.09874	1.00339	1.00516	0.46816	0.16798
wgt mean 0.08402	1.00000	1.00000	-0.00153	0.99047	0.99673	-0.63212	-0.00026

COMPARISON OF FORWARD AND REVERSE RESULTS

Note: weighted means and standard deviations are based on detector noise level

det	scene	scene	net scene	net scene
	mean,md	stdev,sd	mean,nmd	stdev,nsd
	(for/rev)	(for/rev)	(for/rev)	(for/rev)
1	0.99931	0.98545	0.98196	0.98543
2	0.99882	0.97813	0.97544	0.97816
3	0.99857	0.96631	0.97216	0.96630
4	0.99842	0.97462	0.96943	0.97460
5	0.99865	0.96936	0.97482	0.96937
6	0.99823	0.97087	0.97436	0.97089
7	0.99840	0.96268	0.96346	0.96267
8	0.99788	0.96237	0.96145	0.96238
9	0.99969	0.99367	0.97921	0.99363
10	0.99840	0.97751	0.96755	0.97753
11	0.99865	0.97323	0.97207	0.97320
12	0.99774	0.96482 (sr)	0.95650 (nmr)	0.96481
13	0.99863	0.97722	0.96690	0.97724
14	0.99829	0.98017	0.95549	0.98015
15	0.99696	0.96633	0.93792	0.96631
16	0.99674	0.96599	0.93662	0.96599
mean	0.99834	0.97304 (sa)	0.96533 (nma)	0.97304

stdev	0.00074	0.00873	0.01324	0.00873
coef of var	0.07454	0.89722	1.37119	0.89669
minimum	0.99674	0.96237	0.93662	0.96238
maximum	0.99969	0.99367	0.98196	0.99363
wgt mean	0.99832	0.97283	0.96512	0.97283

Ratios of for/rev gains and differences between forward and reverse biases

det b(ref)	% diff		% diff		sd/sr	nmd/nmr (for-rev)	b(avg)
	nmd/nma (for/rev)	sd/sa	nmd/nma (for/rev)	nmd/nmr (for/rev)			
1 0.20242	1.01745	1.01299	0.43999	1.02661	1.02138	0.51100	0.12337
2 0.13269	1.01070	1.00546	0.51995	1.01980	1.01379	0.59095	0.05217
3 0.00718	1.00731	0.99331	1.39912	1.01637	1.00154	1.47011	-0.07333
4 0.09907	1.00448	1.00186	0.26165	1.01352	1.01015	0.33263	0.01851
5 0.03860	1.01006	0.99645	1.35609	1.01915	1.00471	1.42707	-0.04060
6 0.06083	1.00959	0.99801	1.15352	1.01867	1.00627	1.22450	-0.02005
7 0.03055	0.99829	0.98958	0.87568	1.00727	0.99778	0.94666	-0.11069 -
8 0.02859	0.99621	0.98926	0.69950	1.00517	0.99745	0.77048	-0.11057 -

9 0.28727	1.01461	1.02144	-0.67078	1.02374	1.02989	-0.59978	0.20754
10 0.13044	1.00253	1.00483	-0.22962	1.01155	1.01315	-0.15866	0.05000
11 0.07981	1.00721	1.00042	0.67578	1.01627	1.00871	0.74678	0.00066
12 0.00000	0.99108	0.99179	-0.07100	1.00000	1.00000	0.00000	-0.08148
13 0.12247	1.00186	1.00453	-0.26684	1.01087	1.01285	-0.19586	0.04339
14 0.16258	0.99003	1.00756	-1.75524	0.99894	1.01591	-1.68425	0.08102
15 0.02370	0.97183	0.99333	-2.18868	0.98057	1.00156	-2.11771	-0.05564
16 0.02398	0.97048	0.99299	-2.29212	0.97921	1.00121	-2.22114	-0.05829
mean 0.08199	1.00023	1.00024	-0.00581	1.00923	1.00852	0.06517	0.00163
stdev 0.08805	0.01371	0.00897	1.18535	0.01384	0.00905	1.18535	0.08843
coef of var 5438.92334	1.37117 107.39045	0.89727	-20393.19922	1.37110	0.89725	1818.74365	
minimum 0.03055	0.97048	0.98926	-2.29212	0.97921	0.99745	-2.22114	-0.11069
maximum 0.28727	1.01745	1.02144	1.39912	1.02661	1.02989	1.47011	0.20754
wgt mean 0.07992	1.00001	1.00002	-0.00659	1.00901	1.00830	0.06440	-0.00046

HISTOGRAM ANALYSIS REPORT- HEADER PAGE

INPUT DATA: SCENE, float data

DATE OF ACQUISITION: 07/28/2000 12:03:45

TIME: 06/26/2001 16:40:11

SATELLITE: LANDSAT 7

PATH: 202

ROW: 210

BAND: B2

REFERENCE DETECTOR: 12

PROCESSING LEVEL: R1R

NUMBER OF SCANS ANALYZED: 374

GAIN STATE: L

TOTAL # PIXELS USED PER DET: 2178750

PIXELS TAKEN OFF LOW END PER DETECTOR

FORWARD SCANS 0

REVERSE SCANS 0

ALL SCANS 0

PIXELS TAKEN OFF HIGH END PER DETECTOR

FORWARD SCANS 9115

REVERSE SCANS 9037

ALL SCANS

18126

NOTE: BIAS WAS CALCULATED FROM THE IC DATA

TEMPERATURES IN DEGREES C:

MEAN

AMBIENT_PREAMP_LOW_CH	11.5170
BACKUP_SHUTTER_FLAG	11.5150
BAFFLE_HEATER	28.0875
BAFFLE_SUPPORT	22.2060
BAFFLE_TUBE	23.1610
BAND4_POSTAMP	19.0430
BAND7_PREAMP	-4.5240
BLACKBODY_CTL	46.5600
BLACKBODY_ISO	44.3967
CAL_LAMP_HOUSING	10.5760
CAL_SHUTTER_FLAG	11.7056
CAL_SHUTTER_HUB	11.2030
CFPA_CTL	91.4730
CFPA_MONITOR	91.5020
MEM_HEAT_SINK_PS1	14.0210
MEM_HEAT_SINK_PS2	14.3340
MUX_ELECTRONICS	11.0950
MUX_POWER_SUPPLY	8.1720
PANBAND_POSTAMP	18.4130

PRIMARY_MIRROR	12.1430
PRIMARY_MIRROR_MASK	12.1430
SCAN_LINE_CORRECTOR	6.4590
SECONDARY_MIRROR	16.5280
SECONDARY_MIRROR_MASK	15.9010
SILICON_FP_ASSEMBLY	12.4845
TELESCOPE_BASEPLATE	9.9480
TELESCOPE_HOUSING	15.2740

LAMP CURRENTS IN MILLIAMPS:

	MEAN
TEC_LAMP_1I	95.2430
TEC_LAMP_2I	94.2335

Landsat-7 Image Assessment System 06/26/2001 16:40:11

Histogram Analysis tightrope

Product: L71EDC110021017040 Processing Level: R1R

Band B2 Scene 1 Gain L -- PASC IMAGE data

note: rxx_numBadPixFound_HIST = 197890

HISTOGRAM ANALYSIS REPORT- SUMMARY PAGE

INPUT DATA: SCENE, float data

REFERENCE DETECTOR = 12

FOR ALL SCANS:

TOTAL # PIXELS USED PER DET: 2178750
 # PIXELS TAKEN OFF LOW END (BIN 0) PER DETECTOR: 0
 # PIXELS TAKEN OFF HIGH END (BIN 255) PER DETECTOR: 18126

	unweighted	weighted	reference
	detector		
scene mean (counts)	0.2638	0.2648	0.0888
scene stdev (counts)	3.9918	4.0084	0.7503
scene mean for/rev ratio	0.9737	0.9736	0.9752
scene stdev for/rev ratio	0.9805	0.9804	1.0092
scene mean for/all ratio	0.9825	0.9824	0.9870
scene stdev for/all ratio	0.9863	0.9863	1.0045

det	nmd/nma	sd/sa	b(avg)	b(ref)	nmd/nma	sd/sa	b(avg)	b(ref)
	(for/rev)		for/rev		(for-rev)	(for-rev)	b(ref)	

1 0.00257	2.54095	2.82101	0.02629	0.04415	1.01059	1.00517	-0.00198	-
2 0.00254	2.38117	2.63085	0.02513	0.04393	1.00283	0.99810	-0.00180	-
3 0.00900	0.30301	0.18835	-0.16122	0.00905	1.12260	1.03340	-0.03081	-
4 0.00242	2.57204	2.79300	0.02095	0.04315	0.99609	0.99412	-0.00104	-
5 0.00959	0.28276	0.18963	-0.13007	0.01488	1.14075	1.03484	-0.03483	-
6 0.00728	0.31951	0.19101	-0.17818	0.00588	1.09082	1.02860	-0.02115	-
7 0.00600	0.30661	0.18710	-0.16916	0.00756	1.08322	1.03631	-0.01462	-
8 0.00498	0.34472	0.19443	-0.20470	0.00091	1.06141	1.03100	-0.00814	-
9 0.00239	0.30105	0.19967	-0.13446	0.01406	0.96921	1.03339	0.02907	
10 0.00219	2.55867	2.79360	0.02227	0.04340	0.99404	0.99711	0.00015	-
11 0.00614	0.28230	0.19536	-0.11785	0.01717	1.08608	1.03056	-0.01685	-
12 0.00000	0.33530	0.18718	-0.20957	0.00000	1.00168	1.02944	0.01850	
13 0.00032	0.30012	0.19540	-0.14193	0.01266	0.99568	1.03193	0.01827	
14 0.00768	0.32818	0.18856	-0.19608	0.00252	0.90549	1.01818	0.05899	
15 0.00130	2.48144	2.79639	0.02983	0.04481	0.96293	0.98565	0.00465	-
16 0.00773	0.30121	0.18254	-0.17216	0.00700	0.88042	0.99658	0.05856	
mean 0.00224	0.99619	0.99588	-0.10568	0.01945	1.01899	1.01777	0.00356	-

stdev	1.05280	1.23388	0.09443	0.01767	0.07356	0.01813	0.02760
0.00512							
coef of var	105.68252	123.89798	-89.34938	90.89134	7.21914	1.78093	775.46362
-228.51677							
minimum	0.28230	0.18254	-0.20957	0.00000	0.88042	0.98565	-0.03483
0.00959							
maximum	2.57204	2.82101	0.02983	0.04481	1.14075	1.03631	0.05899
0.00773							
wgt mean	1.00000	1.00000	-0.10580	0.01942	1.01885	1.01757	0.00357
0.00224							

PEAKS IN FFT

frequency (lines/cycle)	FFT magnitude	magnitude- background
32.0000	0.0284	-0.0729
16.0000	0.0278	-0.0605
8.0000	0.0178	-0.0302
5.3333	0.0143	-0.0206
4.0000	0.0143	-0.0150
3.2000	0.0148	-0.0112
2.6667	0.0162	-0.0079
2.2857	0.0154	-0.0088
2.0000	0.0192	-0.0093

RESULTS FOR ALL SCANS

Note: weighted means and standard deviations are based on detector noise level

det	scene mean,md (counts)	scene stdev,sd (counts)	detector noise lev (counts)
1	0.673	11.308	0.601
2	0.631	10.545	0.576
3	0.080	0.755	0.579
4	0.681	11.195	0.573
5	0.075	0.760	0.588
6	0.085	0.766	0.591
7	0.081	0.750	0.578
8	0.091	0.779	0.597
9	0.080	0.800	0.612
10	0.678	11.198	0.600
11	0.075	0.783	0.602
12	0.089	0.750 (sr)	0.572
13	0.079	0.783	0.606
14	0.087	0.756	0.589
15	0.657	11.209	0.586
16	0.080	0.732	0.575
mean	0.264	3.992 (sa)	0.589

stdev	0.279	4.946	0.013
coef of var	105.683	123.898	2.178
minimum	0.075	0.732	0.572
maximum	0.681	11.308	0.612
wgt mean	0.265	4.008	0.588

Calculated gain and bias corrections

det b(ref)	nmd/nma	% diff		% diff		sd/sr	nmd/nmr	b(avg)
		sd/sa	nmd/nma	nmd/nmr	& sd/sr			
1 0.04415	2.54095	2.82101	-10.44635	7.57805	15.07104	-66.16591	0.02629	
2 0.04393	2.38117	2.63085	-9.96294	7.10154	14.05508	-65.73392	0.02513	
3 0.00905	0.30301	0.18835	46.67015	0.90369	1.00625	-10.73962	-0.16122	
4 0.04315	2.57204	2.79300	-8.23690	7.67078	14.92136	-64.18678	0.02095	
5 0.01488	0.28276	0.18963	39.43121	0.84329	1.01306	-18.29041	-0.13007	
6 0.00588	0.31951	0.19101	50.34349	0.95291	1.02044	-6.84422	-0.17818	
7 0.00756	0.30661	0.18710	48.41212	0.91441	0.99956	-8.89777	-0.16916	
8 0.00091	0.34472	0.19443	55.74889	1.02808	1.03874	-1.03197	-0.20470	

9 0.01406	0.30105	0.19967	40.49311	0.89785	1.06673	-17.19304	-0.13446
10 0.04340	2.55867	2.79360	-8.77878	7.63089	14.92458	-64.67330	0.02227
11 0.01717	0.28230	0.19536	36.40059	0.84192	1.04371	-21.40306	-0.11785
12 0.00000	0.33530	0.18718	56.69931	1.00000	1.00000	0.00000	-0.20957
13 0.01266	0.30012	0.19540	42.26743	0.89506	1.04389	-15.35165	-0.14193
14 0.00252	0.32818	0.18856	54.03599	0.97874	1.00738	-2.88424	-0.19608
15 0.04481	2.48144	2.79639	-11.93497	7.40057	14.93950	-67.49246	0.02983
16 0.00700	0.30121	0.18254	49.06122	0.89832	0.97522	-8.20896	-0.17216
mean 0.01945	0.99619	0.99588	29.38772	2.97101	5.32041	-27.44358	-0.10568
stdev 0.01767	1.05280	1.23388	27.91598	3.13983	6.59188	27.26208	0.09443
coef of var 89.34938	105.68252	123.89798	94.99197	105.68252	123.89798	-99.33862	-90.89134
minimum 0.00000	0.28230	0.18254	-11.93497	0.84192	0.97522	-67.49246	-0.20957
maximum 0.04481	2.57204	2.82101	56.69931	7.67078	15.07104	0.00000	0.02983
wgt mean 0.01942	1.00000	1.00000	29.38852	2.98237	5.34242	-27.43512	-0.10580

RESULTS FOR FWD SCANS

Note: weighted means and standard deviations are based on detector noise level

det	scene mean,md (counts)	scene stdev,sd (counts)	detector noise lev (counts)
1	0.664	11.176	0.601
2	0.620	10.380	0.576
3	0.084	0.760	0.579
4	0.667	11.003	0.573
5	0.079	0.766	0.588
6	0.087	0.769	0.591
7	0.083	0.756	0.578
8	0.093	0.783	0.597
9	0.077	0.805	0.612
10	0.663	11.022	0.600
11	0.077	0.787	0.602
12	0.088	0.754 (sr)	0.572
13	0.078	0.788	0.606
14	0.081	0.755	0.589
15	0.633	10.969	0.586
16	0.074	0.724	0.575
mean	0.259	3.937 (sa)	0.589

stdev	0.272	4.858	0.013
coef of var	104.876	123.378	2.178
minimum	0.074	0.724	0.572
maximum	0.667	11.176	0.612
wgt mean	0.260	3.953	0.588

Calculated gain and bias corrections

det b(ref)	nmd/nma	% diff		% diff		sd/sr	nmd/nmr	b(avg)
		sd/sa	nmd/nma	nmd/nmr	& sd/sr			
1 0.04288	2.55155	2.82694	-10.24036	7.57401	14.82851	-64.76505	0.02535	
2 0.04267	2.38125	2.62578	-9.76728	7.06851	13.77336	-64.34019	0.02423	
3 0.00456	0.32196	0.19219	50.47873	0.95569	1.00811	-5.33880	-0.17567	
4 0.04195	2.56429	2.78319	-8.18673	7.61184	14.59902	-62.91676	0.02046	
5 0.01005	0.30309	0.19372	44.02670	0.89968	1.01615	-12.15931	-0.14688	
6 0.00224	0.33486	0.19446	53.04939	0.99399	1.02002	-2.58465	-0.18785	
7 0.00457	0.32022	0.19118	50.46621	0.95054	1.00281	-5.35216	-0.17562	
8 0.00158	0.35651	0.19818	57.08759	1.05827	1.03954	1.78485	-0.20786 -	

9 0.01525	0.29737	0.20374	37.36995	0.88272	1.06871	-19.06138	-0.11957
10 0.04232	2.54818	2.78799	-8.98822	7.56400	14.62422	-63.63935	0.02238
11 0.01410	0.29519	0.19908	38.89222	0.87625	1.04424	-17.49487	-0.12562
12 0.00000	0.33688	0.19064	55.44397	1.00000	1.00000	0.00000	-0.19958
13 0.01282	0.30059	0.19925	40.54965	0.89226	1.04513	-15.78132	-0.13233
14 0.00640	0.31287	0.19099	48.37884	0.92873	1.00184	-7.57298	-0.16603
15 0.04419	2.43122	2.77477	-13.19851	7.21681	14.55489	-67.40927	0.03221
16 0.01074	0.28414	0.18325	43.17217	0.84343	0.96121	-13.05290	-0.14325
mean 0.01832	0.99626	0.99596	29.28339	2.95730	5.22424	-26.23026	-0.10348
stdev 0.01769	1.04483	1.22880	27.97653	3.10148	6.44557	27.37309	0.09279
coef of var 0.01830	104.87556	123.37817	95.53720	104.87556	123.37817	-104.35692	-89.67044
minimum -0.00158	0.28414	0.18325	-13.19851	0.84343	0.96121	-67.40927	-0.20786
maximum 0.04419	2.56429	2.82694	57.08759	7.61184	14.82851	1.78485	0.03221
wgt mean 0.01830	1.00000	1.00000	29.28596	2.96840	5.24544	-26.22047	-0.10359

RESULTS FOR REV SCANS

Note: weighted means and standard deviations are based on detector noise level

det	scene mean,md (counts)	scene stdev,sd (counts)	detector noise lev (counts)
1	0.675	11.341	0.601
2	0.635	10.608	0.576
3	0.077	0.750	0.579
4	0.688	11.289	0.573
5	0.071	0.755	0.588
6	0.082	0.762	0.591
7	0.079	0.744	0.578
8	0.090	0.775	0.597
9	0.082	0.795	0.612
10	0.685	11.275	0.600
11	0.073	0.779	0.602
12	0.090	0.747 (sr)	0.572
13	0.081	0.779	0.606
14	0.092	0.756	0.589
15	0.675	11.352	0.586
16	0.086	0.741	0.575
mean	0.266	4.016 (sa)	0.589

stdev	0.282	4.987	0.013
coef of var	106.093	124.182	2.178
minimum	0.071	0.741	0.572
maximum	0.688	11.352	0.612
wgt mean	0.267	4.032	0.588

Calculated gain and bias corrections

det b(ref)	nmd/nma	% diff		% diff		sd/sr	nmd/nmr	b(avg)
		sd/sa	nmd/nma	nmd/nmr	& sd/sr			
1 0.04545	2.52481	2.81241	-10.77701	7.50725	15.18656	-67.67757	0.02733	
2 0.04521	2.37453	2.63077	-10.23872	7.06041	14.20576	-67.19915	0.02603	
3 0.01356	0.28680	0.18598	42.64951	0.85275	1.00425	-16.31612	-0.14487	
4 0.04437	2.57436	2.79965	-8.38440	7.65457	15.11765	-65.54548	0.02150	
5 0.01964	0.26569	0.18720	34.66195	0.79000	1.01085	-24.52724	-0.11205	
6 0.00952	0.30698	0.18905	47.54856	0.91277	1.02085	-11.17897	-0.16670	
7 0.01057	0.29562	0.18448	46.29809	0.87899	0.99617	-12.49764	-0.16099	
8 0.00340	0.33588	0.19222	54.40668	0.99871	1.03797	-3.85454	-0.19973	

9 0.01286	0.30682	0.19716	43.51877	0.91230	1.06462	-15.41028	-0.14864
10 0.04450	2.56345	2.79608	-8.68072	7.62215	15.09837	-65.81032	0.02223
11 0.02024	0.27180	0.19317	33.81901	0.80816	1.04310	-25.38212	-0.10877
12 0.00000	0.33632	0.18519	57.95735	1.00000	1.00000	0.00000	-0.21808
13 0.01250	0.30189	0.19308	43.96566	0.89764	1.04261	-14.94365	-0.15060
14 0.00129	0.34553	0.18758	59.25570	1.02740	1.01291	1.42030	-0.22502 -
15 0.04549	2.52482	2.81516	-10.87422	7.50726	15.20140	-67.76389	0.02756
16 0.00301	0.32273	0.18388	54.81720	0.95961	0.99291	-3.41109	-0.20180
mean 0.02056	0.99613	0.99582	29.37146	2.96187	5.37725	-28.75611	-0.10704
stdev 0.01805	1.05683	1.23662	28.18115	3.14235	6.67756	27.52820	0.09747
coef of var 91.05756	106.09347	124.18179	95.94736	106.09345	124.18179	-95.72990	-
minimum -0.00129	0.26569	0.18388	-10.87422	0.79000	0.99291	-67.76389	-0.22502
maximum 0.04549	2.57436	2.81516	59.25570	7.65457	15.20140	1.42030	0.02756
wgt mean 0.02054	1.00000	1.00000	29.37022	2.97339	5.39984	-28.74896	-0.10716

COMPARISON OF FORWARD AND REVERSE RESULTS

Note: weighted means and standard deviations are based on detector noise level

det	scene mean,md (for/rev)	scene stdev,sd (for/rev)
1	0.98390	0.98543
2	0.97635	0.97851
3	1.09295	1.01311
4	0.96979	0.97460
5	1.11062	1.01452
6	1.06201	1.00841
7	1.05461	1.01596
8	1.03338	1.01076
9	0.94361	1.01310
10	0.96779	0.97753
11	1.05740	1.01033
12	0.97523	1.00923 (sr)
13	0.96939	1.01167
14	0.88158	0.99820
15	0.93750	0.96630
16	0.85717	0.97701
mean	0.99208	0.99779 (sa)

stdev	0.07162	0.01777
coef of var	7.21914	1.78095
minimum	0.85717	0.96630
maximum	1.11062	1.01596
wgt mean	0.99195	0.99759

Ratios of for/rev gains and differences between forward and reverse biases

det b(ref)	% diff		% diff		sd/sr	nmd/nmr (for-rev)	b(avg)
	nmd/nma (for/rev)	sd/sa	nmd/nma (for/rev)	nmd/nmr (for/rev)			
1 0.00257	1.01059	1.00517	0.53814	1.00889	0.97642	3.27095	-0.00198 -
2 0.00254	1.00283	0.99810	0.47262	1.00115	0.96956	3.20543	-0.00180 -
3 0.00900	1.12260	1.03340	8.27457	1.12071	1.00385	11.00128	-0.03081 -
4 0.00242	0.99609	0.99412	0.19800	0.99442	0.96569	2.93089	-0.00104 -
5 0.00959	1.14075	1.03484	9.73620	1.13883	1.00525	12.46084	-0.03483 -
6 0.00728	1.09082	1.02860	5.87106	1.08898	0.99919	8.60054	-0.02115 -
7 0.00600	1.08322	1.03631	4.42670	1.08140	1.00667	7.15745	-0.01462 -
8 0.00498	1.06141	1.03100	2.90660	1.05963	1.00152	5.63841	-0.00814 -

9 0.00239	0.96921	1.03339	-6.40941	0.96758	1.00384	-3.67810	0.02907	
10 0.00219	0.99404	0.99711	-0.30811	0.99237	0.96860	2.42486	0.00015	-
11 0.00614	1.08608	1.03056	5.24571	1.08426	1.00109	7.97578	-0.01685	-
12 0.00000	1.00168	1.02944	-2.73292	1.00000	1.00000	0.00000	0.01850	
13 0.00032	0.99568	1.03193	-3.57536	0.99401	1.00242	-0.84264	0.01827	
14 0.00768	0.90549	1.01818	-11.71658	0.90397	0.98907	-8.99086	0.05899	
15 0.00130	0.96293	0.98565	-2.33266	0.96131	0.95747	0.40033	0.00465	-
16 0.00773	0.88042	0.99658	-12.37732	0.87894	0.96808	-9.65256	0.05856	
mean 0.00224	1.01899	1.01777	-0.11142	1.01728	0.98867	2.61891	0.00356	-
stdev 0.00512	0.07356	0.01813	6.38222	0.07344	0.01761	6.38234	0.02760	
coef of var -228.51677	7.21914	1.78093	-5727.91846	7.21914	1.78091	243.70189	775.46362	
minimum 0.00959	0.88042	0.98565	-12.37732	0.87894	0.95747	-9.65256	-0.03483	-
maximum 0.00773	1.14075	1.03631	9.73620	1.13883	1.00667	12.46084	0.05899	
wgt mean 0.00224	1.01885	1.01757	-0.10827	1.01714	0.98847	2.62204	0.00357	-

References

Reference 1

Landsat 7 System Data Format Control Book (DFCB) Volume IV - Wideband Data. Revision H. Martin Marietta Astro Space. 23007702-IVH. 26 February 1998.

Reference 2

Landsat 7 System Program Coordinates System Standard. Revision B. Martin Marietta Astro Space. PS23007610B. 2 December 1994.

Reference 3

Landsat 7 System Image Assessment System (IAS) Element Specification (Revision 1). NASA Goddard Space Flight Center. 430-15-01-001-1. February 1998.

Reference 4

Landsat 7 System Specification. Revision H. Goddard Space Flight Center. 430-L-0002-H. June 1996.

Reference 5

Landsat 7 Space Segment Technical Description Document - Enhanced Thematic Mapper Plus. Hughes Santa Barbara Research Center. May 1994. Updated by NASA Goddard Space Flight Center. September 1995.

Reference 6

Landsat to Ground Station Interface Description. Revision 9. Goddard Space Flight Center. Greenbelt, Maryland. January 1986.

Reference 7

Landsat 7 System Calibration Parameter File Definition. Revision 1. 430-15-01-002-0. NASA Goddard Space Flight Center. Greenbelt, Maryland. January 1998.

Reference 8

SBRs radiometric algorithm document (appended)

Reference 9

IAS Users Guide

Reference 10

Level 0R data description document

Reference 11

IAS database fields

